AD A100783

DTIC FILE COPY

FOREIGN TECHNOLOGY DIVISION

AERODYNAMIC NOISE AND SUPPRESSORS

by

Dan Qun Fang

DTIC
ELECTE
JUL 0 1 1981

S D

81 06 29 151

EDITED TRANSLATION

FTD-ID(RS)T-1800-80   29 May 1981

MICROFICHE NR: FTD-81-C-000473

AERODYNAMIC NOISE AND SUPPRESSORS

By: Dan Qun Fang

English pages: 294

Source: Aerodynamic Noise and Suppressors, 1978, pp. 1-245
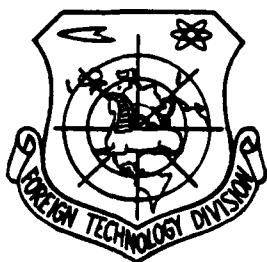
Country of origin: China
Translated by: SCITRAN
                F33657-78-D-0619
Requester: FTD/TQTR
Approved for public release; distribution unlimited.

PREPARED BY:

TRANSLATION DIVISION
FOREIGN TECHNOLOGY DIVISION
WP-AFB, OHIO.

TABLE OF CONTENTS

Summary of Contents

Along with the rapid development of modern industry noise itself becomes one of the international invironmental pollutants. How we will combat noise is an important question of environmental protection. This paper emphasizes the analysis of the mechanisms which produce aerodynamic noise, presents the noise characteristics of typical aerodynamic equipment, investigates the basic principles of eliminating various types of noises and the methods of planning and design, and cites actual applications of noise elimination.

This book uses practical experience as the basis and at the same time incorporates domestic and foreign advanced technology reflecting the basis state of affairs of this branch of learning.

This paper is for the reference of acoustic and aerodynamics workers, scientific research, planning and factory and mine technical personnel and workers involved with the mechanical, metallurgical, construction petrochemical and defense industries and personnel in environmental protection, work safety, and industrial hygiene.

Foreword

Following modern industrial development, machinery has become more powerful, the rotation speed has become faster, and the noise they produce also has become stronger. Noise makes people uncomfortable, and affects their work and rest. It is commonly said that nine out of ten riveters are deaf. This suggests the hearing of workers is affected with long-term exposure to noise. Noise can also affect the general health and cause high blood pressure and heart disease. By diverting one's concentration, it is often the cause of various accidents. Furthermore, under very strong noise, sensitive instruments will malfunction, causing the failure of rockets and spacecraft. Therefore, noise has recently been recognized as an international public hazard. How to combat noise becomes an important concern.

This book mainly discusses aerodynamic noise and sound suppressors. Aerodynamic noise is one of three major types of noise. It is also the one most commonly encountered and most serious in causing damage. Among the sources of aerodynamic noise, there are exhausts from automobiles and tractors, supersonic jet airplanes, air conditioners in modern buildings, air exchangers used in mining, blowers, air compressors, turbines, and internal combustion engines. Chapter 1 introduces the fundamentals of sound waves and noise; Chapter 2 analyzes the mechanisms of aerodynamic noise formation and introduces the noise characteristics of typical aerodynamic equipment; Chapter 3 studies aerodynamic noise control -- the fundamentals and

calculations of various sound suppressors; Chapter 4 discusses the actual applications of sound suppressors.

I would like to thank Ma Ta-You of the Physics Institute, Chinese Science Academy for much advice, Sun Cha-Chi of the Peijing Science Institute for his useful help and his writing of several sections, and other colleagues at the Peijing Science Institute for their leadership and support.

CHAPTER 1. FUNDAMENTALS OF SOUND WAVE AND NOISE

I-1.   Vibrations, Sound Wave and Noises

I-1-1.   Vibrations and Sound Waves

There are all kinds of sound at all hours in our environment, e.g., people talking, wind whistling, cars moving, machines rotating, ... In short, there is sound accompanying us at any time and in any situation. With such a close relationship with sound, we are very much interested in knowing the nature of sound, its character, its production and propagation, as well as its measurement.

When we hit a drum with a hammer, we hear the drum sound. We will find at this moment vibrations of the drum's surface. If we press the surface to stop the vibrations, the sound then disappears. Therefore, it can be concluded that sound is produced from vibrations of certain materials.

Not only   solids can produce sound through vibrations; gases and liquids can do just the same. For example, the siren of the train is caused by the passage of steam through a horn, while the ocean wave produces sound from the vibrations of a liquid.

The sound produced by the vibration of a source can not be heard by us if there is no propagation medium. That is, sound can only propagate in a medium. For a clock enclosed in a glass jar, we can hear the ticking through the air. When the air is pumped away, the sound becomes weaker and weaker and eventually disappears--completely when vacuum is achieved. This clearly demonstrates that, without air, the sound can not be propagated.

However, without air, the sound can still propagate through liquid or solid. By putting our ears against the steel track, we can hear the approaching train at a far distance.

In short, vibrating bodies are sources of sound. Vibration in an elastic medium (gas, liquid and solid) propagates as a wave. This elastic wave is called the sound wave. For a certain frequency range, the sound wave affects human ears to cause a hearing sensation.

We can use Fig. 1.1 to explain the vibrations and the wave:
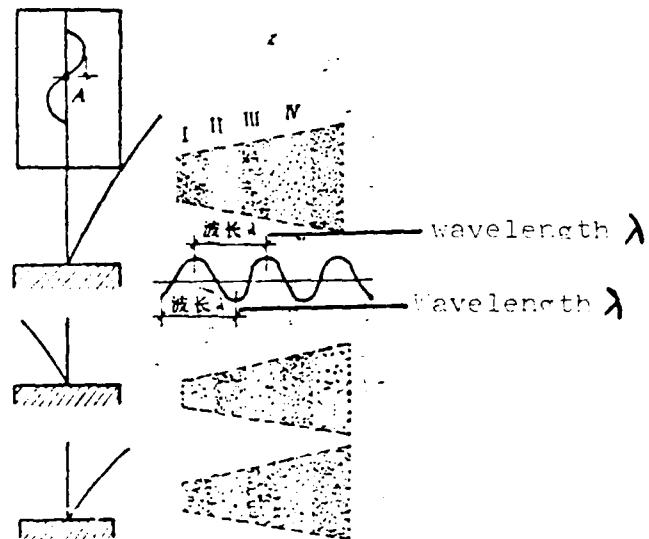
Fig. 1.1. Vibrations and Wave

If one strikes the end of a thin steel ruler, the ruler will oscillate back and forth. This regular oscillation is called vibration. When the ruler bends towards the right, the air to its right is compressed to form a condensation region I. This condensed region I will then compress its neighboring area on the right, II, thus causing the region II to become condensed. On the other hand, when the ruler bends towards the left, leaving an evacuated region on its right, the air of region I will rush into this evacuated region. As a result, the region I becomes less condensed to form a rarefaction region. At this moment

2

region II has become the condensed region. The air there continues to press towards the right, causing the region III to become condensed. When the ruler changes its direction towards the right again, the region I becomes condensed once more, while the region II becomes less condensed by compressing the region III to become condensed.

Due to the elasticity and inertia of the air, the vibrating steel ruler makes the air in its vicinity become more and less condensed alternately. This density modulation process propagates outward in the form of a sound wave with a well-defined velocity. Therefore, the sound wave is basically the result of the density change of the medium.

It should be noted that, while the sound wave propagates, air itself does not actually move along with it. Rather the air particles only oscillate around their equilibrium positions. The same situation occurs in water waves initiated by a stone dropped into the water; any material floating on the water surface only oscillates back and forth without moving away. This indicates that there is no net water flow. Only the water wave propagates.

As we know, the air pressure rises and drops as the density increases and decreases, respectively. Therefore, the propagating process as induced by the density change can also be viewed as that of propagating pressure. When this changing pressure enters human ears, causing the ear drums to vibrate, these signals are interpreted by the nervous system as sound.

As shown in Fig. 1.1., every time the steel ruler makes one complete vibration, air will be affected to form a high-low density wave component. The number of vibrations per second is called the frequency, f, and

its unit is Hertz (abbr. Hz). For human beings, only those vibrations with 20-20,000 Hz can cause a hearing sensation. The ultra-sound with frequencies higher than 20,000 Hz and the sub-sound with frequencies less than 20 Hz are not detectable by human ears.

The propagating speed of a sound wave in a medium is called the sound speed, as expressed by c with units of m/sec. At ambient temperatures (20°C) and under standard atmospheric pressure, the sound velocity in air is 344 m/sec. The sound velocity changes with changing temperatures. At 0°C, c=331.5 m/sec. At any temperature t°C,

$$c = 331.5 + 0.607t \ (m/sec), \tag{1.1}$$

i.e., the sound velocity increases by 0.607 m/sec for every 1°C increase in temperature.

The sound velocity varies with medium. In air it is 344 m/sec; in water, 1450 m/sec; and in steel, 5000 m/sec. Therefore, we can detect the approaching train by sound earlier through the steel rail than through the air.

In a sound wave the distance between two neighboring condensation regions or two neighboring rarefaction regions is called the wave length, λ, with units in m.

The wavelength λ, frequency f, and sound velocity c are three important quantities in the study of sound. They are related by

$$\lambda = \frac{c}{f}. \tag{1.2}$$

At ambient temperatures, if f=20 Hz, then λ= 17.2 m, and if f=20,000 Hz, λ=0.0172 m. Therefore, at ambient temperatures, human ears can detect sound waves with a wavelength range between 0.0172 and 17.2 m. Fig. 1.2 illustrates the relationship between the wavelength and frequency of sound waves at ambient temperature.

Wavelength (m)

```
          20   10    5      2    1   0.5           0.1  0.05
          |    |     |      |    |    |            |     |
     +----+----+-----+------+----+----+------------+-----+----+
     .10   20       5u    100  200   500  1000        5000 10000
```

Frequency (Hertz)
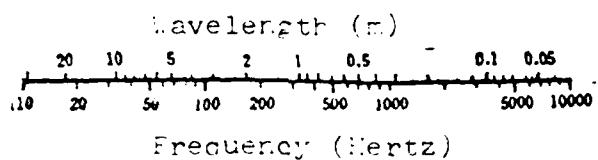
Figure 1.2 Relationship between wavelength and frequency of

a sound wave in air, under ambient temperature.

It is obvious that the wavelengths of a given frequency will be
different in different media.

1.1.2. Noise

What is noise? Noise is one kind of sound wave with all the
characteristics of sound waves.   From the physics viewpoint, noise refers
to sound without a regular pattern of intensity and frequency. However,
under a broader definition, any sound not required by people can be
categorized as noise. For example, piano sound is music. But to people
in sleep or reading it also becomes a form of disturbance.

According to its source,   noise can be basically categorized
into aerodynamic, mechanical, and electromagnetic noise. Aerodynamic
noise is induced by vibrations of gases. When a gas has an eddy current,
or has a sudden change in pressure, there will be noise caused by gas
vibrations. Typical examples include those from blowers, air conditioners,
air compressors, ejectors, jet airplanes, rockets, sirens and exhaust
gases. Mechanical noise is induced by the vibrations of solids.
Through collisions, friction , and transmissions under mechanical forces,
the sheet metals, ball bearings, and gears, etc., of machinery vibrate
to form mechanical noise. Electromagnetic noise is induced by the
changing magnetic field, which causes the electrical components in
generators or transformers to form noise.

According to frequency distributions, noise can be distinguished in terms of noise with or without a tune. A tuned noise has a clear fundamental frequency and its accompanying overtones. It is usually caused by rotating machinery (e.g., blowers). An untuned noise has no well defined fundamental frequency and overtones. A typical example is that caused by exhausting gases.

§ 1.2 Physical Parameters of Noise

Sound pressure (sound pressure level), sound intensity (sound intensity level), sound power (sound power level) and frequency (frequency band) are generally used as physical parameters of noise.

1.2.1. Sound Pressure, Sound Intensity, Sound Power

A sound wave induces oscillations of air particles, which lead to fluctuations in pressure. The variations from static pressure are called the sound pressure, P, with units in N/m^2. In general, sound pressure refers to the effective sound pressure (i.e., the root mean square value).

The threshold audible sound pressure for normal human ears is $2 \times 10^{-5} \ N/m^2$. The sound pressure in a typical room is $0.1 \ N/m^2$, a loud cry has a sound pressure of $0.5-1 \ N/m^2$, the noise from a weaving machine is $3 \ N/m^2$. Very strong noises from jack hammers and air blasters can reach $20 \ N/m^2$, and cause pain in human ears. The threshold sound pressure to cause such pain is $20 \ N/m^2$. When the pressure reaches several hundred N/m^2, it will damage the ear drum (bleeding).

Sound pressure is a common physical quantity for measuring the strength of a given sound. Most receivers (transmitters) respond to sound pressures.

Being one kind of waves, sound has a fixed energy. Therefore, we can also use energy to express the strength of sound propagation. This leads to two other physical quantities: the intensity and the power of sound.

Intensity of sound is measured as the energy passing through a unit area perpendicular to the propagation direction. It is generally expressed by I, with units in Watt/m^2.

The power of sound refers to the total energy delivered by the source in unit time. It is generally expressed by W, with units in watt.

The power W and the intensity I are related by the equation:

$$W = \oint_s I_n dS,$$ (1.3)

where S is the enclosed surface area around the source; I_n is the intensity component along the normal direction of a spherical surface.

In a free sound field (i.e., sound propagates freely without reflection), the sound propagates spherically:

$$I_{Spherical} = \frac{W}{4\pi r^2},$$ (1.4)

where r is the distance in m; and $I_{Spherical}$ is the average intensity in Watt/m^2 at the spherical surface.

If the source is located on the ground in an open area, the sound wave propagates only semi-spherically. Then,

$$I_{Semi-Sph.} = \frac{W}{2\pi r^2},$$ (1.5)

where $I_{Semi-Sph.}$ is the average intensity in watt/m^2 at the semi-spherical surface.

From equations (1.4) and (1.5), it can be seen that the power of a given sound source is a constant. At different points in space, intensities are different, and are inversely proportional to r^2, with r being the distance from the source.

In a free sound field, intensity is related to sound pressure.

$$I = \frac{P^2}{\rho c},\qquad (1.6)$$

where ρ is the density of the medium, c the speed of propagation, the product ρc the specific acoustic resistance of the medium to the sound propagation. For air, at 20^0C and under normal atmospherical pressure, ρc = 413 Rayls. The specific acoustic resistance changes with changing temperature and atmospherical pressure.

In a free sound field, sound power and sound pressure are related:

$$W = 4\pi r^2 \ P^2_{Spherical} \ \rho c \qquad (1.7)$$

where $P_{spherical}$ is the average sound pressure at the spherical surface.

In a hemispherical sound field, sound power and sound pressure are related:

$$W = \frac{2\pi r^2 P^2_{semi-sph.}}{\rho c} \qquad (1.8)$$

where $P_{semi-sph.}$ is the average sound pressure at the hemi-spherical surface.

From the audible region to the threshold of pain, the intensity ranges from 10^{-12} to 1 Watt/m^2.

1.2.2. Level and Decibel

Between the audible region and the threshold of pain, the sound pressure ratio is 10^6:1, i.e., different by one million times. The intensity ratio is 10^{12}:1. It is obvious that it is not practical to use either sound pressure or intensity to express the magnitude of sound energy. Therefore, logarithmic ratios -- levels are introduced. They are sound pressure levels, sound intensity levels and sound power

8

levels. This is the same approach as   in expressing the level
of   wind or an earthquake.

Their mathematical definitions are:

Sound pressure level:

$$L_P = 20 \log (P/P_0) \qquad \text{(decibel)}, \qquad (1.9)$$

with $P_0 = 2 \times 10^{-5}$ N/m^2 as the reference sound pressure.

Sound intensity level:

$$L_I = 10 \log (I/I_0) \qquad \text{(decibel)}, \qquad (1.10)$$

with $I_0 = 10^{-12}$ watt/m^2 as the reference sound intensity.

Sound power level:

$$L_W = 10 \log (W/W_0) \qquad \text{(decibel)}, \qquad (1.11)$$

with $W_0 = 10^{-12}$ watt as the reference sound power.

P_0 and I_0 are, respectively, the audible sound pressure at 1000 Hz
and its corresponding sound intensity. By taking the logarithmic ratio
of P/P_0 and multiplying it by 20, one obtains the sound pressure level
of P. By taking the logarithmic ratio of I/I_0 and multiplying it by
10, one obtains the sound intensity level of I.

The unit of sound pressure level, sound intensity level, and sound
power level is the decibel. This dimensionless unit for levels was first
introduced in electrical engineering. In the latter, the logarithmic
ratio of two power values is often used to express the gain of an
amplifier or the signal-to-noise ratio. Such a unit is called a Bel.
A decibel (db) is one-tenth of a Bel. Therefore, the decibel is the unit of
the logarithmic ratio of two power values, multiplied by 10. For a
network with input power W_1 and output power W_2, the amplification of

the network is $\log(W_2/W_1)$ in Bel, and $10 \log(W_2/W_1)$ in db. When $W_1=0.1$ microwatt, $W_2=1$ microwatt the power gain is

$$10 \log(1/0.1) = 10 \text{ db}$$

When $W_1=1$ watt and $W_2=10$ watt, the power gain is still 10 db:

$$10 \log(10/1) = 10 \text{ db}$$

It is clear then that the gain as expressed in db does not represent the actual power or the values of either input or output powers. Instead, it only indicates the ratio between the output and the input power. On the other hand, 10 db in gain means an increase of 10 to 1, the gain of 20 db means an increase of 100 to 1, and that of 30 db means an increase of 1000 to 1....

In electricity, when the resistance is constant, the power ratio is equal to the square of the voltage ratio:

$$W_2/W_1 = (V_2/V_1)^2$$

where V_2 and V_1 are output voltage and input voltage, respectively. Therefore,

$$10 \log(W_2/W_1) = 10 \log(V_2/V_1)^2 = 20 \log(V_2/V_1).$$

In acoustics, sound power and sound pressure correspond to the electrical power and voltage, respectively:

$$L_W = 10 \log(W_2/W_1) \qquad (db), \qquad (1.12)$$

$$L_P = 10 \log(P_2/P_1)^2 = 20 \log(P_2/P_1) \qquad (db). \qquad (1.13)$$

By replacing W_1 by the reference value W_0 and replacing W_2 by the measured W, Equation (1.12) then becomes Equation (1.11). Similarly, by replacing P_1 by P_0 and P_2 by P, Equation (1.13) changes to Equation (1.9).

From the audible region to the threshold of pain, the sound pressure change is 2×10^{-5}-20 N/m^2 and the sound intensity change is

10^{-12}-1 watt/m^2. By substituting them into Equations (1.9) and (1.10), the changes in sound pressure level and sound intensity level are both 0-120 db.

Figure 3 shows the curves for converting sound pressure, sound intensity, and sound power to sound pressure level, sound intensity level, and sound power level, respectively.

It is clear that, by introducing the concept of levels, one can reduce the order of magnitude in changes in sound pressure or sound intensity and power from 10^6 or 10^{12} to 0-120. (Even with a sound pressure of several hundred N/m^2 beyond the threshold of pain, and a sound power of ten-thousand watt, from the strong noise of a jet airplane, the sound pressure level is still only 140-150 db and sound power level is 160 db). Consequently, this convenient and logical way of expression has been widely accepted.

Since the decibel is a logarithmic unit, it can not be calculated using simple arithmatic. One has to follow the logarithmic operations.
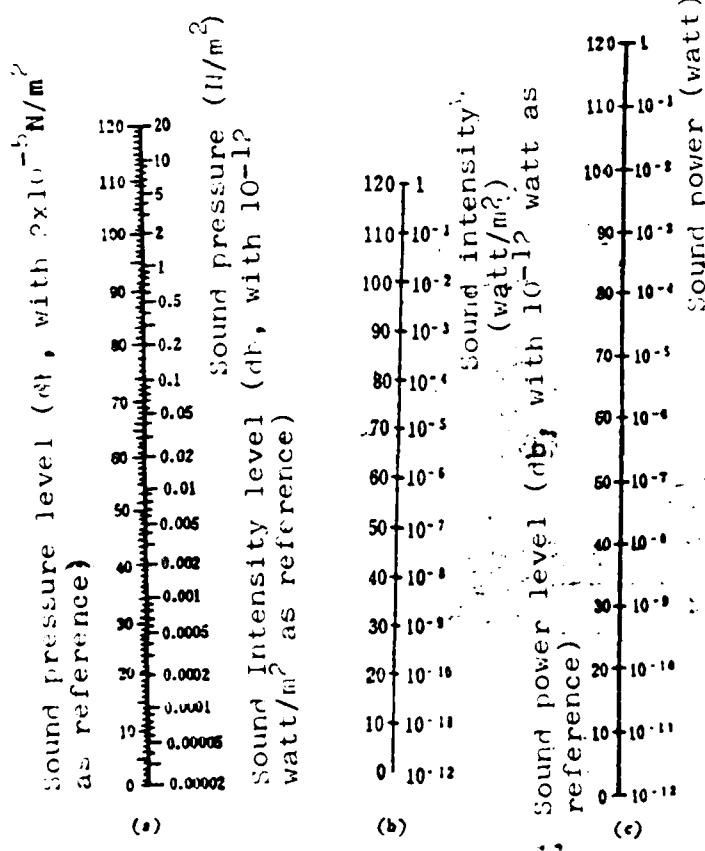
Figure 1.3
Conversion curves for
sound levels

The addition of decibels: The addition of one sound with 90 db to another with 88 db does not equal 178 db. Rather, from Fig. 1.4 or Table 1.1, one finds first the increment $\Delta L = 2.1$ db corresponding to the difference $L_I - L_{II} = 90-88=2$ db; then add this ΔL to the higher L_I value to obtain $L_{Total} = 90+2.1 = 92.1$ db. For adding several decibel together, one should follow this procedure step by step.
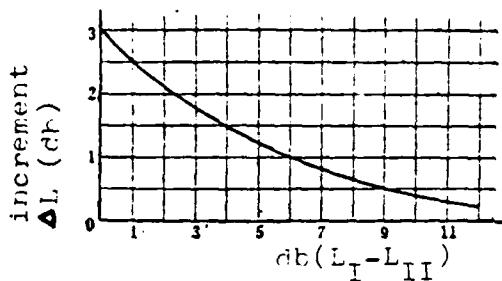
Fig. 1.4 The Increment of Decibel Additions

Table 1.1 The Increment of Decibel Additions

Level difference $L_I - L_{II}$
between I and II $\longrightarrow$

Level increment $\Delta L(db)$ $\longrightarrow$
beyond the higher level
between I and II

I 和 II 的级差 $L_I - L_{II}$	0	1	2	3	4	5	6	7	8	9	10
向 I 或 II 中较高的级的增值 ΔL（分贝）	3.0	2.5	2.1	1.8	1.5	1.2	1.0	0.6	0.6	0.5	0.4

The same procedure should be used to calculate the average of n decibel values, by adding the decibels of all sound components together, and subtracting 10 log n from the summation.

For example, to determine the average value of 95, 93, 90, and 88 db, we can use Fig. 1.4: the sum of 95 and 93 db is 97.1 db; 97.1 and 90 db is 97.9 db; 97.9 and 88 db is 98.3 db; finally, with 10 log 4 = 6, 98.3 − 6 = 92.3 db. The integer decibel value would then be 92.

To let the readers have more direct feeling on levels and decibels, Fig. 1.2 lists the sound power level of several commonly encountered noise sources.

Table 1.2   Sound Power Level of Several Common
Sound Sources

Sound Source	Sound Power Level (decibel)	Sound Power (Watt)
whisper	30	10^{-9}
small electric clock	40	10^{-8}
normal conversation	70	10^{-5}
illegible	100	10^{-2}
blower (large size)	110	0.1
illegible	120	1
	140-150	100-1000
jet airplane	160	10000

1.2.3.   Frequency Band

Audible sound has a frequency range between 20 and 20000 Hz. The two extremes represent a variation of 1000 in ratio. For convenience, we divide the broad frequency range into several sub-groups. They are so-called frequency bands.

In noise measurements the most commonly used bands are based on the ratios of 2 or 1/3.

The band with a ratio of 2 refers to the case where the two extreme frequencies are 2:1.

The central frequencies of commonly used bands of this type are 31.5, 63, 125, 250, 500, 1000, 2000, 4000, 8000, and 16000 Hz. If the central frequency of a given band is f_c, and the upper and lower limiting frequencies are f_u and f_1, then $f_c = \sqrt{f_u \cdot f_1}$, $f_u = \sqrt{2} f_c$, $f_1 = \frac{1}{\sqrt{2}} f_c$, and $f_u = 2f_1$.

The ten frequency bands mentioned above can cover the whole
audible sound range. It makes the measurements simpler. In fact,
in noise control and field measurements, one needs only eight bands
covering 63 - 8000 Hz. This is shown in Table 1.3.

Table 1.3 Octave Frequency Bandwidths (IEC)[1]

Central
  frequency(Hz)
Frequency range
  (Hz)

中心频率(赫)	63	125	250	500	1 k	2 k	4 k	8 k
频率范围(赫)	45—90	90—180	180—355	355—710	710—1400	1400—2800	2800—5600	5600—11200

1) IEC 为国际电工委员会的缩写.

1) IEC is abbr. of International Electrical Engineering Committee

In order to obtain the more detailed frequency spectra, one can
use half-octave or third-octave bands. This is to subdivide a given
frequency band into two or three sections. The central frequencies
of the half-octave bands are: 31.5, 45, 63, 90, 125, 180, 250, 355,
500, 710, 1000, 1400, 2000, 2800, 4000, 5600, 8000, 11200, 16000 Hz;
those of the third-octave bands are: 40, 50, 63, 80, 100, 125, 160, 200,
250, 320, 400, 500, 630, 800, 1000, 1250, 1600, 2000, 2500, 3200, 4000,
5000, 6300, 8000, 10000, 12500, 16000 Hz.

Using the frequency (frequency band) as abscissa, and sound
pressure level (sound intensity level, sound power level) as ordinate,
a noise analysis diagram can be drawn. It provides information on the
components and characteristics of the noise. This is called
frequency spectral analysis. Fig. 1.5 shows the noise frequency spectra
of a 1-n018 type air compressor.

Fig. 1.6 indicates the noise frequency spectra of a D800-21
centrifugal fan .

Fig. 1.7 shows the noise frequency spectra for a K-350-01-1
turbine compressor.

14

Octave sound pressure level (db)

Frequency (Hz)

Fig. 1.5 1-nO18 Type Air Compressor -- Noise Frequency Spectra

Third-octave sound pressure level (db)
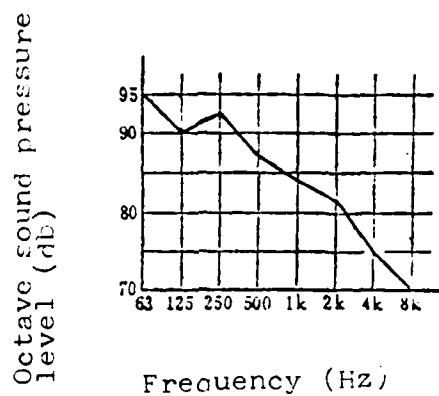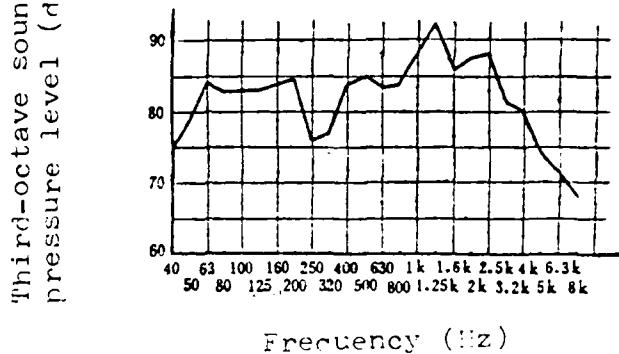
Frequency (Hz)

Fig. 1.6 DS00-21 Centrifugal Fan -- Noise Frequency Spectra

Sound pressure level (db)
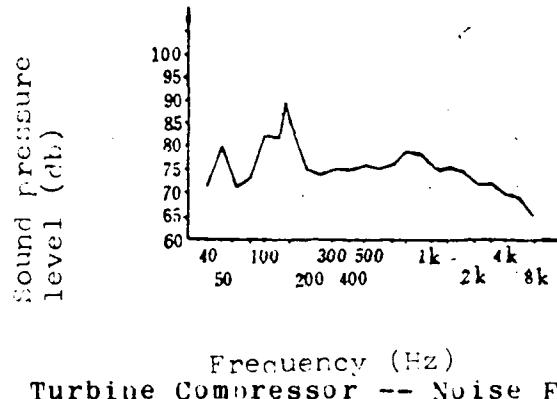
Frequency (Hz)

Fig. 1.7 K-350-01-1 Turbine Compressor -- Noise Frequency Spectra

15

§ 1.3 Propagation of Sound Wave

1.3.1 Reflection, Refraction, Diffraction and Interference of Sound Waves

When a sound wave reaches an obstacle, reflection may occur. The conditions for reflection depend on the wavelength of the sound and the dimensions of the obstacle as well as the smoothness of its surface. When the wavelength is shorter than the dimension of the obstacle, the sound can easily be reflected. When the wavelength is greater than the dimensions of the roughness of the surface, the surface will lead to regular reflections. If the wavelength is about the same as or shorter than the dimensions of the roughness of the surface, the sound wave will end in a diffuse reflection. Since the wavelength of noise ranges from several cm to more than 10 m, the reflection of noise is rather complicated.

The ratio between the reflected sound energy and the incident sound energy is called the reflection coefficient. From a medium with specific acoustic resistance $\rho_1 c_1$ into another medium with $\rho_2 c_2$, the reflection coefficient r_0 of a normal incident sound wave is

$$r_0 = \left(\frac{\rho_1 c_1 - \rho_2 c_2}{\rho_1 c_1 + \rho_2 c_2}\right)^2. \tag{1.14}$$

Table 1.4 lists the specific acoustic resistance of several common media. The negligibly small air resistance (413 Rayls) in comparison with that of steel (390×10^5 Rayls) indicates that a steel plate can practically reflect sound energy completely.

16

Table 1.4 Specific Resistance of Several Media

Media	Sound Velocity (m/s)	Density (kg/m³)	Specific Resistance (kg/m²-s) (Rayl)
Air	344	1.20	413
Water	1450	1000	145×10^4
Steel	5000	7800	390×10^5
Glass	4900-5800	2500-5900	$130 - 340 \times 10^5$
Aluminum	5100	2700	130×10^5

A sound wave can also be refracted when it encounters an interface with different specific acoustic resistance.

In the refraction of sound wave, the propagation direction changes, as shown in Fig. 1.8. The relation between the incident angle θ_1 and the refracted angle θ_2 is

$$\sin \theta_1 / \sin \theta_2 = c_1 / c_2 . \tag{1.15}$$

When a temperature gradient exists, ρ and c vary accordingly, leading to the refraction of sound waves. Similarly, with a wind gradient, refraction of sound waves can also occur.

When sound waves encounter obstacles, openings or holes with dimensions much smaller than the wavelength, diffraction occurs, as shown in Fig. 1.9. Low frequency sound waves have wavelengths up to several meters: diffraction occurs easily.

Fig. 1.8 Refraction of Sound Waves

small hole ——————— 小孔   小屏障 —— small obstacle

large hole ———————— 大孔   大屏障 ———— large obstacle
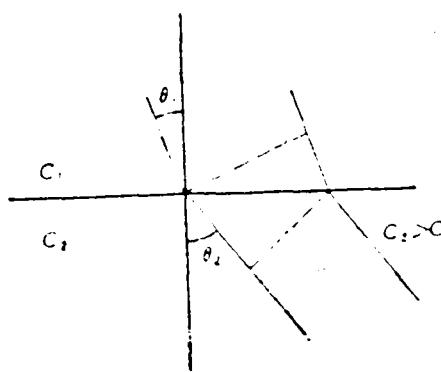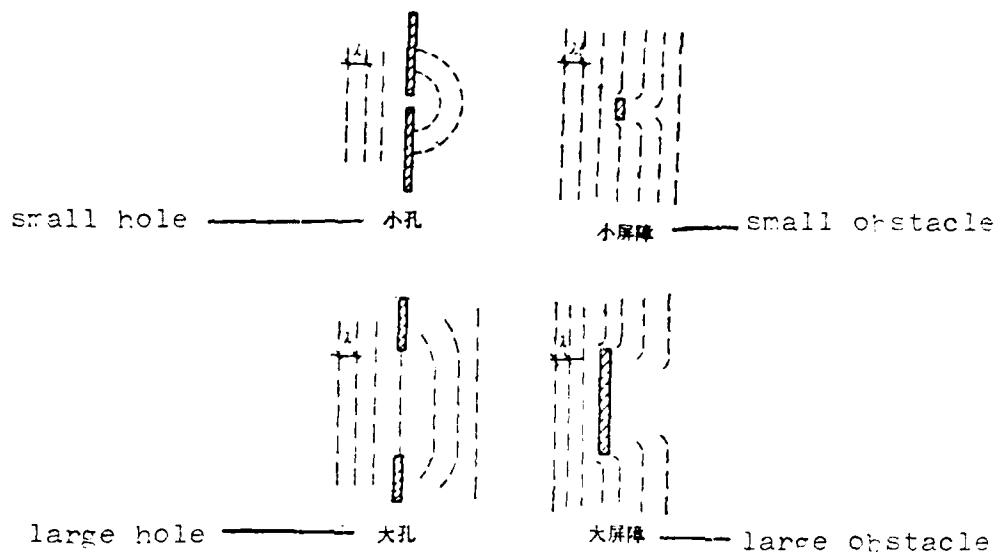
Fig. 1.9 Diffraction of Sound Waves

Sound waves can also superimpose   during propagation. This phenomenon is called interference of sound waves.

When two sound waves with the same frequency arrive at a point in phase, i.e., they cause identical disturbance at that point, the two waves then reinforce each other. The resulting amplitude is the sum of the two individual amplitudes (see Fig. 1.10(a)); if the two waves are out of phase, then they destroy each other partially or completely. The resulting amplitude is the difference of the two individual amplitudes (see Fig. 1.10(b)).

(a)   (b)
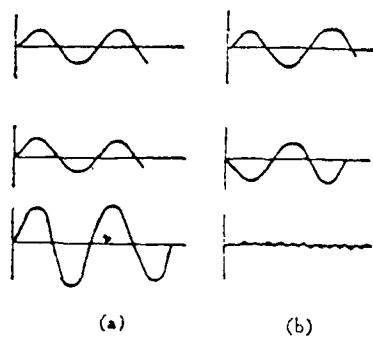
Fig. 1.10 Interference of Sound Waves

18

1.3.2 Attenuation of Sound Waves

If the dimensions of a sound source are much smaller than the distance between the point of measurements and this source, the source can be considered as a point source. A point source produces a spherical wave with its sound pressure value inversely proportional to the distance between the source and the point of measurements (see Eq. (1.7) and (1.8)). As expressed in decibels:

$$L_P = L_W - 20 \log r - k \text{ (db)}, \tag{1.16}$$

where K is a correction factor; in free space, k = 11; in a semi-free space, k = 8.

The difference in sound pressure levels at distance r_1 and r_2 is

$$L_{P_{(r_1)}} - L_{P_{(r_2)}} = 20 \log(r_2/r_1). \tag{1.17}$$

When $r_2/r_1 = 2$, the level decrease is 6 db, i.e., it diminishes by 6 db when the distance doubles. When $r_2/r_1 = 10$, the level decreases by 20 db; when $r_2/r_1 = 100$, the level decreases by 40 db.

If the sound source is a line source, then

$$L_{P_{(r_1)}} - L_{P_{(r_2)}} = 10 \log (r_2 / r_1). \tag{1.18}$$

In this case, the level decreases by 3 db when the distance doubles.

This phenomenon is referred to as the divergence decrease of sound wave due to distance.

During the propagation of sound waves, the absorption by air (caused by the viscosity and heat transfer of air, damping effect of the air molecules' rotational motion) can also cause the sound waves to diminish. As indicated in Table 1.5, the magnitude of this effect depends on the frequency of the sound wave, the air temperature, and the humidity.

19

Table 1.5 Sound wave attenuations (dt/100 m)[1] due

to air absorptions

频率(赫) a	温度(℃) b	c 相 对 湿 度 (%)			
		30	50	70	90
500	−10	0.56	0.32	0.22	0.18
	0	0.28	0.19	0.17	0.16
	10	0.22	0.18	0.16	0.15
	20	0.21	0.18	0.16	0.14
1000	−10	1.53	1.07	0.75	0.57
	0	0.96	0.55	0.42	0.38
	10	0.59	0.45	0.40	0.36
	20	0.51	0.42	0.38	0.34
2000	−10	2.61	3.07	2.55	1.95
	0	3.23	1.89	1.32	1.03
	10	1.96	1.17	0.97	0.89
	20	1.29	1.04	0.92	0.84
4000	−10	3.36	5.53	6.28	6.05
	0	7.70	6.34	4.45	3.43
	10	6.58	3.85	2.76	2.28
	20	4.12	2.65	2.31	2.14
6000	−10	4.11	6.60	8.82	9.48
	0	10.54	11.34	8.90	6.84
	10	12.71	7.73	5.47	4.30
	20	8.27	4.67	3.97	3.63

Key:

a. Frequency (Hz)

b. Temperature (℃)

c. Relative humidity ( )

It is obvious from Table 1.5 that the attenuation is more pronounced for high frequency than for low frequency sound. Therefore, even though airplanes produce strong noise in high, medium and low frequencies, we hear only low frequency noise from a distance because of the effective diminishing effect of the high frequency noise through the air. The closer the airplane is to us, the more the contribution to the noise is from the high frequency components.

In a conduit, the sound wave can be greatly reduced when it encounters sound suppressors.

§ 1.4 The Effect of Noise on Human Bodies and Subjective Evaluation of Noise

1.4.1 The Effect of Noise on Human Bodies

Noise affects health adversely. High noise level (e.g., above 90 decibel (A)) conditions can produce annoyance and discomfort. Continuing exposure to these conditions leads to loss of hearing sensitivity, and sometimes, to deafness. Medical surveys on workers in different industries showed that among several groups (e.g., textile workers, riveters, and generator workers, etc.) hearing loss can reach 50 - 60%, or even 80-90%, if there are no control measures.

Sudden exposure to very intense noises (as high as 150 decibel) can cause severe physical injuries, such as bleeding and rupture of the ear drums, bleeding of Scala Media, and detachment of Helicotrema, and leads to deafness, nausea, vertigo, speech incoherence, concussion, coma and shock. In fact, moderately high levels of noise can already affect the central nervous system - loss of equilibrium between excitation and inhibition of cerebral cortex leads to abnormal conditioned reflexes, disturbance of normal daily activities, irritation and annoyance, and

loss of concentration. Also, people reach a fatigued state much more readily even though no hard physical labor is performed. Since noise acts on the cerebral cortex, industrial workers often lose concentration, and reflexes slow down. Under those conditions, defective products, bodily injuries, and lowered productivity are very common.

Noise probably also affects brain vascular tensions, causing dissolution of neural chromosomes, deformed nuclei, twisting of dendrites, and infiltration of axons. If these physiological changes are not allowed to recover in time, sustained excitation of axons may progress to the involuntary nervous system resulting in pathological conditions. Headache, dizziness, ringing in the ears, nightmares, insomnia, fatigue, and lethargy are often the accompanying clinical symptoms. Health workers found 60-70% of workers in the high noise level factory environment have nervous system related diseases.

The gastrointestinal system can also be affected: abnormal digestive juice secretion, decreased gastric acidity, loss of stomach wall muscle contraction, indigestion, decrease of appetite, ulcers, and other digestive diseases.

Noise also affects endocrine functions: stimulation of adrenal glands, anterior pituitary acidophil increase, excess secretion of pituitary stimulating hormones, and inhibition of sex glands. Female workers' sex gland functions cause erratic menstrual irregularities, and increased abortion risk may also be associated with noise.

In recent years, research on the effects of noise on the cardiovascular system showed that it stimulates the sympathetic nervous system; increases heart rate; disturbs cardiac rhythm; slows down ST-T wave of EKG and increases blood pressure. Under intense noise, the rate of hypertension

is increased many fold compared to no noise condition, clearly illustrating the effect of noise on the cardiovascular system. Noises also affect the involuntary nervous system, causing vasoconstriction, cardiac output decrease, diastolic pressure increase, insufficient perfusion of ventricles, and heart muscle damage . The consensus among the medical professionals is that noise may cause coronary diseases and arteriosclerosis.

Noise can cause blood composition changes too, increasing white cell counts, lymphocyte counts and blood sugar levels. Therefore, under long term exposure to noise, the general level of health is decreased. Even if there are no outright occupational diseases, noise can lead to other associated pathological conditions.

1.4.2 Subjective Evaluations of Noises

In Section 1.2 it has been mentioned that sound pressure and sound pressure level are used as physical parameters for noise. The higher the sound pressure, the stronger the sound; the lower the sound pressure, the weaker the sound. However, the sensation towards sound for a human being's ears depends not only on sound pressure, but also on frequency. Generally it is more sensitive to higher frequencies than to lower frequencies. The hearing sensation is different if frequency is different, even though the sound pressure remains the same. For example, with the same 90 decibel in noise sound pressure level for both K-250 air compressor and small sedans, the former appears to be much louder. It can irritate so much that one can hardly stand it, while the latter does not seem to be loud at all. Therefore, sound pressure level (decibel) can only represent the strength of noise physics.

Based on this characteristic , we introduce a concept for loudness
similar to that for sound pressure level. That is, by taking a 1000 Hz
pure sound as reference sound, any sound with the same effect on hearing
has a loudness value (phon) equal to the sound pressure level (decibel)
of this pure sound. If the noise and the sound pressure level are 100
decibel, and the loudness is the same as that of a reference sound with
frequency 1000 Hz, then the loudness level of the noise is 100 phon.

The loudness level represents the magnitude of the loudness of a
given sound. It unifies the sound pressure level and the frequency into
one unit. Not only does it take into   account the physical effect of a sound,
it also considers the physiological effect of the sound to a human being's
hearing. It is a basic quantity in a subjective evaluation of noise.
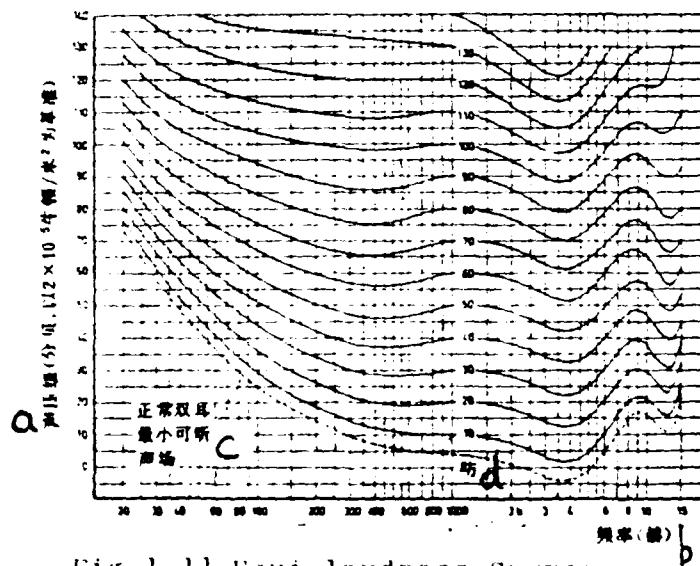
Fig 1.11 Equi-loudness Curves

Key:

a.   ... pressure .... , ... reference

b.   ....

c.   ... ...

d.   ... .

24
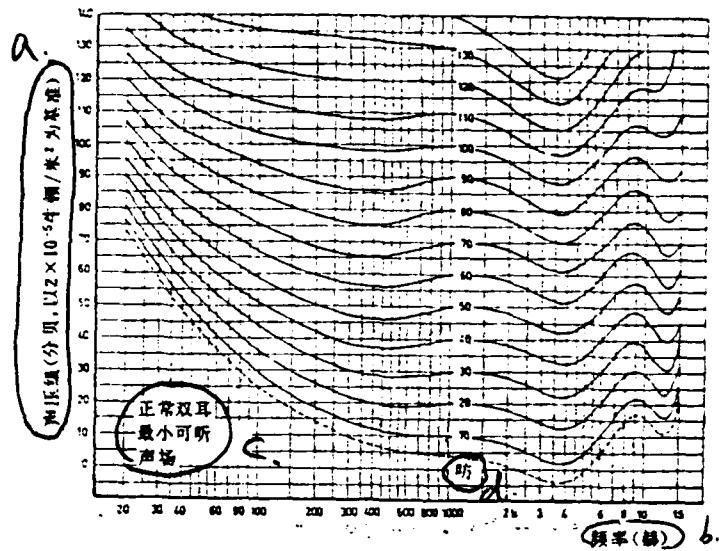
Fig 1.11 Equi-loudness curves

a. sound pressure level (db, 2×10^{-5} N/m^2 as reference)

b. frequency (Hz)

c. Minimum audible sound field for normal ears

d. phon

Using the method based on comparisons with the reference sound, one can obtain the loudness level of a pure tone in the entire audible range. The equi-loudness curves in Figure 1.11 are determined from many experiments. Each curve in the group corresponds to a sound of certain loudness level (phon). Zero phon corresponds to an equi-loudness curve of 2×10^{-5} N/m^2 at 1000 Hz. The lowest audible field is 4 phon.

25

It can be seen from the equi-loudness curves:

1. Human ears are most sensitive to sound with high frequencies, particularly between 3000-4000 Hz, but not sensitive to low frequencies, particularly less than 100 Hz. For the same loudness level of 50 phon, the sound pressure level is 50 db for a sound of 1000 Hz; 42 db for 3000-4000 Hz, 59 db for 100 Hz, and 75 db for 40 Hz. They are all on the same 50-phon curve.

2. When the sound pressure level and frequency are low for a certain sound, the sound pressure level (db) and loudness level (db) are quite different. For example, with a sound pressure level of 50 db, a sound with an ultra-low frequency of 30 Hz is not audible (below the audible region curve), its loudness level is not yet zero phon. For the same 50 db sound pressure level, the loudness level is 25 phon for a 60-Hz sound, 34 phon for a 500-Hz sound, and 50 phon for a 1000-Hz sound.

3. When the sound pressure level reaches beyond 100 db, the equi-loudness curves have gradually levelled off. This indicates that, when the loudness of sound reaches a certain level (higher than 100 db), human ears can no longer distinguish high frequency sounds from low frequency ones. The loudness of a sound depends only on its sound pressure level, and is independent of its frequency.

The equi-loudness curves in Figure 1.11 are introduced by Robinson and Dadson. They have been approved by the 43rd Technical Committee of the International Standards Organization (ISO). Therefore, they are also called the ISO equi-loudness curves.

Loudness levels are relative quantities. Sometimes they need to be converted into natural numbers, i.e., to be expressed in absolute quantities. This leads to the concept of loudness, with its unit the sone.

26

Loudness is the quantity describing the strength of a sound as judged by the hearing sensation. It is directly proportional to a normal person's subjective feeling towards sound. One sone is equal to 40 phon. Every 10-phon increase in loudness level, the loudness doubles. For example, 50 phon is equivalent to 2 sone, 60 phon to 4 sone, etc. This can be expressed as

$$S = 2^{(L_S - 40)/10} \tag{1.19}$$

or

$$L_S = 40 + 10 \log_2 S, \tag{1.20}$$

where S--Loudness (sone); L_S-- loudness level (phon).

This is shown graphically in Figure 1.12.

It is relatively direct to express the degree of noise in terms of loudness, which can be used to calculate directly the percentage increase or decrease of the loudness. For example, a noise has a loudness level of 120 phon, and loudness of 250 sone. After being treated for sound suppression, the loudness level drops to 90 phon and loudness to 32 sone. That is, the total loudness decreases by

$$(250-32)/250 = 87\% .$$

According to the equi-loudness curves, sound measurement equipment often has three built-in weighting networks. They allow different degrees in wave filtering for the incident sound. Weighting network-A simulates the loudness of a pure tone of 40 phon to human ears. When a signal passes through, it attenuates significantly the low and medium range frequencies (less than 1000 Hz). Weighting network-B simulates the reaction of human ears to pure tones of 70 phon. It attenuates the low frequency band of a signal. Weighting network-C simulates the reaction of human ears to pure tones of 100 phon. It has practically the same

effect on the whole audible sound range. Network-A makes a
given sound measurement device sensitive to high frequencies,
but not to low frequencies. This is similar to human ears'
sensation towards noises. Therefore, the level of noise as
measured by network-A is closer to the actual feeling of human
ears. In recent years, in noise measurements and evaluations, the sound level as determined by the network-A is used to represent the degree of noise, called the A-sound level and expressed in db(A) or dBA. There are conversion relationships between the A-sound level and many other noise evaluation quantities. Therefore, the evaluation method for A-sound levels becomes more and more important in noise evaluations.

Table 1.6 lists the A-sound level of several common types of sound.

Noises also interfere conversations (including telephone calls). In situations with relatively high degree of noise, conversation becomes strenuous, and one can even

phon sone
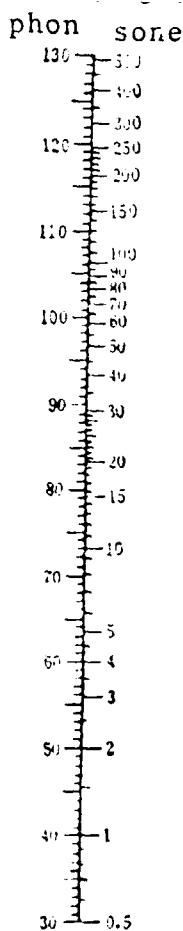
Figure 1.12

Relationship between
loudness level and
loudness

28

hardly hear the other person. However, higher sound pressure level or loudness level does not necessarily cause more interference to conversations. This is because of the fact that conversation sound is mainly confined to three octave bands with center frequencies at 500 Hz, 1000 Hz and 2000 Hz. Noises below 200 Hz or above 7000 Hz, even though with somewhat high sound pressure level and loudness level, do not induce serious interference to conversations. Consequently, speaking-interference-level (SIL) is defined as the average value of the sound pressure levels of the three octave bands -- 500 Hz, 1000 Hz and 2000 Hz. If SIL is less than 60 db, there is no appreciable effect on normal conversations or phone calls. Between 60 and 75 db, conversations and phone calls become somewhat difficult. Above 75 db, it is almost impossible to make phone calls.

In recent years, for airplane noises, another new subjective evaluation parameter is introduced -- perception noise level and degree of noise. The unit for perception noise level is PNdb, equivalent to the loudness level. The unit of degree of noise is NOYS , equivalent to the loudness. They are different from the loudness level and loudness in that they are based on composite sound, while the loudness level and loudness are based on pure tone or frequency-band sound.

Figure 1.13 shows equi-degree of noise curves.

Figure 1.14 shows the relationship curves between the degree of noise(NOYS) and the perception noise level.

Table 1.6 A-sound levels of several common sound sources (distance between sound source and point of measurement: 1-1.5 m)

A-sound level (db (A))	Sound source
20-30	whisper, broadcast room
40-60	common indoor noise
60-70	common conversation, small air conditioner
80	loud discussion, radio, relatively noisy street
90	heavy loaded car, air compressor station, Pumping station, noisy street
100-110	weaver, electric saw, sander, large blower
110-120	jack hammer, ball grinder, diesel generator
120-130	air riveter, propeller airplane
130-150	high-pressure large-volume exhaust, wind tunnel, jet airplane, ground-to-air cannon
above 160	rocket, Airship, missile

Recently, another evaluation method for airplane noises has been introduced internationally, called the effective perception noise level EPNL. It is developed from the basis of perception noise level. Not only does it consider the frequency characteristics of noises, it also considers the continuous time span of the noise effect as well as the individual components in the frequency spectrum. Furthermore, for calculations related to other evaluation methods, e.g., the aeronautic noise

30

index NNI, the equi-effect continuous perception noise level
ECPNL, etc., one can read the literature references (2-5).
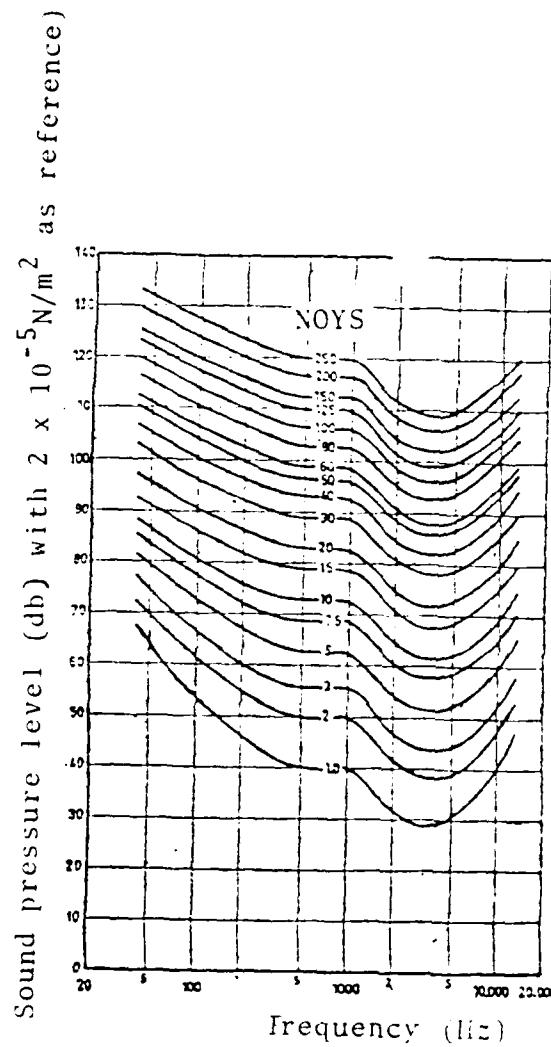
Figure 1.13   Equi-degree curves of noises
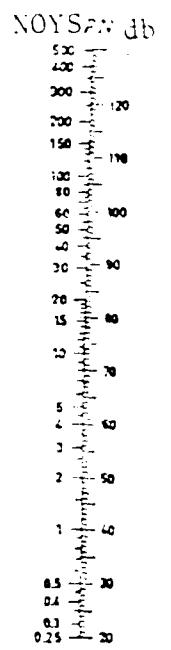
Figure 1.14
Relationship curves
between the degree
of noises (Na) and
the perception noise
level (PN db)

31

§ 1.5   Noise Measurements

1.5.1   Noise Measurement Equipment

Commonly used noise measurement equipment includes sound
level meters, frequency spectrometers, automatic recorders,
magnetic tape recorders, etc.   This section introduces briefly
the characteristics and method of applications of this   equip-
ment.

1. Sound level meters: Sound level meters are the most
common and simplest noise measurement equipment.   With small
volume and light weight, they can easily be carried around.
Not only they can be used individually for sound level measure-
ments, they can also be used along with matching devices or
peripheral equipment   for spectroscopic analysis, vibration
measurements, etc. Examples include the Model SJ-1 general
sound level meters manufactured by the Peijing Radio Factory,
No. II; the Model ND1 precision sound level meters manufactured
by the Kiang-Si Red Sound Equipment Factory; and the Model 2203
precision sound level meters manufactured by the Denmark B & K Co.
Their appearances are shown in Figure 1.15.

Sound level meters are composed of sound transmitters,
amplifiers, sound attenuators, frequency weighting networks,
and effective value indicators.

Figure 1.16 is a block diagram for the sound level meters.

The working principles of sound level meters are: A sound
pressure signal passing through the sound transmitter is converted

32

into an electrical voltage signal, which is fed into the amplifier
to become an electrical signal with a certain power rating. By
further passing through a weighting network with a certain
frequency response, followed by wave rectifying, the signal will
move the indicator in terms of a decibel scale.

Sound transmitters are also called microphones. They are
acoustic-electrical converters. According to the conversion
principles and structures, they can be categorized into three
types: electromotive sound transmitters, piezoelectric electrical
microphones, and condenser microphones.

Electromotive microphones are also called moving-coil
microphones. They are based on the electrical voltage output
induced by the motion of a conductor in a magnetic field. They
are relatively large in size, low in sensitivity, susceptible
to electromagnetic field interference, non-linear in frequency
response, and greatly attenuated at low frequency ranges. However,
they have low background noise   and can work at high temperatures.
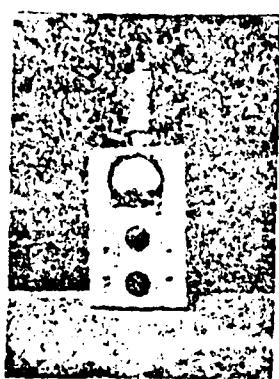
(a) Model SJ-1 general
   sound level meter--
   Peijing

(b) Model ND 1 Precision
   sound level meter--
   Kiang-Si

(c) Model 2203
   Precision sound
   level meter--
   Denmark

Figure 1.15 Appearances of sound level meters

a. microphone b. amplifier   c. attenuator d. weighting networks
e. wave analyzer f. indicator
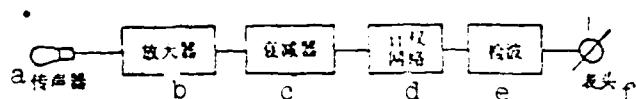
Figure 1.16 Block diagram of a sound level meter

Piezoelectric microphones are also called crystal microphones. They are energy converters based on the electrical voltage output induced by the strain of crystals with piezoelectric characteristics (e.g., Rochelle salt, ammonium dihydrogen phosphate, etc.). Microphones of this type are simple in structure, low in price, flat in frequency response, but more sensitive to temperatures.

Electromotive microphones and piezoelectric microphones are often used in general sound level meters.

Condenser microphones are composed of two electrode plates, which yield an electrical capacitance, in terms of one vibrating diaphragm and another back electrode. A D.C. electrical voltage (charging voltage) is applied between the diaphragm and the back electrode, thus forming a constant charging condition. When the diaphragm vibrates under a sound pressure effect, the change in capacitance between the electrodes produces an electrical voltage corresponding to the sound pressure. Microphones of this type are high in sensitivity, with a flat frequency response to a very broad range of frequencies. Their output characteristics are stable, with practically no change between the temperature range of $-50^\circ C$ and $+150^\circ C$ and the relative humidity range between 0 and 100%. Therefore, they are suitable for precision measurements. Precision sound level meters do use condenser microphones.

34

However, the materials and processing requirements of such microphones are very strict, and the manufacturing costs are high. Furthermore, they require highly stable D.C. voltages and amplifiers in their applications.

The characteristics of condenser microphones are closely related to their volumes. The smaller the volume, the broader is the frequency response range, the smaller the effect from the noise propagation directions, the ability in sustaining higher sound intensities, but the lower the sensitivity. Table 1.7 is a partial list of specifications and characteristics of the CH-series condenser microphones manufactured by the Peijing Radio Equipment Factory, No.1.

The electronic amplifier in condenser microphones needs to have a high gain. The amplification characteristics are flat in the audible frequency range (20-20,000 Hz). It should have low background noise and high stability. The attenuator requires an attenuation of 10 db in each step.

There are three common frequency weighting networks, designed by following the human ear's response to sound (see section 1.4.2). Some sound level meters include an additional weighting network-D, which simulates the frequency characteristics of a noise level curve with 40 Na. to evaluate the airplane noises. The frequency characteristics of weighting networks-A, -B, -C, and -D are shown in Fig. 1.17.

a. Model Number   b. Diameter (mm)   c. frequency response (± ? db)
d. sensitivity (250 Hz)   e. temperature coefficient (-40 - 10°C)
f. dynamic range (db)

a. 型号	b. 直径 (毫米)	c. 频率响应 (±2分贝) Hz	d. 灵敏度 (250赫) uV/mbar	e. 温度系数 -40~10℃ (分贝) db/°C	f. 动态范围 (分贝)
CH 11	24	20—18000赫	5 毫伏/微巴	0.02 分贝/℃	20—146
CH 13	12	25—40000赫	1 毫伏/微巴	0.02 分贝/℃	32—160
CH 16	6	30—70000赫	0.1 毫伏/微巴	0.02 分贝/℃	70—180
CH 18	3	30—140000赫	0.? 毫伏/微巴	0.02 分贝/℃	90—184

Table 1.7   Specifications and characteristics of the
CH-series condenser microphones
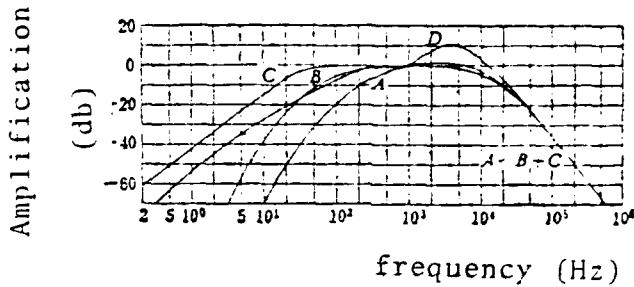
Figure 1.17   Frequency characteristics of weighting
networks -A, -B, -C, and -D

In noise measurements, Network-A is usually specified for
the sound with more than 55 db, called the A-sound level as
expressed by dBA; network B for the medium intensity sound with
55-85 db, called the B-sound level as expressed by dBB; and
network C for the stronger noise with more than 85 db, called
the C-sound level as expressed by dBC. However, as stated in
Section 1.4.2, network-A is always used in recent years in the
noise measurements and evaluations, whether the sound is strong
or weak. This is because of the fact that A-sound level is
closer to human ears' perception characteristics to noises. For
some sound level meters, such as the Model 2207 sound level meters

from Denmark, there is only the network-A, without other networks.

In noise measurements, one has to only read out the values on the A-, B-, and C-scales of a sound level meter in order to roughly estimate the frequency characteristics of a noise, without using a frequency analyzer. As shown in Figure 1.1b, if the readings are the same on the A-, B-, and C-scales, then the noise sound energy is mainly concentrated at the high frequency bands. Therefore, the noise shows high frequency characteristics. If the A-scale reading is higher then the C-scale reading by 1-2 db, then the noise has a peak value between 2000 and 5000 Hz. If the C-scale reading is equal to the B-scale reading and is greater than the A-scale reading, then the noise has a medium frequency characteristics. If the C-scale reading is greater than the B-scale reading, which is greater than the A-scale reading, then the noise has a low frequency characteristics.

Currently, there are two kinds of sound level meters: the general and the precision meters. International Electrical Engineering Council (IEC) has standard specifications for these two kinds of meters: The general sound level meters have a frequency range of 20-8000 Hz, while the precision meters have a frequency range of 20-12500 Hz.

Most sound level meters can not be used to measure impulse sound. Impulse sound level meters have to be used, e.g., the Denmark-manufactured Model 2204 and 2209 sound level meters. Sound level meters of this type have already taken into account the perception characteristics of human ears towards impulse sound. They also have D-networks, and can be used for airplane noise measurements.

Sound level meters' indicator readings are effective values. There are fast and slow damping for the indicators. For measuring noises with small fluctuations, fast-scale should be used. When the fast-scale-measured noises have fluctuations more than 4 db, slow scale should then be used.

Sound level meters are generally powered by batteries. It is necessary to check the voltages before use, to check whether it satisfies the normal working requirements of the sound level meters.

Sound level meters also require regular calibrations. For the sound level meters by the Denmark B & K Co., Model 4240 Noise Generators from the same Co. can be used for calibration. They produce constant noise level at 108 db. Model 4220 piston type generators produce constant sound pressure level at 124 db. For the sound level meters manufactured by the Kiang-Si Red Sound Equipment Factory, Model Nx6 piston type sound generators, which produce sound with $124^{\pm}0.2$ db, can be used. For those sound level meters without standard noise sources, calibrations can be made roughly in a weaving room of a fabric factory. This is because a typical weaving room has a constant noise of $104^{\pm}1$ db.

2. Frequency analyzers: Frequency analyzers are equipment for analyzing the frequency spectrum of noises. They are composed mainly of amplifiers and wave filters. If a noise passes through an octave band filter, one can obtain an octave band frequency spectrum of the noise. If a noise pases through a third-octave band filter, one can obtain a third-octave band frequency spectrum of the noise. If it passes through a narrow bandwidth filter, one can then obtain a narrow bandwidth frequency spectrum of the noise.

38

In the measurement of aerodynamic machinery and sound suppressors, octave band and third-octave band frequency analyzers are generally used. The central frequencies and the corresponding frequency ranges for octave band analyzers are shown in Table 1.3. The central frequencies and the corresponding frequency ranges for third-octave band analyzers are shown in Table 1.8.

Table 1.8   Central frequencies and corresponding
frequency ranges for third-octave band
frequency analyzers (IEC)

a. 中心频率(每)	b. 频率范围(赫)	a. 中心频率(赫)	b. 频率范围(赫)
50	45—56	1000	900—1120
63	56—71	1250	1120—1400
80	71—90	1600	1400—1800
100	90—112	2000	1800—2240
125	112—140	2500	2240—2800
160	140—180	3150	2800—3550
200	180—224	4000	3550—4500
250	224—280	5000	4500—5600
315	280—355	6300	5600—7100
400	355—450	8000	7100—9000
500	450—560	10000	9000—11200
630	560—710	12500	11200—14000
800	710—900		

Key: a. Central frequency (Hz); b. Frequency range (Hz)

Using the Chinese Model SJ-1 general sound level meters, Model TLB-1 third-octave frequency wave filters, and octave band wave filters together, one can make octave or third-octave band frequency spectral analysis. It can also be done with the Denmark Model 2203 precision sound level meters with Model 1013 octave band wave filters, or Model 1616 third-octave and octave band wave filters.   39

Loudspeakers or sound level meters and wave filters can also be combined to make a device called frequency spectrometer (e.g., Denmark Model 2112, 2114 spectrometer). It can not only measure the sound level, it can also analyze the frequency spectrum. Model ND 2 octave band sound level meters, which are new products from the Kiang-Si Red Sound Equipment Factory, are indeed the portable frequency spectrometers.

Octave band analysis is often used in evaluating allowable noise standards as well as the noise control standard. It can also give a general noise indication for given equipment. For aerodynamic equipments, octave band is enough. If detailed analysis is required, third-octave band can be used. For tuned noise and noise with pure sound peaks, or for tests on sound absorbing materials and basic tests on sound suppressors, more detailed analysis is required to determine the width of resonance peaks. One can then use narrow band continuous analyzers based on constant hundredth-octave bandwidth. For instance, with a Denmark Model 2107 frequency analyzer, the bandwidth can be adjusted between 6 and 29% of any central frequency. Extra-plated continuous analyzers have even higher frequency selectivity. Their bandwidths do not depend on the central frequencies, but are 5, 20, 50, and 200 Hz. They are called constant bandwidth analyzers (such as the Denmark Model 2014 analyzers).

Noise measurements with analyzers require a certain time. One needs 8 measurements for an octave-band analysis, and 24 measurements for a third-octave analysis. To measure the

40

frequency spectrum of a time-dependent noise, such as from a passing-through automobile or a suddenly-approaching airplane, measurements become obviously impossible. Instantaneous frequency analyzers are then needed. With the Denmark model 3347 real-time analyzers or the Japanese model SA-10 real-time analyzers, one can simultaneously (in fractions of a second) observe the third-octave band frequency spectra on a TV screen.

3. Automatic and magnetic-tape recorders: Automatic recorders are equipment which automatically record sound levels. Along with frequency spectrometers, they can quickly and accurately measure, analyze, and record the noise levels and the frequency spectra. They can also automatically record the time dependence of noises. This brings great convenience to noise measurements.

The Chinese model SJ-1 general sound level meters, model TLB-1 band pass filters, and model NJ1 recorder in a matched set; or the Chinese model NP-1 frequency analyzer and model NJ1 recorder in a matched unit can both serve the purpose to automatically measure and record the noise levels and frequency spectra. The Denmark model 2305 recorder and model 2112 or 2114 frequency spectrometer can also form a unit to automatically analyze and record the spectra of octave band and third-octave band.

Automatic recorders can also be used to measure the time of sound mixing.

Magnetic tape recorders are also called recorders. They can be used to record noises quickly. This is particularly

41

meaningful for field measurements. The recorded noises can
be later carefully analyzed for their frequency characteristics.
With oscilloscopes one can also observe the travelling wave
shapes of any impulse noises and discrete noises recorded on
the magnetic tapes.

Magnetic tape recorders should have good frequency responses,
broad dynamic ranges, low background noises, and long-time
stability to avoid loss of fidelity.

In recent years, integral sound level meters also become
available. They are also called noise dosage meters. They can
integrate the sound levels as a function of time, and bring great
convenience to noise measurements.

1.5.2 Noise measurement methods and calculations

For typical noise measurement, A-sound levels and octave-
band noise spectra are mainly measured. Sometimes, in order to
analyze the noise characteristics, spectra of third-octave band
or even narrow noise frequency band have to be determined. For
aeronautic noises, the measurements are mainly on perception
sound levels, which are actually the D-sound levels. For machinery
evaluations, one also has to measure the sound power and the
directional characteristics of the noise source.

1. Simple field measurements: In industrial and mining
locations, there are many noise sources, and the size of in-
dividual rooms have also limited sizes. In noise measurements,
microphones should be set as close to the radiant surface of
machineries as possible. This way, the direct sound field of
a given noise source is large enough, such that interferences

due to other noise sources or reflections are relatively small. However, the distance can not be too close, otherwise the sound field will not be stable.

Generally speaking, for aerodynamic machinery situated on ground in factories, such as air compressors, blowers, steam turbines, etc. with dimensions around 1 m, microphones can be arranged at 1 m away and 1.5 m high to evaluate the radiant noise of the equipment. If the equipment is very small, such as small blowers, with dimensions less than 30 cm, microphones can be set at 30 cm from the equipment. For medium size machinery with dimensions around 0.5 m, the point of measurement can be 0.5 m from the surface. For extremely large machinery or dangerous equipment (e.g., airplanes, rockets, cannons), one can choose a position at 5-10 m or even further away (e.g., 50m, 100m, etc).

If the equipment has non-homogeneous radiant noise in different directions, measurements should first be made at different positions surrounding the equipment, 1 m from them and 1.5 m above ground. The main noise evaluation reference is then based on data taken at a point where the A-sound level is maximum. Other reference data include the A-sound levels at several other points and the frequency spectra. Otherwise, one can determine the distributions of the noise in different directions, thus determining the directional characteristics of the equipment's noise.

43

Aerodynamic equipment's intake and exhaust gas noises often override those radiated from the structures. To well design appropriate sound suppressors, one has to carefully measure the intake and exhaust gas noises in terms of their sound levels (A-sound levels and overall sound pressure levels) and corresponding frequency spectra (octave bandwidths, third-octave bandwidths, narrow bandwidths).

For intake gas noises, the point of measurement can be chosen at 1 m from the gas inlet, along the axial direction. In order to understand the radiation behaviors, measurements can also be made at 0.5-10 m or even further away from the gas inlet, along the axial direction.

For exhaust gas noises, particularly those of high speed, high temperature, and gases containing water and oil, microphones should be set at a horizontal distance of 0.2-1 m from the outlet, or at 0.5-1 m from the outlet in the 45^0 direction with respect to the exhaust pipe. Measurements at large distances can also be made to understand the radiating conditions.

The above-mentioned are methods for field measurements of radiating noises from machinery. If it is necessary to understand the noise effect on health, the points of measurements can then be chosen to be those of workers' ears (people should be away at this time); or where workers often work (e.g., work benches, next to machinery, aisles). The height of measuring positions is that of the ears.

To know the environmental pollution due to certain machinery, the points of measurement can be chosen at those places of interest, or at positions 10, 50, 100, 200, 500, 1000 m or even further away from the noise source.

For street automobiles and tractors, the points of noise measurement are often selected at 7.5 m away from the vehicles' body, and 1.2 m above ground.

In every measurement, the point of measurement should be identified, along with the model numbers of the measuring devices and the working conditions of the equipment being measured.

To have accurate measurements, one has to pay attention to the following concerns: To avoid the interference due to background noises. The so-called background noises are noises from the environment when the noise source being studied ceases to function. If the ambient noises are stronger than the one being studied, no meaningful measurements can be made. In general, the A-sound levels of a noise source and the sound pressure levels at all frequency bands to be measured should be higher by 10 db than the corresponding ambient sound levels, the interference due to background noises can then be avoided. If the differences are less than 10 db, Table 1.9 is needed for corrections.

Table 1.9 Correction factors for background noises

	3	4~5	6~9
(db)	3	2	1

Δ -- difference between measured noise and background noise

δ -- noise level to be subtracted from the measured noise

For example, if the measured noise for a blower is 95 db(A)
and the background noise is 90 db(A), the noise of the blower
after correction should be 95 db - 2 db = 93 db(A).

In field noise measurements, apart from the correction for
background noises, one should also be aware of the sound field
characteristics of the noise source. For instance, Figure 1.18
shows the sound field distribution of a noise source in a garage;
the noise level at a given point inside the garage is a function
of the distance from the sound source. We should try to choose
a point of measurement in far-away free field areas. Such areas
can be roughly found, based on the principle that noise level
in a free field decreases by 6 db when the distance doubles.
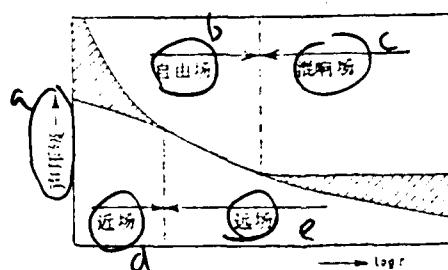
Key:

a. sound pressure level
b. free field
c. mixing sound field
d. near field
e. far-away field

Figure 1.18 Sound field distribution of a
noise source

In noise measurements, the effect due to reflections should
also be avoided. Otherwise, the measured noise is stronger than
the actual noise. To avoid reflected sound, microphones should
be set far away from reflection surfaces (such as walls,
other equipment, etc); in general the distance should be above
2-3 m.

Beyond the background noise and reflection effect, different effects can also be caused by wind, electromagnetic fields, vibrations, humidity, etc. Quite large errors can be particularly induced by wind. Therefore, air streams should be avoided. If they can not be avoided completely, microphones can be modified with covers or nose-cones.

2. ISO near-field measurement methods

For reference, specifications for near-field sound level measurements proposed by the International Standards Organization are listed.

To avoid the background noises and reflected sound effect, near-field measurements are used, which measure the noise levels near and surrounding the equipment of interest. In this method, a surface surrounding the equipment (called the defined surface), which has similar shape as that of the equipment's surface, is selected. The surface should be as simple as possible and allow simple calculations. Its distance from the equipment is determined by the actual situations, but should be as close as possible.

The average values of measured sound levels at several points on the defined surface are converted to a noise level for a reference radius. If the defined surface has an area of S (m^2), the average surface noise level is L_{pd}(db), the average sound level L_{pr} on a semi-spherical surface with a radius d (m) is

$$\overline{L}_{pr} = L_{pd} - 20 \log (d/r), \qquad (1.21)$$

where $r = \sqrt{\dfrac{S}{2\pi}}$ -- effective semi-spherical radius of the defined surface.

47

Using this method, the average error is 0.7 db if the scattering of readings is less than 5 db. The average error is less than 2.5 db if the scattering is within 10 db. Above 10 db, this method is not useful anymore.

For all machinery included in a given specification, the reference radius is the same. Selection should be made among 1, 3, and 10 m.

For instance, in near-field noise level measurements on 12V four-stroke diesel engines (N = 1200 hp, n = 1500 rpm) in a given diesel engine testing station, the points of measurement can be chosen from a rectangular surface   comprised of side/ vertical faces and top face (excluding bottom face) 1 m away from the generator. A-sound level measurements are to be made at a total of 29 points on this surface (8 points each at the plane of the crank, cylinder, and compressor, 5 points along the horizontal axis of the diesel engine; see Figure 1.19 for the plane view). The average value of these A-sound levels (db(A)) is calculated, and then converted according to Equation (1.21) to the corresponding A-sound level for a reference radius d = 3 m of a semi-spherical surface.
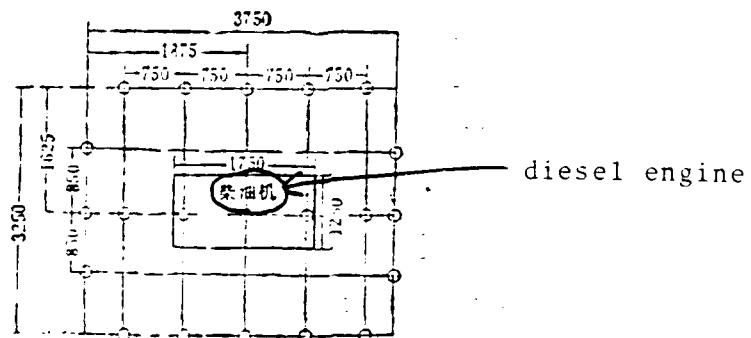

Figure 1.19   Selected points for near-field noise
              measurements (plane view) for a diesel
              engine   48

3. Method for measurements of sound power levels of machinery: To more objectively express the noise characteristics of machinery, the noise power levels and their directionalities are often needed. This is because, under a given working condition, the sound power level is constant, not like the sound pressure level which varies with distance. Meanwhile, due to a particular functional relationship between the sound power level and the sound pressure level of a given noise source, the latter at different environments and at different points of measurement can be estimated if the sound power level is known. Therefore, in noise control, sound power level is an important physical quantity.

However, both sound power level and sound power can not be directly measured. They are calculated under special conditions from the measured sound pressure levels. There are generally four methods for determining and calculating sound power levels and sound power: free-field method, expansion-field method, semi-expansion-field method, and near-field method.

Free-field method: In a free field,

$$L_w = \overline{L}_p + 10 \log S \quad (db), \qquad (1.22)$$

where L_w -- sound power level; $\overline{L}_p$ -- average sound pressure level; S -- surface area of the testing sphere (or semi-sphere).

$\overline{L}_p$ is the measured sound pressure level at the spherical surface (or semi-spherical surface) with its center at the machine and a radius of r. The value of r should be chosen to

49

be large enough such that the sound pressure and the particle velocity are in phase at the point of measurement. Under normal conditions, r is twice the dimensions of the machine.

If the machine is located inside a sound suppression room or other more ideal free-fields, the sound source radiates a spherical wave, then Equation (1.22) changes to

$$L_w = \bar{L}_p + 10\log 4\pi r^2 = \bar{L}_p + 20\log r + 11 \qquad (db), \qquad (1.23)$$

where $\tilde{L}_r$ -- average sound pressure level as determined from several points on a spherical surface with a radius r.

If the machine is set on hard outdoor ground with no reflection from surroundings, or the dimensions of the sound source are much smaller than those of the room, where no reflection occurs, the sound source radiates semi-spherically. Equation (1.22) then changes to

$$L_w = \bar{L}_p + 10\log (2\pi r^2) = \bar{L}_p + 20\log r + 8 \qquad (db), \qquad (1.24)$$

where $\bar{L}_p$ -- the average sound pressure level as determined from several points on a semi-spherical surface with a radius r.

In directionality measurements, for a spherical radiation, then

$$DI = L_p - L_{ps} \qquad (db), \qquad (1.25)$$

where DI -- directional characteristics in the direction of measurement; L_p -- sound pressure level at a distance r from the center along the direction of measurement; L_{ps} -- average sound pressure level on the testing spherical surface with a radius r.

50

If the machine is set on ground, radiating semi-spherically,
then, $DI = L_p - L_{ps-s} + 3$ (db)   (1.26)
where L_{ps-s} is the average sound pressure level as determined from the
semisphere with radius r.

Expansion-field method: In an expansion-field (e.g., sound-
mixing room, or rooms with very long sound-mixing time),

$$L_w = \overline{L_p} + 10 \log R - 6 \quad (db), \quad\quad\quad (1.27)$$

where $R = \dfrac{Sa}{1-a}$ -- room constant; S -- total surface area
of room, m^2; a -- average sound absorbing coefficient for the
interior surface of room. or,

$$L_w = \overline{L_p} + 10 \log V - 10 \log T - 14 \quad (db), \quad\quad\quad (1.28)$$

where T -- sound-mixing time; V -- room volume, m^3.

The expansion-field method does not yield directional characteris-
tics. Furthermore, its accuracy is related to the flatness of
the noise source's frequency characteristics. It is not appro-
priate for machinery with peak frequency components.

Semi-expansion-field method: A semi-expansion-field, where
the room does not absorb completely or reflect completely, is
between a free-field and a sound-mixing field. (This is often
encountered in field measurements.) The following equation can be
used for measurements and calculations:

$$L_w = \overline{L_p} - 10 \log \left(\frac{1}{2\pi r^2} + \frac{4}{R} \right) \quad (db). \quad\quad\quad (1.29)$$

Calculations of this kind are tedious and not very accurate.
Recently, sound power levels are also determined by the standard
sound source method.

The so-called standard sound source is a special sound source
which radiates enough homogeneous sound power spectra over given

51

frequency bands. Such standard sound sources have their sound power levels L_{ws} first determined in laboratories, before they are used in field measurements. The average sound pressure level $\overline{L}_p$ is measured from the semi-spherical surface with a radius r(m) and the noise source as the center. After turning off the noise source, average sound pressure level $\overline{L}_{ps}$ is determined at the same position with the noise source replaced by the standard sound source. Therefore, the sound power level for the noise source being investigated is

$$L_w = L_{ws} + \overline{L}_p - \overline{L}_{ps} \qquad (1.30)$$

It is easier and more accurate to measure sound power levels using the standard sound source method.

The semi-spherical expansion-field method can only provide limited information on the directionality of the sound radiation.

Near-field method. If because of the shapes and installation conditions of a noise source which make the above-mentioned methods impractical, sound power levels of the sound source can then be determined by the near-field method. By using Equation (1.21) to find $\overline{L}_{pr}$ and substituting it into Equation (1.25), the sound power level of a given machine can be obtained.

In recent years, due to the popularity of A-sound level, another term A-power level is introduced. It is the A-weighting sound power level. Calculations are still to be done according to Equations (1.22) - (1.30). However, L_w and L_p in the equations are replaced by L_{w_A} and L_A.

52

4. Calculations of loudness level and perception noise level: The loudness level is calculated from the following method, after the sound pressure level of the noise is first measured: The octave-band or third-octave-band spectra are first determined, followed by converting each frequency band's sound pressure level to the loudness index using Figure 1.20, then the total loudness level is calculated from Equation (1.32)

$$S_t = S_m + F(\Sigma S_i - S_m) \qquad (\text{sone}), \qquad (1.31)$$

where S_t -- total loudness, sone; ΣS_i -- sum of the loudness indices for all frequency bands; S_m -- the maximum value of individual loudness index; F is determined by the bandwidth used in spectral analysis:

bandwidth	F
octave band	0.3
third-octave band	0.15

After the total loudness S_t is calculated, the total loudness (sone) can be converted to the total loudness level (phon) using Equation (1.20) or the curves in Figure 1.21.

If accurate calculations are not required, the total sound pressure level L_c and the A-sound level L_A can be read out from sound level meters. From the difference between L_c and L_A, the value of (phon-L_c) can be found from Figure 1.21. By adding this value to L_c, the loudness level (phon) is obtained. or, with the values of L_c and L_A, the loudness level (phon) is directly found from Figure 1.22. The loudness value (sone) can then be

53

calculated from Equation (1.20).

Key:

a. loudness index
b. octave-band sound
   pressure level (db)
c. frequency (Hz)
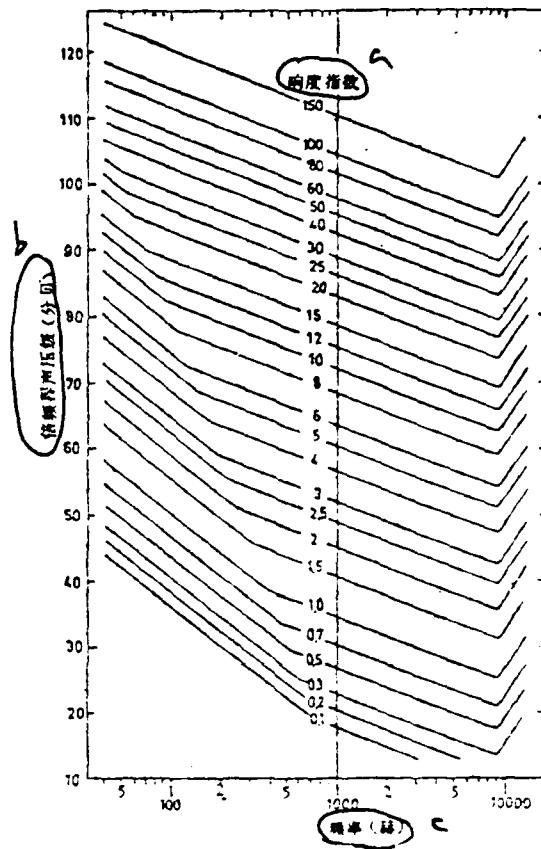
Figure 1.20   Equi-loudness Index table
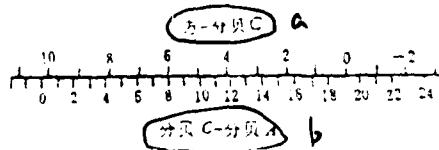
Key: a. phon - dBc
      b. dBc - dBA

Figure 1.21   Estimation of the loudness levels from
          the A- and C- weighting network readings of sound
          level meters

Key:

a. scale-c reading on a
   sound level meter (dBc)
b. phon
c. scale-A reading on a
   sound level meter (dBA)
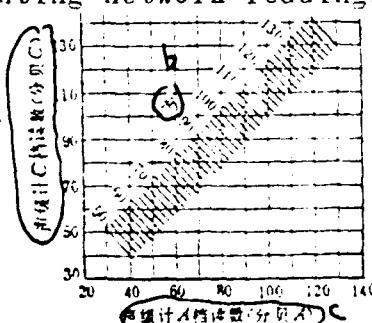
Figure 1.22   Estimation of the loudness level (phon)
          from the A- and C-weighting network readings of
          sound level meters   54

For example, we obtain the C-scale reading of the noise sound level L_c =130 db for a given generator, the A-scale reading is L_A =122 db. From Figure 1.21, the (phon-dbC) value is 6, corresponding to dbC - dbA = 8 db. Therefore, the loudness level of the generator is

$$L_s = dbC + (phon - dbC) = 130 + 6 = 136 \text{ phon.}$$

For perception noise level, a similar method is used for calculations. The octave or third-octave band sound pressure level is first measured for a given aeronautic noise. From Figure 1.13 the noise level for each frequency band is obtained from the equi-noise level curves, and the overall noise level N_T is then calculated from Equation (1.32):

$$N_T = N_m + F(\Sigma N - N_m) \quad (NOYS) \tag{1.32}$$

where N_m -- the maximum of the noise levels; ΣN -- sum of the frequency band noise levels; F is determined from the following table

Bandwidth	F
Octave band	0.30
Third-Octave band	0.15

Then, following Equation (1.33) or Table 1.10 and Figure 1.14, the total noise level can be converted to the perception noise level:

$$\text{Total PN db} = 40 + 33.3 \log N_T . \tag{1.33}$$

55

If accurate values are not required, the total sound
pressure level L_c and the A-sound level L_A can also be read
out from sound level meters. The difference $L_c - L_A$ is obtained.
From Figure 1.23, the value of (PN db – dbC) is found. The
sum of this value and dbC is the perception noise level PN db.
or, directly from Figure 1.24, the PN db can be obtained from
the values of L_A and L_c.

In recent years, sound level meters with a D-network have become
available. Therefore, with Equation (1.34), the perception
noise level can be directly calculated from the D-scale reading:

Perception noise level PD db = L_D + 9.   (1.34)

This way, measurements and calculations are greatly simplified.
For example, a given airplane has a noise with L_D = 140 db, its
perception noise level is then 140 + 9 = 149 (PN db).

Table 1.10   Noise level (NOYS) converted to perception
noise level (PN db)

Key: a. NOYS; b. PN db

Perception noise level [PN db] - dBC
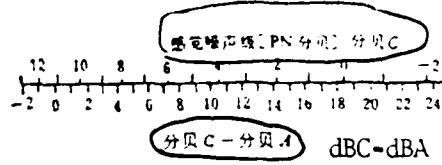

Figure 1.23 Line diagram for estimation of perception
noise level from the C- and A-scale weighting
network readings of sound level meters

Key:
   a. Scale-C reading on a
      sound level meter (dBC)
   b. PN-db
   c. Scale-A reading on a
   sound level meter (dBA)
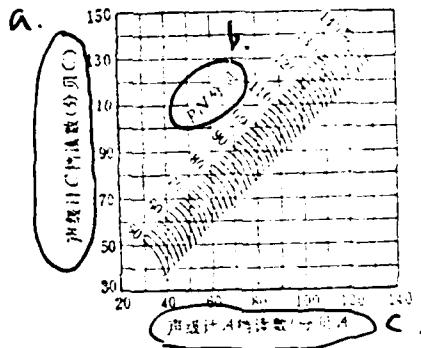
Figure 1.24 Estimation of perception noise level from
the C- and A-scale weighting network of sound
level meters

§ 1.6　Allowable Noise　Standards

To what degree should noise　be controlled to be most
reasonable?　Is it best to completely eliminate noise?　No,
this is not necessary, and not economical.　In factories and
cities, it is most important to make sure that no deafness or
other diseases are caused by noise.　Consequently, there is
a need for standards to safe-guard hearing and health.　To
guarantee that living and working areas (such as residential
areas, industrial areas, business districts, institutions,
schools, hospitals, etc.) are not disturbed by noise,　we need
noise standards for different regions as well as different
locations.

Noise standards are very complicated. They are related
to acoustics, psychology, physiology, health science, and the
technology and economic conditions.　The following are the
noise standards (ISO standards) recommended by the 43rd Techni-
cal Committee (acoustics) of the International Standards
Organization.

1.6.1　Noise standards as expressed in terms of noise rating
NR values.

The ISO standards of 1961 as shown in Figure 1.25 are com-
posed of a group of noise rating curves (i.e., NR curves).
Their noise level range is between 0 and 130 db, and a frequency
range of 63-8000 Hz in eight frequency bands.

In this group of noise rating curves, the sound pressure level of the octave band at 1000 Hz is equal to the noise rating value N. The relation between N and the sound pressure levels for the octave bands at 63, 125, 250, 500, 1000, 2000, 4000, and 8000 Hz is as follows:

$$L_p = a + bN \quad (db), \tag{1.35}$$

where a and b are constants, with their values given is Table 1.11.

To make a convenient reference, the corresponding sound pressure level for an octave band for the noise rating values N is also shown in Table 1.12.

1. Allowable noise standards for hearing protection: For hearing not to be damaged by noises, one should first consider the noises of three octave bands at 500, 1000, and 2000 Hz for general conversations. For a broad frequency band noise with continuously more than 5 hours daily, at 500, 1000, and 2000 Hz, the noise rating value is set not to go beyond N 85.

Under certain conditions, with less than 5 hours daily for a broad band noise, one can allow a standard higher than N 85. The upper limit is determined by Figure 1.26. This standard allowing 12 db is based on the temporary audible field shift[1] at 2000 Hz. This is shown in Figure 1.26 by the dashed lines. As confirmed by hearing tests, continuously

---

1) Under the influence of noises, hearing ability of human ears decreases; after a certain time with the noise stopped, hearing ability will recover. This effect is called the temporary audible field shift.   59

Figure 1.25 Noise rating value curves

Table 1.11 Values of a and b

倍 频 带 频 率	a (分 贝)	b (分 贝)
63	35.5	0.790
125	22.0	0.870
250	12.0	0.930
500	4.8	0.974
1000	0	1.000
2000	−3.5	1.015
4000	−6.1	1.025
8000	−8.0	1.030

Key:
a. octave band sound pressure level (0 db = 2 x 10⁻⁵ N/m²)
b. central frequency of octave band
c. noise rating value

Key:
a. octave band
b. db

60

Figure 1.25 Noise rating value curves

Table 1.11 Values of a and b

倍 频 带 频 率	a (分 贝)	b (分 贝)
63	35.5	0.790
125	22.0	0.870
250	12.0	0.930
500	4.8	0.974
1000	0	1.000
2000	−3.5	1.015
4000	−6.1	1.025
8000	−8.0	1.030

Key:
a. octave band sound pressure level (0 db = 2×10^{-5} N/m²)
b. central frequency of octave band
c. noise rating value

Key:
a. octave band
b. db

60

Table 1.12 Corresponding sound pressure level (db)
for each octave band with a noise rating value N[1]

N	63	125	250	500	1000	2000	4000	8000
0	35.5	22.0	12.0	4.8	0	−3.5	−6.1	−8.0
5	39.4	26.3	16.6	9.7	5	1.6	−1.0	−2.8
10	43.4	30.7	21.3	14.5	10	6.6	4.2	2.3
15	47.3	35.0	25.9	19.4	15	11.7	9.3	7.4
20	51.3	39.4	30.6	24.3	20	16.8	14.4	12.6
25	55.2	43.7	35.2	29.2	25	21.9	19.5	17.7
30	59.2	48.1	39.9	34.0	30	26.9	24.7	22.9
35	63.1	52.4	44.5	38.9	35	32.0	29.8	28.0
40	67.1	56.4	49.2	43.8	40	37.1	34.9	33.2
45	71.0	61.1	53.6	48.6	45	42.2	40.0	38.3
50	75.0	65.5	58.5	53.5	50	47.2	45.2	43.5
55	78.9	69.8	63.1	58.4	55	52.3	50.3	48.6
60	82.9	74.2	67.8	63.2	60	57.4	55.4	53.8
65	86.8	78.5	72.4	68.1	65	62.5	60.5	58.9

N	63	125	250	500	1000	2000	4000	8000
70	90.8	82.9	77.1	73	70	67.5	65.7	64.1
75	94.7	87.2	81.7	77.9	75	72.6	70.8	69.2
80	98.7	91.6	86.4	82.7	80	77.7	75.9	74.4
85	102.6	95.9	91.0	87.6	85	82.8	81.0	79.5
90	106.6	100.3	95.7	92.5	90	87.8	86.2	84.7
95	110.5	104.6	100.3	97.3	95	92.9	91.3	89.8
100	114.5	109.0	105.0	102.2	100	98.0	96.4	95.0
105	118.4	113.3	109.6	107.1	105	103.0	101.5	100.1
110	122.4	117.7	114.3	111.9	110	108.1	106.7	105.3
115	126.3	122.0	118.9	116.8	115	113.2	111.8	110.4
120	130.3	126.4	123.6	121.7	120	118.3	116.9	115.6
125	134.2	130.7	128.2	126.6	125	123.4	122.0	120.7
130	138.2	135.1	132.9	131.4	130	128.4	127.2	125.9

Key:
a. An additional octave band with 31.5 Hz was added in 1971 to the ISO noise rating value curves. The values are listed in the following table.

[1] 1971 年公布的 ISO 噪声评价曲线又加了一个 31.5 赫的倍频带,其值如下表所示:

N	0	5	10	15	20	25	30	35	40
31.5	55.4	58.8	62.2	65.6	69.0	72.4	75.8	79.2	82.6
N	45	50	55	60	65	70	75	80	85
31.5	86.0	89.4	92.9	96.3	99.7	103.1	106.5	109.9	113.3
N	90	95	100	105	110	115	120	125	130
31.5	116.7	120.1	123.5	126.9	130.3	133.7	137.1	140.5	143.9

working for 5 hours at N 85, followed by a 2-minute stop, the
audible field rises by 12 db. At higher noise rating values,
one reaches this stage at a shorter working time period. The
relation is shown in Figure 1.26. Therefore, if the noise
effect lasts for 50 minutes, from Figure 1.26, the allowable
standard is N 95.

Key:
a. temporary audible
   field shift (db) at
   2000 Hz
b. action time (sec)
c. noise rating value
d. recommended allow-
   able value for temp-
   orary audible field
   shift at 2000 Hz
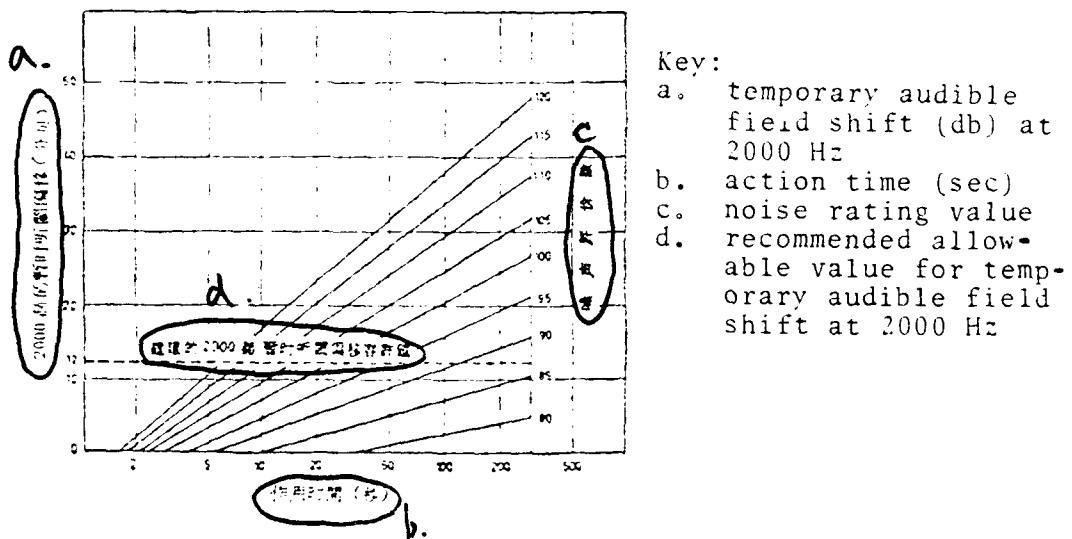
Figure 1.26   Noise rating values for short working
              periods

Under certain conditions, the effect of broad band noise
in a working day is not continuous. The allowable noise curves
are then determined in Figure 1.27. The abscissa is the time
period (minutes) of the noise effect, the ordinate is the time
interval between noise occurrences. The dashed lines indicate
the number of times daily for the allowed effect. The solid
lines indicate the noise rating values N.

62

For example, in an eight-hour working day with 20 minutes working for each 2 hours, the allowable noise rating value is N 100.

2. Allowable noise standards for comprehensible conversations: Under normal conditions, conversations at a distance within 2 m can be clearly heard. Therefore, one should also consider the conversational frequencies at 500, 1000, and 2000 Hz. Table 1.13 shows, at different noise rating values N, the relation between the distance and the degree of comprehensibility. The N values should be calculated from the sound pressure levels of 500, 1000, and 2000 Hz measured at the human ears' positions.

For telephone conversations, Table 1.14 should be used.

3. Allowable standards based on the interference of noises: These standards are introduced because of the fact that noises interfere with normal work and rest, and that noise makes people feel disturbed and uncomfortable. Therefore, the standards are different between day and night, summer and winter, city and countryside, as well as between continuous and pulsed noises. For instance, nighttime should be quieter than daytime, and summertime (with windows open) should be quieter than wintertime (with windows closed). Accordingly, the standards should be higher for nighttime and summertime than for daytime and wintertime. Pulsed sound makes one more uncomfortable than continuous sound does. Therefore, the restrictions on pulsed sound are more stringent. 63

The method of determination involves first the calculations, within the frequency range 31.5-8000 Hz, of the N value from the measured octave-band sound pressure level of the noise, then comparison with Table 1.15 and 1.16, followed by corrections with Table 1.17.


Key:
a. time interval (min)
b. allowable number daily
c. noise rating value
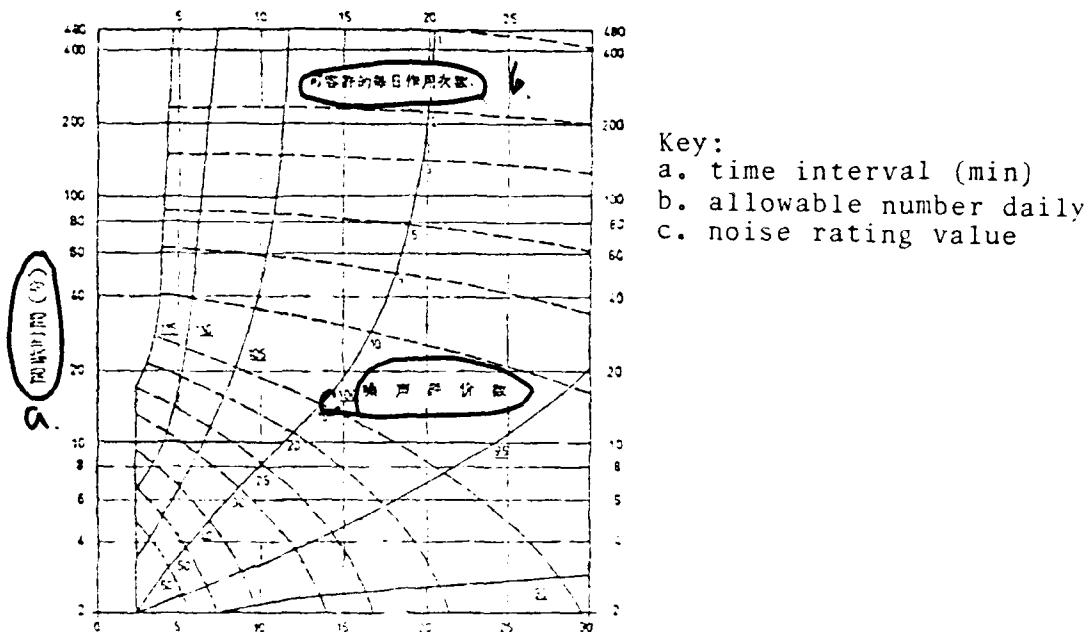
Figure 1.27   Limits for pulsed noises

Table 1.13

噪声评价数 N	正常交谈时的距离(米)	大声交谈时的距离(米)
40	7	14
45	4	8
50	2.25	4.5
55	1.25	2.5
60	0.7	1.4
65	0.4	0.8
70	0.22	0.45
75	0.13	0.25
80	0.07	0.14
85	—	0.8

Key:
a. noise rating value N
b. distance (m) for normal conversation
c. distance (m) for loud conversation

Table 1.14

(a) 噪 声 评 价 数 N	(c) 通 话 情 况
50	(d) 良 好
60	(e) 稍 有 困 难
75	(f) 困 难
75 以上 (b)	(g) 不 可 能

Key: a. noise rating value N; b. above 75; c. conversation condition; d. good; e. with some difficulty; f. difficult; g. impossible

Table 1.15 Evaluation standards for noise interference

(a) 噪声评价数 N	场 (b) 所
20—30	(c) 寝室,病房,电视间,住宅,戏院,电影院,会议室,阅览室,大礼堂
30—40	(d) 大办公室,商店,机关,小餐厅,会场
40—50	(e) 大餐厅,教室,有打字机的办公室,中学
50—60	(f) 大打字机室
60—70	(g) 工厂

Key: a. noise rating value N; b. location;
c. dormitory, patient room, TV room, residence, theater, conference room, reading room, auditorium;
d. large office, store, institution, small restaurant, meeting room;
e. large restaurant, classroom, office with typewriters, high school
f. large typing room; g. factory

Table 1.16

表 1.16 住宅区的群众反映 (a)

(b) 校 正 的 N 数	反 (e) 应
40 以下 (c)	(f) 没有意见
40—50	(g) 有少数人有意见
45—55	(h) 相当多的人有意见
50 以上 (d)	(i) 极其不满

Key: a. comments from residents; b. correction value of N;
c. below 40; d. above 50; e. comments; f. no comment;
g. comments from a few people; h. comments from many people;
i. many complaints

Table 1.17   Correction values for noise rating values

(mainly for residential areas)

噪 声 因 素	可 能 条 件	所得 N 值的修正数 (分贝)
噪声的脉冲特性	由若干纯音形成	+ 5
	宽带噪声	0
噪声因素(脉冲性)	脉冲	+ 5
	稳态	0
重复性 (噪声作用时间 大于30 秒)	连续作用: 1 次/分	0
	10—60 次/时	— 5
	1—10 次/时	— 10
	4—20 次/天	— 15
	1—4 次/天	— 20
	1 次/天	— 25
习 惯 性	完全生疏	0
	明白习惯	— 5
	熟悉习惯	— 10
时 间	仅在白天	— 5
	傍晚	+ 5
	夏季	0
	冬季	— 5
环 境	农村	+ 5
	郊区	0
	城市住宅区	— 5
	轻工业区	— 10
	重工业区	— 15

a. industrial factors

b. noise frequency spectral characteristic

c. nature factors

d. repeatability

e. familiarity

f. time

g. location

h. possible condition

i. broad band noise formed several pure tone

n. rural area
   suburb
   residential area in the city
   light industrial areas
   heavy industrial areas
o. Revised numbers of N values
   surveyed (dB)

66

1.6.2 Noise standards based on A-sound levels

In 1967, the International Standards Organization introduced again a new ISO noise evaluation based on A-sound levels. There are conversion relationships between A-sound levels and noise rating values NR. For most noises (with the exception of aeronautic noises), the NR values are lower than the A-sound levels by 5 db, i.e.,

$$L_A = N + 5. \tag{1.36}$$

1. Allowable noise standards for hearing protection: To protect hearing, the allowable noise standards are defined, based on the working time period under the noise conditions. For instance, with an 8 hour working period, the allowable A-sound level for continuous noises is 90 dbA. With half of the time period, the allowable noises can be raised by 3 dbA. If the daily working period is 4 hours, the allowable noise is 93 dbA; and 96 dbA for a 2 hour working period. The upper limit is 115 dbA. That is, under all conditions, the noise can not go beyond 115 dbA in order to protect hearing.

Recently, it has been suggested internationally that the allowable continuous noise is 85 dbA for a daily work of 8 hours. This number has been accepted in several countries.

Under many conditions, the noise levels in factories are not constant. Furthermore, operators do not work under a given noise level either. To take this into consideration, ISO introduced in 1971 another noise evaluation standard based on equi-effect continuous A-sound levels.

67

The definition of an equi-effect continuous A-sound level is: In a certain position in the sound field, and in a certain time interval there are several discontinuous A-sound levels prevailing. Based on the average energy, one can use one A-sound level to express the strength of the noise in this time interval. This A-sound level is called the equi-effect continuous A-sound level. The equation is

$$L_{ee} = 10 \log \left(\frac{1}{T} \int_0^T 10^{0.1L} \, dt \right) \quad \text{(db)}$$

$$(1.37)$$

where L_{ee} -- equi-effect continuous A-sound level, db; T-- the time interval under consideration; L-- the instantaneous value of the varying sound levels.

From Equation (1.37) it can be seen that, for a stable noise over a period of time, the A-sound level is the equi-effect continuous A-sound level.

ISO introduces the concept of a weekly equi-effect A-sound level and its regulations: If there is only one constant continuous noise effect, then the equi-effect continuous A-sound level is just the A-sound level. For instance, if the noise inside a certain machine room is stable, and the total number over a weekly 40 hour period is 100 db(A), then the equi-effect continuous A-sound level is also 100 db(A). On the other hand, if the noise effect is not constant, but is changing with time, then the equi-effect continuous A-sound level for that noise is

$$L_{ee} \text{ db(A)} = 70 + 10 \log \Sigma E_i \text{ (db)}, \quad (1.38)$$

$$E_i = (\Delta t_i / 40) \, 10^{0.1(L_i - 70)}, \quad (1.39)$$

where E_i -- exposure index corresponding to the noise portion with its sound level (A) equal to L_i; Δt_i -- time period for the weekly 40 hours' sound level L_i db(A) $\pm$ 2.5 db. For instance, consider the noise inside a machine room. In a 40 hour period, there are 20 hours with 110 db(A), 10 hours with 90 db(A), and 10 hours with 100 db(A). Then the equi-effect continuous A-sound level for the room is

$$L_{ee} = 70 + 10 \log \sum E_i$$
$$= 70 + 10 \log \left[\frac{20}{40} 10^{0.1(110-70)} + \frac{10}{40} 10^{0.1(90-70)} + \right.$$
$$\left. + \frac{10}{40} 10^{0.1(100-70)} \right] = 107 \quad db(A)$$

Based on the equi-effect continuous A-sound levels, ISO has investigated the noise exposure of a large number of workers with different working periods. The noise-caused deafness rates were studied (see Table 1.18). From this table one can see that, with L_{ee} below 80 db(A), the hazards are null. No noise-caused deafness occurred. It took 40 years at 85 db(A) to reach a hazard rate of 10%, 10 years at 90 db(A), 5 years at 95 db(A), and less than 5 years at above 100 db(A). Accordingly, under normal conditions, L_{ee} of 85-90 db(A) is the allowable noise standard for hearing protection.

2. Evaluation standards based on noise interference: ISO again introduced in 1971 the A-sound level standard based on social reactions. The main point is that the allowable noise is 35-45 db(A) for outdoors in residential areas.

69

Table 1.19 gives correction factors for the noise standards at different time periods.

Table 1.20 gives correction factors for the indoor noise standards for residential areas.

See Table 1.21 for the correction factors of noise standards of different areas.

The outdoor noise standards in residential areas can also be expressed in Table 1.22.

Table 1.23 shows the noise standards for non-residential areas.

Table 1.18 Relationship between the 0-45 years' equi-effect continuous A-sound levels and the hearing hazard rates [1]

a. equi-effect A-sound level (dB A)

b. percentage of persons with damaged hearing and hazards rate

c. percentage

d. number of years of noise exposure

e. hazards rate (%)

f. persons with damaged hearing (%)

i. persons with hearing damage refer to those losing more than 25 dB at the three 500, 1000, 2000 Hz octave bands

70

Table 1.19 Correction factors for noise standards
at different time periods

a. time   b. daytime   c. evening
d. night   f. -1. to -15   e. correction value (dBA)
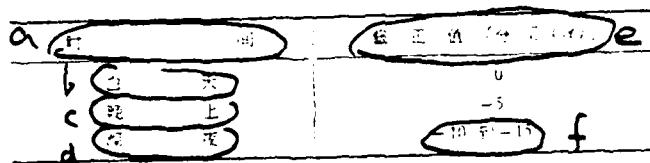
Table 1.20 Correction factors for indoor noise
standards
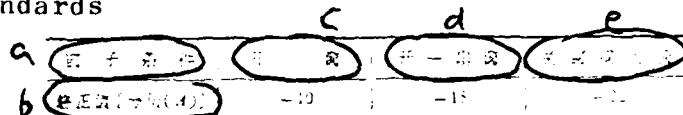
a. window condition   b. correction value (dBA)
c. open windows   d. one window open
e. closed windows or no window

Table 1.21 Correction factors for noise standards
at different locations
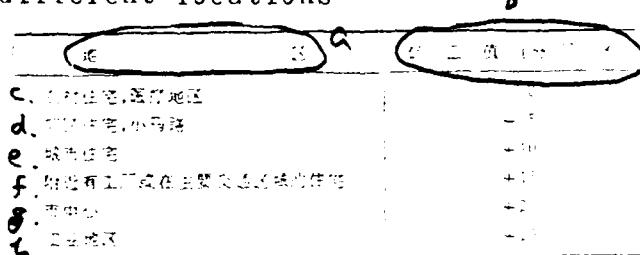
a. location   b. correction value (dBA)
c. rural areas, hospital areas
d. suburban, small streets
e. city dwelling areas
f. houses adjacent to industrial or commercial districts
g. city center
h. industrial areas

71

Table 1.22   Allowable A-sound levels for residential
areas' outdoor noise

地区	容许 A 声级 [分贝(A)]		
	白天	晚上	深夜
农村	35	30	25
郊区	40	35	30
市区	45	40	35
办公地区	50	45	40
城市街道	55	50	45
重工业区	60	55	50

a. location   b. allowable A-sound level (dbA)

c. daytime   d. evening   e. night

f. rural area   g. suburb   h. city

i. office area   j. city streets   k. heavy industrial area

Table 1.23   Allowable A-sound levels for non-
residential areas' noises

类别	容许 A 声级 [分贝(A)]
大会议室,阅览室,小电话总机室等	35
办公室,带打字机的办公室,休息室	45
大型打字机室	55
各种用途机器室	45～55

a. location   d. large meeting room,
                                     reading room, ...
b. allowable A-sound level (dbA)   e. machine room with
                                     different purposes
c. large office, ... , small ...

In recent years, studies have been made on 100 factories'
noise by the "Industrial Noise Standards Research" Group
supported by the Peijing Workers' Protection and Science
Research Institute, the Peijing Otorhinolaryngology Research
Institute, the Chinese Science Academy's Psychology Research
Institute, the Peijing Medical Institute, the Peijing Municipal

72

Health and Epidemiology Station, etc. Analyses were done on
the effects of different sound levels on close to ten-thousand
workers of varying working years, in terms of their hearing,
ear-nose-throat, blood pressure, pulse, EKG and nervous systems.
These led to the relationships between the A-sound levels and
hearing, the A-sound levels and changes of EKG(ST-T), and the
A-sound levels and incidence rate of nervous breakdowns. They
also evaluated the principal frequencies of mandarin. Based on
these, they have summarized the noise effects on hearing,
coronary, nervous systems, and proposed the following industrial
noise standards: For new industries, machine rooms should not
have noise standards exceeding 85 db(A). Consequently, over
95% of the workers will not become deaf over long working years,
and most of them will not have noise-caused coronary and nervous
diseases. For existing industries, considering economic and
technical conditions and feasibilities, the noise standards
can be temporarily set at 90 db(A), and gradually reduced to
85 db(A).

At the same time, the Peijing Workers' Protection and
Science Research Institute also tested and analyzed the environ-
mental noises of 50 streets. Close to ten-thousand residents'
psychological and acoustic reactions were investigated and
studied. According to the results, they have made statistical
and psycho-physical evaluations. They proposed the following
suggestions for the residential noise standards near factories:
Daytime (5 a.m. to 10 p.m.): 50 db(A), nighttime (10 p.m. to
5 a.m.): 45 db(A).

73

Chapter 2   Aerodynamic Noise

Following the development of modern industry and scientific technology, aerodynamic machinery has   more and more applications. It becomes   the necessary equipment   in both domestic economics and defense industries.   However, aerodynamic processess all produce noises, and these noises are more often encountered and more dangerous.   Particularly for the modern technological development, aerodynamic machinery   promoted greatly the power efficiencies, and increased rotating speeds, thus also generated stronger noise.   For instance, large scale turbine generator systems, high pressure/large volume exhaust streams and jet airplanes have noise power levels as high as 150-160 db.   The sound power is as high as 1000-10000 watts.   For saturn rockets the sound power levels even reach 195 db, and the sound power reaches 25-40 billion watt.[6]   Some high sound intensity aerodynamic noises not only seriously damage human health, but also lead to the failure of automatic control equipment   and sensitive testing facilities through "acoustic fatigues".   Therefore, the control of aerodynamic noise   has special meaning in modern technology.

The production mechanism and properties of aerodynamic noise   are discussed below.

§2.1   Formation of aerodynamic noise   and the types of the sound sources

Aerodynamic noise is   produced through the unstable processes

of gases, or the disturbance of gases and the interactions between gases and materials.

Turbulent gases have the continuity equation

$$\frac{\partial \rho}{\partial t} + \frac{\partial (\rho v_i)}{\partial x_i} = Q,$$

(2.1)

where ρ --- density; v_i --- wind velocity in the x_i direction: t --- time: Q --- flux from source per unit time and unit volume.

The motion equation

$$\frac{\partial (\rho v_i)}{\partial t} + \frac{\partial}{\partial x_i} (\rho v_i v_j + p_{ij}) = F_i,$$

(2.2)

where F_i --- the generalized force in unit volume; $\rho v_i v_j$ --- shear compressive stress tensor: $p_{ij} = p\delta_{ij} + \eta\left[-\frac{\partial v_i}{\partial x_j} - \frac{\partial v_j}{\partial x_i} + \frac{2}{3}\frac{\partial v_k}{\partial x_k}\delta_{ij}\right]$ ---pressure and viscosity-related compressive stress tensor; η --- viscosity coefficient.

$$\delta_{ij} = \begin{cases} 1 & \text{when } i = j, \\ 0 & \text{when } i \neq j, \end{cases}$$

Differentiating (2.1) with respect to time and to differentiating (2.2) with respect to x_i, through manipulations one obtains

$$\frac{\partial^2 \rho}{\partial t^2} = \frac{\partial Q}{\partial t} - \frac{\partial F_i}{\partial x_i} + \frac{\partial^2}{\partial x_i \partial x_j}(\rho v_i v_j + p_{ij}),$$

(2.3)

and further obtains

$$\frac{\partial^2 \rho}{\partial t^2} - c_0^2 \frac{\partial^2 \rho}{\partial x_i^2} = \frac{\partial Q}{\partial t} - \frac{\partial F_i}{\partial x_i} + \frac{\partial^2 T_{ij}}{\partial x_i \partial x_j},$$

(2.4)

75

where

$$T_{ij} = \rho v_i v_j + p_{ij} - c_s^2 \rho \delta_{ij}. \tag{2.5}$$

From Equation (2.4) it can be seen that, when the flux Q from source varies with time, the generalized force F_i varies with space, or the compressive stress tensor T_{ij} varies, aerodynamic noise will be produced.

In general, for sound radiation problems, one has to solve the wave functions with certain boundary conditions. The mathematical derivations are very complicated. The simpler way is to find solutions for basic spherical radiations. Of course, this kind of radiation is idealized. But it has real meaning. This is because most radiators are similar to spherical sound sources when their dimensions are much smaller than the wavelengths. In addition, many complicated sound radiations can be resolved into sound radiations of simplified configurations. For aerodynamic noises, in terms of the sound source characteristics, there are three main groups: single source, dipole source, and quadrupole source.

Single source is also called zeroth order source. When high speed streams are periodically exhausted from the outlet, or when steady streams are periodically shut off, then the flux Q from the source varies with time and produces a single-source radiation. A single source resembles a pulsed sphere. It evenly expands and contracts. Its radiation directionality is spherical (Figure 2.1). The wave function of a single source radiation is

76

$$\frac{1}{r^2}\frac{\partial}{\partial r}\left(r^2\frac{\partial \varphi}{\partial r}\right) = \frac{1}{c^2}\frac{\partial^2 \varphi}{\partial t^2},$$

$$(2.6)$$

where φ---velocity potential.

    a. sound source category

    b. schematic diagram of
       sound source

    c. radiation characteristics

    d. directionality

    e. sound power

    f. single source

    g. dipole source

   h. quadrupole source
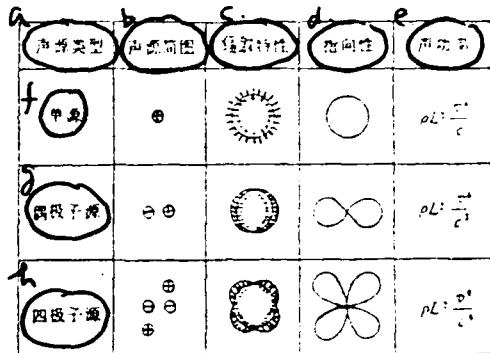
Figure 2.1 Radiation categories of aerodynamic noises

Following certain mathematical derivations, [2,3,5,7,8] one can obtain the sound power of a single source

$$W \propto \rho L \frac{v^4}{c} = \rho L v^3 M,$$

$$(2.7)$$

where ρ --- gas density, kg/m^3; L--- relevant length, m: v--- flow rate, m/s; c--- sound velocity, m/s; M--- Mach number, equal to v/c, dimensionless.

Double source (dipole source): Double-source radiation occurs when stream and materials interact such that the generalized force F_i varies with space. Blowers, air handlers, etc. have noises of this kind.

77

A double source can be viewed as a pair of single sources
with their separation distance shorter than the wavelength.
Its directionality is of the S-shape. The radiation is stronger
along the axis, and weaker in the direction perpendicular to the
axis (Figure 3.1)

The wave motion equation for a double-source is

$$\frac{1}{r^2}\frac{\partial}{\partial r}\left(r^2\frac{\partial \varphi}{\partial r}\right) + \frac{1}{r^2 \sin\theta}\frac{\partial}{\partial \theta}\left(\sin\theta \cdot \frac{\partial \varphi}{\partial \theta}\right)$$
$$= \frac{1}{c^2}\frac{\partial^2 \varphi}{\partial t^2}.$$

$$(2.8)$$

Following certain mathematical derivation, [2,3,5,7,8] the
sound power of a double-source can be obtained as

$$W \propto \rho L^2 \frac{v^6}{c^3} = \rho L^2 v^3 M^3.$$

$$(2.9)$$

Quadrupole source: When high speed gases are exhausted as
a jet, compressive stress tensor $T_{i,j}$ varies to produce quadru-
pole radiation. A quadrupole source can be viewed as two pairs
of dipole sources at 180° to each other. Its directionality is
shown in Figure 3.1. The sound power of a quadrupole source is

$$W \propto \rho L^2 \frac{v^8}{c^5} = \rho L^2 v^3 M^5.$$

$$(2.10)$$

§2.2 Fan noise

Air handlers, blowers, propeller airplanes, rotating com-
pressors, motors with cooling fans, etc. produce noise which
arises mainly from the rotating fans.

78

Fan noise is composed of the noise from rotation and noise from eddy currents.

Rotation noises: They are also called blade noises. They are produced because the rotating blades periodically make impact on air particles, and lead to fluctuations of the air pressure. This pressure fluctuation can be resolved, through Fourier series, into one steady component and a series of vibration components, as shown in Figure 2.2. The steady component is the required air pressure for the aerodynamic equipment. The vibration components are the rotation noise from the blades.

a. steady component
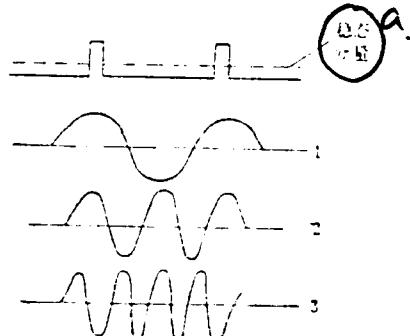
Figure 2.2 Schematic diagram showing the Fourier
components of the rotation noise from
a fan
1, 2, and 3 are, respectively, the 1st,
2nd, and 3rd order harmonic wave.

The frequency of the rotation noise is the same as the number of impacts on air particles by the blades. The value is

$$f_i = (nZ/60)i, \qquad (2.11)$$

where n--- revolutions per minute; Z--- number of blades; i = 1, 2,3,....--- harmonic wave index. For a fan with Z symmetrically arranged blades, when it rotates at n revolutions per minute, the fundamental frequency of the rotating noise is

$$f_1 = nZ/60. \qquad (2.12)$$

This fan has rotating noise with harmonic waves with $f_2 = 2f_1$, $f_3 = 3f_1$, ...

For example, for a Model K-4250 turbine blower, with the number of blades Z = 13, when n = 2600 rpm,

$$f_1 = nZ/60 = (2600 \times 13)/60 = 560 \text{ Hz},$$

$$f_2 = 2f_1 = 1120 \text{ Hz},$$

$$f_3 = 3f_1 = 1680 \text{ Hz}.$$

Experimental results as shown in Figure 2.3 (analyzer is a narrow band wave filter), peak values occur at 560, 1120, and 1680 Hz.

a. sound pressure level (db)

b. db
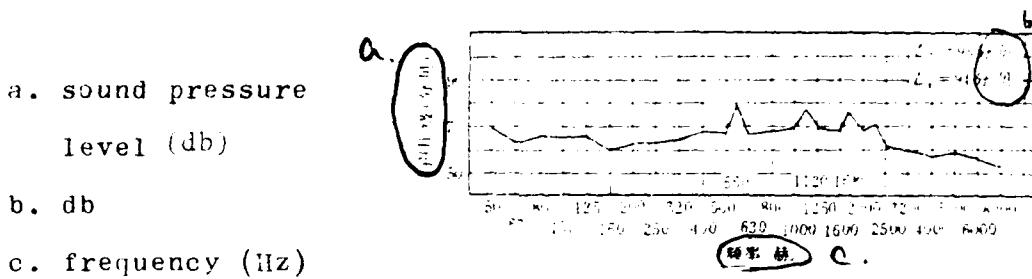
c. frequency (Hz)

Figure 2.3 Noise frequency spectrum of a K-4250 blower

$$n = 2600 \text{ rpm}, \quad Q = 4250 \text{ m}^3/\text{min}$$

Eddy current noise: When blades rotate and produce eddy currents in the surrounding gases, such eddy currents will further

80

break into a series of independent small eddy currents, due to the effect of viscosity. The processes of eddy current formation and their breaking-up lead to the vibration of air, causing the formation of compressive and expansive regions, resulting in the occurrence of noise.

The eddy current frequency is

$$f_i = sh(v/D)i, \tag{2.13}$$

where sh--- Stowreu-Hali number, in the range of 0.14-0.20 and generally taken as 0.185; v--- relative velocity between the gas and materials; D--- the projection of the front width of a body in the direction normal to the velocity plane; i = 1, 2, 3, ... --- harmonic wave index.

When the fan rotates, the eddy current frequency is determined by the relative velocity between the blade and the gas. The tangential velocity of the rotating blades varies with the distance from the center of rotation. From the center to the maximum circumference, the velocity varies continuously. Therefore, the eddy current noises of fans show clearly continuous spectra.

As far as fan noises are concerned, the rotation noises dominate for machinery with high power and large tangential velocities, such as airplane propellers, large blowers, etc. On the other hand, as in air-conditioners, the eddy current noises dominate.

The noise frequency spectra of rotating machinery often have base lines in the form of continuous spectra over broad

81

frequency ranges. On top of them are several peaks (not notice-
able at low power and slow rotating speeds). This is the result
of mixing between the rotation noise and eddy current noise..

For wind generators or any other aerodynamic equipment
utilizing fans (e.g., wind tunnel), the fan noise dominates.
In addition, wind guide plates, elbows, cross-sectional varia-
tions, local obstacles, the shell of centrifugal wind generators,
etc. also produce not too small eddy current noise. The re-
sonance of the wind generators' shells and the wind pipes can
also produce noise, particularly when the aerodynamic equipment
is not well installed, with a lack of dynamic equilibrium, or
when the shells are broken. In these cases, noise increases
significantly.

Figures 2.4- 2.11 show experimental results on noise pro-
duced by aerodynamic equipment with fans (testing points are
generally selected at 1 m from the equipment and 1.5 m high).

a. octave-band sound pressure
   level (db)
b. frequency (Hz)
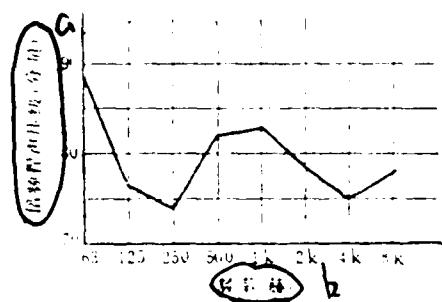
Figure 2.4   Noise frequency spectrum of Brown-
             Bovery steam generators.
             n = 1000 rpm,   N = 4200 kW

82

a. octave-band sound pressure

level (db)
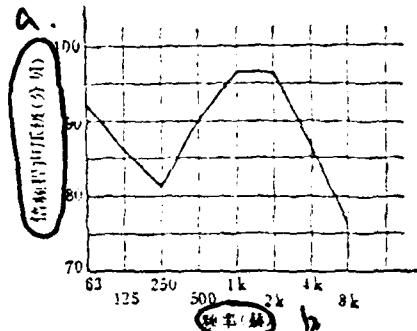
b. frequency (Hz)

Figure 2.5 Noise frequency spectrum of ALG blowers,

n = 3200 rpm, Q = 1400 - 1600 m^3/min

a. octave-band sound pressure

level (db)
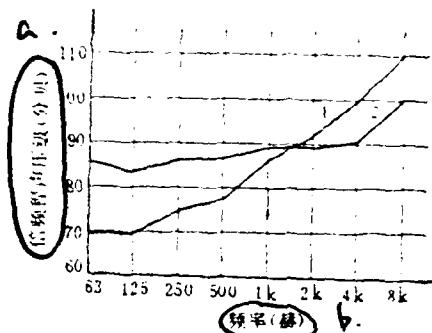
b. frequency (Hz)

Figure 2.6 1---noise frequency spectrum of 6500 air

blowers,   n = 1450 rpm, Q = 6500 m^3/min

2---noise frequency spectrum of 3500 air

blowers,   n = 965 rpm, Q = 3500 m^3/min

a. octave-band sound pressure

level (db)
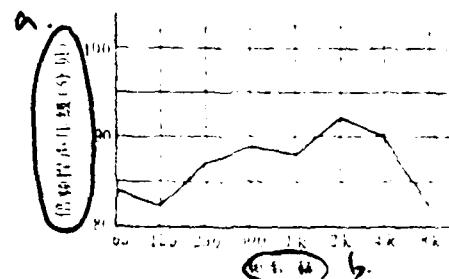
b. frequency (Hz)

Figure 2.7   25000 m^3/hr turbine compressors.

n = 4320 rpm, Q = 25000 m^3/min

83

a. octave-band sound pressure

level (db)
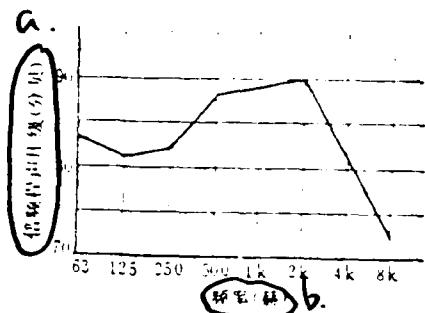
b. frequency (Hz)

Figure 2.8 Noise frequency spectrum of D50-11 com-
pressors,   n = 8890 rpm, Q = 50 m^3/min

a. octave-band sound pressure

level (db)
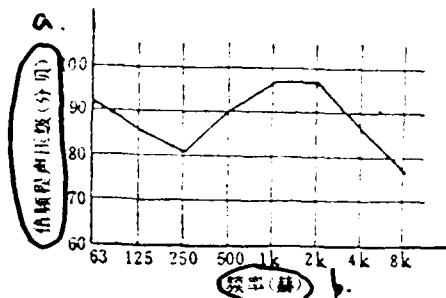
b. frequency (Hz)

Figure 2.9 Noise frequency spectrum of 1JB51-2
electrical generators.

a. octave-band sound pressure

level (db)
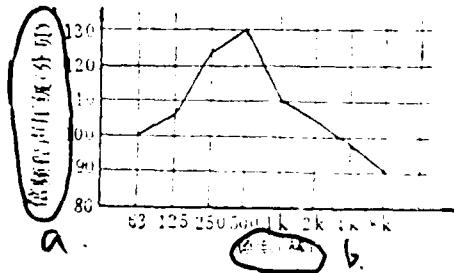
b. frequency (Hz)

Figure 2.10   Noise frequency spectrum of a certain wind
tunnel. This wind tunnel uses two Model
LS4 Rotz blowers to supply wind,
n = 970 rpm, Q = 5000 m^3/min

a. sound pressure level (db)
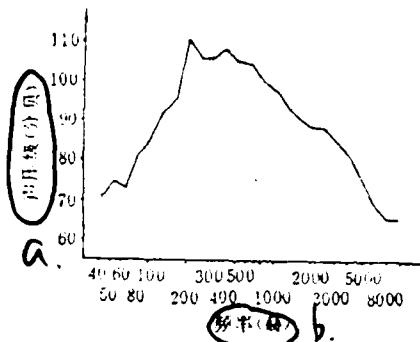
b. frequency (Hz)

Figure 2.11 Noise frequency spectrum of ZBY-24-16B main

fans. n = 750 rpm, q_t = 50-120 m^3/sec

In terms of sound source characteristics, the fan noises belong to double sound sources, i.e., dipole sources. The solution for the dipole radiation equation (2.4) is

$$\rho = \frac{1}{4\pi c_0^2} \frac{\partial}{\partial x_i} \int_v \frac{F_i\left(\mathbf{y},\ t - \frac{|\mathbf{x} - \mathbf{y}|}{c_0}\right)}{|\mathbf{x} - \mathbf{y}|} dV,$$

(2.14)

where $\mathbf{y}$ --- the coordinate of the fluid unit dV under consideration; $\mathbf{x}$ --- the coordinate of the testing point in a far field outside the stream; $r = |\mathbf{x} - \mathbf{y}|$ --- distance between the unit volume and the testing point.

In a far field, equation (2.14) can be simplified to become

$$\rho \approx \frac{1}{4\pi c_0^3} \frac{x_i}{r^2} \int \frac{\partial}{\partial t} F_i dV.$$

(2.15)

Through certain mathematical derivations, one can obtain the equation (2.9) for the sound power of dipole sources. From equation (2.9), the sound power of dipole sources is proportional to the sixth power of velocity. This is in agreement with

85

experimental results. Figure 2.12 shows typical examples of the relationship between noise and tangential velocity for various rotating blades. It can be seen that, the fan noise sound power is more or less proportional to the sixth power of the tangential velocity of the blades, and sometimes it is proportional to the 5.5th power.

a. sound power level (db)

b. m/s
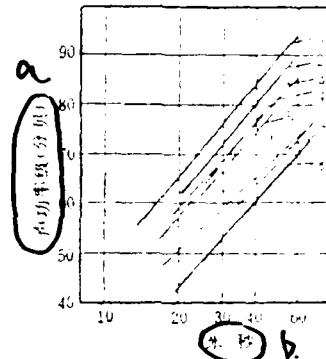
Figure 2.12 Relationship between the noise and the tangential velocity for rotating blades with different cross sections

1 --- W = constant x v^6;

2-7 --- blades with different snapes;

8 --- w = constant x $v^{5.5}$

The sound power of fan noise is also proportional to the square of the fan diameter, and is related to the resistance coefficient of the fan and the shape of the fan. In mathematical terms

$$W \propto \rho \xi^2 D^2 \frac{v^6}{c^3},$$ (2.10)

where ξ --- normal resistance coefficient; v--- tangential velocity; D--- fan diameter.

86

E.Ya. Yudin gave [7] the sound power for smooth blades of wind generators

$$W = K \frac{\rho_0}{c^3} (\xi s h)^2 v^6 l D,$$

(2.17)

where k = 0.04 --- proportional coefficient; v --- tangential velocity; l --- length of blades; D --- transverse length of blades, such as diameter. For rotating bodies with rough surfaces, the sound power is

$$W = \frac{1}{7} K \frac{\rho_0}{c^3} (s h \xi)^2 (1 - K_n)^6 v_R^6 D R (1 - \bar{d}^2) Z$$

(2.18)

where v_R --- tangential velocity of the tip of the rotating blades; D --- transverse dimensions of the rotating blades in the direction perpendicular to the impact flux; R --- radius of rotating blades; $\bar{d}$ --- the ratio between the radius of the cover tube of the rotating body and the radius R: Z --- number of rotating blades; k_n = 0.05.

When actual testing data are lacking, the sound power levels of wind equipment noise can be estimated from the following equation:

$$L_w = \tilde{L}_w + 10 \log (Q H^2) \quad (db),$$

(2.19)

where $\tilde{L}_w$ --- specific sound power level of the wind generator, the sound power level of a same class of wind generators with unit wind volume (m³/hour) and unit wind pressure (1 mm water column); $_Q$ --- flow volume of the wind generator (m³ hour): H --- total wind pressure of the wind generator, mm water column.

87

The Chinese model 4-62, model QDG, and model 4-72 wind generators have specific sound power levels $\tilde{L}_w$ as shown in Table 2.1. [10]

Table 2.1   Specific sound power levels of several
kinds of wind generators

a. model of the
   wind equipment

b. model

c. (db)

a (model of the wind equipment)											
4-62 (b)			QDG (b)			HDG (b)			4-72 (b)		
$\bar{Q}$	$\frac{L_w}{}$ (c)	η	$\bar{Q}$	$\frac{L_w}{}$ (c)	η	$\bar{Q}$	$\frac{L_w}{}$ (c)	η	$\bar{Q}$	$\frac{L_w}{}$ (c)	η
0.05	34	0.5	0.1	27	0.12	0.68	35	0.78	0.05	40	0.60
0.1	24	0.68	0.14	23	0.16	0.77	34	0.92	0.10	32	0.70
0.14	23	0.73	0.18	22	0.20	0.54	26	0.85	0.15	22.5	0.81
0.18	25	0.72	0.2	22	0.25	0.86	21	0.87	0.20	19	0.91
0.22	28	0.65	0.24	23	0.3	0.9	23	0.85	0.25	21	0.87
0.26	35	0.5	0.28	28	0.35	0.75	28	0.74	0.30	27	0.76

1) $\bar{Q}$ in the Table is the flow volume coefficient:

$$\bar{Q} = \frac{Q}{\frac{\pi}{4} \times D^2 \times v \times 3600},$$

where D --- fan diameter of the wind generator, m; v --- tangential velocity of the wind generator fan, m/s; Q --- flow volume of the wind generator, m^3/hour.

2, η is the wind generator's total pressure efficiency. The sound power level of each frequency band for the wind generator

$$L_{w_i} = L_w + \Delta L_w \quad \text{db}, \tag{2.20}$$

where ΔL_w --- correction value for each frequency band's sound power level for the wind generator, db.

88
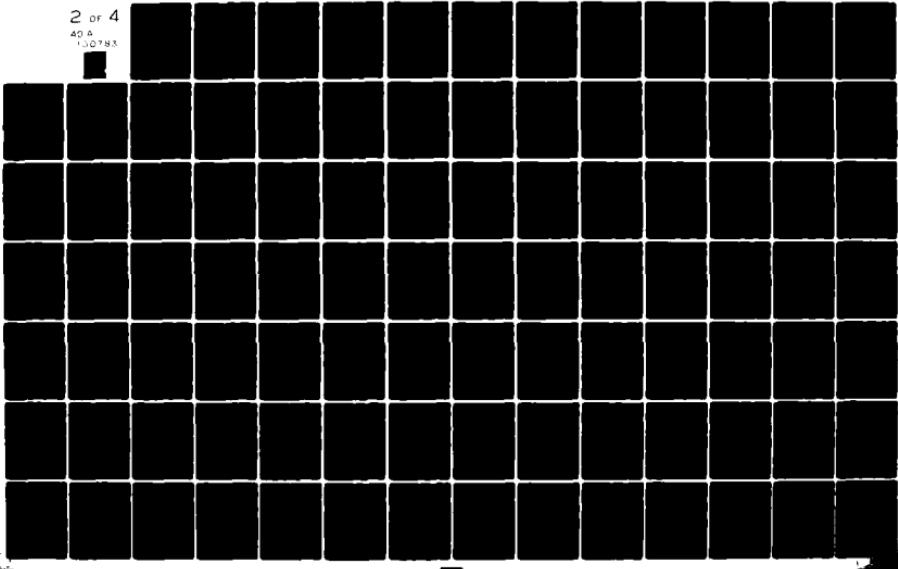
L. L. Brenak [9] derived the correction value ΔL_w curve as shown in Figure 2.13 for both centrifugal type wind generator and the axial flow type wind generator. As seen from the figure, the axial flow wind generator has relatively flat frequency characteristics, which decreases somewhat at low and high frequencies. For the centrifugal type wind generator, the sound power level is high at low frequencies, and decreases with increasing frequency at a slope of 5 db/octave band.

a. axial flow fan

b. centrifugal fan

c. sound power frequency-band level, the db number with the total sound power as the reference standard
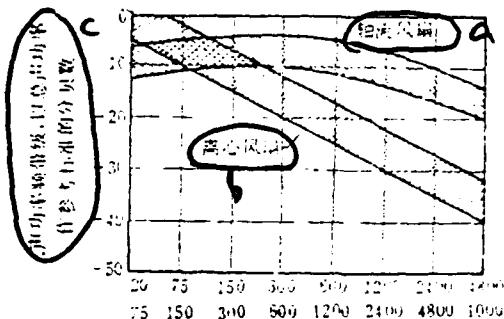
Figure 2.13 Correction curves for sound power levels at each frequency band

Table 2.2 [10] gives the ΔL_w values for several wind generators. From this one can calculate the sound power level of each frequency band.

After the sound power level is obtained, the total sound pressure level and the sound pressure level for each frequency band can be calculated from equation (1.16). Finally the frequency spectrum curves can be obtained.

Table 2.2 ΔL_w values of several wind generators[1]

通风机 类型 中心频率(赫) ΔL_w (分贝)	63	125	250	500	1k	2k	4k	8k
d 离心风机,叶片向前弯	−3	−7	−11	−15	−19	−23	−27	−31
e 离心风机,叶片向后倾	−2	−8	−14	−20	−26	−32	−38	−44
f 轴流风机	−9	−7	−6	−6	−7	−10	−13	−17

1) Model 4-62 wind generator, flat blades back-tilted;

Model 4-72 wind generator, airplane wing type blades

back tilted;

Model QDG wind generator, curved blades strongly back

tilted;

Model HDG wind generator, curved blades back tilted:

Model 9-57 wind generator, blades bending forward.

a. central frequency (Hz)

b. (db)

c. wind generator type

d. centrifugal wind generator, blades bending forward

e. centrifugal wind generator, blades back tilted

f. axial flow wind generator

§2.3 Jet Noise

Air compressors, blowers, chemical reactors, high pressure
vessels, jet sprayers, steam boilers, and jet airplanes, in the
process of exhausting or ejecting gas into atmosphere, disturb
the steady state of the atmosphere and cause great disturbance.
This is due to the turbulent mixing of the high speed gas par-
ticles and the low speed gas particles in their surroundings.
Strong jet noises can thus be produced. Jet noises have sound
power levels as high as 130-160 db, with the sound levels at
110-150 db(A) near the exhaust outlet, seriously polluting the
quietness of the surrounding.

For instance, the noise level is 110-125 db(A) at 1 m from
the exhaust outlet of an air compressor (with pressure below 10
atmospheres). The noise level gradually increases with increas-
ing exhaust pressure, as shown in Figure 2.14.

a. A-sound level (dbA)
b. 1 m from the exhaust outlet
c. meter pressure
d. atmosphere
e. flow volume
f. m^3/min
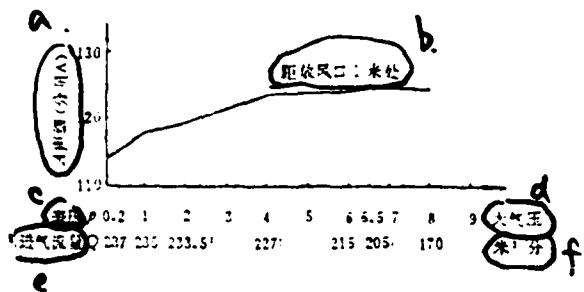
Figure 2.14 Exhaust noise level for Model K-250
Air compressors

Such noises are strong, making people feel pressure on their
chests, headaches and facial heating. In passing nearby, it seems
that a stream of air enters the ear, causing aching and itching.

91

Another example is boilers of medium pressures (30 atmos-
pheres). At 1 m from the exhaust outlet, exhaust steam has a
noise of 135-140 db(A). For high pressure boilers (100 atmos-
pheres) it reaches 140-150 db(A). Therefore, in exhausting steam
from high pressure/large volume steam boilers, if no sound sup-
pression is used, interference at different degrees can reach up
to several kilometers: For instance, students can not hear the
orders of gym teachers in schools, some patients in hospitals
will shiver such that nurses can not give them shots, and few
people will not be woken up from sleep.

Jet noise increases with increasing flow rate. For medium
and small blowers (wind volume at approximately 1000 m^3/min),
when being exhausted, noise of 120 db(A) is produced near the
exhaust outlet. For large blowers (such as Model K-4250 blowers
with wind volume at 4250 m^3/min) the noise can reach as high as
130-140 db(A). Table 2.3 shows the variation of noise, caused
by exhausting a model K-4250 blower, with flow rate.

Table 2.3 Exhaust noise from a Model K-4250 blower

a. wind volume (m^3/min)
b. 1 m from exhaust
   outlet
c. near the exhaust
   outlet
d. db
e. remarks
f. wind pressure
   1.2 kg/cm^2
g. wind pressure
   1.6 kg/cm^2
h. m^3/min.

a	b	c		e
h	d	d	d	d
3600	110	106	127	125
3750	111	107	128	126
3900	111	107.5	12.	12.
4050	112	108.5	12.	127
4250	113	110	130.5	12.
4450	114	119	135	131
4600	124	123	13.	13.
4900	126	125	130.5	13.

92

Large-scale blowers have high intensity, broad spectral exhaust noise, overshadowing other sounds in their surroundings (such as conversations, broadcasting, automobiles, and trains' traffic signals and other signals for dangerous situations), and make people feel uncomfortable. If there is no sound reduction mechanism when large-scale blowers are exhausted in a certain factory, the whole area near this factory and up to several kilometers away will lose its quietness.

Noise from jet airplanes is well known to people. For instance, the noise as measured under an jet airplane is 135-150 db(A). At a distance of 25 m away, the noise is still as high as 120 db(A). Therefore, jet airplanes not only affect the ground crew's health, but also disturb the normal working and resting of residents along their flying courses.

In terms of sound source characteristics, jet noise belongs to quadrupole sources. For quadrupole sources, Equation (2.4) can be simplified to

$$\frac{\partial^2 \rho}{\partial t^2} - c_0^2 \nabla^2 \rho = \frac{\partial^2 T_{ii}}{\partial x_i \partial x_i},$$

(2.21)

where ρ --- gas density, c_0 --- sound velocity in a static medium; T_{ij} --- compressive stress tensor at any point in space.

Compressive stress tensor T_{ij} is mainly determined by the kinetic energy flux tensor $\rho v_i v_j$. The change in kinetic energy flux is balanced by action forces. In pure air streams, the change in action force is due to the change in pressure. Higher pressure causes higher density, yielding the source of noise.

93

For far fields, i.e., at distances much greater than the
sound source dimensions and the sound wavelengths, Equation (2.21)
has the solution (in terms of sound power) as

$$W = \frac{1}{4\pi^2 \rho_0 c_0^5} \int_V \int_S \left(\frac{x_i x_j}{x^2}\right)^2 \left[\frac{\partial^2 T_{ij}}{\partial t^2} dV\right]^2 dS,$$

$$(2.22)$$

where V--- jet fluid volume; S--- area enclosing the jet stream.

Equation (2.11) can be more directly expressed as

$$W = K \frac{\rho_c^2 V_c^8}{\rho_0 c_0^3} D^2 \frac{1}{\left(0.6 \dfrac{T_0}{T_c} + 0.4\right)^2},$$

$$(2.23)$$

where ρ_c, ρ_0 --- density of the jet stream and the surrounding
medium; T_c, T_0--- absolute temperature of the jet stream and the
surrounding medium; V_c--- jet stream velocity; D--- diameter of
the exhaust opening; K--- proportionality constant.

It can be seen that, the sound power of jet noise is pro-
portional to the eighth power of the jet stream velocity. This
is the famous eighth-power theorem. In the meantime, the sound
power of jet noise is also related to factors such as the dia-
meter of exhaust opening, the gas density, temperature of the
medium, etc. With

$$L_i = \frac{\rho_c^2 V_c^8}{\rho_0 C_0^3} D^2 \frac{1}{\left(0.6 \dfrac{T_0}{T_c} + 0.4\right)^2}$$

$$(2.24)$$

94

representing the Lighthill number, Figure 2.15 gives the relation-
ship between the sound power of jet noise and the Lighthill
number. This is obtained from analyzing some gases' jet noise
including the jet noise of jet airplanes.

a. sound power (watt)

b. Figure 2.15 Relationship between
   the sound power of jet noise
   and the Lighthill number

c. mm

d. jet generators
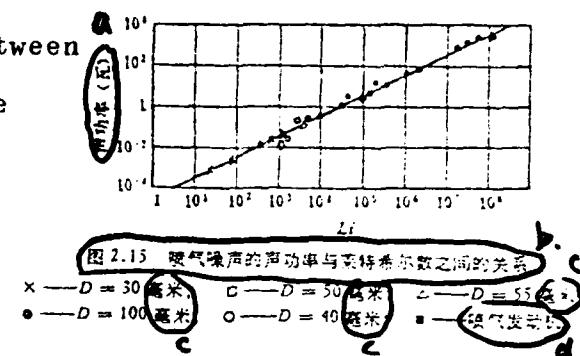
From these data we have the value for the coefficient
$K = 2.8 \times 10^{-5}$ in equation (2.23).

Figure 2.16 shows the flow pattern of jet streams. There
are two sections for the whole jet stream: The initial section
and the main body section. The initial section has a fixed core
velocity; its length is about 5 times the diameter of the exhaust
opening. The main section extends much further.

a. core

b. turbulent area
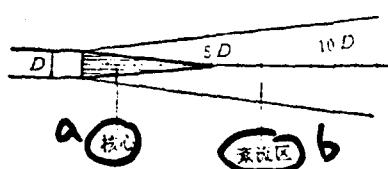
Figure 2.16 Flow pattern of jet streams

Figure 2.17 shows the relationship between the variation
of the sound power radiated from a given portion of the jet stream
and the distance X of that portion from the exhaust opening, i.e.,
the relationship between $\dfrac{dW}{Wd\left(\frac{X}{D}\right)}$ and X/D. In the initial sec-
tion covering a distance from the exhaust opening equal to 5 times
the diameter of the opening, the noise sound power of a unit volume
comprises more than one-half of the total jet stream's sound power.
Furthermore, the unit volume radiation has a noise sound power
independent of the distance of this unit volume from the exhaust
opening. In the main body section further away from the exhaust
opening, radiated sound power of the jet stream's unit volume
decreases drastically in seventh power with increasing distance
from the exhaust opening. Therefore, jet noise is caused mainly
by the jet section within a distance from the jet opening 6 times
the diameter of the opening. This point has an important meaning
in jet noise control. Currently for jet airplanes, noise control
is indeed made within a distance from the jet opening 6 times the
diameter of the opening. The noise is greatly reduced.
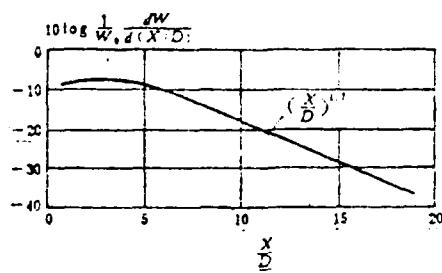
Figure 2.17 Radiated noise sound power from jet streams

96

Jet noise has a broad continuous frequency spectrum. Also, at different observation positions, the frequency spectra are very different. As can be seen from Figure 2.18, jet streams near the jet opening radiate mainly high frequency noise. Since the pressure is high and flow rate is high, the radiated noise sound levels are rather large. When the distance from the jet opening increases, the low frequency components gradually increase.

The relationships between the third-octave frequency band of jet noise and D, V_c, sh are [15]:

$$sh = \frac{fD}{V_c} , \qquad\qquad (2.25)$$

$$X/D < 4, \quad sh = (\frac{0.2}{X/D})^{0.38} , \qquad\qquad (2.26)$$

$$X/D \geq 4, \quad sh = (\frac{1.8}{X/D})^{1.43} , \qquad\qquad (2.27)$$

The strength of jet noise is also different at different directions. As shown in Figure 2.19, the maximum radiation occurs within $\varphi = 30^\circ$, which is the angle with the jet stream axis.

a. sound pressure level (db)
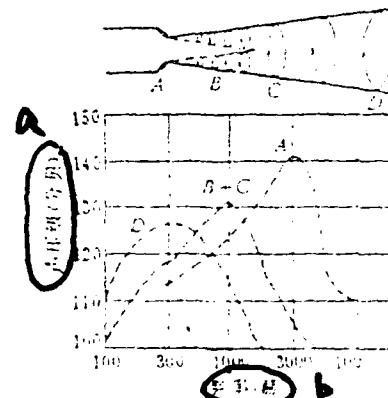
b. frequency (Hz)

Figure 2.19   Comparisons of noise sound levels and frequency spectra at different parts of jet streams

97

a. db
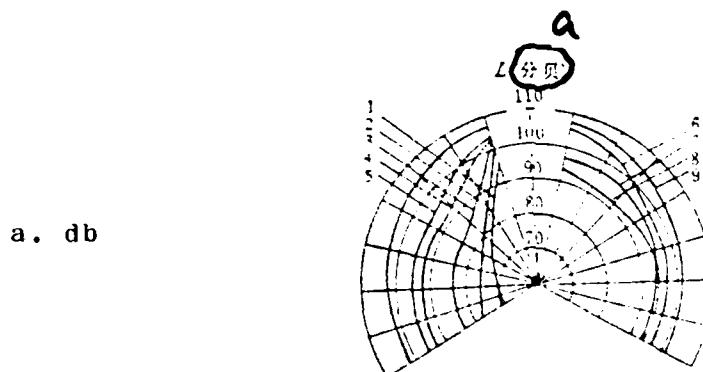
Figure 2.19 Directional characteristics of jet noise

D = 80 mm; 3 m from jet opening; U_c = 280 m/s

1. 50 Hz; 2. 100 Hz; 3. 200 Hz; 4. 400 Hz; 5. 800 Hz;

6. 1600 Hz; 7. 3200 Hz; 8. 6400 Hz; 9. Total sound

pressure level

For far sound fields, using Equation (2.17) and Figure 2.20
one can calculate the noise sound pressure level L_p at a distance
r from the jet opening and an angle φ :[7]

$$L_p = 10 \quad \log \frac{W}{W_0} \cdot \frac{1}{4\pi r^2} + 10 \log \phi$$

$$= L_W - 20 \log r - \theta + (1 + b)\, 10 \log \phi , \qquad (2.28)$$

where θ = 11 db in spherical radiation; θ = 8 db in semi-spherical
radiation; b = 0.3 $(T_c - T_0)/T_0$.
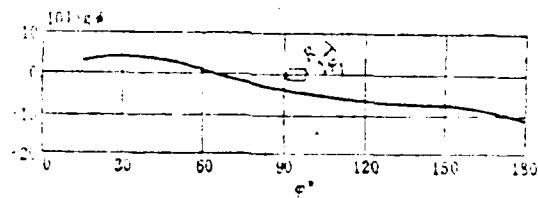
Figure 2.20   Abstract directional characteristics of
jet noise

98

For near sound fields, at distances smaller than one diameter from the edges and larger than two diameters from the jet opening, noise sound pressure level can be determined from the following equation:

$$L_p = L_w + \frac{40}{\sqrt{\Pi_c}} - 0.6\frac{X}{D} - 20\frac{\sigma}{D} \cdot \quad (2.29)$$

where Π_c --- pressure drop at the jet opening; σ --- distance from the edge of the jet (choosing opening angle $2\alpha = 20^0$).

Frequency can be calculated from the following equation:

$$f = \frac{c_0}{2D\sqrt{\Pi_c - 1.9}}. \quad (2.30)$$

Figure 2.21 shows the directional characteristics of jet airplanes.

Figures 2.22-2.24 are exhaust noise frequency spectra for, respectively, model K-250 air compressors, model K-4250 blower relieve valves, medium pressure (31 kg/cm^2) steam boilers. It can also be seen that, near such jet noise sources, noises are obviously of the high frequency types. However, even the low frequency components also reach quite high levels. Within some ten meters from the exhaust outlet, there is still basically high frequency sound which irritates hearing. Further out the low frequency sound then dominates.
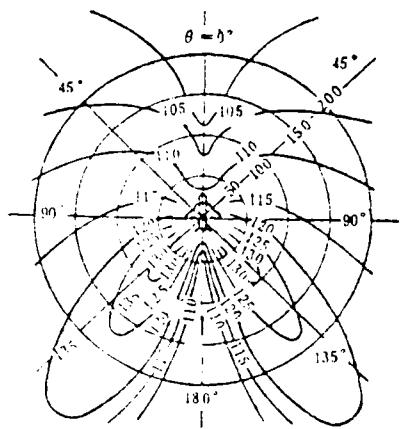
(a) Equi-noise-sound-
level curves (axial
distance (m)) for jet
airplanes
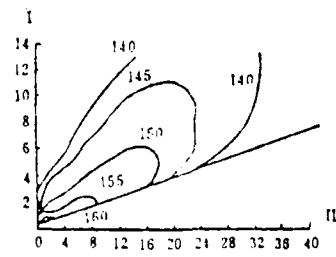
(b) Near sound field of jet
airplanes

I--- perpendicular dis-
tance from jet
opening (m);

II-- distance from the
jet opening along
the axis (m)

Figure 2.21

100

a. m^3/minute

b. Frequency (Hz)

c. Sound pressure
   level (db)
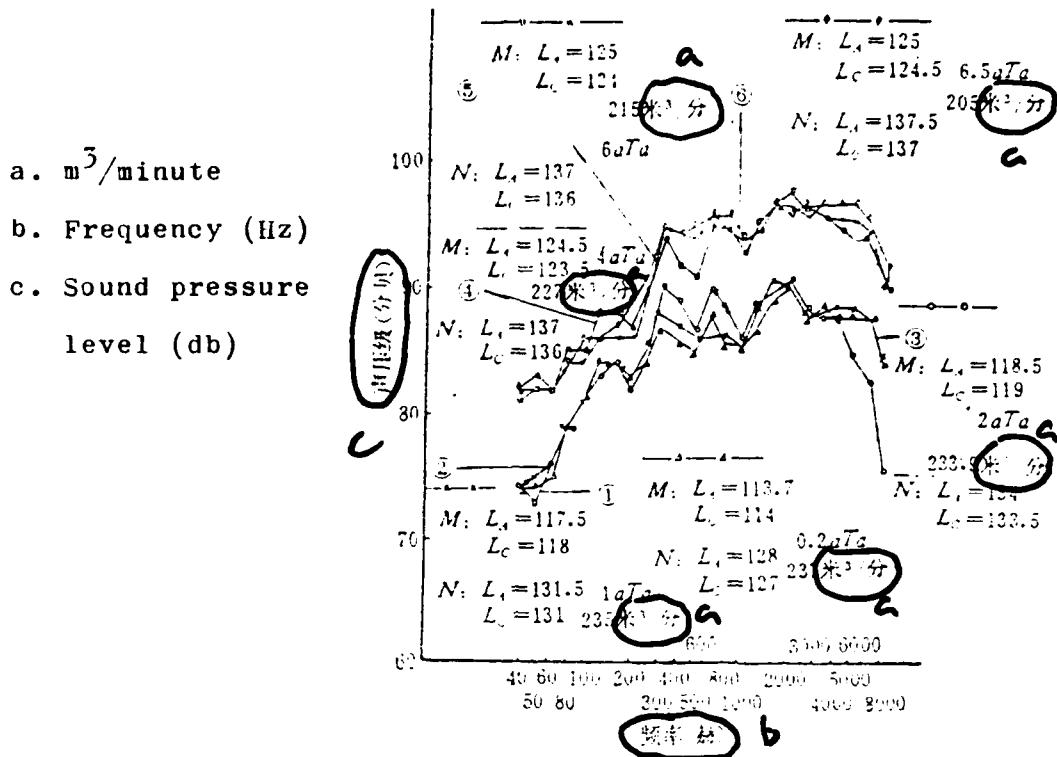
Figure 2.22   Exhaust noise frequency spectra (under
              different pressures) for model K-250
              air compressors

Test point M: 1 m from exhaust opening, sideway;

Test point N: 0.2 m from exhaust opening, direct below;

(1)---pressure 0.2a Ta, flow volume 237 m^3/min;

(2)---pressure 1a Ta, flow volume 235 m^3/min:

(3)---pressure 2a Ta, flow volume 233.9 m^3/min;

(4)---pressure 4a Ta, flow volume 227 m^3/min;

(5)---pressure 6a Ta, flow volume 215 m^3/min:

(6)---pressure 6.5a Ta, flow volume 205 m^3/min:

a. octave-band sound
   pressure level (db)
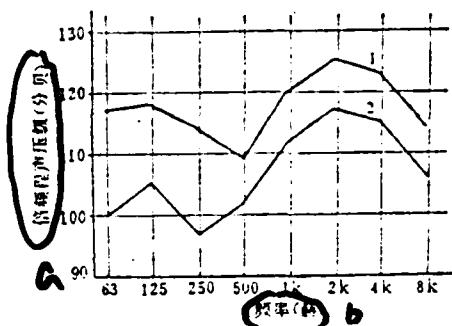
b. frequency (Hz)

Figure 2.23   Noise frequency spectra for the exhaust
              valves of model K-4250 blowers

1. complete exhaust test point

2. small-volume exhaust 0.5 m from the exhaust
   valve

a. sound pressure
   level (db)

b. db
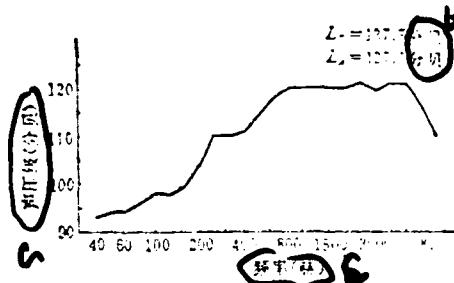
c. frequency (Hz)

Figure 2.24   Complete exhaust noise frequency spectra
              for medium pressure (31 kg/cm^2) steam
              boilers

Test point: 1 m from the exhaust opening

§2.4 Periodic Exhaust Noise

Generators and other aerodynamic machinery, which exhaust
gases periodically, produce strong noise.   The latter seriously
disturbs the quietness of city streets and industrial areas.   For
instance, typical internal combustion engines, at 0.5 - 1 m from
the exhaust opening (45° direction), produce noise with sound
levels at 90-120 db (A).   Some internal combustion engines produce
noise higher than 130-140 db.   Automobiles, tractors, and motor-
cycles with such generators will produce noise with sound levels
at 75-90 db (A) when moving on streets.   If internal combustion
engines are used in city engineering processes (e.g., well drill-
ing, electrical generation, etc.) or on trains, since the power
and rotating speed are both high, noise above 100 db will be
produced in the neighboring areas.   Such noise is   much higher
than that allowed under ambient noise standards, and will clearly
affect the work and rest of a large population.   In several coun-
tries, to avoid the city noise interference, there are window-
less dormitories and windowless schools.   Lighting and air-
changes are all provided by electrical lighting and air-condi-
tioners.

Periodic exhaust noise is   caused mainly by the fluctuations
of gas pressures.   In terms of sound source characteristics, it
is close to single source.   As stated before, a single source is
like a vibrating sphere which expands and contracts evenly.   The
periodic   pressure fluctuations cause the surrounding medium to
oscillate periodically in density, thus producing noise.

103

For a single source, the solution of Equation (2.4) is

$$\rho = \frac{1}{4\pi c_0^2}\int_V \frac{\partial}{\partial t} Q\left(y, t - \frac{|x-y|}{c_0} \frac{dV}{|x-y|}\right),$$

(2.31)

where y --- the coordinate of the fluid unit dV under considera-
tion; x --- coordinate of the test point in a far sound field.

In a far sound field, $|x-y| \approx |x|$, Equation (2.31) can
be simplified to

$$\rho \approx \frac{1}{4\pi c_0^2 |x|} \frac{\partial}{\partial t}\int_V Q(y, t)\, dV.$$

(2.32)

In a far sound field, the relationship between the sound
power of single source radiation and the density ρ is

$$W = 4\pi r^2 \frac{\rho^2}{\rho_0} c_0^3,$$

(2.33)

where r is very large,

$$\rho^2 \sim \frac{1}{c_0^4 r^2} f^2 Q^2 V^2,$$

(2.34)

where $f \sim \frac{\partial}{\partial t}$ --- oscillation frequency, approximately equal to
v/L (v is velocity, L is the relevant length).

By substituting Equation (2.34) into Equation (2.33), Equa-
tion (2.7) can be obtained to relate the sound power W to density
ρ , flow velocity v, length L, and sound velocity c.

2.4.1 Exhaust noise from internal combustion engines

We will now study in detail the relationship between the
periodic exhaust noise of internal combustion engines and the
parameters.

104

a. sound pressure level
   (db)
b. exhaust volume (cc)
c. axial horsepower
c. torque (kg.m)
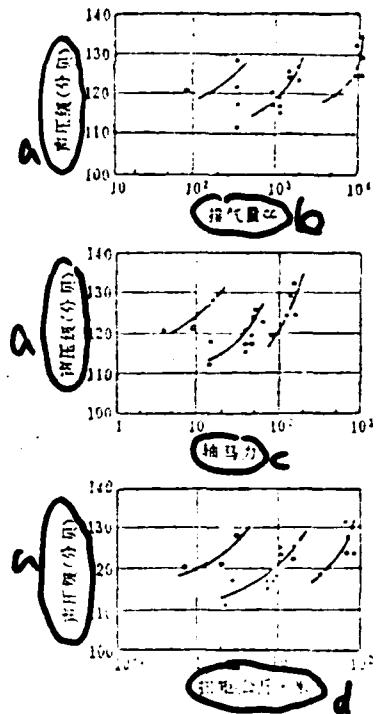
Figure 2.25   Relationship between the exhaust noise
              from automobile engines and the exhaust
              volume, axial horsepower, and torque
              (60% of specified speed)

We know that the combustion of gasoline or diesel fuel
inside a cylinder produces very high pressure. When the exhaust
valve is open, violent pressure fluctuation will occur, leading
to the formation of exhaust noise.   The sound power of engine
exhaust noise depends mainly on the power (axial horsepower) of
the engine, exhaust volume (or the cylinder volume), torque,

105

average effective pressure inside cylinder, area of the exhaust opening, rotating speed, etc.

a. sound pressure level (db)

b. actual average effective pressure x area of exhaust opening (kg)
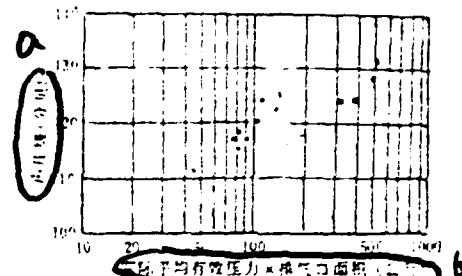
Figure 2.26 Automobile gasoline engine and diesel engine: Relationship between the exhaust noise and the actual average effective pressure times the area of exhaust opening (60% of specified rotating speed)

a. sound pressure level (db)

b. actual average effective pressure x area of exhaust opening (kg)
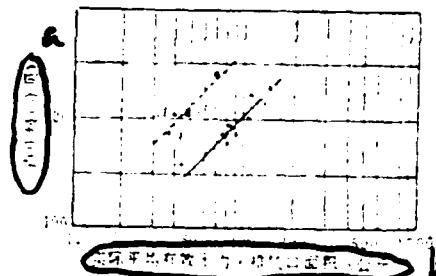
Figure 2.27 Two-stroke and four-stroke automobile engine: Relationship between exhaust noise and actual average effective pressure times the area of exhaust opening

Figure 2.25 - 2.27 [16] are, respectively, relationships between the automobile engine exhaust noise and the exhaust volume, axial horsepower, and torque, and relationships between the automobile engine exhaust noise and the actual average effective pressure times the area of exhaust opening (test point

106

at 45° and a distance of 0.5 m from the exhaust opening). In
the Figures A refers to air cooling; the symbol without a letter
refers to water cooling; o is for a 2-stroke gasoline engine;
● is for a 4-stroke gasoline engine; ▢ is for a 2-stroke diesel
engine; and ■ is for a 4-stroke diesel engine.
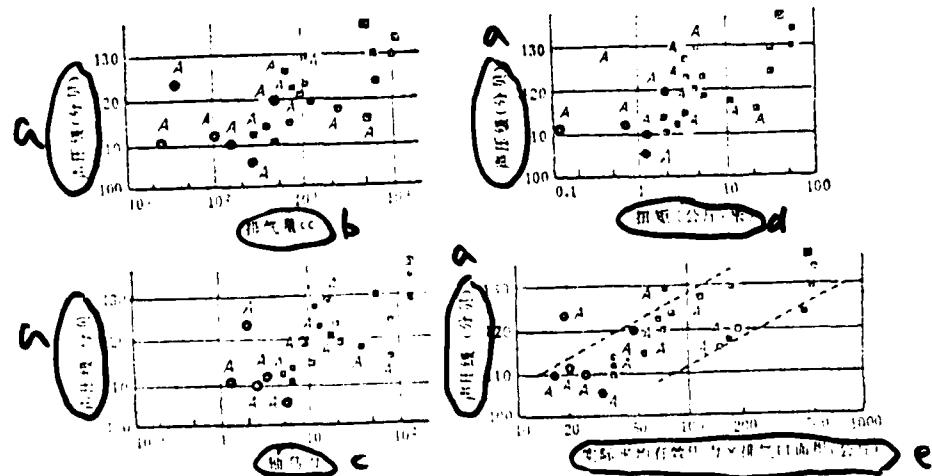
Figure 2.2S Engines used in industry and agriculture:
Relationship between the exhaust noise and the exhaust
volume, axial horsepower, torque, and actual average
effective pressure times area of exhaust opening

a. sound pressure level (db),   b. exhaust volume cc,

c. axial horsepower,   d. torque (kg·m),   e. actual average
effective pressure x area of exhaust opening (kg)

107

Figure 2.28-2.30 are respectively, the relationships between
the engineering and agricultural engines' exhaust noises and the
exhaust volume, the axial horsepower, and torque; the relation-
ships between the engines' exhaust noises and the actual average
effective pressure times the area of the exhaust opening; and
the relationships between the sound power levels of the engines'
exhaust noises and the engines' rotating speed and actual average
effective pressure (same testing points as before). Symbols with
A refer to air cooling; symbols without a letter refer to water
cooling. ◎ is for 2-stroke gasoline engines, ⊙ is for 4-stroke gasoline engines,
▣ is for 2-stroke diesel engines, and ▣ is for 4-stroke diesel engines.

a. sound pressure level (db)
b. actual average effective
   pressure x area of exhaust
   opening (kg)
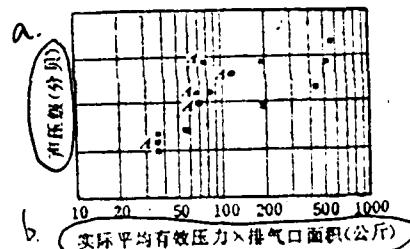
Figure 2.29 Comparisons between water-cooling and
           air-cooling 4-stroke engines used in engineering
           and agriculture.

a. exhaust gas sound power
   level (db)
b. number of rotations of the
   engine (rpm)
c. kg/cm^2
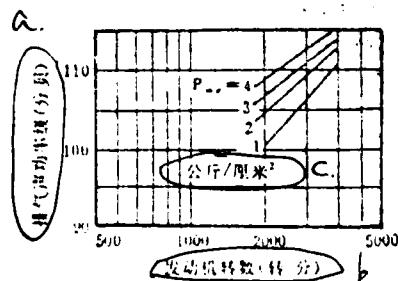
Figure 2.30 Exhaust noises' sound power level with
           a constant actual average effective pressure P_{mt}

108

It can be seen that engine exhaust noises increase with increasing exhaust volume, axial horsepower, torque, and the cylinder's actual average effective pressure times the area of the exhaust opening. When the actual average effective pressure is small, the exhaust noises increase rapidly with increasing engine rotating speed. However, with increasing actual average effective pressure, the effect of rotating speed gradually drops. Therefore, the exhaust noises are greatly affected by the cylinder's actual average effective pressure.

When the rating of engines increases, the amplitude variation of the noises from engines of the same kind is between 10-18 db.

For example, the Chinese model 4115 T internal combustion engines widely used in tractors, electrical productions, irrigation, automobiles and city constructions have total sound pressure levels increased from 111 db to 123 db and A-sound levels from 100 db to 118 db, when they change from idling rotation to 55 horsepower. (see Table 2.4 and Figure 2.31)

Table 2.4 Noises from model 4115 T internal
combustion engines
(at 45°, 0.5 m away from the exhaust opening)

Condition	Total sound pressure level (db)	A-sound level (db)
idling	111	100
10 horsepower	113	108
22 horsepower	117	112
55 horsepower	123	118

a. Octave-band sound

   pressure level (db)
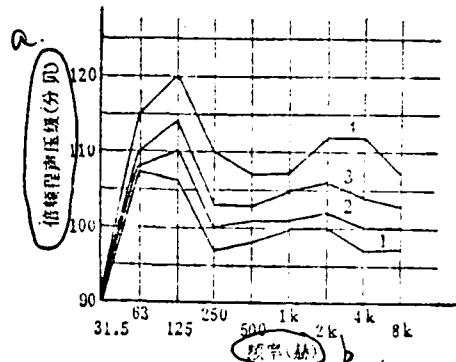
b. frequency (Hz)

Figure 2.31 Frequency spectrum of exhaust noises from

   model 4115T internal combustion engines

   1. idling;   2. 10 horsepower;   3. 22 horsepower;

   4. 55 horsepower

Testing point: at 45°, 0.5 m from the exhaust opening

Another example is the Chinese model BJ212 gasoline engines

(75 horsepower). From 500 rpm and 0.5 kg/cm^2 to 3800 rpm and

4.5 kg/cm^2, the total sound pressure level changes from 110 db

to 128 db, and A-sound level from 105 db to 122 db (see Table 2.5)

Table 2.5 Noises from model BJ212 gasoline engines

(at 45°, 0.5 m from the exhaust opening)

Condition	total sound pressure level (db)	A-sound level (db(A))
500 rpm, 0.5 kg/cm^2	105	110
1000 rpm, 1.75 kg/cm^2	111	119
2000 rpm, 2.75-3.75 kg/cm^2	119	125
3800 rpm, 4.5 kg/cm^2	122	128

The literature gives several quantitative formulas for the

engines' noises. They are given below:

110

Following T. Priede[17]:

4-stroke, diesel engines, without increased pressure:

$$L_A = 30 \log N + 50 \log B - 31.5 \text{ (db)};\qquad(2.35)$$

4-stroke, diesel engines, with increased pressure:

$$L_A = 40 \log N + 50 \log B - 66.5 \text{ (db)};\qquad(2.36)$$

2-stroke, diesel engines:

$$L_A = 40 \log N + 50 \log B - 54.5 \text{ (db)}.\qquad(2.37)$$

Gasoline engines [18]:

$$L_A = 50 \log N + K \text{ (db)},\qquad(2.38)$$

where L_A --- noise level of engines, db(A); N --- rotating speed of engines, rpm; B --- cylinder diameter (or radius), inches; K --- constant.

The above equations refer to the L_A values corresponding to the engines at maximum power, and at 0.9 m from the engines.

Soroka and Chien [19] made a study and analysis on diesel engines with 100-660 mm stroke length and 250-3000 rpm. They obtained the following equation at 1 m from the engines,

$$L_A = 69 + 30 \log C_m + 5 \log S + 5 \log Z \text{ (db)},\qquad(2.39)$$

where C_m --- average velocity of piston, m/s: S --- stroke length; Z --- number of cylinders.

Cimac [20] investigated 4-stroke diesel engines with 10-8000 horsepower and 200 rpm. At 1 m from the engines,

$$L_A = 10 \log (n_N/n_0) + 5.5 \log (N_{eN}/N_0)$$
$$- 30 \log (n_N/n) + 55 \text{ (db)},\qquad(2.40)$$

111

where n_N --- specified number of rotations, rpm; n --- working number of rotations, rpm; N_{eN} --- specified power, horsepower; N_0 --- 1 horsepower; n_0 --- 1 rpm.

Based on the noise measurement data for Chinese model 4115T and 4115L high speed, medium size diesel engines, the relationship between the noise level L_A and the power level N_e of the engines can be expressed by the empirical equation:

$$L_A = a + 13.5 \log N_e, \qquad (2.41)$$

where for model 4115T diesel engines, a = 94.5 db (10-55 horsepower); for model 4115L diesel engines, a = 97.5 db (10-65 horsepower); testing point at 45° and 0.5 m from the exhaust opening of the engines.

The frequency spectrum of engine exhaust noises can be calculated following Equation (2.42):

$$f_i = \frac{nZ}{60\tau} i, \qquad (2.42)$$

where i = 1,2,3, ... --- harmonic wave index; n --- number of rotations of the engine's main axis, rpm; Z --- number of cylinders; τ --- stroke coefficient (for 2-stroke engines, $\tau = 1$; for 4-stroke engines, $\tau = 2$).

Figure 2.32 and 2.33 are the noise frequency spectra (third octave band) of, respectively, the model 411R 4-cylinder engines and the 1500-horsepower diesel engines.

a. third octave band

   sound pressure level

   (db)
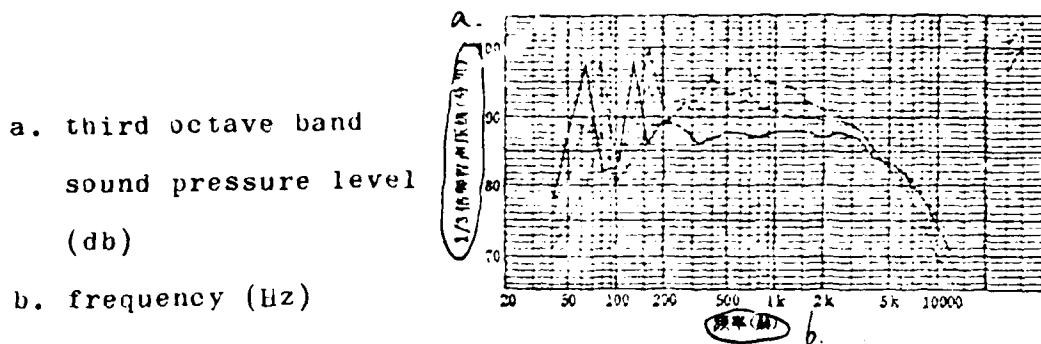
b. frequency (Hz)

Figure 2.32 Noise frequency spectrum of FIAT model

411R 4-cylinder engines

$N = 2.6$ horsepower, $n = 2600$ rpm (no load);

$N = 33.3$ horsepower, $n = 2340$ rpm (normal);

$N = 39$ horsepower, $n = 2300$ rpm (full load);

$N = 35.2$ horsepower, $n = 1910$ rpm (over load)

a. third octave band sound

   pressure level (db)

b. db
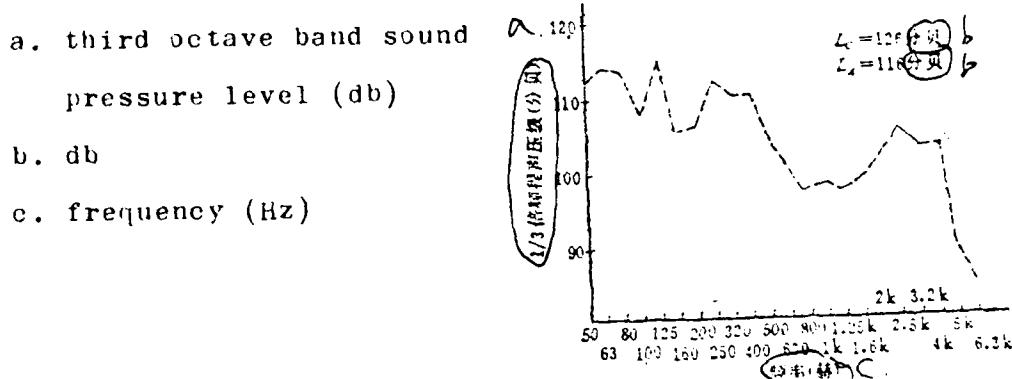
c. frequency (Hz)

Figure 2.33 Noise frequency spectrum of 1500-horsepower

diesel engines.

testing point: at 45^{0} and 1 m from the exhaust opening

Using the model 411R engine as an example, with 4 cylinders,

4- stroke, $Z = 4$ and $\tau = 2$:

113

At no load conditions, n = 2600 rpm, f_1 = 87, f_2 = 174, f_3 = 261, f_4 = 348, ...

At normal working conditions, n = 2340 rpm, f_1 = 78, f_2 = 156, f_3 = 234, f_4 = 312, ...

At full load conditions, n = 2300 rpm, f_1 = 77, f_2 = 154, f_3 = 231, f_4 = 308, ...

At over load conditions, n = 1910 rpm, f_1 = 64, f_2 = 128, f_3 = 192, f_4 = 256, ...

The measurements are made with a third-octave band analyzer. Therefore, at no load, normal working and full load conditions, peak values all show up at 80, 160, 250, and 320 Hz. At over load conditions, the peak values occur at 63, 125, 200, and 250 Hz.

Internal combustion engines' exhaust noises have clearly low frequency characteristics in their spectrum. But the medium and high frequency noises also reach certain levels. The medium frequency noises are induced by the higher harmonic waves of the fundamental frequency, and the high frequency noises are caused by the eddy current noises induced at the exhaust, combustion inside the cylinders, explosion sound, as well as the impact, vibrating parts and self-vibration of the pipe walls.

2.4.2 Noises of the volume-type compressors and blowers

Volume-type compressors and blowers (e.g., piston-type compressors, threaded rod compressors, Rotz blowers) have noises belonging to the periodic exhaust noise category. The mechanism

114

of their noise production is more or less the same as those in internal combustion engines. Among them, the Rotz blowers and the threaded rod compressors have noise as high as 110-140 db(A). Near them, one will feel pressure in the chest, headaches, dizziness, facial heating, and whole-body powerlessness. They not only affect the working condition of machine rooms, but also cause relatively large interference for the surrounding offices, dormitories, schools, and streets.

Rotz blowers are one kind of volume-type gas compressors. They move gases through the rotation of a pair of kidney-shaped gears perpendicular and tightly fitted to each other. The gas flow rate is constant. The pressure can be adjusted within a specified range according to the application requirement.

When the Rotz blowers are used, the two gears rotate relative to each other, periodically compressing the air, leading to the fluctuation of the surrounding air's pressure. Periodic exhaust noise is thus produced. In the meantime, when the gears rotate, the surface forms eddy currents. These eddy currents also produce eddy current noises when they break up at the gears' surface. In general, the periodic exhaust noise is the main component of the Rotz blowers.

The noise strength of Rotz blowers is related to the flow rate, rotating speed and pressure. The noise is stronger if the flow rate is higher, the rotation is faster and the pressure is higher. In general, for a given rotating speed and pressure, the noise increases by 6 db(A) when the flow rate doubles. The noise

115

increases by 3-4 db(A) when the pressure increases by 1000 mm

water column. When the rotating speed is doubled, the noise

increases by 6-10 db(A). Table 2.6 shows the experimental values

of noises from several Chinese-made Rotz blowers. Table 2.7 lists

the experimental values of noises from LGA-80-5000 Rotz blowers

under different pressure conditions. From these tables we can see

the relationship mentioned above.

Table 2.6 Experimental values of noise from several

Chinese-made Rotz blowers

(testing point: 1 m from the inlet along the axial

direction)

a. model number

b. flow rate (m³/min)

c. rotating speed (rpm)

d. pressure (mm water

column)

e. noise level (db(A))

f. production location

g. Chang-Sha

h. Shiang-hai

i. Wu-Han

j. Tien-Jing

a	b	c	d	e	f
D36×35—30/5000	36	960	5000	117	
SD36×35—40/7000	40	1450	7000	125	g
D36×70—60/5000	60	960	5000	123	
D36×60—80/5000	80	1450	5000	129	
D60×45—120/3500	120	960	3500	121	
D60×75—200/3500	200	960	3500	127	
D60×75—200/5000	200	960	5000	128	
LGA-30/3500	30	580	3500	112	h
LGA-40/5000	40	730	5000	116	
LGA-80/5000	80	730	5000	122	
D36×35—40/3500		1450	3500	125	i
D36×35—40/5000		1450	5000	129	
D36×60—80/3500		1450	3500	131	
D36×60—80/5000	80	1450	5000	134	
D36×35—40/3500	40	960	3500	115	j
D36×70—80/5000		960	5000	122	

116

Table 2.7 Experimental values of noises from LGA-50-
5000 Rotz blowers under different pressure conditions
(testing point: 1 m from the inlet along the axial
direction)

a. pressure (mm water
column)

b. noise level (db(A))

c. no load

正 力（毫 米 水 柱）	噪 声 级 [分 贝 (A)]
压 数	105
1000	108
2000	112
3000	115
4000	119
5000	122

Figure 2.34 shows the noise frequency spectra of several
Rotz blowers.

a. octave-band sound
pressure level (db)

b. model number of
wind generators

C. frequency (Hz)

117
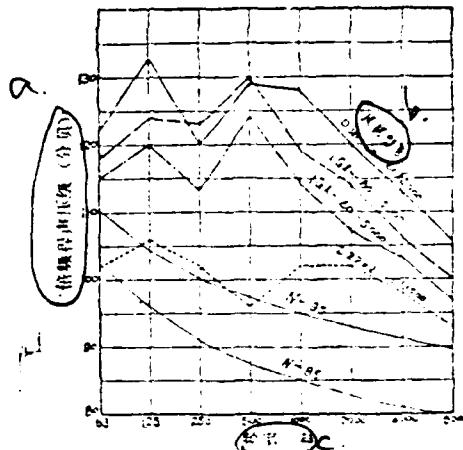
Rotz blowers produce noises with broad continuous spectra, having peak values at low and medium frequency bands. When the pressure is relatively low, i.e., when the load is small, the peak value often occurs at the octave-band with 125 Hz. When the pressure rises to specified values, a peak value in the octave-band with medium frequency of 500 Hz will also appear. This indicates that, along with increasing working pressure, there is a tendency for the noise to increase at medium and high frequencies.

2.4.3 Jackhammer's exhaust noise and the steam-siren's noise

Noises from the jackhammer's exhaust and the steam-siren also belong to periodic exhaust noises.

For example, for the Chinese-made model 0130 jackhammers with pulse frequency of 1800 per minute, there are two exhausts for every piston impact. Therefore, the peak values should occur at 60 Hz and 120 Hz. By placing a microphone in the exhaust stream, the peak values are found to occur just at 63 Hz and 125 Hz, using a third-octave band frequency spectrometer (see Figure 2.35).

a. third-octave band
   sound pressure level
   (db)
b. frequency (Hz)
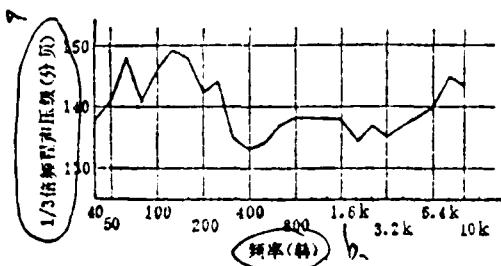
Figure 2.35 Exhaust noise frequency spectrum for jackhammers

118

Another example is the steam-siren. The fundamental frequency is equal to the number of times in a unit time to let exhaust into the atmosphere. With z as the number of holes on the rotating disk of the siren, n being the number of rotations (rpm), then the steam-siren has peak values at

$$f_i = nz/60. \tag{2.43}$$

§2.5 Other aerodynamic noises

2.5.1 Flying noises

In recent years supersonic flight has been developed very fast. Jet airplanes, rockets, space-ships, ... have more and more power, and larger and larger velocities. Strong noise is therefore produced. For instance, the sound power level can reach 160 db for turbo-jet airplanes having back combustion equipment. The sound power reaches 10,000 watt. For jet airplanes the sound power level reaches as high as 170 db and the sound power reaches 100,000 watt. For space-ships the sound power level even reaches 180-193 db, and the sound power reaches several million or tens of million watt. Table 2. 5 [22] gives the results from a 1964 study at a Japanese air base on the airplane landing noises. The base has mainly airplanes of the following models: F-105, F-102, F-100, B-47, B-52, B-57, T-33, T-39, KC-50, C-97, C-124, C-130, C-133, C-135, S-55, H-43, and Boeing-707. These airplanes produced ground noise as high as 55-129 db, obviously causing serious interference for the environment.

119

Table 2.9   1964 airbase noise measurements (airplane

landing)

(600 m from the run-way)

a. month

b. day

c. db (highest

   sound)

d. Total value

e. 7am to 6pm

   (daytime)

f. 7pm to 6am

   (nighttime)

g. db

h. and higher

i. times

a	b	c	d	e	f	
10	14	116	275	105	45	
	15	120	231	143	44	
	16	118	172	113	43	2
	17	124	156		31	3
	18	107	117	78	31	2
	19	115	133		35	30
	20	122	175	114		25
	21	135	143		14	
	22	116	146		25	4
	23	114	81	62	11	2
	24	125	235	144	45	7
	27	123	84	42	25	4
	28	121	230	157		1
	31	120	213		46	12
11	17	125	307	153	45	2
	18	127	255			23
	19	117	125		45	23
	20	125	225			
	21	122				
	22	117				
	23	116	235			
	24	120				4
	25	125				

Another example is the Los Angeles International Airport in
the United States. During the 24 hours every day, there is one
jet airplane taking-off or landing for about every two minutes.
There are five elementary schools under the flight path. When
the airplanes pass over, the noise inside classrooms can reach
as high as 50-90 db. The outdoor noises are 100-120 db, seriously
affecting the classes.

120

Table 2.9 lists the equi-effect perception noise level EPNL values for several airplanes' take-off and landing. It can be seen that the airplanes have rather high noises.

Table 2.9   EPNL values [3,23] of several airplanes' noises

a. airplane model

b. EPNL values(db) for take-off noise

c. EPNL values (db) for landing noise

d. without treatment

e. sound suppression at the jet opening

f. sound suppression for the whole airplane body

g. Boeing

h. Trident

i. Concorde

j. Tu

k. Ilys

a. 飞机类型	b. 起飞噪声的EPNL值(分贝)			c. 降落噪声的EPNL值(分贝)		
	d. 未处理	e. 喷口消声	f. 整个机体消声	d. 未处理	e. 喷口消声	f. 整个机体消声
VC 10	110	106		115	110	
DC 8	115	103	93	116	104	101
DC 9	98	93	90	110	110	98
g. 波音 707	114	103	93	119	104	101
g. 波音 727	99	95	91	109	99	96
g. 波音 737	101	92	90	111	102	99
h. 三叉戟 I	100	96		108	104	
h. 三叉戟 II	109	105		109	105	
h. 三叉戟 III	105	103		110	104	
BAC 111	98	92		104	98	
i. 协和	114			115		
g. 波音 747	108			107		
DC 10	99			106		
j. 图-104	108					
j. 图-124	102					
j. 图-154	100					
k. 伊尔-62	103					

At this time the supersonic airplane   flight noises are the world's strongest noise sources. Along the flight path of supersonic airplanes, thousands and ten-thousands of residents are disturbed seriously. On January 29, 1962, for example, three U.S.

121

military airplanes passed through a Japanese city with highest speed at low elevation. Window glass of many residential houses was shattered and fluorescent light tubes fell down, causing great damage. Another example occurred in 1970 at a city and surrounding villages in Germany. Due to the very strong supersonic boom, several hundred cases of damage were reported. Most of them involved shattered glass, raised roofs, and damaged doors.

There have been extensive discussions concerning the noise from the Concorde airplanes. To have some handle on their effect, England made eleven supersonic flights in 1967, with a total of 50-million people affected. This resulted in 12,000 cases of complaint, 788 cases of lawsuits, and a large sum of payment for damages. Based on the actual testing, when the Concorde type airplanes take off, the ground noise is 114 EPN db. For DC-8, Boeing 707, it is 93 EPN db. Trident-I has 96 EPN db (see Table 2.9)

Supersonic flight noise not only disturbs people, it also excites the chickens and dogs, causes milk cows to stop producing milk, and pigs, horses, and cows to be affected in their growth.

Furthermore, supersonic flight noise can also cause equipment and control devices to have sound fatigue, leading to damage in structures and failure in controls.

Supersonic exhaust noise is the main component of the noise from supersonic jet airplanes and rockets. Supersonic jets produce tremendous shock waves, causing the pressure and temperature of the medium to rise rapidly. This leads to large disturbance

122

of the surrounding air, producing strong supersonic jet noises.

Figure 2.36 [24] shows the sound pressure level curves for the near-field noises of the turbo-jet generators and JATO rockets. It can be seen that, turbo-jet generators (jet velocity at 565 m/s) have major noises coming from downstream at a distance equal to six times the diameter of the jet opening. Beyond 10 times the diameter of the jet opening the radiation of noise is small. Rockets (jet velocity at 1800 m/s) have the major noises coming from the mixing zone of the supersonic core, downstream at a distance 20-40 times the jet openings.

Based on the noise data for rockets and jet airplanes one
can see that, with increasing jet velocities, the sound power of
noise from supersonic exhaust deviates from the eighth-power law.
Instead, it is proportional to the third power of the velocity,
as shown in Figure 2.37 [25]. In terms of equation it becomes

$$W = k \frac{\rho^2}{\rho_0} v^3 D^2,$$ (2.44)

where W -- sound power; $k = (0.5 - 1) \times 10^{-2}$ -- coefficient; ρ, ρ_0
-- medium density of the jet stream and the surroundings; v -- jet
velocity; D -- diameter of the jet opening.

a. distance along the
   radial direction
   (in terms of the
   diameter of the
   jet opening)
b. distance along the
   axial direction
   (in terms of the
   diameter of the
   jet opening)
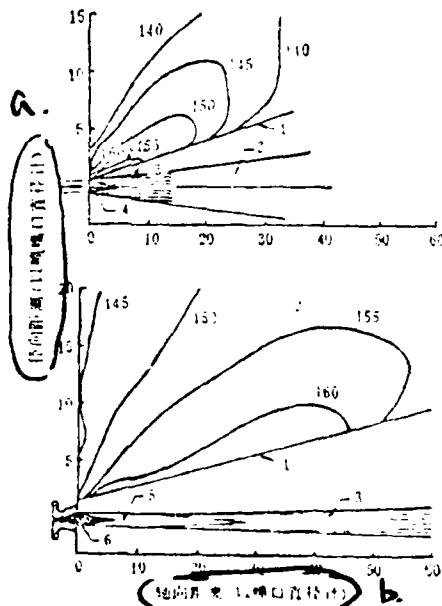
Figure 2.36 Near-field equi-sound pressure level curves for
   turbo-jet engines (upper) and JATU rockets (lower).
   Parameters for the turbo-jet engines: thrust 4360 kg, jet
   velocity 505 m/s, pressure ratio 2.2 at the jet opening,
   diameter of the jet opening being 0.505 m.

124

Parameters for the JATO rockets: thrust 454 kg, jet velocity 1800 m/s, pressure ratio 60 at the jet opening, diameter of the jet opening being 0.007 m.

1. boundary of measurements;   2. total eddy currents;

3. mixing zone;   4. core;   5. supersonic core;

6. exit velocity

a. sound power (watt)

b.   jet engine

c. constant

d. rocket

e. model jet

f. jet engine with
   pre-heating
   equipment

g. velocity (m/s)
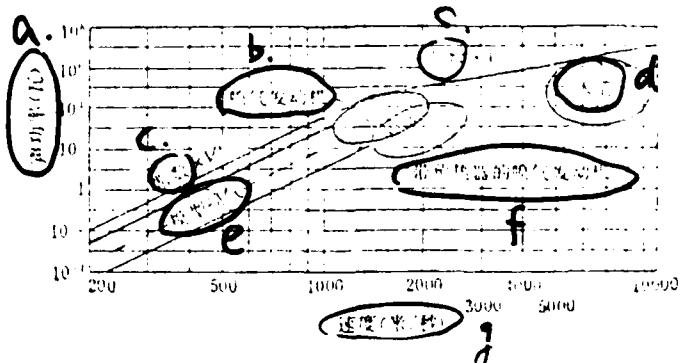
Figure 2.37 Relationship between jet velocity and the
            sound power of noise from jet airplanes and rockets.

Based on theories and a large number of experiments, Equation (2.44) is applicable in the range with the Mach number $M > 2$. That is, when the jet velocity is above twice of the sound velocity, the sound power of noise from jet exhaust is proportional to the third power of the velocity. Equation (2.23) is applicable for the range with $M = 0.5 \sim 2$. That is, when the jet velocity is between one-half and twice   the sound velocity, the sound power of noise

125

from jet exhaust is proportional to the eighth power of the velocity. In general, jet airplanes fly with supersonic velocities, but with lower velocities in taking-off and landing.

When airplanes and rockets fly with supersonic velocities, they produce a strong booming sound, which is the noise caused by the shock waves from bodies with supersonic motions. Such noise has the N wave structure. The boom rises in a time interval of 0.01 second, continues for 0.1-0.2 second with pressure increase at about 100 N/m^2. It sounds like some sudden explosion. The previously mentioned glass-shattering and roof-blowing away, etc. are indeed caused by such sonic booms. In these days supersonic flight becomes more and more popular. For instance, the *Russian-made model Tu-144 planes have a flying* velocity of 2.35 Mach (i.e., 2.35 time the sound speed with the sound speed at 1200 km/hour), the American-made model Boeing-2707 planes with 2.9 Mach, the English-French-made Concord planes with 2 Mach, and military planes with maximum velocities as high as 5 Mach. Therefore, the sonic boom has attracted more and more attention from people.

Figure 2.36 shows the characteristics of the boom sound pressure wave in free space and near the ground. They are expressed in terms of the strength ΔP, pulse rise time τ and the total lasting time span T.
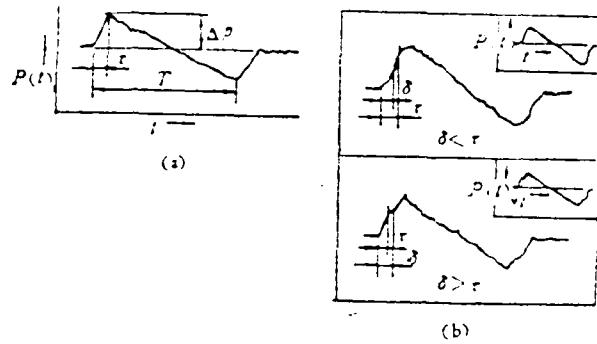
Figure 2.38   Boom sound pressure wave configurations

(a) in free sound field   (b) near ground

Due to reflections, the pressure wave shapes become compli-
cated at the ground surface.   They are formed from two almost
singular N waves, which have time difference δ. The value of δ
is determined by the height h of the reflection surface and inci-
dent angle θ, following the mathematical relation:

$$\delta = 2h\cos\theta/c.$$

(2.45)

For first-order approximation (neglecting the refractive effect
occurring during   propagation in the atmosphere) this can be
written as

$$\delta = \frac{2h\sqrt{M^2-1}}{Mc},$$

(2.46)

where M is the Mach number and c is the sound speed.

The boom's energy spectral density is

$$F(\omega) = \int_0^{T+\tau} P(t)\, e^{-i\omega t}\, dt,$$

(2.47)

where $P(t)$ is the wave pressure.

For N wave with intensity ΔP_0 , in a free sound field [5],

127

$$F(\omega) = \frac{2 \Delta P_0}{\omega^2 b(a - b)} (a \sin b\omega - b \sin a\omega)$$

$$= \frac{2 \Delta P_0}{\omega^2 b(a - b)} \left(\tau \sin \frac{\omega T}{2} \cos \frac{\omega \tau}{2} \right.$$

$$\left. - T \cos \frac{\omega T}{2} \sin \frac{\omega \tau}{2} \right), \tag{2.48}$$

where $a = (T + \tau)/2$; $b = (T - \tau)/2$.

The energy in the frequency band ω_1 to ω_2 is equal to

$$\frac{1}{\pi} \int_a^n |F(\omega)|^2 d\omega. \tag{2.49}$$

The boom effect occurs for supersonic flights along their flight path over several thousand kilometers. The effect reaches side distances of 50-80 kilometers, with victims up to tens of thousand people. Under the boom effect, people get headaches, humming in the ears, plugged noses, shivering, and fright. When a boom suddenly occurs, temporary shock can also occur. If a person is situated under boom sound for 5 minutes, he will become dizzy for the whole day.

During the supersonic flight, in addition to the supersonic exhaust noise and the boom sound, another important noise source is the attached surface layer. High speed jet airplanes and guided missiles have their internal noise mainly determined from the attached surface layer's noise. The sound power of the attached surface layer's noise rises rapidly with increasing flying speed (approximately at 2.75th power of the speed).

2.5.2 Combustion noise

Recently, combustion noise has increased both in number and

128

intensity. For instance, combustion rotating machinery, internal combustion engines, heating furnaces at oil refineries, city waste combustion, etc. all produce rather high intensity noise. This causes some concern to people.

Combustion noise is due to the pressure waves induced by combustion, which lead to noise generation.

Figure 2.39 shows the experimental results on noise from heating furnaces.

Figure 2.40 is the sound frequency spectrum of noise from model 6522 D1 combustion gas rotating machinery, near the combustion chamber.

Figure 2.41 [4] shows the combustion noise from a small scale internal combustion engine.

a. octave band sound
   pressure level (db)
b. frequency (Hz)
c. (a) 12.0 million kCal
   cylindrical furnace
   (oil burning)
d. (b) 10.0 million kCal
   cylindrical furnace
   (gas burning)
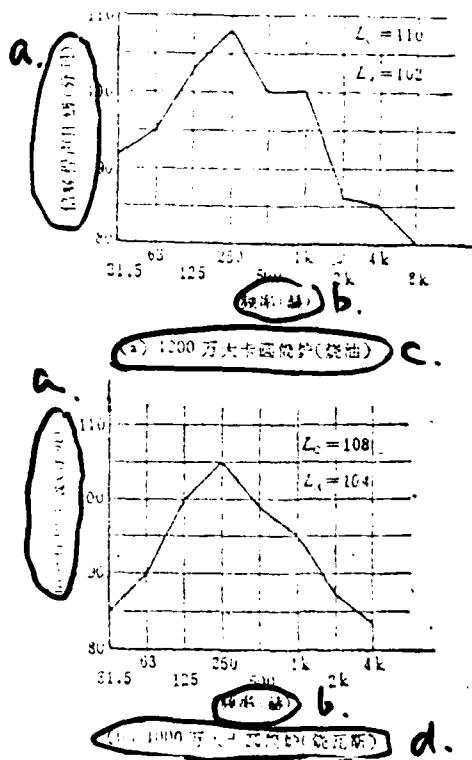
Figure 2.39 noise frequency spectrum of heating furnaces

next the users, of 120 decibels (A) or

a. octave band sound
   pressure level (db)
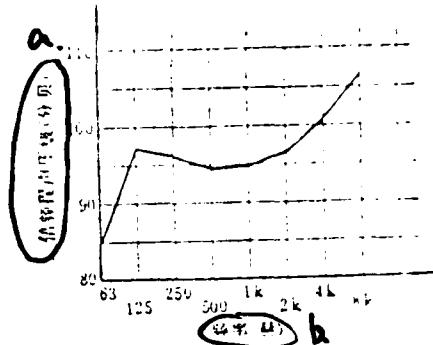
b. frequency (Hz)

Figure 2.40   noise frequency spectrum for Model 6522 D1
              combustion gas rotating machinery near the combustion
              chamber

a. sound power level (db)

b. frequency (Hz)
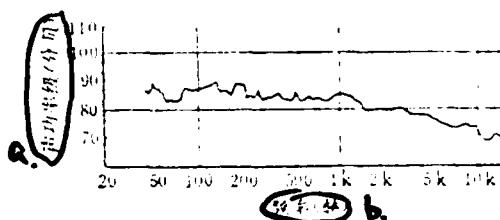
Figure 2.41   combustion noise from a small-scale
              internal combustion engine

2.5.4 Wind sound

Wind sound is caused by the impact of gas streams against
stationary objects. The main components are those from eddy
currents and the noise associated with the breaking up of eddy
currents.

The sound power from wind rises drastically with increasing
stream velocity, proportional to the sixth power of velocity.
When the velocity is low, it is proportional to the 5.5th power
of velocity. It is also related to the cross-sectional area of
the object, normal direction friction coefficient, and the gas

130

density, in terms of the following mathematical equation:

$$W \propto \rho S \xi^2 v^4,$$ (2.50)

where W -- sound power; ρ -- gas density; S -- cross-sectional area
of object; ξ -- object's normal direction friction coefficient;
v -- stream velocity.

For stationary long cylinders, the wind noise due to the
stream flow has its sound power the same as that in Equation (2.17).
However, in this case l is the length of the cylinder; D is the
transverse direction length (diameter) of the cylinder. K has a
value determined by the geometric shape of the object, the Mach
number M and the Reynold number Re. For a smooth object with
stream-lined body, the K value is small. For rough bodies with
large friction, the K value is relatively large.

Figure 2.42 [26] is the curve showing the relationship between
the total sound pressure level and flow speed, for noise produced
by the stream perpendicular to the model 4131 condenser microphone's
membrane. It can be seen that, when the flow speed is 5-10 m/s,
the noise has a total sound pressure level at 70-80 db. When the
flow speed reaches beyond 50 m/s, the noise's total sound pressure
level already reaches 100 db. Therefore, in designing air change
and circulation systems and sound suppressors, the stream speed
has to be limited. Otherwise, due to the too high speed, the air
changer's ducts and the interior of sound suppressors will produce
very high wind sound, such that the sound suppressors can no longer
be effective. They may even serve a negative function.

131

a. total sound pressure

  level (db)

b. m/s
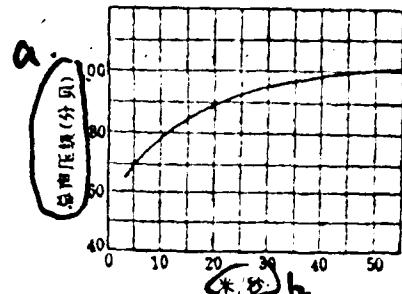
Figure 2.42   Relationship between stream speed and

noise level

The frequency of wind noise is determined by Equation (2.13).
Figure 2.43 [27] shows the frequency spectrum of wind noise produced
by the air, when the air flows at speed v of 33 m/s around a long
cylinder of 5 mm in diameter D. It can be seen that, at the funda-
mental frequency f_1 = (0.185)(33/0.005) = 1330 Hz and its second
harmonics f_2 = 2 x 1330 = 2660 Hz, the noise has obvious peaks.

When the wind blows the electrical cables or ships' holding
cables, one often hears such tuned sound. However, under many
conditions, due to the complicated shapes of objects, as well as
the different degrees in roughness of their surfaces, the noise
produced has no regular patterns.   Therefore, the resulting wind
noise forms a continuous spectrum, with no clear fundamental
frequency or harmonics.

a. sound pressure level (db)

b. frequency (Hz)

c. Hz
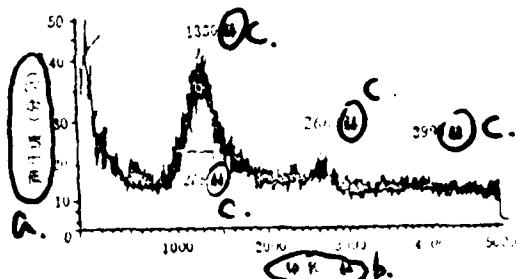
Figure 2.43   Frequency spectrum of wind noise produced

by air flowing around a cylinder

132

CHAPTER 3. FUNDAMENTAL PRINCIPLES AND CALCULATIONS OF SOUND SUPPRESSION

§ 3.1 Introduction

A sound suppressor is a device for prohibiting the transmission of sound while allowing the gas flow. It is an important technique for reducing aerodynamic noise. If such a device is installed along the flow path of aerodynamic equipment, the noise level of such equipment can then be reduced.

There are many kinds of sound suppressors. The three basic types include frictional sound suppressors, reactive sound suppressors, and frictional-reactive combined sound compressors.

The frictional sound compressor is based on the absorption of sound by certain materials. The frictional sound compressor is constructed with sound absorbing materials fixed on the inner surface of the flow path, or fixed according to certain patterns along the flow path. When sound enters the device, it will be absorbed by the absorbing materials. This is an analogy of the resistance in an electrical circuit, which dissipates electrical energy through heat juction. This kind of sound suppressor has advantages for a broad spectrum of medium and high frequencies, particularly in the high frequency range which irritates hearing. Their disadvantages lie in the corrosion by certain gases, and short life in high temperature and steam applications. They have relatively poor efficiency for low frequency noise.

Reactive sound suppressors are also called sound wave filters. They are based on the principle of sound wave filtering, e.g., resonance sound suppressors, expansion -type sound suppressors, and interference sound suppressors. They have advantages at low frequencies, with simple structure and good resistance to high temperatures, gas corrosion and impact wear. Their disadvantages include narrow frequency ranges and poor efficiency at high frequencies.

Some aerodynamic noises have very broad frequency ranges such that either resistive or reactive sound suppressors alone can not solve the problems. Resistive-reactive combined sound suppressors are therefore employed, with the characteristics of both types of suppressors. They have not only resistive sound absorbing materials, but also acoustic filtering components such as resonant cavities and expansion volumes. Consequently, they are effective for broad ranges of frequencies. However, having the sound absorbing materials, they have short life in applications involving high temperatures (particularly with flames), corrosive gases, and high speed gas flow conditions.

Recently, to reduce aerodynamic noises with relatively broad frequency ranges, and in the meantime to enhance the effectiveness under high temperatures and steam and corrosive gas flow, noise control workers have constantly carried out research on improving designs of all-metallic sound suppressors. One new product is the suppressor based on metallic plates with fine holes. The plates themselves have both resistive and reactive properties. With proper arrangement, they can be very effective for broad frequency ranges, and sustain high temperature, steam, corrosive gas applications. They can function

134

well even when the gas flow contains large amounts of moisture. There
is some difficulty in the processing (e.g., in welding) of the required
thin plates (less than 1 mm in thickness).

The quality of a sound suppressor is mainly based on three con-
siderations below:

1. The characteristics of sound suppression (sound reduction and
spectral properties): The sound reduction can be measured in terms of
transmission loss and insert loss; for field measurements, it can also
be expressed through the decrease in loudness levels between the exhaust
outlet and the inlet.

Transmission loss is the difference in sound energy between the
inlet and the outlet. By its definition:

$$\Delta L_w = 10 \log W_1/W_2 = L_{W_1} - L_{W_2} \quad (db) \tag{3.1}$$

where ΔL_w is the transmission loss, L_{W_1} the inlet sound power level,
and L_{W_2} the transmitted sound power level.

Since the sound power level can not be measured directly, trans-
mission loss is generally determined through the measured sound pressure
levels. With a sound transducer located inside the sound suppressor,
one measures the sound level (total sound pressure level and A-sound
level) at constant intervals between the inlet and the outlet. The
relation between the noise reduction and distance can be derived. The
total sound reduction of the sound suppressor can then be calculated.
This method is free of interference from background noises, and reflects
correctly the characteristics of the sound suppressor as well as the
sound reduction process. However, the measurements are tedious, and

135

accurate measurements can hardly be made in high speed gas flow. Therefore, approximate transmission loss is often determined by measuring the sound level (total sound pressure level and A-sound level) at various holes drilled through and along the wall of the sound suppressor.

A simpler method for measuring transmission loss is based on the difference at two ends. That is, the transmission loss is the difference in average sound level (total sound pressure level and A-sound level) between the inlet and the outlet. This method is sensitive to background noises. To avoid interference caused by high speed gas flow, this method can also be used with sound levels measured at some reference holes through the suppressor wall near its inlet and outlet.

In field measurements, transmission loss as measured by inserting a given sound suppressor into the flow path is more often used to evaluate the quality of such a suppressor. That is, at one or several points in an aerodynamic device, the average sound levels (total sound pressure level and A-sound level) are measured with and without the installation of the sound suppressor. By inserting the suppressor into the flow path, this method can be used even if the aerodynamic device involves high temperature, high flow rate, and corrosion to transducers, or it has walls not suitable for hole drilling. The weakness of this method is that, with strong background noises, no accurate measurement can be made,

To avoid interference due to background noises in evaluation of a given sound suppressor, one can also rely on the sound level

136

changes at the exhaust outlet (or gas inlet). The sound reduction
is determined by measuring the difference with and without the sound
suppressor, in the average sound levels (total sound pressure level
and A-sound level) at one or several points with known distances
from the exhaust outlet (or gas inlet).

The transmission loss, the insert loss, and the sound level
changes at the exhaust outlet are the main indicators of the effective-
ness of a given sound suppressor. The larger these values are, the
better the sound suppression. However, the results are sometimes
different from different methods. One has therefore to indicate
the method being employed in each measurement.

It is not enough to evaluate a given sound suppressor simply
by considering the total sound pressure level and A-sound level. One
has to know its spectral characteristics in terms of the sound
reductions at different frequencies of frequency bands. Individual
measurements at specified frequencies or bands have to be made.
They are often expressed in octave or third-octave bands.

Irrespective of which method is used, the background noise
correction must be made, using Fig. 1.4 or Table 1.1.

With the sound reduction determined in levels (db), one can
calculate then, through certain relationships, the sound power level
difference (db), sound power difference (watt), loudness level
difference (fon), loudness difference (sone), etc.

.2. Aerodynamic properties of sound suppressors: The aerodynamic
properties are also important in evaluating a given sound suppressor.
Since every suppressor has to be installed along the flow path, it

137

will undoubtedly affect the aerodynamic characteristics of the aerodynamic device. If only the effectiveness in sound reduction is taken into consideration, but the aerodynamic aspect is ignored, a sound suppressor can sometimes reduce greatly the efficiency of an aerodynamic device, or even cause the device to become completely inoperable. For an air-changer having a sound suppressor with too large flow resistance, the device will have too low air pressure to deliver enough air flow. If the resistance from a sound compressor is too high in an internal combustion engine, the engine may end with too low power to start.

The aerodynamic characteristics of sound suppressors are mainly defined in terms of resistive dissipation and the resistance coefficient. The resistive dissipation arises from the friction of the inner surface, the elbow, the holes, and the conduit cross section variations of the sound suppressor. It is usually expressed in terms of the total pressure difference between the inlet and the outlet of the suppressor. If the flow rates are equal at the two locations, one can then use the static pressure difference. (Appendix 1 lists resistive dissipation associated with some common networks.)

Once the dynamic pressure P_d and the resistive dissipation Δp of a given sound suppressor is determined under different wind velocities, one can calculate the average resistance coefficient ξ from Equation (5.2):

$$\xi = \frac{\overline{\Delta p}}{\bar{p}_m}, \qquad\qquad (5.2)$$

with $\overline{\Delta p}$ being the total average pressure difference between the inlet and the outlet of sound suppressor, and $\bar{p}_d$ being the average dynamic

pressure at the cross section containing the point of measurement.

3. Specifications of sound suppressor (dimensions, prices, useful life, etc): Specification of a given sound suppressor is also an indicator of its quality. With the same sound reduction capability and aerodynamic characteristics, it would be better to have smaller dimensions, lower prices, and longer useful life.

§ 3.2   Sound Absorbing Materials and Sound Absorbing Structures

3.2.1   Sound Absorbing Materials

Sound absorbing materials are materials which can absorb sound energy incident on them. When sound waves enter the fine openings of such materials, the air and tiny fibers inside vibrate to dissipate the sound energy into heat through friction and viscosity. Therefore, most sound absorbers are soft and porous. There are fine holes at the surface. These holes extend deep into the materials and are interconnected. Therefore, sound waves can enter easily. Examples of good absorbing materials include fiber glass, mineral fiber, asbestos, wool, cotton, Kaolon fiber, sea-weed, foam plastics, wood chip board, sugarcane fiber board, aerated concrete, sound absorbing brick, etc.
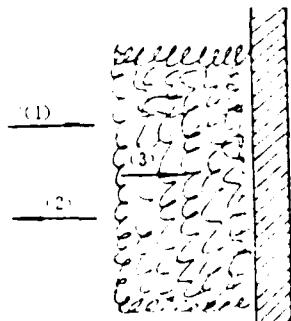

Figure 3.1   The mechanisms of sound absorption in sound absorbing materials

Fig. 3.1 shows schematically the process of sound absorption. When incident sound wave (1) arrives at the surface of a porous material, the wave (2) is reflected from the surface, while the wave (3) enters the material. Part of this sound wave (3) is absorbed.

139

The un-absorbed portion is reflected by the rigid wall, and passes once more through the porous material before reaching the surface. This repeated process allows most of the sound to be absorbed. Only a small portion is returned to the air.

For practical purposes, the physical parameter describing the sound absorption ability of a material is most often the sound absorption coefficient α. It is defined as the ratio of the absorbed sound energy to the incident energy. That is

$$\alpha = \frac{E_a}{E_i} = \frac{E_i - E_r}{E_i}, \tag{5.5}$$

where E_i = incident sound energy, E_r = reflected sound energy, and E_a = absorbed sound energy.

It is obvious from Equation (5.5) that, with a perfect reflective surface ($E_i = E_r$), $\alpha = 0$; for a perfect absorption surface ($E_r = 0$), $\alpha = 1$. For general materials, the sound absorption coefficient has a value between 0 and 1. The larger the absorption coefficient is, the better the sound absorption effect.

The quality of a sound absorbing material is sometimes expressed in terms of sound resistance Z_A. It is the ratio between the sound pressure on a given cross section and the passage value of this cross section (volume velocity or linear velocity multiplied by the cross-sectional area):

$$Z_A = p \cdot V \quad \text{(sound-ohm)} \tag{5.4}$$

Sound resistivity is the resistance per unit area.

There is a conversion relationship between the sound resistance and the sound absorption coefficient.

For an incident angle θ (the angle with the normal direction of the absorbing structure),

140

$$\alpha_\theta = 1 - \left| \frac{Z_a \cos\theta - \rho c}{Z_a \cos\theta + \rho c} \right|.$$

$$(3.5)$$

For diffuse incidence,

$$\alpha = \int_0^{\pi/2} \alpha_\theta \sin 2\theta\, d\theta.$$

$$(3.6)$$

When the sound resistance is independent of the incident angle, this integration can be expressed as

$$\alpha = 8 \left[\frac{\bar{R}}{\bar{R}^2 + \bar{X}^2} - \left(\frac{\bar{R}}{\bar{R}^2 + \bar{X}^2} \right) \ln(\bar{R}^2 + 2\bar{R} + \bar{X} + 1) \right.$$

$$\left. + \bar{R} \left(\frac{\bar{X}}{\bar{R}^2 + \bar{X}^2} \right) \left(\frac{\bar{R}^2}{\bar{X}^2} - 1 \right) \operatorname{arctg} \frac{\bar{X}}{\bar{R} + 1} \right],$$

$$(3.7)$$

where $\alpha =$ diffuse incidence sound absorption coefficient; $\bar{R} = \dfrac{R}{\rho c}$, and $\bar{X} = \dfrac{X}{\rho c}$ are, respectively, the real and imaginery part of the sound resistance.

The sound absorbing ability of a porous material is determined by the following factors:

1. Flow resistance R of the material: It is the resistance to air flow through the openings; it is defined as the ratio between the static pressure difference across the material and the linear velocity of the air flow, provided that a steady flow is maintained with low flow rate:

$$R = \frac{\Delta p}{v} \quad (\text{MKS Rayls}[1]).$$

$$(3.8)$$

1) MKS Rayls means kg m-s in the MKS unit system

Specific flow resistance r is the flow resistance with unit thickness of the material. Its unit is Rayl/cm. Typical specific flow resistance values are between $10-10^7$ MKS Rayls/cm.

2. Porosity q: This is the ratio between the air volume to the total material volume. In this case, only the interconnected air passages accessible to air flow is taken into account, not including totally enclosed air pockets. Common porous materials have porosity above 70%, most of them above 90%. For example, mineral fiber has porosity of 80%, and fiber glass has porosity higher than 90%.

3. Structural factors: This is a physical quantity determined by the structural characteristics of a sound absorbing material. In the theory of sound absorption by porous materials, models are made by assuming the arrangement of capillaries is along the directions perpendicular to their wall thickness. In reality, the air bubbles, spacings and configurations in the porous materials are rather irregular. To arrive at an agreement between the theory and the fact, a correction factor would be required. This is the structural factor. It usually has a value between 2 and 10. When one kind of capillaries is arranged randomly, the structural factor is 3.

It is known from both theory and experiment:

1. When the thickness is sufficiently large, the sound absorption coefficient is greater if the specific flow resistance and the structural factor are small.

2. When the thickness is not large, r maintains the best value; when $r = 10^3$ MKS Rayls/cm, the sound absorption coefficient is high --

142

as in fiber glass and mineral fiber of a given density; but when r = 10 MKS Rayls/cm and r = 10^4-10^5 MKS Rayls/cm, the sound absorption coefficient is relatively low -- as in wood chip board and sugar-cane fiber board. Therefore, in studying sound absorption materials and product development, it is practical to control flow resistance in order to raise the sound absorptive ability of porous materials.

3. With given specific flow resistance r and structural factor s, the low and medium frequency absorption coefficient generally increases with increasing thickness of materials. For soft and low density materials, if flow resistance is in the range of 10^2-10^3 MKS Rayls/cm, one has to increase the thickness to enhance the sound absorption effect for low frequencies. If the flow resistance is very large, as up to 10^5 MKS Rayls/cm, there will not be much improvement in the sound absorption coefficient even the thickness is increased. Consequently, there is no need for very thick board materials with higher density.

There are two common laboratory methods for determining the sound absorption coefficient of materials:

1. Sound-mixing room method: Through the measurement of the sound absorption coefficient during the sound mixing period in a sound-mixing room, the sound absorption coefficient α_m of a material for a diffuse incident sound can be determined.

Assume the sound mixing time in an empty room is t_e, then

$$t_e = 0.161 \, V/A, \tag{5-9}$$

where V is the volume of the room, in m^3; and A the total sound absorption in the empty room, in m^2, $A = \alpha_{\hat{e}} S$.

Assume the sound mixing time is t_m in a room equipped with sound absorption material samples, then

$$t_m = 0.161 \ V / (S\alpha_e + S_m\alpha_m) \qquad (3.10)$$

where S_m is the sample's surface area, in m^2. From Equations (3.7) and (3.8), we have

$$\alpha_m = \frac{0.161 \ V}{S_m} \left(\frac{1}{t_m} - \frac{1}{t_e} \right) . \qquad (3.11)$$

With the sound-mixing room method, one needs very large area of the sound absorption material samples, as well as very long time requirements of the laboratory (sound mixing room). Therefore, it takes more effort.

2. Standing wave tube method: The standing wave tube method can be used to measure the sound absorption coefficient when the wave propagates in a direction perpendicular to the surface of the material. The testing arrangement is shown in Figure 3.2. This method is mainly based on the measurement of the standing wave, which occurs as a result of the reflection from the sound absorption surface of a longitudinal, single wavelength, plane wave. (If the tube diameter is not small enough and the inner surface of the tube is very smooth, the loss at the tube surface can be neglected.)

a. Rigid wall
b. cavity
c. sample material
d. testing tube
e. loudspeaker
f. sound frequency resonator
g. transmitter cart
h. frequency spectrometer
i. Scale
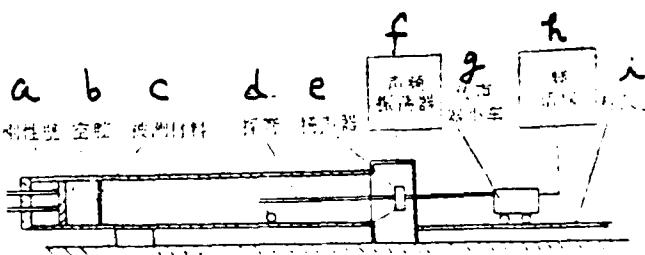
Fig. 3.2 Schematic Arrangement of the
Standing Wave Tube Test

144

For a given material and frequency, the ratio between the maximum and the minimum value of the sound pressure in the tube is a constant. If this constant is n, the sound absorption coefficient for a normal incident sound:

$$\alpha = \frac{4}{n + \frac{1}{n} + 2} \qquad (3.12)$$

For some standing wave tubes and spectrometers, the sound absorption coefficient can be read out directly from the indicators on the instruments. Therefore, this method is simple and is convenient for making relative studies among different sound absorption materials. However, the method is valid only for plane waves (i.e., for sound waves with wavelengths greater than 1.7 times the diameter of the tube).

Tables 3.1-3.4 show the testing data for the sound absorption coefficient of materials in this country [1].

From testing results on sound absorption materials we know that:

1. As far as sound absorption ability is concerned, different sound absorption materials have the following order according to their effectiveness in sound absorption: fiber glass, mineral fiber, Kaplon fiber, seaweed, asbestos, industrial wool blanket, perforated fire brick, sound absorbing brick, perforated concrete, wood chips, wood fiber board, sugar-cane fiber board, etc. The sound absorption characteristics of foam plastics are not stable. They depend on the fabrication techniques, the continuity of the materials, and the sizes of the capillaries. Some of them have high sound absorption coefficient close to that for fiber glass.

---

1) The sound absorption coefficient values in this chapter are based on the various testing data as gathered in China.

Table 3.1 Sound absorption coefficient (Tube testing method) of fiber glass, glass cotton, mineral residual cotton and their products

a. Material   b. Thickness, cm   c. Density, kg/m^3

d. Sound absorption coefficient at various frequencies

e. Production location

a. 材料名称	b. 厚度 厘米	c. 密度 公斤/米³	d. 各频率下的吸声系数 125	250	500	1000	2000	4000	e. 产地
"baked" fiber glass — 熟玻璃丝	5	80	0.06	0.08	0.18	0.44	0.72	0.82	Tien-jing
	5	100	0.07	0.10	0.25	0.65	0.77	0.94	
	5	130	0.10	0.12	0.31	0.76	0.85	0.90	
	9	70	0.12	0.30	0.72	0.95	0.91	0.97	
	9	100	0.18	0.44	0.89	0.95	0.95	0.99	
	2	200	0.10	0.14	0.18	0.75	0.95	0.94	Peijing
	4	200	0.13	0.26	0.53	0.95	0.94	0.95	
	6	200	0.25	0.33	0.82	0.94	0.87	0.82	
	9	200	0.30	0.54	0.94	0.95	0.85	0.84	
raw fiber glass — 生玻璃丝	5	80	0.07	0.11	0.27	0.65	0.82	0.82	Tien-jing
	5	130	0.12	0.21	0.54	0.95	0.94	0.94	
ultrafine glass cotton — 超细玻璃棉	5	20	0.10	0.35	0.85	0.85	0.86	0.86	Shiang-hai
	10	20	0.25	0.60	0.85	0.87	0.87	0.85	
	15	20	0.50	0.90	0.85	0.85	0.86	0.90	
	5	12	0.06	0.16	0.68	0.95	0.93	0.90	Nan-tung
	5	17	0.06	0.19	0.71	0.95	0.91	0.90	
	5	24	0.10	0.30	0.85	0.85	0.85	0.85	
phenolic aldehyde fiber glass board (with the hard skin layer removed) — 酚醛玻璃纤维板（去掉表面硬皮层）	2	100	0.05	0.08	0.22	0.42	0.76	0.90	Shiang-hai
	4	100	0.08	0.21	0.55	0.93	0.90	0.95	
	6	100	0.15	0.37	0.73	0.95	0.90	0.95	
	8	100	0.25	0.55	0.80	0.92	0.96	0.95	
mineral residue cotton — 矿渣棉	6	240	0.25	0.55	0.78	0.75	0.87	0.91	Peijing
	8	240	0.35	0.65	0.65	0.75	0.88	0.92	
	6	300	0.35	0.43	0.55	0.67	0.78	0.92	
	5	150	0.30	0.64	0.93	0.78	0.93	0.94	
	7	200	0.32	0.63	0.76	0.83	0.90	0.92	
asphalt mineral cotton blanket — 沥青矿棉毡	1.5	200	0.08	0.09	0.18	0.40	0.74	0.82	Tai-yuan
	3	200	0.10	0.18	0.50	0.68	0.81	0.84	
	4	200	0.16	0.38	0.61	0.70	0.81	0.90	
	6	200	0.19	0.51	0.67	0.70	0.85	0.85	

146

Table 3.2 Sound absorption coefficient of fibrous materials and their products (Tube testing method)

a. material b. thickness, cm c. density, kg/m³

d. sound absorption coefficient at various frequencies

e. production location

a		b	c	d						e
材料名称		厚度 厘米	重度 公斤/米³	各频率下的吸声系数						产地
				125	250	500	1000	2000	4000	
industrial wool blanket	工业毛毡	1	370	0.04	0.07	0.21	0.50	0.52	0.57	Peijing
		3	370	0.10	0.28	0.55	0.60	0.60	0.59	
		5	370	0.11	0.30	0.50	0.50	0.50	0.52	
		7	370	0.18	0.35	0.43	0.50	0.53	0.54	
seaweed	海草	1	100	0.10	0.10	0.14	0.25	0.77	0.86	
		3	100	0.10	0.14	0.17	0.65	0.80	0.94	
		5	100	0.10	0.19	0.50	0.94	0.85	0.85	
coarse hemp	粗大麻	3	90	0.07	0.09	0.15	0.35	0.66	0.62	
fine hemp	细大麻	3	90	0.08	0.10	0.17	0.37	0.70	0.72	
asbestos chip	石棉屑	2.5	210	0.06	0.35	0.50	0.46	0.52	0.65	
wood chip	木屑	2.5	160	0.03	0.09	0.26	0.60	0.70	0.70	
cotton	棉絮	2.5	10	0.03	0.07	0.15	0.30	0.62	0.60	
Sugarcane fiber board	甘蔗板	1.3	190	0.09	0.13	0.21	0.40	0.35	0.40	Shang-hai
		2	190	0.09	0.14	0.21	0.25	0.37	0.40	
wood fiber board	木丝板	2		0.15	0.15	0.16	0.34	0.78	0.52	Peijing
		4		0.19	0.20	0.48	0.79	0.42	0.70	
		8		0.25	0.53	0.82	0.63	0.84	0.59	
hemp fiber board	麻纤维板	1.3	260	0.07	0.09	0.14	0.18	0.27	0.30	Shang-hai
		2	260	0.09	0.11	0.16	0.22	0.28	0.30	
sunflower stem board	向日葵杆 芯板	2	150	0.07	0.09	0.22	0.42	0.55	0.56	Shang-hai
		2.2	320	0.12	0.13	0.15	0.34	0.52	0.53	
paper board	纸板	1	250	0.11	0.12	0.13	0.23	0.22	0.23	Shang-hai
soft wood chip board	软木屑板	2.5	260	0.05	0.11	0.25	0.63	0.70	0.70	

147

Table 3.3 Sound absorption coefficient of foam plastics materials
(Tube testing method)

a. Material b. thickness, cm c. density, kg/m³

d. sound absorption coefficient at various frequencies

e. production location

a. 材料名称	b. 厚度 厘米	c. 密度 公斤/米³	d. 各频率下的吸声系数						e. 产地
			125	250	500	1000	2000	4000	
polyamino-ester foam plastics (聚氨脂泡沫塑料)	3	56	0.07	0.16	0.41	0.87	0.75	0.72	
	4	56	0.09	0.25	0.65	0.95	0.73	0.79	
	5	56	0.11	0.31	0.41	0.75	0.86	0.81	
	3	71	0.11	0.21	0.71	0.65	0.64	0.65	Tien-jing
	4	71	0.17	0.30	0.76	0.56	0.67	0.65	
	5	71	0.20	0.32	0.70	0.62	0.68	0.65	
	2.5(细 孔)f	40	0.04	0.07	0.11	0.16	0.31	0.53	
	3(小 孔)g	40	0.06	0.12	0.23	0.46	0.86	0.82	Peijing
	5(大 孔)h	40	0.06	0.13	0.31	0.65	0.70	0.82	
	4	45	0.10	0.19	0.36	0.70	0.75	0.80	
	6	45	0.11	0.25	0.52	0.87	0.74	0.81	Shiang-hai
	8	45	0.20	0.40	0.95	0.90	0.98	0.85	
amino-formic acid foam plastics (氨基甲酸泡沫塑料)	2.5	25	0.05	0.07	0.26	0.87	0.64	0.67	Tien-jing
	5	36	0.21	0.31	0.86	0.71	0.86	0.82	
polyether ethylene foam plastics (聚醚乙烯泡沫塑料)	1	26	0.04	0.04	0.06	0.08	0.16	0.24	Peijing
	3	26	0.04	0.11	0.38	0.89	0.75	0.86	
urea aldehyde (尿荃米波罗)	3	20	0.10	0.17	0.45	0.67	0.65	0.85	Chung-chun
	5	20	0.22	0.29	0.40	0.68	0.95	0.94	
phenolic aldehyde foam plastics (酚醛泡沫塑料)	1	28	0.05	0.10	0.26	0.55	0.52	0.62	Tai-yuan
	2	16	0.08	0.15	0.30	0.52	0.56	0.66	
hard polychloroethylene foam plastics (硬质聚氯乙烯泡沫塑料板)	2.5(光 面)i	10	0.04	0.04	0.17	0.56	0.28	0.58	
	2.5(凹凸面)j	10	0.04	0.05	0.11	0.27	0.52	0.67	
	4.5(光 面)k	40	0.02	0.05	0.12	0.07	0.15	0.10	

f (fine holes)   i (smooth surface)
g (small holes)   j (rough surface)
h (large holes)   k (smooth surface)

Table 3.4 Sound absorption coefficient of building materials (tube testing method)

a. material   b. thickness, cm   c. density, kg/m^3

d. sound absorption coefficient at various frequencies

e. production location

a 材料名称	b 厚米	c 容重	d 各频率下的吸声系数						e 产地
			125	250	500	1000	2000	4000	
perforated brick 加气泡孔砖	3.5	370	0.08	0.22	0.38	0.45	0.65	0.66	Peijing
	5.5	620	0.20	0.40	0.60	0.52	0.65	0.62	
	5.5	850	0.15	0.40	0.57	0.48	0.50	0.60	
	5.5	1100	0.13	0.20	0.22	0.30	0.29	0.29	
sound absorbing quartize brick 石英砂吸声砖	6.5	1500	0.08	0.24	0.78	0.43	0.40	0.40	Chung-chun
foam glass 泡沫玻璃	4	1240	0.11	0.32	0.52	0.44	0.52	0.33	
	4	1690	0.11	0.21	0.31	0.32	0.42	0.32	
	4	1870	0.11	0.22	0.32	0.34	0.43	0.32	
foam glass brick 泡沫玻璃砖	5.5	340	0.03	0.08	0.42	0.37	0.22	0.33	Chung-chun
perforated concrete 加气混凝土	5	500	0.07	0.13	0.10	0.17	0.31	0.33	
	5(穿孔φ5) f	500	0.11	0.17	0.48	0.33	0.47	0.35	Peijing
	6(穿孔φ5) g	500	0.10	0.10	0.10	0.48	0.20	0.30	
concrete expanded pearlite board 水泥蛭比	5	350	0.16	0.46	0.64	0.48	0.56	0.5	Peijing
珍珠岩板	8	350	0.34	0.47	0.40	0.3	0.48	0.55	Shiang-hai
foam concrete (white) 泡沫品混凝土 (白)	4.4	210	0.09	0.31	0.52	0.43	0.50	0.50	
(yellow) (黄)	2.4	290	0.06	0.19	0.55	0.84	0.52	0.50	Sheng-yang
(brown) (棕)	4.2	300	0.11	0.25	0.45	0.45	0.57	0.53	
(grey) (灰)	4.1	340	0.13	0.26	0.51	0.53	0.55	0.54	
asbestos-vermiculite board 石棉蛭石板	3.4	420	0.22	0.30	0.39	0.41	0.50	0.50	Peijing
vermiculite board 蛭石板	3.8	240	0.12	0.14	0.35	0.39	0.55	0.54	

f (with holes φ5)
g (with holes φ6)

149

Some of them have low values like that for wood fiber board. There are some foam plastics containing independent air bubbles not allowing air circulation, such as the polyethylene styro-foam. Air vibrations due to sound waves can not be transmitted to the interior of the materials. Strictly speaking, this kind of material can only be categorized as soft material, but not porous material. They have different mechanisms for sound absorption from that for porous materials. When sound waves are incident on such materials, the latter vibrate as a result. The internal friction dissipates energy, and causes the attenuation of the sound wave. Consequently, the sound absorption characteristics are also different from that for porous materials. For one particular sound wave frequency, they will resonant. Near this resonance frequency, they have a very high sound absorption coefficient. The efficiencies for sound absorption are greatly reduced for other frequencies.

2. Relationship between the thickness of a material and the sound absorption coefficient: The sound absorption coefficient generally increases with increasing frequency, and reaches a constant for a given frequency. With thicker materials, the sound absorption efficiency for low and medium frequencies can be enhanced. However, considering the economics, the thickness can not be increased without a limit.

There is practically no effect on high frequency absorption by increasing the thickness of materials. For fiber glass with thickness more than 1 cm, the high frequency average sound absorption coefficient is generally above 0.90. For mineral fiber with thickness more than 4 cm, the high frequency average sound absorption coefficient is about 0.85. For plastics with thickness more than 4 cm, if flow resistance

150

is low, the high frequency average sound absorption coefficient is about 0.90; if flow resistance is high, the high frequency average sound absorption coefficient is 0.80-0.85; and if the flow resistance is very high, then the high frequency average sound absorption coefficient is below 0.75. Industrial wool blanket, sound absorbing brick, etc. have high frequency average sound absorption coefficient below 0.7.

Most sound absorbing materials have good high frequency sound absorption properties. There is no upper limit for frequencies as far as sound absorption is concerned. Therefore, relatively thin sound absorption materials would be enough for high frequency sound. On the other hand, one needs thick materials to absorb low frequency sound.

5. The effect of sound absorption materials' density on the sound absorption coefficient: Since the density of a sound absorption material is directly related to the flow resistance, it has a certain effect on the sound absorption coefficient. If the density is 10-20 kg/m^3 for ultrafine fiber glass, the resonant sound absorption coefficient is 0.90-0.99 and the high frequency average sound absorption coefficient is 0.90. If the density is 25-30 kg/m^3 for ultrafine fiber glass, the resonant sound absorption coefficient is 0.80-0.90 and the high frequency average sound absorption coefficient is 0.80. For ultrafine fiber glass with density of 35-40 kg/m^3, the resonant sound absorption coefficient is reduced to 0.70-0.80 and the high frequency average sound absorption coefficient is reduced to 0.70. But in contrast to this, the low frequency sound absorption coefficient increases, for ultrafine fiber glass, if the density is decreased from 35-40 kg/m^3 to 25-30 kg/m^3 or from 25-30 kg/m^3 to 10-20 kg/m^3.

151

For most sound absorption materials, if the density increases, the low frequency sound absorption efficiency increases while the high frequency sound absorption efficiency decreases. Therefore, one has to reasonably select the density of the sound absorption materials to achieve best sound absorption results.

Apart from density and thickness, the sound absorption ability of a material also depends on environmental factors such as temperature, humidity, and air currents.

1. The effect of temperature: When temperature increases, the peak sound absorption efficiency moves towards higher frequencies. When the temperature decreases, it moves towards lower frequencies. This effect is due to the change in wavelength through change in temperature. It should be noted that, in selecting sound absorption materials, one should not go beyond the working temperature range of a given material. Otherwise, not only is the material not effective, it will also deteriorate fast. (In Appendix 2 some thermal properties of sound absorption materials are given. They may be used as reference in material selection.)

2. The effect of humidity: The absorption of moisture or water causes the change of a material's properties, as well as sealing off passages and small holes inside the material. This leads to a reduction in porosity of a porous material, affecting the sound absorption characteristics of a sound absorption material.

Table 3.5 shows the water-soaking effect on sound absorption of fiber glass. It can be seen that water-soaking first causes the reduction in high frequency sound

Table 3.5 Effect of water absorption on the sound absorption capability of glass cotton (glass cotton blanket, density 25 kg/m³, 5 cm thick)
Key: a. water content (%);
b. sound absorption coefficient at various frequencies.

a. 含水率 (%) / b. 各频率的 吸声系数	250	500	1 K	2 K
0	0.25	0.65	0.92	0.98
5	0.25	0.63	0.89	0.82
20	0.20	0.58	0.50	0.70
50	0.05	0.15	0.40	0.30

absorption coefficient, followed by the extension of this effect towards lower frequencies when the water amount increases.

3. The effect of air stream: Apart from the fact that air stream blows some fibers away, it also causes the change of the sound wavelength. This leads to the shift in peak efficiency of sound absorption towards either higher or lower frequencies.

3.2.2 Sound Absorbing Structures

As mentioned before, one has to greatly increase the thickness of sound absorbing materials. This is not economically sound. Therefore for low frequencies, resonance sound absorbing structures are often used for sound absorption.

A single resonator is shown in Figure 3.3: a cavity of volume V, a small hole with diameter d through its wall, the neck length l. This kind of resonator is called the Helmholtz resonator.

When sound waves reach the resonator, the air inside the neck of the hole moves back and forth under the sound wave pressure. This moving air has a constant mass. It resists the velocity change caused by the sound wave, just as the inductor in an electrical circuit has the effect of moderating the change in electrical current. At the same time, when sound waves enter the neck of the hole, part of the sound energy is dissipated into heat through friction and resistance. Such friction and resistance are equivalent to the electrical resistance in an electrical circuit. Also, the air-filled cavity has the effect of resisting the pressure change from the small hole. This is an analogy to a capacitor in an electrical circuit, which resists the voltage change across its terminals.

Figure 3.3 The structure of a single-unit resonator
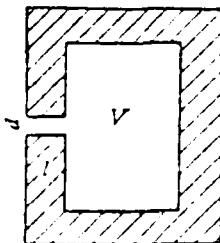
When the sound waves have a frequency equal to the natural frequency of the resonator, resonance will occur. The vibration amplitude is at its maximum. The air column moves back and forth in the neck of the hole with a maximum velocity, as well as a maximum frictional energy dissipation. The sound energy absorption is therefore also a maximum. Such a sound absorbing structure is called a resonance sound suppressor.

It should be made clear that the condition for Helmholtz resonators to be applicable is that the wavelength of the sound wave must be greater than the dimensions of the resonance cavity. Furthermore, dimensions of the opening on the cavity wall must be much smaller than those of the cavity. Only noises with low frequency and long wavelength can satisfy these conditions. Therefore, in general, Helmholtz resonators are useful for low frequency noises only.

Then, to what factors are resonance frequencies related? According to electrical circuit theory, the resonance frequency for a circuit:

$$f_r = \frac{1}{2\pi}\sqrt{\frac{1}{LC}},$$

(5.13)

where L is the inductance and C is the capacitance. By comparing sound and electricity, we can derive the resonance frequency in a sound system:

$$f_r = \frac{c}{2\pi}\sqrt{\frac{S}{l_k V}},$$

(5.14)

where c is the sound speed; S is the area of the small hole; $l_k = l + t_k$ is the effective neck length; l is the neck length or the board thickness for a board with drilled holes; t_k is a correction factor, for a circular hole, $t_k = 0.8d$; and V is the volume of the cavity.

154

For a single resonator, the frequency bandwidth Δf with sound absorption coefficient greater than 0.5 is

$$\Delta f = 8\pi^2 \frac{V}{\lambda_r^3} f_r.$$

(3.15)

Single resonators are highly selective in sound absorption. With narrow bandwidths they can only absorb noises with very simple sound. In industrial applications one often has to use multiple resonators. That is, to have many holes rather than just one on a board. When the number of holes is n, the resonance frequency is

$$f_r = \frac{c}{2\pi}\sqrt{\frac{ns}{l_k V}}$$

(3.16)

or

$$f_r = \frac{c}{2\pi}\sqrt{\frac{P}{l_k D}} \, ,$$

(3.17)

where p is the degree of openings, i.e., the ratio between the area of openings to the total surface area. (The relations between P and the hole dimensions and the distance between holes can be found in Appendix 5.) D is the cavity depth.

To make it convenient for calculations, Equation (3.17) is expressed in a diagram (see Appendix 4).

The sound absorption coefficient at resonance frequency is:

$$\alpha = \frac{4r_A}{(1 + r_A)^2} \, ,$$

(3.18)

where r_A is the relative sound resistance. It is determined by the flow resistance r, the effective opening length l_k, and degree of openings P. In a mathematical representation:

155

$$r_4 = \frac{r}{\rho_0 c_0} \frac{l_k}{P}.$$

$$(3.19)$$

The bandwidth for a multiple resonator with sound absorption coefficient greater than 0.5 is

$$\Delta f = 4\pi \frac{l_r}{\lambda_r} D.$$

$$(3.20)$$

Several values of α and Δf as determined by the tube method are given below:

1. Fixed hole diameter and cavity depth, variable degree of openings: Figure 3.4 shows the sound absorption coefficient of a resonator with the degree of openings P = 1-8%, board thickness t=2.5 mm, hole dimensions ϕ 10 mm, and cavity depth D=150 mm.

Figure 3.5 shows the sound absorption coefficient of a resonator with P=0.5-8.5%, board thickness t=2.5 mm, hole dimensions ϕ 5 mm and cavity depth D=150 mm.

From Figures 3.4 and 3.5, it can be seen that the sound absorption efficiency is better when the degree of openings P is in the range of 1-3%. For absorption bandwidth [1] above 150 Hz, particularly for resonators

---

[1] The absorption bandwidth referred here is the frequency bandwidth corresponding to sound absorption coefficients higher than 50%

---

with P=1.5-2.5%, the sound absorption efficiency is even better. For example, with P=2%, two resonators with hole dimensions ϕ 10, and ϕ 5 have bandwidth reaching about 300 Hz.

When the value of P reaches 4%, there is a small reduction in sound absorption coefficient (90%) at the resonance peak, meanwhile the bandwidth is also reduced to below 150 Hz. When the value of P is above 5%,

156

both the sound absorption coefficient at resonance peak and the band-width have significant decrease. When the value of P is above 3%, the sound absorption coefficient drops appreciably that the maximum value is not beyond 40-50%. When the value of P is reduced to a certain level (e.g., 0.5%), the resonator will not be sufficiently effective. Therefore, the sound absorption coefficient at resonance peak as well as the bandwidth are much lower than those at P=1-3%.

(a) sound absorption coefficient α (%)
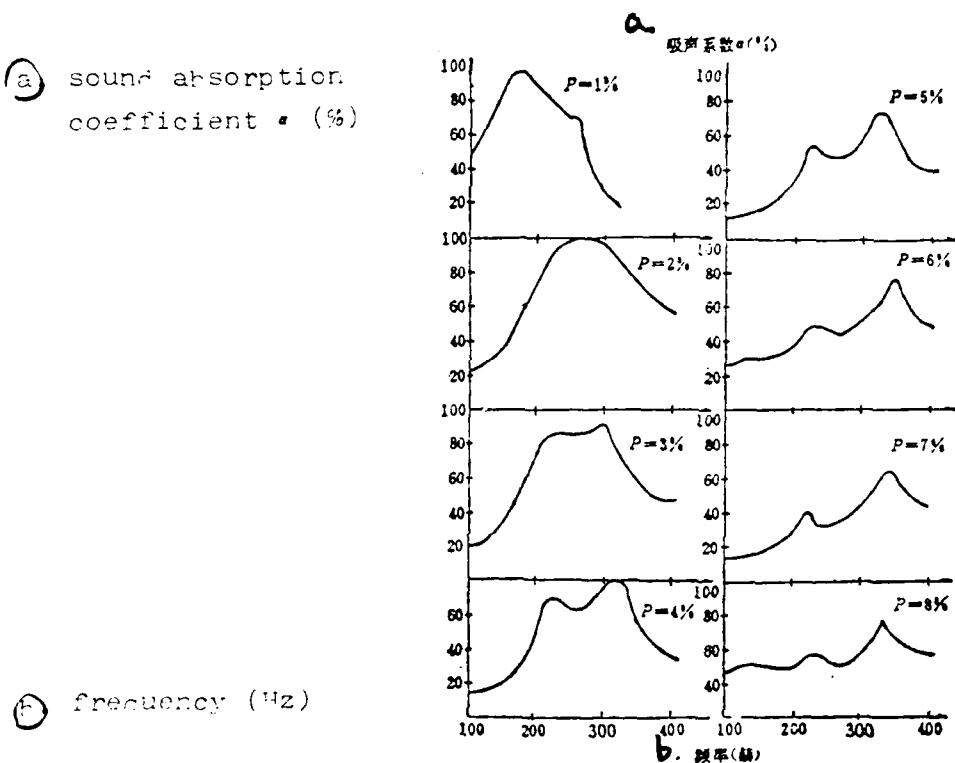
(b) frequency (Hz)

Figure 5.4   Sound absorption coefficient of resonators with different degrees of openings (1)
(Test resonator: Hole dimension φ 10 mm, board thickness t = 2.5 mm, cavity depth D = 150 mm)

157

a. sound absorption
   coefficient α (%)
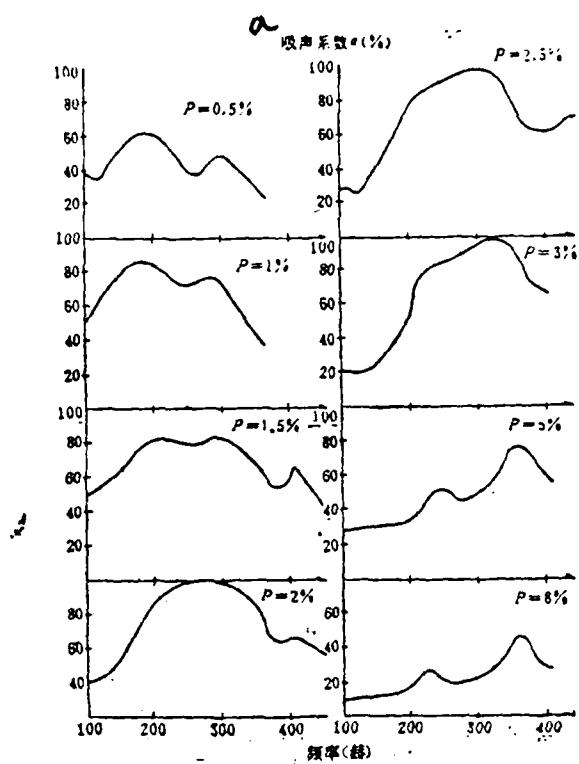
b. frequency (Hz)

Figure 3.5   Sound absorption coefficient of resonators with
              different degrees of openings (2)
              (Test resonator: hole dimensions φ5 mm, board
              thickness t = 2.5 mm, cavity depth D = 150 mm)

It can also be seen from experimental results that there is a shift
between resonance frequency data and theoretical values as calculated
from Equation (3.12).   For low degree of openings, experimental values
are higher than theoretical values, and vice versa.

2. Fixed degree of openings and cavity depth, variable hole dimensions:
Figure 3.6 shows the sound absorption coefficient for resonators with
hole dimensions between 2-10 mm, degree of openings P= 2%, cavity depth
D = 150 mm, and board thickness t = 2.5 mm.   It can be seen from the

158

a. sound absorption
   coefficient α (%)

b. frequency (Hz)

c. frequency (Hz)
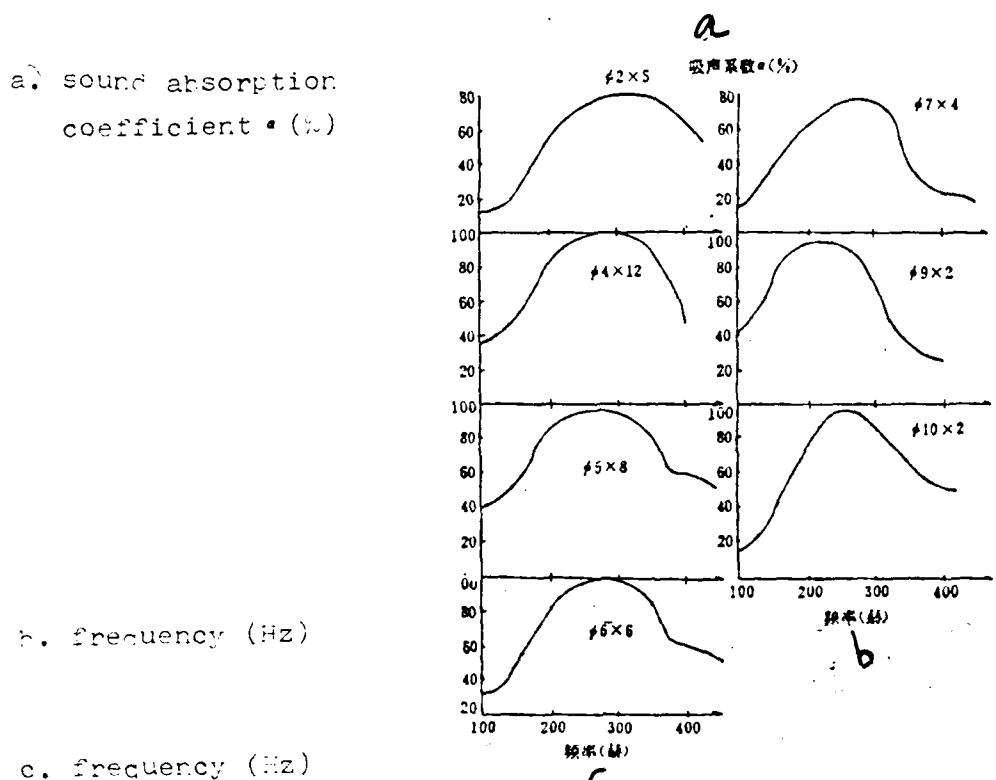
Figure 5.6   Sound absorption coefficient of resonators with variable hole diameters, fixed degree of openings (2%), cavity depth (150 mm), board thickness (2.5 mm)

a. h = 20 cm
b. h = 15 cm
c. h = 10 cm
d. h = 5 cm

e. frequency (Hz)
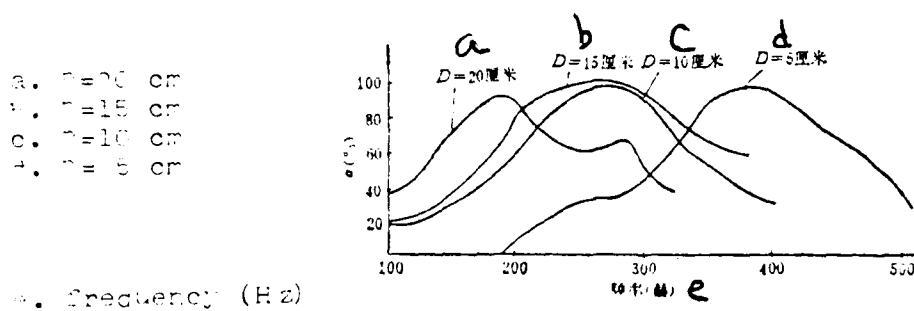
Figure 5.7   Sound absorption coefficient of resonators with variable cavity depth (5-20 cm), fixed degree of openings (2%), hole diameter (φ 10), and board thickness (2.5 mm).

159

figure that, in the range of $\phi 2 - \phi 10$mm, smaller hole dimensions yield greater resonance bandwidth, but the difference is not appreciable. Therefore, in this range, there is no significant influence on both sound absorption coefficient and bandwidth due to the changing hole dimensions.

3. Fixed degree of openings and hole diameter, variable cavity depth: Figure 3.7 shows experimental curves for sound absorption coefficient of resonators with cavity depth D = 5-20 cm, degree of openings P = 2%, hole dimension $\phi 10$ mm, board thickness t = 2.5 mm, cavity depth D = 5-20 cm. As shown in this figure, the resonance frequency shifts towards lower frequencies with decreasing cavity depth.

To extend the bandwidth of resonators, one can also combine the resonance cavity and resistive sound absorbing materials. That is, by filling the resonator with resistive sound absorbing materials, the sound absorbing bandwidth can be extended through the increase of the resistance in the resonance cavity. Table 3.6 shows examples of such combined sound absorbing structures. In general, with the degree of openings within 10%, there are effects of both resonance and resistance. When the degree of openings is above 20%, there is almost no resonance. Under this condition, the board with holes is not a resonance structure anymore, it is only a wide surfaced board then.

The low frequency sound absorbing characteristics can be varied by retaining a layer of air behind the sound absorbing materials. When the thickness of this air layer is increased, the low frequency sound

160

absorbing coefficient increases, with a moderate decrease in high frequency sound absorbing coefficient. When the distance between material and the wall surface is just below $\lambda/4$, the sound absorbing coefficient is at its maximum; when the distance is equal to $\lambda/2$, the sound absorbing coefficient is at its minimum.

As indicated by experimental results, the effect due to the air layer is different for sound absorbing materials with different thickness. The thinner the sound absorbing material is, the greater the influence on sound absorption due to the air layer. It is not practical to have too thin sound absorbing materials. Table 5.6 shows several examples of such combined sound absorbing structures.

Sometimes one can use sound absorbing wedges, as shown in Figure 5.9 to obtain very high sound absorbing coefficient.

The best height of wedge h is approximately equal to one half of the wavelength corresponding to the lowest frequency in the sound to be absorbed. Such a sound absorbing wedge can have a sound absorbing coefficient as high as 0.98, i.e., it can absorb the sound energy almost completely. If the requirement is not so high, the wedge can be appropriately shortened. The sound absorbing wedge in Figure 5.9 has a sound absorbing coefficient higher than 0.90, starting from 100 Hz.
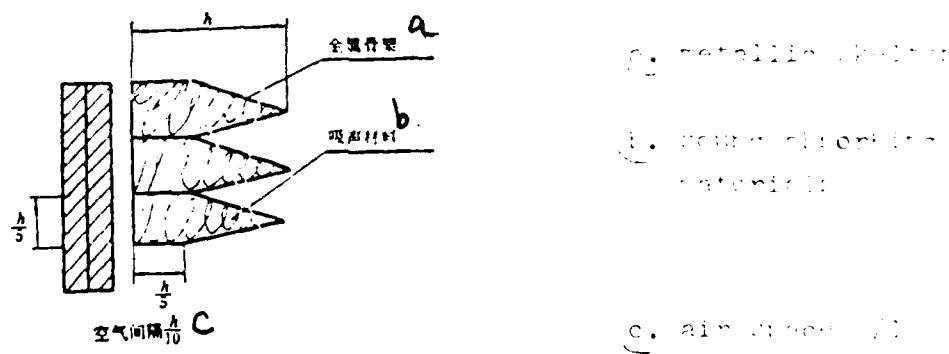
Figure 5.9 Sound Absorbing Wedges
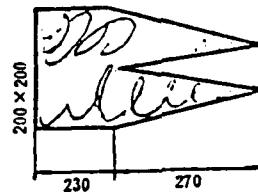
Figure 3.9 One Simple Sound Absorbing Wedge

Table 3.6 Sound absorption coefficient of combined sound absorbing structures

a. structure   b. thickness, cm   c. density, kg/m^3

d. sound absorption coefficient at various frequencies

e. production location

结构名称	厚度 厘米	密度 公斤/米³	125	250	500	1000	2000	4000	产地
超细玻璃棉 前贴φ5,2%,板厚1毫米,穿孔钢板	15	25	0.85	0.70	0.60	0.41	0.25	0.25	
前贴φ5,5%,板厚1毫米,穿孔钢板	15	25	0.60	0.65	0.60	0.55	0.40	0.30	上海
前贴φ9,10%,板厚1毫米,穿孔钢板	6	30	0.38	0.63	0.60	0.56	0.54	0.44	
前贴φ9,20%,板厚1毫米,穿孔钢板	6	30	0.13	0.63	0.60	0.66	0.69	0.67	
沥青矿渣棉后留 空腔2.5厘米	3	200	0.19	0.47	0.68	0.68	0.78	0.92	太原
空腔4厘米	3	200	0.36	0.64	0.74	0.70	0.75	0.87	
空腔6.5厘米	3	200	0.36	0.66	0.66	0.64	0.78	0.90	
聚氯乙烯泡沫塑料2厘米,后改玻璃棉留4厘米			0.13	0.55	0.88	0.68	0.70	0.90	
同上,但空腔为6厘米			0.60	0.90	0.76	0.65	0.77	0.90	
矿棉吸声板厚1.8厘米		300	0.06	0.15	0.50	0.84	0.82	0.85	北京
同上,但留空腔3厘米		300	0.20	0.45	0.52	0.65	0.72	0.78	
同上,但留空腔7厘米		300	0.40	0.58	0.68	0.80	0.85	0.80	

ultrafine glass cotton inlet φ5, , 1 mm thick, steel plate with holes
ditto φ5, 5
ditto φ9, 10
ditto φ9, 20

asphalt mineral residual cotton blanket, back with 2.5 cm cavity
cavity 4 cm
cavity 6.5 cm
polyvinyl ethylene foam plastics, 2 cm, back with 4 cm glass cotton blanket
same as above, except 6 cm cavity
1.8 cm mineral sound absorbing cotton.
same as above, except 3 cm cavity
same as above, except 7 cm cavity

Chiang-hai

Tai-yuan

162

Metallic sound absorbing structures with ultrafine holes are
basically combined sound absorbing structures with cavities and metallic
boards, which have thickness of less than 1 mm and ultrafines holes
with dimensions less than ϕ 1 mm. The degree of openings is between
0.5 and 5%. Such structures are basic acoustic components with both
sound resistance and sound mass. Their cavities have also the effect
of a sound capacitor and form a resonance system along with the boards
with ultrafine holes.

Ma Ta-You derived the relative sound resistance and relative sound
mass, respectively, for metallic sound absorbing boards with ultrafine
holes as the following:

$$(3.21)$$

$$r_A = \frac{0.335}{d^2} \frac{t}{P} k_r,$$

$$m_A = 0.294(10^{-3}) \frac{t}{P} k_m,$$

$$(3.22)$$

where k_r and k_m are, respectively, the sound resistance constant and
the sound mass constant:

$$k_r = \sqrt{1 + \frac{x^2}{32}} + \frac{\sqrt{2} x}{8} \cdot \frac{d}{t},$$

$$(3.23)$$

$$k_m = 1 + \frac{1}{\sqrt{9 + \frac{x^2}{2}}} + 0.85 \frac{d}{t} \quad x = 0.21 \, d \sqrt{f}.$$

$$(3.24)$$

Based on the Equations (3.21) – (3.24), for boards with very small
hole dimensions, the r_A values are greater than those with normal size
holes, but the m_A values are smaller.

The resonance frequency of sound absorbing structures with boards
of ultrafine holes is the same as that in Equation (3.14). However, in
this case the parameter l_k is

163

$$l_k = t + 0.8d + PD/3, \tag{3.25}$$

where PD/3 is a tail correction factor, and D is the cavity depth.

Resonance sound absorption coefficient is the same as that in Equation (3.18), and is generally above 0.90. The absorption angular bandwidth (bandwidth multiplied by 2π) is approximately equal to the ratio r_A/m_A between the sound resistance r_A and the sound mass m_A. This ratio can be obtained from Equations (3.21)-(3.24):

$$\frac{r_A}{m_A} = \frac{1140}{d^2} \frac{k_r}{k_m}. \tag{3.26}$$

It can be seen from Equation (3.26), the smaller the hole dimension r is, the greater r_A/m_A is. Therefore, boards with hole diameters less than 1 mm can have much greater sound absorption bandwidth than those for boards with normal size holes. This is one of the special characteristics of sound absorbing structures with boards of ultrafine holes.

Extensive experiments indicate that, when the boards have thickness t = 0.2-1 mm, hole dimensions $\phi 0.2 - \phi 1$ mm, and degree of openings P = 0.5-4%, the sound absorbing effect is relatively good. It is even better when P = 1-2.5%. When t > 1 mm, d > $\phi 1$ mm, the sound absorbing coefficient decreases appreciably with too large or too small degree of openings. Experimental results on single-layer sound absorbing structures with boards of ultrafine holes are shown in Table 3.7. It can be seen from this table that good sound absorbing structures with boards of ultrafine holes have more than 6 third-octave frequency bandwidths. One can also choose to use double-layer sound absorbing structures in order to obtain greater bandwidth. In this case there are two resonance peaks. The resonance frequencies are:

164

$$f_{i} = \frac{c}{4\pi}\sqrt{\frac{P_{1}}{D_{1}l_{1}}}\left\{\sqrt{\left(\frac{P_{1}}{P_{2}}+\sqrt{\frac{D_{1}}{D_{2}}}\right)^{2}-1}\right.$$
$$\left.+\sqrt{\left(\frac{P_{1}}{P_{2}}-\sqrt{\frac{D_{1}}{D_{2}}}\right)+1}\right\},$$

$$(3.27)$$

Figure 3.7 Sound absorption coefficient of a single-layer board with fine holes

a. frequency (Hz) b. sound absorption coefficient c. cavity depth, cm
d. specification e. hole diameter ϕ0.8mm, board thickness t=0.8mm, P=1%
f. hole diameter ϕ0.8mm, board thickness t=0.8mm, P=2%

a 频率（赫）	孔径 φ0.8 毫米, 板厚 $t=0.8$毫米, $P=1\%$ (e)				孔径 φ0.8 毫米, 板厚 $t=0.8$毫米, $P=2\%$ (f)				孔径φ0.8毫米, 板厚$t=0.8$毫米, $P=1\%$ (e)	孔径φ0.8毫米, 板厚$t=0.8$毫米, $P=2\%$ (f)	
	5	10	15	25	3	5	10	20	20	15	20
100	0.06	0.24	0.35	0.63	0.07	0.05	0.12	0.40	0.26	0.12	0.12
125	0.05	0.24	0.37	0.72	0.08	0.05	0.10	0.40	0.28	0.18	0.19
160	0.05	0.33	0.54	0.92	0.09	0.05	0.14	0.50	0.35	0.19	0.26
200	0.11	0.58	0.77	0.97	0.14	0.07	0.33	0.72	0.51	0.30	0.30
250	0.29	0.71	0.85	0.99	0.11	0.17	0.46	0.83	0.67	0.43	0.50
320	0.36	0.82	0.92	0.97	0.12	0.17	0.63	0.95	0.77	0.96	0.55
400	0.61	0.98	0.97	0.76	0.17	0.36	0.77	0.80	0.71	0.81	0.54
500	0.87	0.96	0.87	0.38	0.15	0.60	0.92	0.54	0.52	0.57	0.45
630	0.99	0.84	0.65	0.10	0.25	0.76	0.50	0.27	0.34	0.52	0.41
800	0.62	0.46	0.30	0.99	0.44	0.54	0.53	0.07	0.31	0.36	0.27
1 k	0.76	0.40	0.20	0.40	0.56	0.78	0.31	0.77	0.42	0.32	0.35
1.25 k	0.44	0.15	0.20	0.09	0.81	0.57	0.23	0.40	0.37	0.22	
1.6 k	0.20	0.07	0.32	0.17	0.65	0.56	0.06	0.13	0.28	0.46	0.36
2 k	0.12	0.29	0.15	0.12	0.40	0.22	0.40	0.25	0.40	0.33	0.36
2.5 k									0.25	0.35	0.31
3.2 k									0.27	0.35	0.33
4 k									0.30	0.34	
5 k									0.25	0.32	0.35

g. 备注 h. 管测法 i. 混响室法

Remarks 1. tube testing method 2. reverberation room method

165

$$f_{r_1} = \frac{c}{4\pi}\sqrt{\frac{P_2}{D_1 l_2}}\left\{\sqrt{\left(\frac{P_1}{P_2} + \sqrt{\frac{D_1}{D_2}}\right)^2 - 1}\right.$$
$$\left. - \sqrt{\left(\frac{P_1}{P_2} - \sqrt{\frac{D_1}{D_2}}\right)^2 + 1}\right\},$$

(5.28)

where l_1, D_1 and P_1 are, respectively, the front cavity board thickness, the cavity depth and the degree of openings; l_2, D_2 and P_2 are, respectively, the back cavity board thickness, the cavity depth, and the degree of openings.

Anti-resonance frequency is

$$f_x = \frac{c}{2\pi}\sqrt{\frac{P_2}{l_2}\left(\frac{1}{D_1} + \frac{1}{D_2}\right)}.$$

(5.29)

Figure 5.10 is a schematic diagram of the sound absorbing characteristics of double-layer sound absorbing boards with ultrafine holes. Such double-layer boards, if appropriately arranged, can yield very broad absorption bandwidths. Table 5.5 lists the sound absorption coefficient for several standard double-layer boards with ultrafine holes in combination. From this table, it can be seen that the bandwidth of a good double-layer sound absorbing structure with boards of ultrafine holes can reach above 10 third-octave frequency bandwidths.
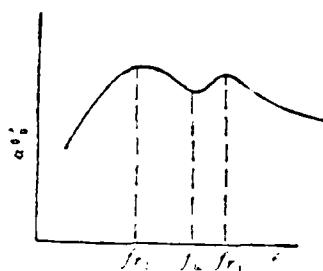
Figure 5.10   Schematic diagram showing the sound absorbing characteristics of a double-layer sound absorbing board with ultrafine holes.

Table 3.8 Sound absorption coefficient of double-layer boards with
fine holes

a. frequency (Hz)   b. sound absorption coefficient   c. both cavity depth, cm
d. specification
e. hole diameter φ0.8mm, board thickness t=0.8mm, P=2.5%+1% [1]
f. hole diameter φ0.8mm, board thickness t=0.8mm, P=2%+1%
g. hole diameter φ0.8mm, board thickness t=0.8mm, P=3%+1%
h. hole diameter φ0.8mm, board thickness t=0.8mm, P=5%+3%
i. hole diameter φ0.8mm, board thickness t=0.8mm, P=2.5%+2%
j. hole diameter φ0.8mm, board thickness t=0.8mm, P=2%+1%
k. hole diameter φ0.8mm, board thickness t=0.8mm, P=2%+1%

l. front cavity
m. back cavity

o. remarks   p. tube testing method   q. sound mixing-room method

r. P2.5%+1% refers to: degree of openings for the front layer board = 2.5%,
                        and degree of openings for the back layer board = 1%.

频率(Hz) a	e 孔径φ0.8毫米, 板厚 t=0.8毫米, P=2.5%+1% [1] 前腔:3 后腔:7	前腔:5 后腔:5	f 孔径φ0.8毫米, 板厚 t=0.8毫米, P=2%+1% 前腔:4 后腔:16	g 孔径φ0.8毫米, 板厚 t=0.8毫米, P=3%+1% 前腔:8 后腔:12	前腔:8 后腔:12	h 孔径φ0.8毫米, 板厚 t=0.8毫米, P=5%+3% 前腔:2 后腔:1	i 孔径φ0.8毫米, 板厚 t=0.8毫米, P=2.5%+2% 前腔:1 后腔:3	j 孔径φ0.8毫米, 板厚 t=0.8毫米, P=2%+1% 前腔:10 后腔:10	前腔:5 后腔:10	k 孔径φ0.8毫米, 板厚 t=0.8毫米, P=2%+1% 前腔:8 后腔:12
100	0.25	0.17	0.47	0.44	0.37			0.24	0.19	0.41
125	0.26	0.18	0.58	0.48	0.40			0.29	0.25	0.41
160	0.43	0.29	0.77	0.75	0.62			0.32	0.31	0.46
200	0.60	0.50	0.95	0.86	0.81			0.64	0.50	0.83
250	0.71	0.69	0.99	0.97	0.92			0.79	0.79	0.91
320	0.86	0.88	0.93	0.99	0.99			0.72	0.79	0.69
400	0.83	0.97	0.78	0.97	0.99			0.67	0.62	0.58
500	0.92	0.97	0.54	0.93	0.95			0.70	0.67	0.51
630	0.70	0.74	0.51	0.93	0.90			0.79	0.60	0.54
800	0.53	0.74	0.75	0.96	0.88	0.27	0.88	0.74	0.57	0.60
1k	0.65	0.99	0.86	0.64	0.66	0.55	0.88	0.64	0.68	0.61
1.25k	0.94	0.70	0.42	0.41	0.50	0.61	0.52	0.43	0.65	0.60
1.6k	0.65	0.38		0.30	0.25	0.71	0.40	0.42	0.53	0.55
2k	0.35	0.24		0.15	0.17	0.54	0.45	0.42	0.46	0.51
2.5k						0.70	0.95	0.42	0.35	0.47
3.2k						0.95	0.63	0.39	0.34	0.32
4k						0.45	0.34	0.42	0.35	0.30
5k						0.22	0.33	0.28	0.26	0.23

注 O 生 | P 管 测 法 | Q 混 响 室 法

1, P2.5%+1%为前层微穿孔板穿孔率2.5%,后层微穿孔板穿孔率1%.

§ 3.3 Resistive Sound Suppressors

Resistive sound suppressors remove sound through sound absorbing
materials arranged along the stream passages. Figure 3.11 shows
simplified pictures of several resistive sound suppressors.

For example, Figure 3.11(a), (b), and (c) are the simplest tube-type
sound suppressors, which are also referred to as straight-through sound
suppressors. Their characteristic is that the stream passes through
them without changing directions. Such sound suppressors have many
methods for calculation, e.g.,

(a)　　　　(b)　　　　(c)

(d)　　　(e)

(f)　　　(g)　　　(h)

(i)　　　(j)

(k)　　　(l)
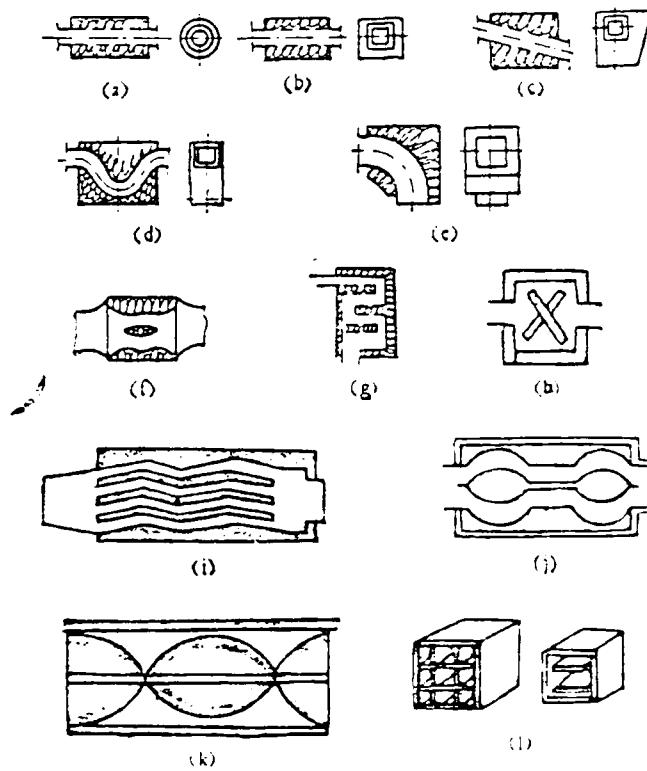
Figure 3.11　Simplified diagrams of several resistive
sound suppressors

1. Belov Equation:

$$\Delta L = 1.1 \frac{\varphi(\alpha)P}{S} l \quad (db);$$

(5.30)

2. Sabine Equation:

$$\Delta L = \frac{1.05 \alpha_m^{1.4} P}{S} \quad (db);$$

(5.31)

3. Rogers Equation:

$$\Delta L = 4.34 \frac{1 - \sqrt{1 - \alpha}}{1 + \sqrt{1 - \alpha}} \cdot \frac{P}{S} \cdot l \quad (db);$$

(5.32)

4. Brüel Equation:

$$\Delta L = 1.5 \alpha \cdot \frac{P}{S} \cdot l \quad (db);$$

(5.33)

5. Cremer Equation:

$$\Delta L = 1.1 \alpha_m \frac{P}{S} \cdot l \quad (db);$$

(5.34)

6. Joule Equation:

$$\Delta L = 1.085 \alpha_m \frac{P}{S} \cdot l \quad db;$$

(5.35)

with ΔL -- the amount of sound being suppressed, db; P -- perimeter of the active parts, m; l -- length of the active parts. m; S -- cross-sectional area of the active parts, m^2; α -- sound absorption coefficient of the sound absorbing materials (standing wave tube method, normal incidence); α_m -- sound absorption coefficient of sound absorbing materials (sound mixing room method, random incidence).

169

The relationship between α and $\varphi(\alpha)$ is given in Table 3.9

Table 3.9 Relationship between α and $\varphi(\alpha)$

α	0.1	0.2	0.3	0.4	0.5	0.6	0.7	0.8	0.9	1.0
$\varphi(\alpha)$	0.1	0.2	0.35	0.5	0.65	0.9	1.2	1.6	2.0	4.0

Among the previous equations, (3.32) and (3.33) are close to the Belov equation, (3.35) is close to the Sabine equation.

Since the Sabine equation is applicable only for the following conditions: rectangular tube passages with dimensional ratio 1:1 – 1:2, frequencies between 125 – 2000 Hz, tube cross-sectional area approximately between 23 – 45 cm, sound absorption coefficient between 0.2 – 0.8 as determined by sound mixing room method, this equation has a relatively narrow range of application. Therefore, we will mainly discuss the Belov equation (3.30).

Equation (3.30) is derived by simplifying the theory on plane waves under special conditions. It leads to relatively large discrepancies from real situations. The calculated values are often greater than experimentally determined values.

From experiments, when $\alpha \leqslant 0.6$, theoretical and experimental values are relatively close; when $\alpha > 0.6$, $\varphi(\alpha)$ increases rapidly and theoretical values become greater than experimental values. According to experience, when α is between 0.6–1.0, φ' = 1–1.5. Therefore, by simplifying equation (3.30) to equation (3.36), and Table 3.9 to Table 3.10, there will be then a better agreement between theoretical and experimental values.

170

$$\Delta L = \frac{\varphi(a)Pl}{S} \quad (\text{db}).$$

$$(3.36)$$

Table 3.10 Relationship between a and $\varphi(a)$
(values based on experience)

a	0.1	0.2	0.3	0.4	0.5	0.6 - 1.0
$\varphi(a)$	0.1	0.25	0.40	0.55	0.7	1 - 1.5

Furthermore, $\varphi(a)$ is not only related to the sound absorption coefficient, it is also related to the area of the passage. When the passage area is larger, high frequency sound waves propagate along the passage as a narrow sound beam, with little or no contact with the sound absorbing materials. Consequently, the sound suppression is greatly reduced. By defining the upper limit frequency f_u as the frequency at which the sound absorption effect shows drastic decrease, then

$$f_u = Kc/D \quad (\text{Hz}),$$

$$(3.37)$$

where K -- proportionality constant, 1-2, taken as 1.8 generally; c -- sound speed, m/s; D -- average perimeter value of the passage cross-section, diameter of a circular cross section, m.

For frequencies lower than f_u, the sound suppression can be calculated. from Equation (3.36). Theoretical values agree with experimental values. For frequencies higher than f_u, sound suppression decreases significantly.

171

The P/S term in Equation (3.30) is equal to $\dfrac{\pi D}{\frac{\pi D^2}{4}} = \dfrac{4}{D}$ for a cylindrical sound suppressor. For a square sound suppressor, it is equal to $4D/D^2 = 4/D$; and for a rectangular one, $2(D_1+D_2)/D_1 D_2$.

(a) Circle   (b) Square   (c) Rectangle
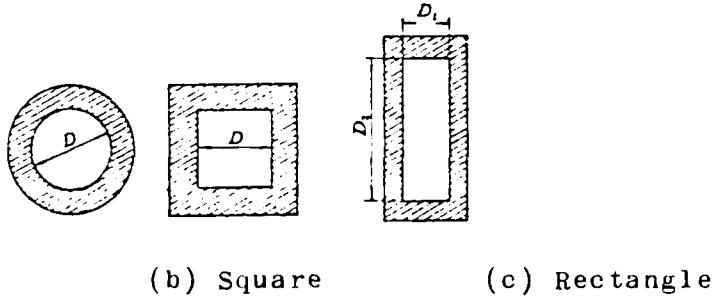
Figure 3.12   The cross sections of three types of sound suppressors

Therefore, Equation (3.30) can be reduced to the following for cylindrical and square sound suppressors:

$$\Delta L = \frac{4\varphi(\alpha)l}{D} \quad \text{(db)}, \tag{3.38}$$

and for rectangular sound suppressors:

$$\Delta L = \frac{2(D_1 + D_2)\varphi(\alpha)l}{D_1 D_2} \quad \text{(db)}. \tag{3.39}$$

For example, in designing one cylindrical sound suppressor: For a sound reduction of 25 db, a passage diameter of 250 mm, and an average sound absorption coefficient $\bar{\alpha} = 0.5$, what should be the length of the sound suppressor?

Solution: We know that $\Delta L = 25$ db and $D = 0.25$ m. From Table 3.10, when $\alpha = 0.5$, $\varphi(\alpha) = 0.7$, then from Equation (3.38)

$$l = \frac{\Delta L \times D}{4\varphi(\alpha)} = \frac{25 \times 0.25}{4 \times 0.7} = 2.23 \text{ m},$$

i.e., the length of sound suppressor should be selected as 2.23 m.

172

The structure of a tube type sound suppressor is simple and can be easily manufactured. It also has good aerodynamic characteristics. When air flow volume is low, tube type sound suppressors are generally used. When flow volume is high, the cross section of the passage has to be large to maintain low flow rate; the effect of sound suppression is therefore reduced (particularly for high frequencies). Therefore, sound suppressors are often made into bee-hive or plate types (see figure 3.11 (l),(m)).

Bee-hive type sound suppressors are actually made by combining many small tube type sound suppressors in parallel. Calculations can be done by Equation (3.38). Their advantages lie in the good efficiencies for medium and high frequencies. However, with more complicated structures, the resistance is higher.

For bee-hive type sound suppressors, each unit passage can control about 200x200 mm.

Plate type sound suppressors are made by combining a row of rectangular sound suppressors in parallel. Each passage is equivalent to a rectangular sound suppressor. Calculations can be done by Equation (3.39). The structures of such sound suppressors are not complicated, have relatively good sound suppression efficiencies at medium and high frequencies, and do not have too high resistance.

In general, the inter-plate distance for plate-type sound suppressors should be chosen as 100-200 mm. The thickness of the plate, according to the frequency characteristics of the noise source, can be chosen as 25-120 mm.

173

In engineering applications, in order to raise the sound suppression efficiencies for high frequencies, the plate-type sound suppressors are often modified to become bend-plate type sound suppressors (see Figure 3.11(i)). In these type sound suppressors, the multi-reflections of the sound wave increase the opportunity for the sound wave to make contact with the sound absorbing materials. This greatly increases the sound absorption effect, particularly at high frequencies. However, bend-plate type sound suppressors have higher resistance than the plate-type ones. Bend-plate type sound suppressors should, in principle, be "opaque"; but in order to reduce resistance, the bending angle is best at less than 20°.

To further increase the sound suppression effect, maze type sound suppressors are sometimes used as shown in Figure 3.11 (g), (h). These types of sound suppressors allow the sound wave to have many times of normal incidence, along with multi-reflections. Sound reductions are significantly enhanced. However, the flow rate can not be too high. Otherwise, it will produce strong re-generated noises, and makes the sound suppressor become useless. The resistance of maze-type sound suppressors is also relatively high, leading to a high pressure drop. It is not appropriate in applications with strict resistance-loss conditions.

In recent years, to satisfy high sound suppression efficiencies, and in the mean time not to affect the aerodynamic characteristics, sound suppressors are often made into sound stream type, as shown in Figure 3.11(d), (e), (f), (j), (k) and Figure 3.13.

174

Such sound suppressors have the sound absorbing materials in sinusoidal or near sinusoidal shapes. Not only do they yield high sound absorption efficiencies through multi-reflections of the sound wave, but they also allow air to pass through smoothly. Therefore, both requirements of high sound absorption efficiency and low resistance are met. However, with more complicated manufacturing processes, their prices are higher.

(a)   (b)

(c)   (d)

(e)
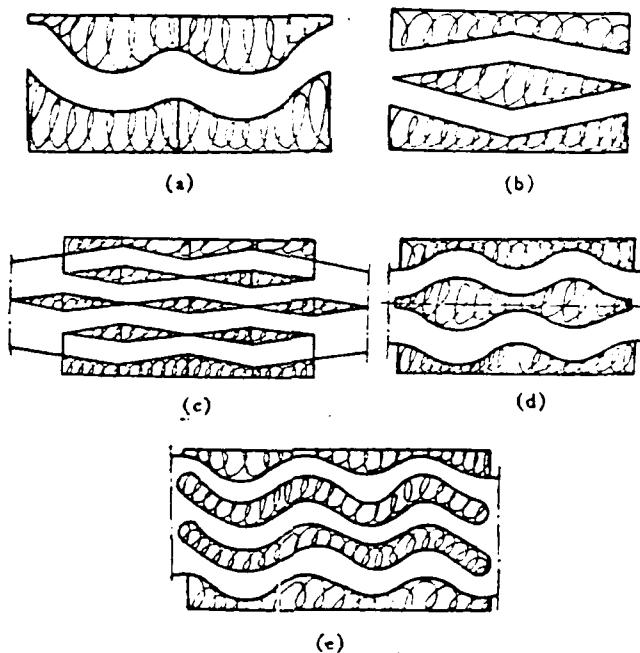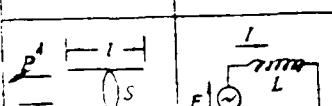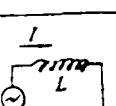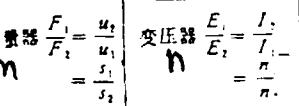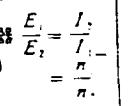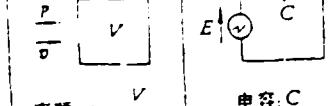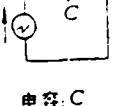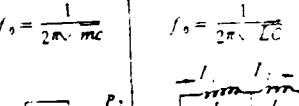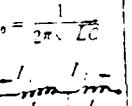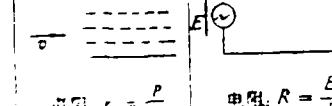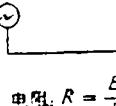
Figure 3.13. Schematic diagrams of several sound stream type sound suppressors

§ 3.4 Reactive Sound Suppressors

The most common reactive sound suppressors include the expansion-room type and the resonance type sound suppressors. Besides, there are other sound suppressors based on interference, bends, obstacles, and perforated plates, etc. Their basic principles are the applications of appropriate combinations of the internal sound resistance, sound capacitance, and sound mass of the sound suppressors, which either reflect the noise back to its source or absorb the noise effectively. Their functions are very much like the wave filters in alternating electrical circuits. Therefore, they are also called acoustic filters. Their difference from resistive sound suppressors is that they have no sound absorbing materials,

Table 3.11 Schematic comparisons between acoustic passages and equivalent electrical circuits for some common acoustic systems

a. sound system
b. electrical system
c. sound pressure
d. electrical potential
e. volume speed
f. electrical current
g. acoustic mass
h. electrical inductance
i. acoustic capacitance
j. electrical capacitance
k. acoustic resistance
l. electrical resistance
m. acoustic transformer
n. transformer

The amount of sound reduction (transmission loss) of a reactive sound suppressor is

$$\Delta L_w = \frac{\text{time average of incident sound energy } (W_\lambda)}{\text{time average of transmitted sound energy } (W_t)} \ . \tag{3.40}$$

If the sound wave in the passage of a sound suppressor is a plane wave, sound pressure is much smaller than the air pressure; there will be no reflection at the rear end of the sound suppressor. We can derive the sound suppression equation under these conditions, along with the assumption that no sound energy can pass through the wall surface of the sound suppressor. (Amount of sound suppression in terms of transmission loss, same for the following). Let the incident wave have a wave function of ϕ_i, and the reflected wave have a wave function of ϕ_r, at any point in the passage. Since the wave is a plane wave, then

$$\phi_i = A e^{ikx - i\omega t}, \qquad \phi_r = B e^{-ikx - i\omega t} \qquad k = \frac{\omega}{c}.$$

The sound pressure P and the particle velocity V are, respectively,

$$P_i = \rho_0 \frac{\partial \phi_i}{\partial t} = -i\omega\rho_0 A e^{ikx - i\omega t} = P^{(+)} e^{ikx - i\omega t} \ (\text{N/m}^2)$$

$$P_r = \rho_0 \frac{\partial \phi_r}{\partial t} = -i\omega\rho_0 B e^{ikx - i\omega t} = P^{(-)} e^{-ikx - i\omega t} \ (\text{N/m}^2)$$

$$V_i = -\frac{\partial \phi_i}{\partial x} = -ik A e^{ikx - i\omega t} = \frac{1}{\rho_0 c} P^{(+)} e^{ikx - i\omega t} \ (\text{m/s})$$

$$V_r = -\frac{\partial \phi_r}{\partial x} = +ik B e^{-ikx - i\omega t} = -\frac{1}{\rho_0 c} P^{(-)} e^{-ikx - i\omega t} \ (\text{m/s})$$

The time average of incident sound wave energy is

$$\overline{W} = \frac{1}{2} \operatorname{Re}(P_i \widetilde{V}_i S) = \frac{1}{2} \frac{S}{\rho_0 c} |P^{(+)}|^2 \quad (\text{watt}) \tag{3.41}$$

where $\widetilde{V}_i$ is the complex conjugate of V_i.

From Equations (3.40), (3.1) and (3.41) one can obtain the amount of sound reduction (amount of sound suppression) between two points in the passage:

$$\Delta L = 10 \log \frac{\overline{W}_1}{\overline{W}_2} = 10 \log \left| \frac{P_1^{(+)}}{P_2^{(+)}} \right|^2 \quad (\text{db}) \tag{3.42}$$

where $P_1^{(+)}$ and $P_2^{(+)}$ represent, respectively, the forwarding sound pressure at point 1 and point 2 in the passage.

3.4.1 Single expansion-room type sound suppressor

The simplest reactive sound suppressor is the single expansion-room sound suppressor, as shown in Figure 3.14. For an expansion-room of length l_1, small-tube cross-sectional area of S_1, large tube cross-sectional area of S_2, the expansion ratio of this sound suppressor is

$$m = S_2 / S_1 \; .$$
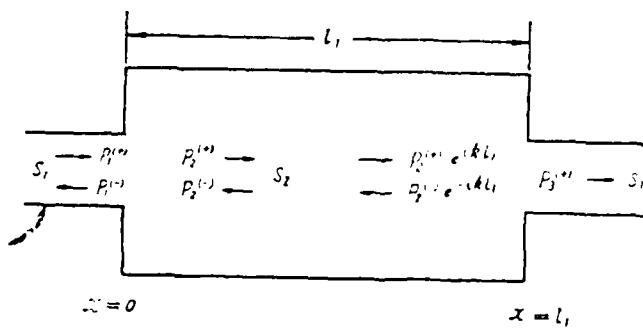
Figure 3.14 Single expansion-room type sound suppressor

178

At the entrance of the expansion room, x = 0; at the rear end, x = l_1; and at the points of continuation, pressures are in equilibrium and the volume flow is continuous.

At x = 0,

$$P_1^{(+)} + P_1^{(-)} = P_2^{(+)} + P_2^{(-)},$$
$$S_1(P_1^{(+)} - P_1^{(-)}) = S_2(P_2^{(+)} - P_2^{(-)}).$$

At x = l_1

$$P_2^{(+)} e^{ikl_1} + P_2^{(-)} e^{-ikl_1} = P_3^{(+)},$$
$$S_2(P_2^{(+)} e^{ikl_1} - P_2^{(-)} e^{-ikl_1}) = S_1 P_3^{(+)}.$$

Through manipulations,

$$\frac{P_3^{(+)}}{P_1^{(+)}} = \cos kl_1 + i\,\frac{1}{2}\left(m + \frac{1}{m}\right)\sin kl_1$$

and

$$\left|\frac{P_3^{(+)}}{P_1^{(+)}}\right|^2 = 1 + \frac{1}{4}\left(m - \frac{1}{m}\right)^2 \sin^2 kl_1.$$

By substituting into Equation (3.42), one has

$$\Delta L_w = 10\log\left[1 + \frac{1}{4}\left(m - \frac{1}{m}\right)^2 \sin^2 kl_1\right]\ (\text{db}).$$

$$(3.43)$$

This equation can also be expressed by Figure 3.15.
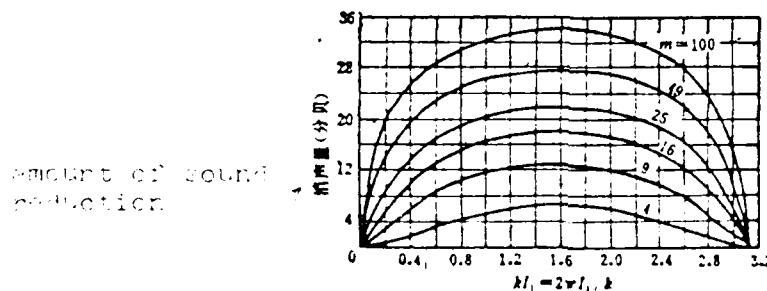
Figure 3.15 Sound Suppression of Single Expansion-room Sound Suppressors

179

In engineering, for convenience, Equation (3.43) is often converted into Table 3.12. It can be seen from this Table that, when the sound suppression is determined by the expansion ratio m, the maximum sound suppression is related to frequency as

$$\sin^2 k l_1 = 1,$$
$$k l_1 = \frac{2\pi f}{c} l_1 = \frac{\pi}{2}, \frac{3\pi}{2}, \cdots,$$
$$f_n = \frac{(2n+1)c}{4 l_1} \ (\mathrm{Hz}) \quad n = 1, 2, 3, \cdots.$$

It is obvious then that, when l_1 increases, the frequency f_n with maximum sound suppression moves towards lower frequencies. Figure 3.16 shows the effect of the tube length l_1 on the sound suppression characteristics of sound suppressors.

It should be pointed out that sound pressure values, rather than sound energy, are actually measured. The maximum value of sound pressure at the entrance of the sound suppressor is $|P^{(+)} + P^{(-)}|$, but not $|P^{(+)}|$. Therefore, the measured sound suppression ΔL is greater than the one calculated from (3.43). When $P^{(+)}$ and $P^{(-)}$ are in phase, it is at the maximum. This maximum sound suppression is

$$\Delta L = 10\log\left[\left|\frac{P_1^{(+)}}{P_1^{(+)}}\right| + \left|\frac{P_1^{(-)}}{P_1^{(+)}}\right|\right]^2$$
$$= 10\log\left[1 + \frac{1}{2}\left(m - \frac{1}{m}\right)^2 \sin^2 k l_1 \right.$$
$$\left. + \left(m - \frac{1}{m}\right) \sin k l_1 \sqrt{1 + \frac{1}{4}\left(m - \frac{1}{m}\right) \sin^2 k l_1}\right] \quad (3.44)$$
$$(\mathrm{db})$$

From the sound suppression ΔL_P one can determine ΔL_w with the correction curve as shown in Figure 3.17.

Table 3.1? The amount of sound reduction at different frequencies f and different expansion ratios m

扩张比 m (分贝) 消声量 ΔL 频率 f (赫)	0.125 f_0	0.375 f_0	0.625 f_0	0.875 f_0	f_0[1]	1.25 f_0	1.5 f_0	1.75 f_0	1.875 f_0
5	1.5	4.5	7	7.8	8	7.4	5.5	2.5	1
10	3	9	12.5	14	14.1	13	10.5	5.5	2
15	5	12.7	16	17.4	17.5	16.9	13.5	7.5	2.5
20	7	15.2	18	19.8	20	19	16.8	10.7	5
25	8	17.5	20	21.3	21.5	21	18	12	5.5
30	9.5	18	22	23	23.1	22.5	20	13	6
35	11	19	23	24.2	24.5	24	21.5	15	7.5
40	12.5	21.5	24.5	26	26.2	25.5	22.5	17	9

1) f_0 的消声量 ΔL 是单室扩张室式消声器的最大消声量,即当 $\sin^2 Kl = 1$ 时的消声量. 此时式 (3.43) 变为 $\Delta L_{最大} = 20 \log 1/2 (m + 1/m)$ 分贝.

a. expansion ratio m

b. amount of sound reduction ΔL (db)

c. frequency (Hz)

d. The amount of sound reduction ΔL at f_0 is the maximum sound reduction for a single expansion-room type sound suppressor i.e., the sound reduction at $\sin^2 Kl = 1$. Under this condition, equation (3.43) becomes $\Delta L_{max} = 20 \log 1/2(m + 1/m)$ db.
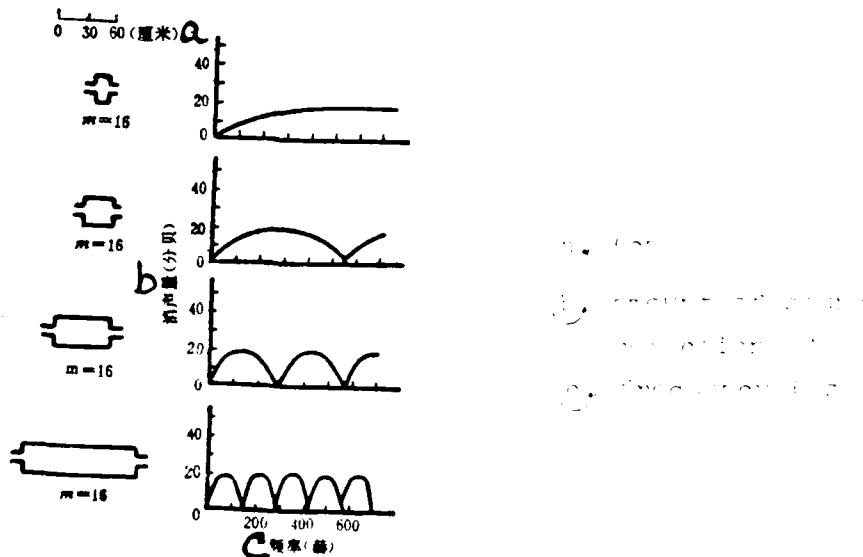
Figure 3.1? Relationship between sound reduction and the length l, for single expansion-room type sound suppressors

181
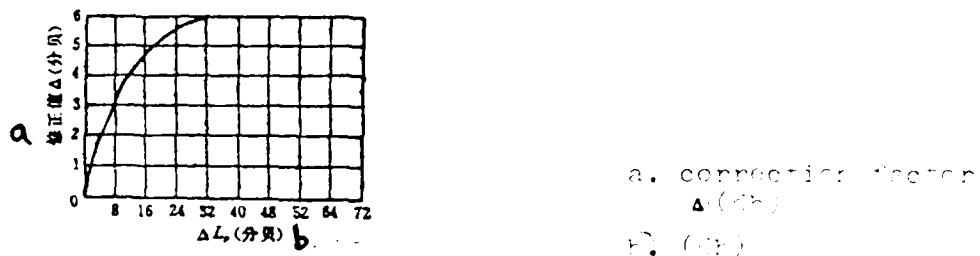
Figure 3.17 Relationship between ΔL_p and ΔL_w

$$\Delta L_w = \Delta L_p - \Delta \quad (db)$$

Furthermore, if the inlet and exhaust tube have different lengths in their cross sections as shown in Figure 3.18, then for a single expansion-room sound suppressor:
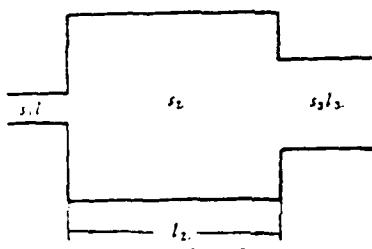
Figure 3.18

$$\Delta L_w = 10\log\frac{1}{4}\left[\left(1 + \frac{m}{m_{23}}\right)^2\cos^2 kl_1 \right.$$
$$\left. + \left(m + \frac{1}{m_{23}}\right)^2\sin^2 kl_2\right] + 10\log\frac{m_{23}}{m} \quad (db). \tag{3.45}$$

3.4.2 Double expansion-room type sound suppressors with external connecting tube

A double expansion-room type sound suppressor with external connecting tube is shown in Figure 3.19. Following the same deductions as in the previous section:

For the cross section at x = 0

$$P_1^{(+)} + P_1^{(-)} = P_2^{(+)} + P_2^{(-)} ,$$
$$P_1^{(+)} - P_1^{(-)} = m(P_2^{(+)} - P_2^{(-)});$$

132

For the cross-section at $x = x_1$,

$$P_2^{(+)}e^{ikl_1} + P_2^{(-)}e^{-ikl_1} = P_3^{(+)} + P_3^{(-)},$$
$$m(P_2^{(+)}e^{ikl_1} - P_2^{(-)}e^{-ikl_1}) = P_3^{(+)} - P_3^{(-)};$$

For the cross-section at $x = x_2$,

$$P_3^{(+)}e^{i2kl_2} + P_3^{(-)}e^{-i2kl_2} = P_4^{(+)} + P_4^{(-)},$$
$$P_3^{(+)}e^{i2kl_2} - P_3^{(-)}e^{-i2kl_2} = m(P_4^{(+)} - P_4^{(-)});$$

For the cross-section at $x = x_3$,

$$P_4^{(+)}e^{ikl_1} + P_4^{(-)}e^{-ikl_1} = P_5^{(+)},$$
$$m(P_4^{(+)}e^{ikl_1} - P_4^{(-)}e^{-ikl_1}) = P_5^{(+)};$$
$$m = \frac{S_2}{S_1}.$$

After manipulations,

$$\frac{P_1^{(+)}}{P_5^{(+)}} \cdot \frac{1}{16m^2}[(m+1)^4 e^{-i2k(l_1+l_2)} - (m^2-1)^2 e^{+i2k(l_1+l_2)}$$
$$- 2(m^2-1)^2 e^{-i2kl_2} + 2(m^2-1)^2 e^{+i2kl_2}$$
$$- (m^2-1)^2 e^{-i2k(l_1-l_2)} + (m-1)^4 e^{+i2k(l_1-l_2)}]$$
$$= \mathrm{Re}\left[\frac{P_1^{(+)}}{P_5^{(+)}}\right] - i\,\mathrm{Im}\left[\frac{P_1^{(+)}}{P_5^{(+)}}\right],$$

where

$$\mathrm{Re}\left[\frac{P_1^{(+)}}{P_5^{(+)}}\right] = \frac{1}{16m^2}[4m(m+1)^2\cos 2k(l_1+l_2)$$
$$- 4m(m-1)^2\cos 2k(l_1-l_2)],$$

$$\mathrm{Im}\left[\frac{P_1^{(+)}}{P_5^{(+)}}\right] = \frac{1}{16m^2}[2(m^2+1)(m+1)^2\sin 2k(l_1+l_2)$$
$$- 2(m^2+1)(m-1)^2\sin 2k(l_1-l_2)$$
$$- 4(m^2-1)^2\sin 2k\,l_2].$$
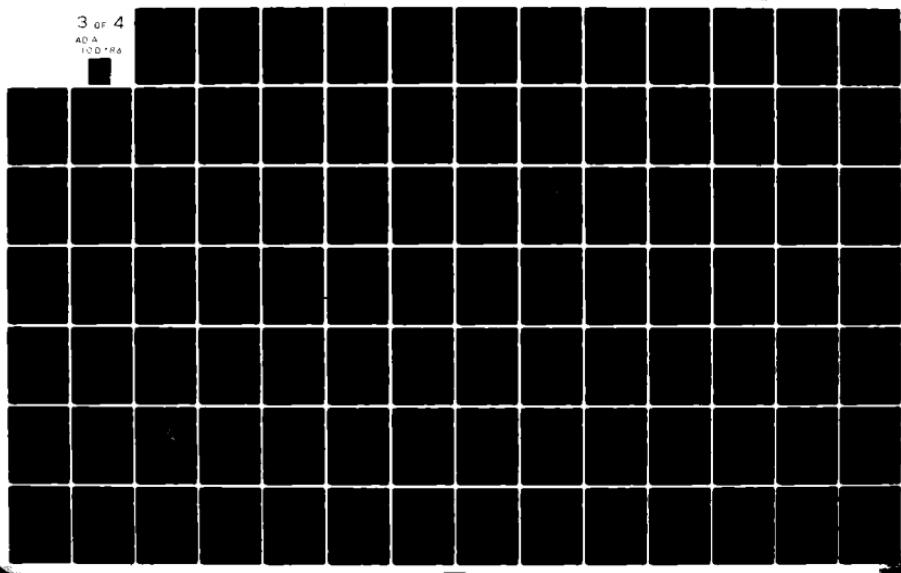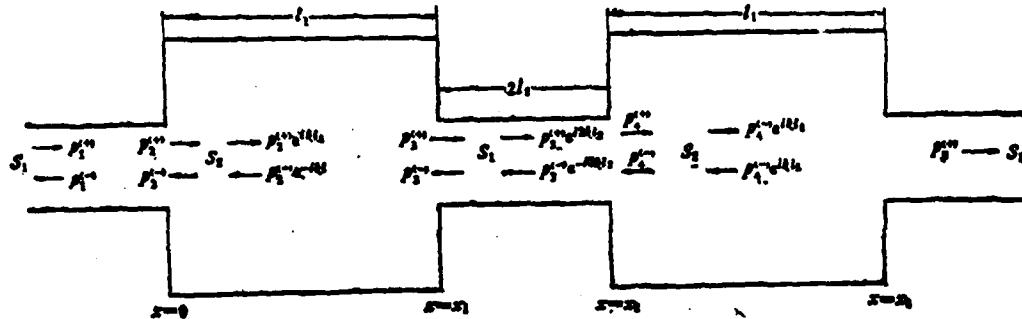
Figure 3.19   Double expansion-room type sound suppressor
with external connecting tube

Sound suppression is

$$\Delta L_{W} = 10\log\left\{\left[\mathrm{Re}\left(\frac{P_1^{(+)}}{P_3^{(+)}}\right)\right]^2 + \left[\mathrm{Im}\left(\frac{P_1^{(+)}}{P_3^{(+)}}\right)\right]^2\right\} \quad (\mathrm{db})$$

$$(3.46)$$

Figure 3.20 shows the characteristics of one double expansion-room sound
suppressor with external connecting tube.

a. (cm)
b. amount of sound
    reduction (db)
c. frequency (Hz)
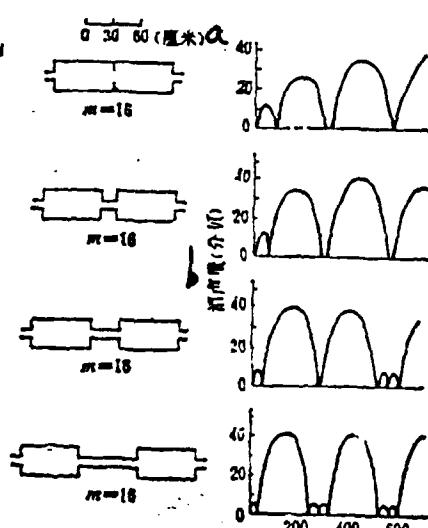
Figure 3.20   The characteristics of one double expansion-
room sound suppressor with external connecting
tube   184

a. sound source
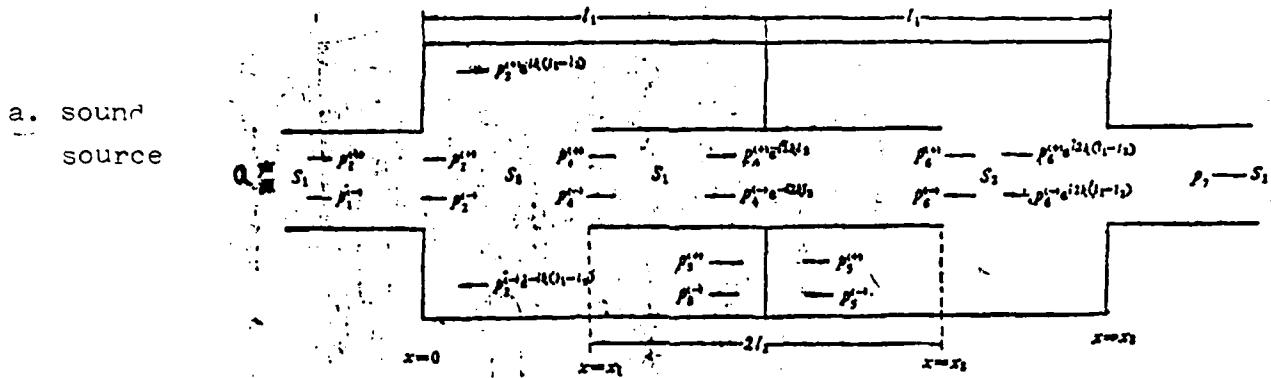
Figure 3.21

The lower-limit critical frequency of a double expansion-room sound suppressor is

$$f_\ell \doteq \frac{c}{2\pi} \frac{1}{\sqrt{m l_1 l_2 + l_1/3\,(l_1 - l_2)}} \quad (Hz) \tag{3.47}$$

3.4.3 Double expansion-room type sound suppressors with internal connecting tube

Figure 3.21 is a schematic diagram of an internally connected double expansion-room type sound suppressor. Following the same deductions of Sections 3.4.1 and 3.4.2, we have

For the cross section at $x = 0$,

$$P_1^{(+)} + P_1^{(-)} = P_2^{(+)} + P_2^{(-)},$$
$$P_1^{(+)} - P_1^{(-)} = m(P_2^{(+)} - P_2^{(-)});$$

For the cross section at $x = x_1$,

$$P_2^{(+)} e^{ik(l_1 - l_2)} + P_2^{(-)} e^{-ik(l_1 - l_2)} = P_3^{(+)}$$
$$+ P_3^{(-)} = P_4^{(+)} + P_4^{(-)},$$
$$m(P_2^{(+)} e^{ik(l_1 - l_2)} - P_2^{(-)} e^{-ik(l_1 - l_2)}) = P_4^{(+)} - P_4^{(-)}$$
$$+ (m - 1)(P_3^{(+)} - P_3^{(-)});$$

185

For the cross-section at x = x_2 ,

$$P_1^{(+)} e^{i2kl_1} + P_6^{(-)} e^{-i2kl_1} = P_3^{(+)} + P_3^{(-)} = P_5^{(+)} + P_5^{(-)},$$

$$P_1^{(+)} e^{i2kl_1} - P_1^{(-)} e^{-i2kl_1} + (m-1)(P_3^{(+)} - P_3^{(-)})$$
$$= m \cdot (P_6^{(+)} - P_6^{(-)});$$

For the cross-section at x = x_3 ,

$$P_6^{(+)} e^{ik(l_1-l_2)} + P_6^{(-)} e^{-ik(l_1-l_2)} = P_7^{(+)},$$

$$m \left(P_6^{(+)} e^{ik(l_1-l_2)} - P_6^{(-)} e^{-ik(l_1-l_2)} \right) = P_7^{(+)}.$$

Due to the total reflection at the dividing wall of the two expansion rooms, we have

$$P_3^{(-)} = P_3^{(+)} e^{i2kl_1}, \quad P_5^{(-)} = P_5^{(+)} e^{-i2kl_1}.$$

Finally,

$$\frac{P_1^{(+)}}{P_7^{(+)}} = \cos 2k\,l_1 - (m-1)\,\sin\,2k\,l_1 \tan k l_1$$

$$- \frac{i}{2}\left\{\left(m + \frac{1}{m} \right) \sin 2k\,l_1 + (m-1)\tan k l_1 \right.$$

$$\left. \left[\left(m + \frac{1}{m} \right) \cos 2k l_1 - \left(m - \frac{1}{m} \right) \right] \right\}$$

$$= \mathrm{Re}\left[\frac{P_1^{(+)}}{P_7^{(+)}} \right] - i\mathrm{Im}\left[\frac{P_1^{(+)}}{P_7^{(+)}} \right].$$

Sound suppression is

$$\Delta L = 10\log\left\{ \left[\mathrm{Re}\!\left(\frac{P_1^{+}}{P_7^{(+)}} \right)\right]^2 + \left[\mathrm{Im}\left(\frac{P_1^{+}}{P_7^{(+)}} \right)\right]^2 \right\} \quad (\text{db}) \tag{3.48}$$

which has a same lower-limit critical frequency as in Equation (3.47).

This type of sound suppressors has sound suppression characteristics determined by m, $2l_2/l_1$, and l_1: large m yields good sound suppression; l_1 and $2l_2$ determine the frequency characteristics of the sound suppressors With m fixed (m = 16), Figure 3.22 shows the dependence of sound suppression characteristics on the length of the internal connecting tube; with $l_1 = 2l_2$, Figure 3.23 shows the dependence of the sound suppression characteristics on m.

a. cm
b. amount of
   sound
   reduction (db)
c. frequency (Hz)
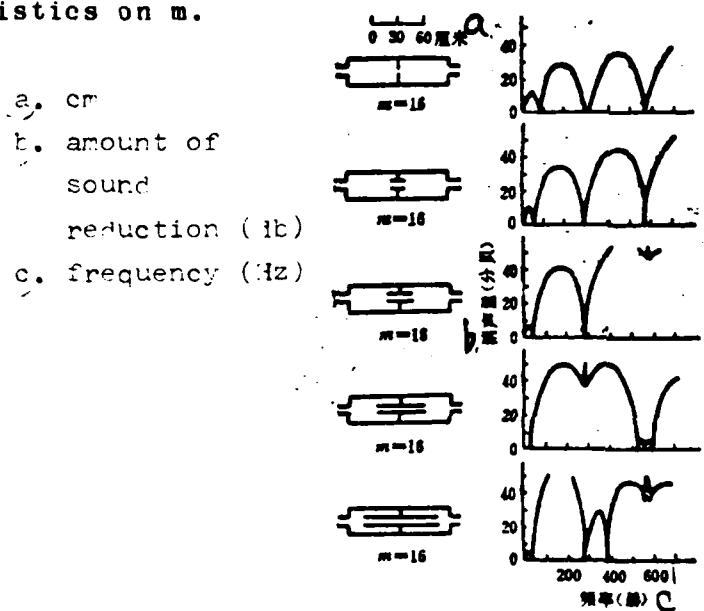
Figure 3.22   The effect of internal connecting tube length
             on the characteristics of sound suppression

a. cm
b. amount of sound reduction
   (db)
c. frequency (Hz)
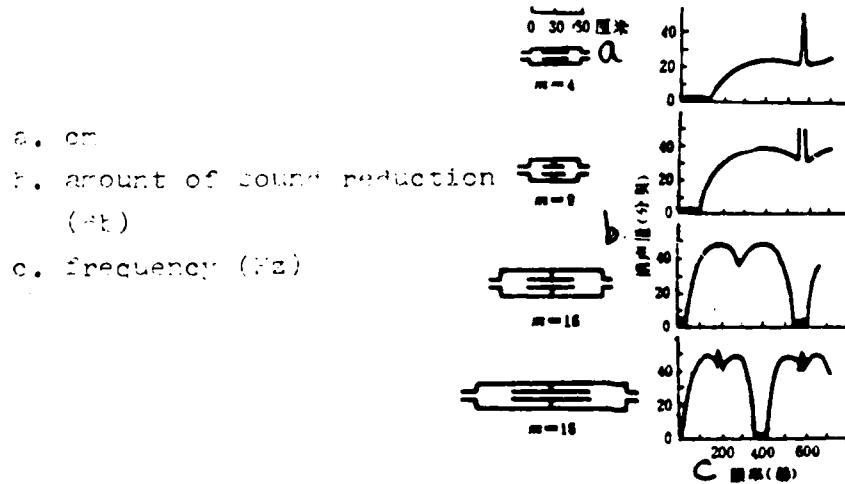
Figure 3.23   Under the condition of $l_1 = 2l_2$

·187

Table 3.13 lists several examples of low-limit critical frequencies of double expansion-room type sound suppressors

3.4.4 Improvement of frequency characteristics for expansion-room type sound suppressors

Based on the discussions in the three previous sections, it is clear that, even though expansion-room type sound suppressors have good sound suppression properties in certain bandwidths, they have problems in the existence of periodical transmittable frequencies. That is, it is possible for the sound suppressors to miss periodically noises with certain frequencies. Such sound waves can propagate directly through without being suppressed. To overcome this difficulty, one can use the method of inserting tubes.

The sound suppression of an expansion-room sound suppressor with inserted tubes is

$$\Delta L = 10\log\left\{\left[\text{Re}\left(\frac{P_i}{P_t}\right)^2 + \text{Im}\left(\frac{P_i}{P_t}\right)\right]^2\right\},$$

(3.49)

where

Table 3.13 Several examples of lower-limit critical frequency for double expansion-room type sound suppressors
(c = 375 m/s, $\theta = 50^\circ$C)

序 a 号	m	l_1 (*)b	l_2 (*)b	f_T (#)c
1	16	0.608	0.0304	85.8
2	16	0.608	0.076	59.9
3	16	0.608	0.152	44.0
4	16	0.608	0.304	31.7
5	16	0.608	0.076	59.9
6	16	0.608	0.152	44.0
7	16	0.608	0.304	31.7
8	16	0.608	0.455	26.1
9	4	0.304	0.152	123.2
10	9	0.304	0.152	84.0
11	16	0.912	0.455	21.2

a. number
b. (m)
c. (Hz)

188
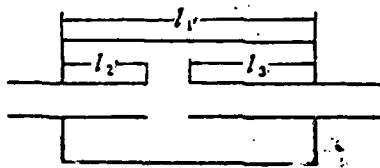
Figure 3.24   Schematic diagram showing inserted tubes in
an expansion-room type sound suppressor

$$\text{Re}\left(\frac{P_i}{P_t}\right) = \frac{1}{4m\,(1+\cos 2k\,l_2)}\{4m\cos k(l_1 - l_2)$$
$$+\,(3m-1)\cos k\,(l_1 + l_2)$$
$$+\,(m+1)\cos k\,(l_1 - 3\,l_2)\},$$
$$\text{Im}\left(\frac{P_i}{P_t}\right) = \frac{1}{4m\,(1+\cos 2k\,l_2)}\{2(m^2+1)\sin k(l_1 - l_2)$$
$$+\,(2m^2-m+1)\sin k\,(l_1 + l_2)$$
$$+\,(m+1)\sin k\,(l_1 - 3l_2)\},$$

where P_i -- incident sound pressure of sound suppressor; P_t -- transmitted
sound pressure of sound suppressor; m -- expansion ratio; l_1 -- length
of sound suppressor; l_2 -- length of inserted tube.

According to Equation (3.49), when the inserted tube in a single
expansion-room type sound suppressor has a length of $(1/2)\,l_1$, it can
eliminate the passage of frequencies $(n/2l)c$ $(n > 0$, integers) with n
being odd. When the inserted tube has a length of $(1/4)\,l_1$, it can
eliminate the passage of frequencies with n being even. This way, by
inserting one tube into the single expansion-room sound suppressor with
$(1/4)$ $\left(l_2 = \frac{l_1}{4}\right)$,   and another tube into another end with $(1/2)\left(l_2 = \frac{l_1}{2}\right)$,

189·

one can obtain the sound suppression curves for non-passing-through frequencies.

To eliminate passing-through frequencies, one can also use a combination of several expansion rooms with different lengths, as shown in Figure 3.25.
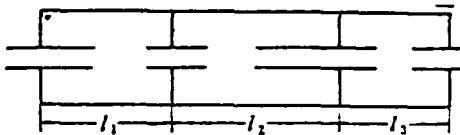

Figure 3.25   Sound suppressor based on a combination of
several expansion rooms with different lengths

In this way, the passing-through frequencies are different for each expansion room. With several sections in combination, the sound suppression curve can become more flat. However, since there are overlapping effects between different sections, we can not calculate the amount of sound suppression by addition.

Figure 3.26 is a schematic diagram of the frequency characteristics of a modified expansion-room type sound suppressor. It can be seen that not only the over-all sound suppression curve is flat, the amount of sound suppression is also relatively large.

In engineering applications, to avoid the loss due to a sudden change in cross sections, plates with drilled holes are often used to connect the expansion rooms, as shown in Figure 3.27.

In this case, the degree of openings is required to be above 30%. This way, for sound waves, one can control the frictional loss variation due to the sudden changes of passage cross sections, but not affect the sound suppression efficiencies. As far as air stream is concerned, it is the same as the addition of one section of wall surface with through

190

holes. The passage frictional loss is much lower than that from the

sudden changes of cross-section.

Figure 3.26 Schematic diagram of
the sound suppression frequency
characteristics of a modified
expansion-room type sound supp-
ressor.

Key:
a. Schematic diagram
b. Amount of sound reduction (db)
c. Remarks on each section
d. Sound suppression characteristics
   of the first expansion-room (in-
   serted tube with length l_1)
e. Sound suppression characteristics
   of the second expansion-room (in-
   serted tube with length l_2)
f. Resonance curves of inserted tube
   with length l_3; its peak frequency
   value is the same as that trans-
   mittable with odd order in the
   l_1-characteristics
g. Resonance curves of inserted tube
   with length l_4; its peak frequency
   value is the same as that trans-
   mittable with even order in the
   l_1-characteristics
h. Resonance curves of inserted tube
   with length l_5; its peak frequency
   is the same as that transmittable
   with odd order in the l_2-characteristics

i. Resonance curves of inserted tube with length l_6; its peak frequency is the same
   as that transmittable with even order in the l_2-characteristics
j. Combined sound suppression characteristics between the first and the second
   expansion room
k. Overall sound suppression characteristics curve
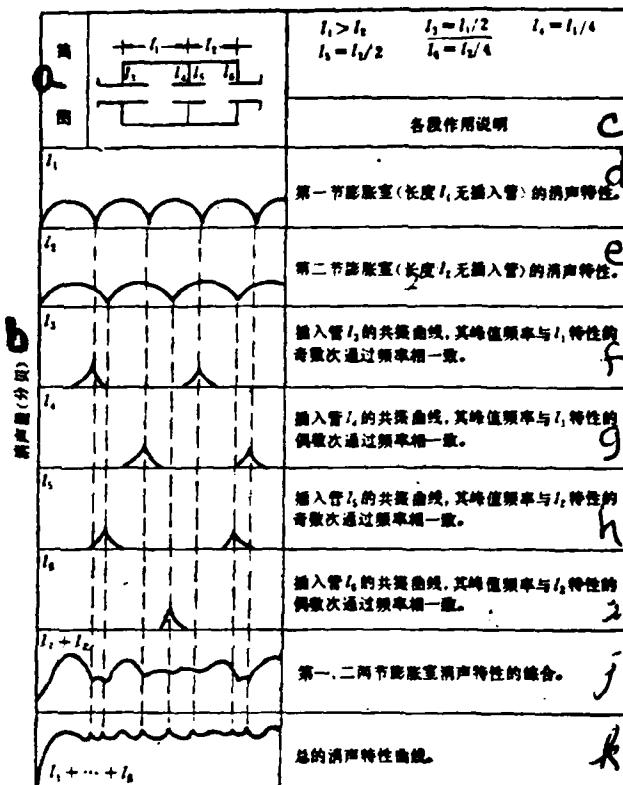
Figure 3.27 Schematic diagram of expansion rooms connected by loards
   with through-holes $l_3 = l_1/4$, $l_4 = l_1/2$, $l_5 = l_2/2$, $l_6 = l_2/4$

191
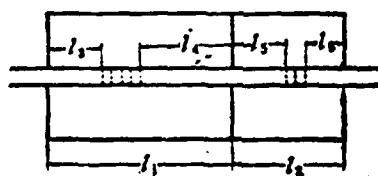
3.4.5 Resonance sound suppressors

Figure 3.28 is a schematic diagram of a resonance sound suppressor. Its passage tube is connected to the Helmholtz resonator. According to the theory in Section 3.2.2, when the sound wavelength is sufficiently long as compared to the dimensions of sound suppressor, the air column inside tube l can be considered as an uncompressed mass component, called the acoustic mass m_A, equivalent to the electrical inductance. The friction and resistance in the neck are called the acoustic resistance r_A, equivalent to the electrical resistance. The air inside the cavity V can be considered as an undisplaced elastic component, called the acoustic capacitance c_A, equivalent to the electrical capacitance. From Table 3.11:

$$m_A = \frac{\rho l}{S},\tag{3.50}$$

$$r_A = \frac{\rho \omega k}{2\pi},\tag{3.51}$$

$$c_A = \frac{V}{\rho c^2}.\tag{3.52}$$
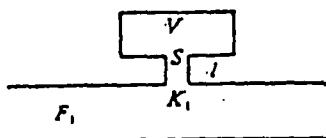
Figure 3.28   Schematic diagram of a resonance sound suppressor

Sound energy propagated through the passage of a sound suppressor is absorbed due to resonance. The resonance frequency f_r is determined by Equation (3.14). When the sound wavelength is sufficiently large as compared to the dimensions of the resonator, one can obtain the amount of sound suppression (amount of sound reduction) for a single cavity resonance sound suppressor:

$$\Delta L = 10 \log \left[1 + \frac{\alpha + 0.25}{\alpha^3 + \beta^2 \left(\frac{f_r}{f} - \frac{f}{f_r} \right)^2} \right] \quad (\text{db})$$ (3.53)

where $\alpha = r_A \frac{F_1}{\rho c}$; $\beta = \frac{F_1}{\sqrt{GV}}$; r_A -- acoustic resistance; F_1 -- cross-sectional area of the passage of sound suppressor; ρ -- air density; c -- sound speed; V -- volume of resonator; f -- frequency of the sound to be suppressed; f_r -- resonance frequency;

$$G = \frac{S}{l + 0.8d}$$ the degree of transmission; (3.54)

l -- neck length of the resonator; d -- hole diameter of the resonator; S -- hole area.

Resonance frequencies are determined from Equation (3.14). In calculating the amount of sound suppression, $S/l_t = G$ is often substituted into Equation (3.14) to obtain

$$f_r = \frac{c}{2\pi}\sqrt{\frac{G}{V}} \qquad \text{(Hz)} .$$

(3.55)

The amount of sound suppression at resonance frequency is

$$\Delta L = 10\log\left[1 + \frac{a\ r\ 0.25}{a^2}\right]$$
$$= 20\log\left[1 + \frac{1}{2a}\right] \quad \text{(db)}$$

(3.56)

Calculations of the acoustic resistance r_A for resonators are very complicated. Under general conditions, when there are no resistive type sound absorbing materials near the neck, acoustic resistance is small and can be ignored. Therefore, Equation (3.55) can be converted into

$$\Delta L_w = 10\log\left[1 + \left(\frac{\sqrt{GV}/2F_1}{\frac{f}{f_r} - \frac{f_r}{f}}\right)^2\right] \quad \text{(db)}$$

(3.57)

Few of the resonators in engineering applications have only one hole. Most of them are structures based on combinations of sound absorbing boards with multi-holes. Calculations of their sound suppression are the same as Equation (3.57), but the G-value is

$$G = \frac{nS}{t + 0.8d},$$

(3.58)

where n-- number of holes; t-- thickness of the board with holes.

The amount of sound suppression for resonance sound suppressors is shown in Figure 3.29.

194
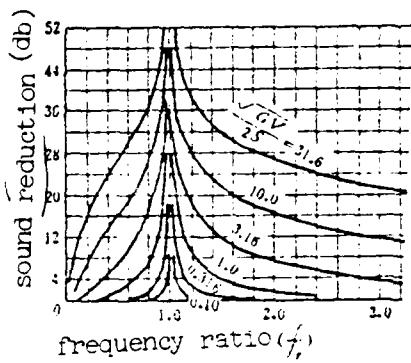
Figure 3.29   Sound suppression curves for resonance
sound suppressors

Equation (3.57) is for the sound suppression of pure tones.
Sometimes it is necessary to calculate the amount of sound suppression for a given frequency band.

The amount of sound suppression ΔL for an octave band is

$$\Delta L = 10 \log (1 + 2K^2) \quad \text{db}, \qquad (3.59)$$

$$K = \frac{\sqrt{GV}}{2F_1}, \qquad (3.60)$$

the sound suppressions for its two neighboring octave bands are

$$\Delta L = 10 \log (1 + 8K^2/49) \quad \text{db}, \qquad (3.61)$$

for a third-octave band,

$$\Delta L = 10 \log (1 + 19 K^2) \quad \text{db}, \qquad (3.62)$$

for the four neighboring third-octave bands:

$$\Delta L_1 = 10 \log (1 + 2K^2) \quad \text{db}, \qquad (3.59)$$

$$\Delta L_2 = 10 \log (1 + 0.67K^2) \quad \text{db}, \qquad (3.63)$$

$$\Delta L_3 = 10 \log (1 + 0.31K^2) \quad \text{db}, \qquad (3.64)$$

$$\Delta L_4 = 10 \log (1 + 8K^2/49) \quad \text{db}, \qquad (3.65)$$

195

To make calculations convenient, Equation (3.59), (3.61), (3.62), (3.64), and (3.65) are expressed in terms of Table 3.14.

For example: Design a resonance sound suppressor for an exhaust pipe with its inner diameter as 10 cm, such that the sound suppression is 15 db for the octave band with its central frequency as 125 Hz.

Solution: Sound suppression ΔL = 15db, resonance frequency f_r = 125 Hz, passage cross-sectional area $F_1 = (\pi/4)10^2$ cm^2. By substituting the ΔL value into Equation (3.18) or from Table 3.14 we have

$$15 = 10 \log (1 + 2K^2), \quad K = 4.$$

Substituting the G value in Equation (3.55) into Equation (3.60),

$$K = (\sqrt{GV}/2F_1) = (2\pi f_r/c)(V/2F_1),$$

$$V = (c/2\pi f_r)(2KF_1) = (34000/2\pi \times 125) \times 2 \times (\pi/4)10^2$$
$$= 13600 \text{ cm}^3.$$

Based on the required volume V of the resonator, a concentric-cylindrical resonance sound suppressor can be designed. With its inner diameter still to be 10 cm, the outer shell tube diameter is 30 cm, and the length of the cavity is 22 cm. From Equation (3.55),

$$G = \left(\frac{2\pi f_r}{c}\right)^2 V = \left(\frac{2\pi \times 125}{34000}\right)^2 \times 13600 = 7.23.$$

Table 3.14 Calculation Table for sound Suppression at various frequency bands for resonance sound suppressors

a. 频带类型 ΔL / K	0.2	0.4	0.6	0.8	1.0	1.5	2	3	4	5	6	8	10	15
b. 倍频程和相邻第一个 1/3 倍频程 $10\log[1+2K^2]$	1.1	1.2	2.4	3.6	4.8	7.5	9.5	12.8	15	17	18.6	20	23	27
c. 1/3 倍频程 $10\log[1+19K^2]$	2.5	6.0	9.0	11.2	12.9	16.4	19	22.6	25.1	27	28.5	31	33	36.5
d. 相邻第一个倍频程和相邻第四个 1/3 倍频程 $10\log[1+8/49\,K^2]$	0	0	0.2	0.4	0.8	1.5	2.2	3.9	5.5	7.0	8.4	10.5	12.5	16.6
e. 相邻第二个 1/3 倍频程 $10\log[1+0.67K^2]$	0	0.5	1.0	1.6	2.2	4.0	6.5	8.5	10.8	12.5	14	16.5	18.4	21.8
f. 相邻第三个 1/3 倍频程 $10\log[1+0.31K^2]$	0	0.2	0.5	0.9	1.2	2.2	3.5	5.8	8.8	9.5	10.8	13	15	18.5

a. type of band

b. octave band and the nearest neighbor third octave band

c. third-octave band

d. the nearest neighbor octave band and the fourth nearest neighbor third-octave band

e. the second nearest neighbor third-octave band

f. the third nearest neighbor third-octave band

By selecting the inner wall thickness t = 2 mm and hole diameter = 3 mm, then substituting them along with the G value into Equation (3.58), the number of holes can be obtained:

197

$$n = \frac{G(t + 0.8d)}{S} = \frac{G(t + 0.8d)}{\frac{\pi}{4}d^2} = \frac{G(t/d + 0.8)}{\frac{\pi}{4}d}$$

$$= \frac{7.23(0.2/0.5 + 0.8)}{\frac{\pi}{4} \times 0.5} = 22.$$

By evenly arranging the 22 holes across the inner wall of the resonance sound suppressors, the purpose of sound suppression can be achieved.

To arrive at higher sound suppressions, one can use resonance sound suppressors in series, yielding multi-room resonance sound suppressors. Their sound suppressions are

$$\Delta L_w = 8.69 N \, \text{arch} \left| \cos\left(Kl_1\frac{f}{f_r}\right) + \frac{\sqrt{GV}/2F_1}{\frac{f}{f_r} - \frac{f_r}{f}} \right.$$
$$\left. \times \sin\left(Kl_1\frac{f}{f_r}\right) \right| \quad (db),$$

(3.66)

where N-- room number; l_1-- length of the connecting tube between two neighboring rooms; $K = 2\pi f_r/c$.

Resonance sound suppressors are sometimes made in a concentric tube style for engineering applications (see Figure 3.30). Their sound suppressions (sound reductions):

$$\Delta L_w = 10\log\left[1 + \frac{1}{4}\left(\frac{S_h/F_1}{\frac{S_h}{kG} - \frac{S_b}{S_h}t_{\cot kl_c}}\right)\right],$$

(3.67)

where S_h-- cross-sectional area of the small hole; F_1-- area of the inner tube passage; S_{bt}-- cross-sectional area of the concentric cavity; l_c-- length of the cavity, $l_c = \frac{l}{2}$ if the hole is near the middle of the cavity; G-- rate of transmission. If there is only one hole, calculation is done following Equation

198

(3.54); for n holes, following Equation (3.58).

Multi-hole concentric resonance sound suppressors are shown in Figure 3.31.
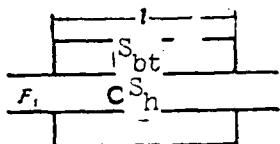
Figure 3.30 Concentric tube type resonance sound suppressors
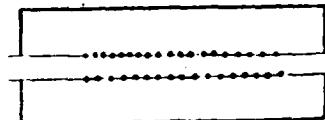
Figure 3.31 Schematic diagram of multi-hole concentric resonance sound suppressors

3.4.6. Interference sound suppressors

Interference sound suppressors are based on the principle of sound wave attenuations due to interference, as shown in Figure 3.32. A side tube is built into the main passage, to allow a portion of the sound energy to be diverted through it. If the difference between the length of this side tube l_1 and the main passage length l is equal to one-half of the wavelength (or odd multiples of the half-wavelength), then

$$l_1 = l + \frac{\lambda}{2}(2n + 1) \quad n = 1, 2, 3, \ldots, \quad (3.65)$$

When the two sound waves meet, due to their opposite phases, the sound energy can be greatly reduced.

Interference sound suppressors are suitable only for well tuned sound, and the sound suppression efficiencies are good only if the tune is stable and not changing.

199
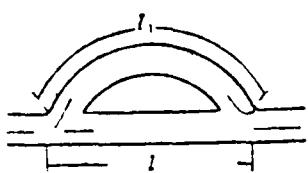
Figure 3.32 Schematic diagram
of interference sound sup-
pressors
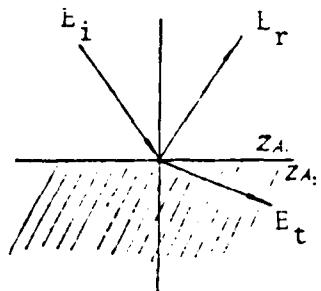
Figure 3.33 Reflection
of a sound wave at
interface of two media
with different acoustic
resistances

3.4.7 Sound attenuations induced by perforated screens, elbows,
and drastically changed cross-sectional areas

When sound waves propagate and encounter perforated screens,
elbows, or drastically changed passage cross-sectional areas,
the situations are equivalent to changes of acoustic resistances.

When sound waves reach an interface involving different
acoustic resistances, a significant portion of sound energy is
reflected back. This reflection is similar to that of a light
wave when it encounters an interface with different dielectric
constants, as shown in Figure 3.33.

Perforated screens: Perforated screens are acoustic com-
ponents combining acoustic mass and acoustic resistance. In
Figure 3.34, when the distance between holes is greater than the
diameter of the holes, the acoustic impedance per area a^2 is

$$Z_A = r_A + j\omega m_A,$$

(3.09)

200

where r_A and m_A are defined in Equation (3.50) and (3.51). They can be more specifically written as

$$r_A = \frac{1}{\pi r^2} \rho_0 \sqrt{2\omega\eta} \left[\frac{t}{r} + 2\left(1 - \frac{S_c}{S_a}\right) \right],$$

$$(3.70)$$

$$m_A = \frac{1}{\pi r^2} \left[t + 1.7r\left(1 - \frac{r}{a}\right) \right],$$

$$(3.71)$$

where $S_c = \pi r^2$; $S_a = a^2$; t = screen thickness; η -- viscosity coefficient, $\eta = 1.56 \times 10^{-5} m^2$/sec for air under standard conditions.

With n holes, the acoustic impedance is equal to $1/n$ times the impedance for a single-hole.

It should be pointed out that the two equations above are applicable only for $r(m) > \frac{0.01}{\sqrt{f}}$, and $r < 10/f$.

Figure 3.35 and 3.36 give the experimental data of sound reduction induced by perforated screens. These experiments yield the sound reduction values as determined by the inserted tube method in a sound suppression room and with a stable pressure sound source.
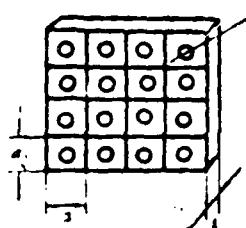

Figure 3.34   Structures of perforated screens
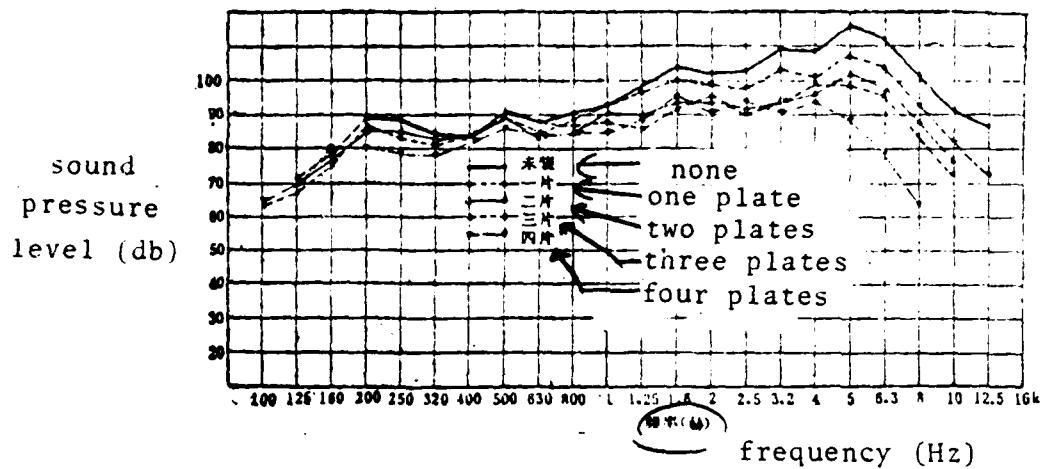
Figure 3.35 Sound suppression curves for perforated
   screens
   perforated screens: hole diameter Ø10; screen
   thickness t=2mm; degree of openings P=10%;
   distance between screens = 10cm
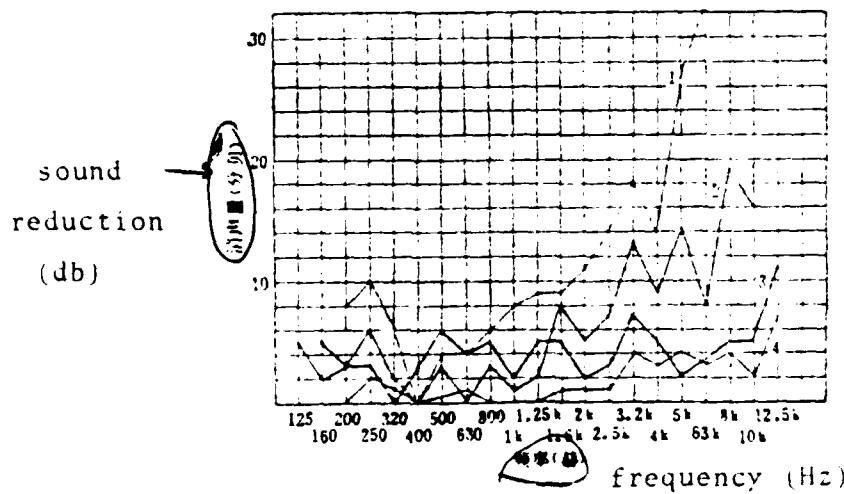

Figure 3.36 Sound suppression curves with varying
   degrees of openings P
   Fixed perforated screens with hole diameter Ø10,
   board thickness t=2mm, number of boards = 4,
   1--P=10%; 2--P=20%; 3--P=30%; 4--P=40%

202

Drastic changes in cross-sectional areas: As shown in
Figure 3.37, for S_1: $Z_{A_1} = \rho c S_1$,   for S_2: $Z_{A_2} = \rho c S_2$,   i.e., the
acoustic impedance changes from $\rho c S_1$ to $\rho c S_2$. from S_1 to S_2.
Sound suppression follows Equation (3.43).

Elbows: As shown in Figure 3.38, sound waves are reflected
by the tube wall at the elbows. The degree of noise reduction
is related to the angle of the elbows, the tube dimensions,
and the wavelength. If the tube is equipped with sound absorbing
materials, the efficiencies are even better at high frequencies.

Table 3.15 lists the estimated values of sound reduction
ΔL for a 90^0 elbow. [30] In this case, the length of the sound
absorbing surface along the side of the tube should be greater
than 2.4 times the width of the side of the tube.
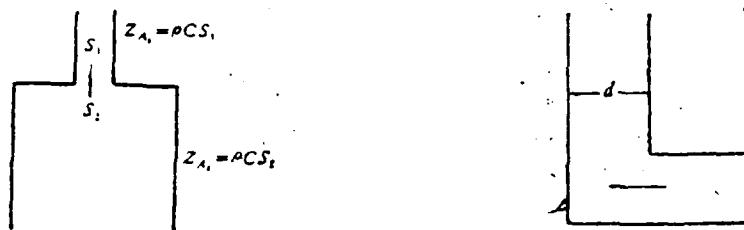
Figure 3.37   Drastic changes
in cross-sectional areas

Figure 3.38   A 90^0 elbow

Table 3.15 Estimated values (db) of sound suppression for 90°-elbows

d/λ	无吸声饰面		有吸声饰面		d/λ	无吸声饰面		有吸声饰面	
	无规入射	平面波入射	无规入射	平面波入射		无规入射	平面波入射	无规入射	平面波入射
0.1	0	0	0	0	1.5	4	8	10	13
0.2	0.5	0.5	0.5	0.5	2	5	7	10	13
0.3	3.5	3.5	3.5	3.5	3	3	8	10	14
0.4	6.5	6.5	7.0	7.0	4	3	10	10	14
0.5	7.5	7.5	9.5	9.5	5	3	11	10	18
0.6	8.0	8.0	10.5	10.5	6	3	12	10	19
0.8	7.5	8.5	10.5	11.5	8	3	14	10	19
1.0	6.0	8.0	10.5	12.0	10	3	15	10	20

a. surface without sound absorption
b. surface with sound absorption
c. non-regular incidence
d. plane wave incidence

3.4.8 Sprinkling sound suppression [31]

By evenly sprinkling water towards noise-producing steams, one can also achieve a certain sound suppression effect. This is called the sprinkling sound suppression. The principles are as follows:

1. The density ρ and sound speed c of the medium change after being sprinkled. This causes a change in acoustic impedance, and the reflections of the sound waves.

2. The friction produced during the mixing of two media causes the dissipation of energy, and reduces a portion of the sound.

If there is no heat transfer between steam and water, and the mixture is also a homogeneous fluid with density ρ and elastic modulus E, then the sound speed is

$$c = \sqrt{\frac{E}{\rho}} = \sqrt{\frac{E_1 E_2}{[xE_2+(1+x)E_1][x\rho_1+(1-x)\rho_2]}}, \qquad (3.72)$$

where ρ_1 --water density; ρ_2 --steam density; E_1 --water elastic modulus; E_2 --steam elastic modulus; x--volume percentage of water; c--sound speed of the mixture.

The reflection coefficient is determined by Equation (1.14). It can be re-written here as

$$r_0 = \left[\frac{\rho c - \rho_2 c_2}{\rho c + \rho_2 c_2}\right]^2,$$

(3.73)

where ρc --mixed parameter of water and steam; $\rho_2 c_2$ --steam parameter.
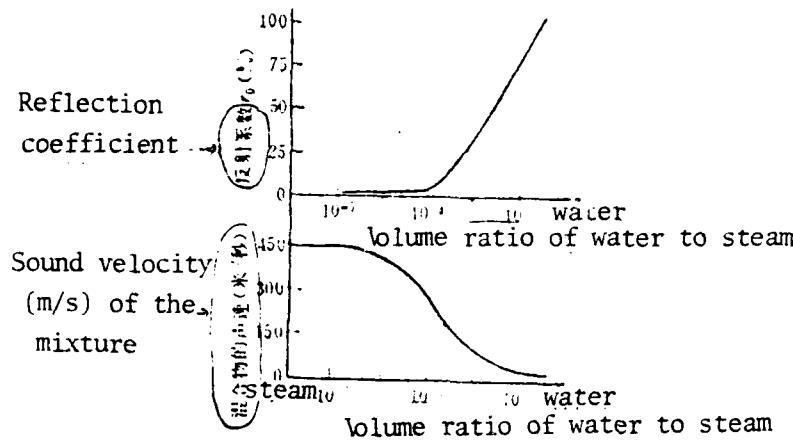
Figure 3.39   The effect of sprinkling to steam on
sound speed and reflection coefficient

Figure 3.39 shows the relationship between the volume ratio of water and steam and the sound speed of the mixture. It also shows the relationship between this volume ratio and the reflection coefficient r_0. It can be seen that, as sprinkling increases, sound speed decreases. When the amount of water approaches that

of steam, sound speed decreases to a limiting value. The reflection coefficient increases with increasing sprinkled water volume. The increase in r_0 is slow when the volume ratio is between 10^{-5}-$10^{-3}\%$. It increases fast when r_0 is above 10^{-3}.

Sound suppression (sound reduction) due to sprinkling is

$$\Delta L = 20\log \frac{\rho c}{\rho_2 c_2} + 10\log \frac{1}{1-r_0} \qquad \text{(db)}. \qquad (3.74)$$

Figure 3.40 shows the sound suppression curves corresponding to various amounts of water sprinkled to steam.

Figure 3.41 is a schematic diagram of the structures of sprinkling sound suppressors.[31]

§3.5 Resistive-reactive combined sound suppressors and perforated-tiles sound suppressors

To have good sound suppression effect over a broad frequency range, one can use resistive-reactive combined sound suppressors (Figure 3.42). Figure 3.42 (a)-(c) are expansion-room-reactive combined sound suppressors; Figure 3.42 (d)-(f) are resonator-reactive combined sound suppressors; Figure 3.42(g) is a perforated screen-reactive combined sound suppressor; Figure 3.42(h) is a perforated screen, elbow-reactive combined sound suppressor.


sound reduction (db)

Volume ratio of water to steam
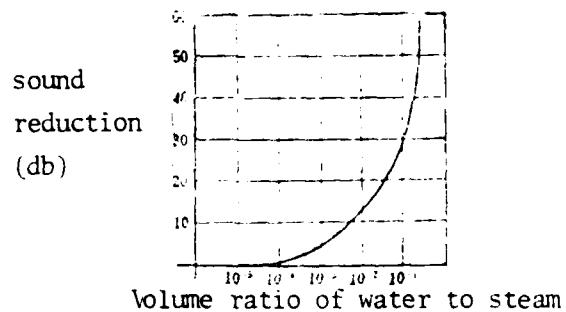
Figure 3.40   Sound suppression at various rates of sprinkling

206

exhaust tube

multi-hole cylindrical box, inner-wall
holes for exhausting gas

automatic regulator

water supply tube

cylindrical box (with its area greater
than that of the exhaust tube)

valve

exhaust inlet
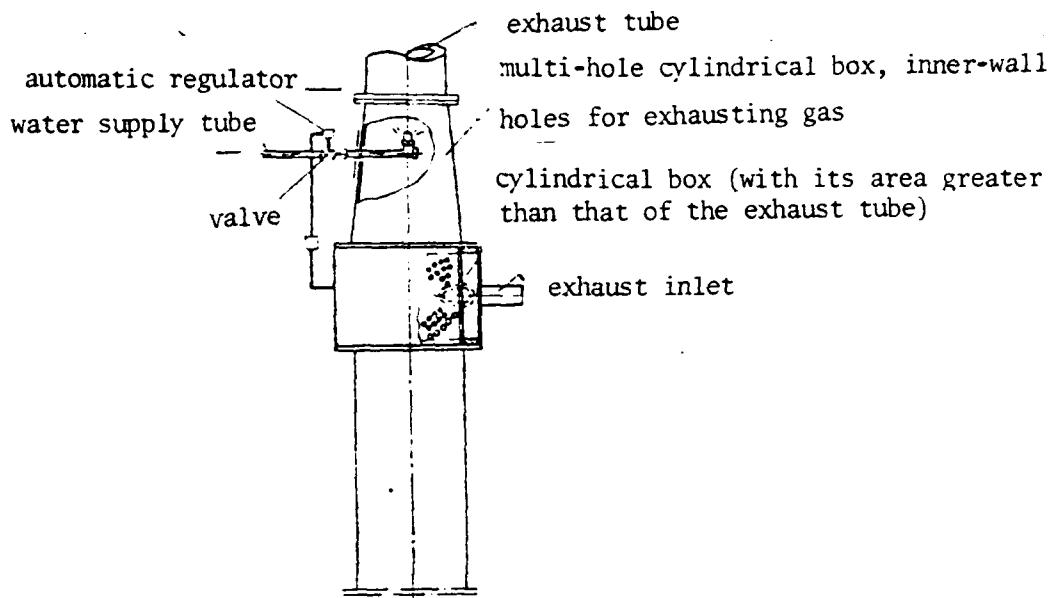
Figure 3.41   Sprinkling sound suppressors

Perforated-tile sound suppressors based on a structure of perforated tiles are good sound suppressors having both intrinsic resistive and reactive characteristics. They have much better frequency characteristics than those for common resistive type sound suppressors.

Metallic perforated sound suppressors are made of pure metal, thin plates. Therefore, they can sustain high temperatures, stream impact, oily mist, and water bubbles. These behaviors are very important for aerodynamic equipment with special requirements. Besides, since they do not have powders as often produced by multi-hole sound absorbing materials, they are particularly suitable for advanced air conditioners which require clean sound suppression systems.

207
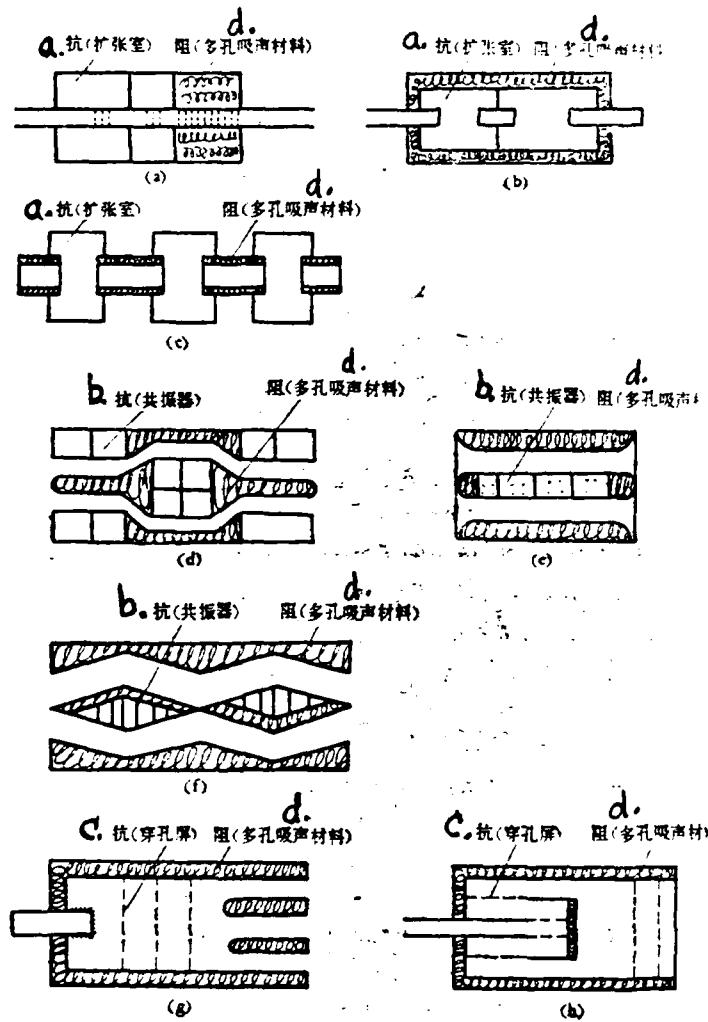
Figure 3.42   Schematic diagrams of several reactive-resistance
combined sound suppressors

a.   reactive (expansion room)
b.   reactive (resonator)
c.   reactive (screen with holes)
d.   resistive (perforated sound-absorbing materials)

Perforated-tiles have low degrees of openings, dense and small holes, and low frictional coefficients; therefore, resistive loss is low for sound suppressors of this type.

One can also use perforated-tiles as sound suppressor components, which can then be combined with multi-hole sound absorbing materials, expansion-rooms, resonance cavities, perforated screens, etc. Many different types of combined sound suppressors based on perforated-tiles can be made to solve the noise problems of aerodynamic equipment under different conditions.

Figure 3.43 shows schematic diagrams of several perforated-tile sound suppressors and combined units with perforated-tiles.

Figure 3.44 and 3.45 show the experimental data on sound suppression for two perforated tile sound suppressors.


(a)

(b)

(c)

(d)

(e)

(f)

(g)

209

a. 微穿孔板 φ0.5, /0.5, P2.7%

c. 消声器中流速30米/秒

b. 消声量(分贝)

d. 频率(赫)

63 125 250 500 1k 2k 4k 8k
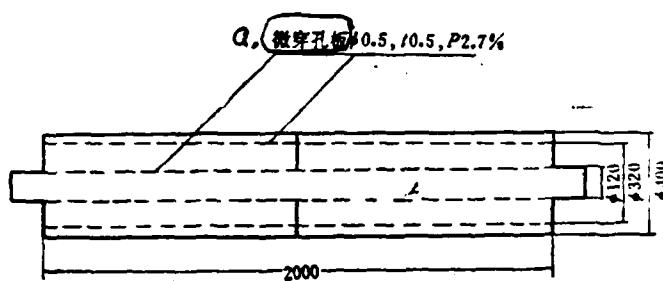
Figure 3.44 Tube-type perforated
 plate sound suppressors and
 their sound reduction data

a. perforated plate
b. sound reduction (db)
c. flow rate (30 m/s) inside the
 sound suppressor
d. frequency (Hz)

a. 微穿孔板 φ0.8, /0.8, P2.5% **a.** 微穿孔板 φ0.8, /0.8, P1%

c. 消声器中流速为10~15米/秒
阻损<1毫米水柱

b. 消声量(分贝)

d. 频率(赫)

63 125 250 500 1k 2k 4k 8k
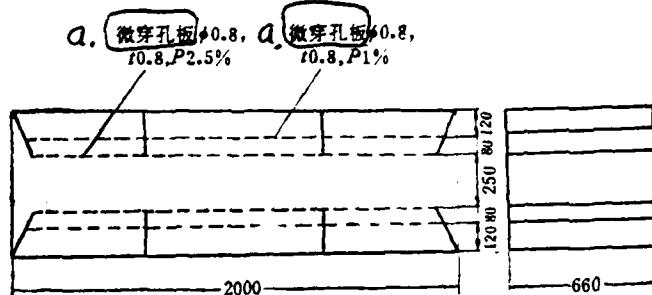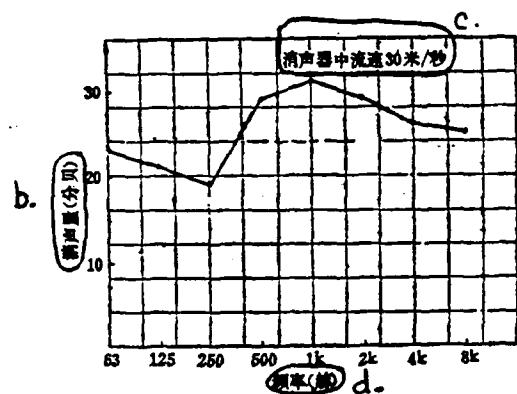
Figure 3.45 Rectangular perforated
 plate sound suppressors and their
 sound reduction data

a. perforated plates
b. sound reduction (db)
c. flow rate (10 - 15 m/s) inside
 the sound suppressor; flow
 loss < 1 mm water column
d. frequency (Hz)

210
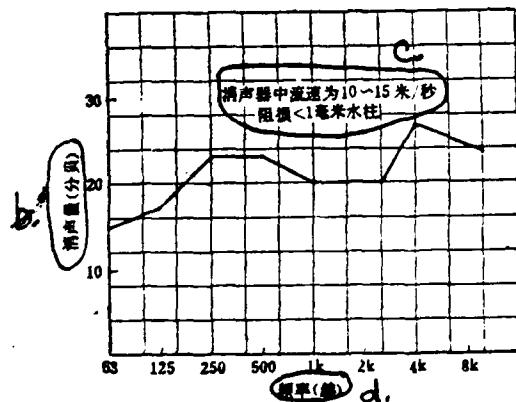
§ 3.6   Relationship between the air flow rate and the
sound reduction properties of sound suppressors

When air flows through sound suppressors with high veloci-
ties, it affects significantly the sound reduction properties.
For a sound suppressor with good sound reduction characteristics
at static and low velocities, high air flow rates can greatly
deteriorate its effectiveness. With poor design or construction,
not only that sound reduction can not be achieved, a sound sup-
pressor can even become a noise amplifier for certain frequencies.

Figure 3.46 and Figure 3.47 are the sound reduction curves
under various flow rates for, respectively, the tube-type per-
forated plate sound suppressor (abbr. perforated sound suppressor)
and the tube-type sound suppressor with glass cotton (abbr.
cotton-type sound suppressor). Their structures are schematically
shown in Figure 3.48 and Figure 3.49.
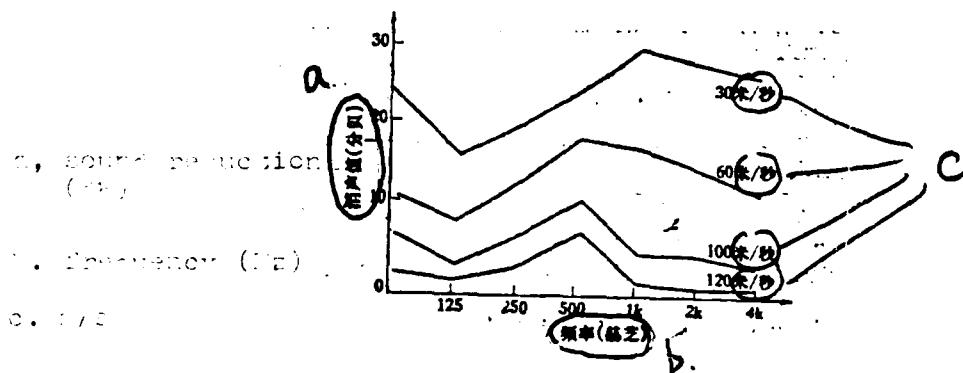
Figure 3.46   Sound reduction curves at various flow
rates for a 2-m long perforated sound
suppressor

211

a. sound reduction
   (dB)

b. frequency (Hz)

c. m/s
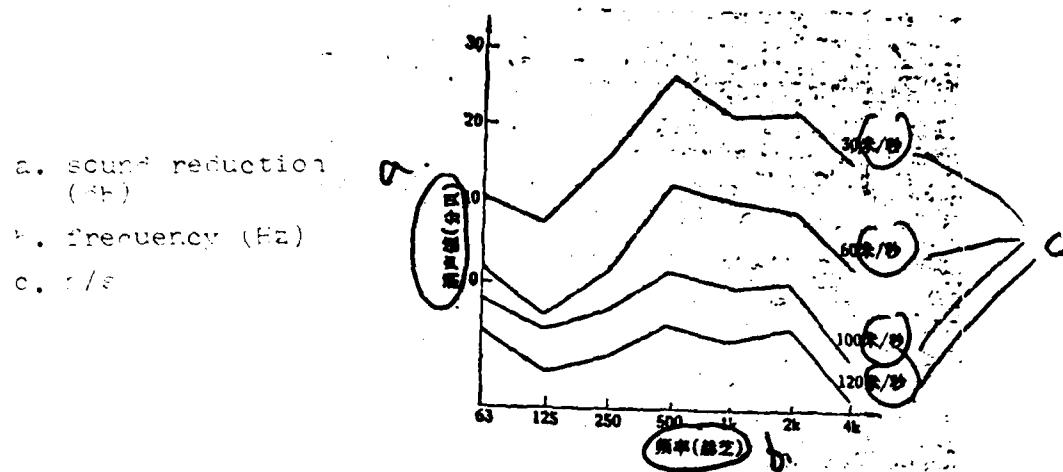
Figure 3.47　Sound reduction curves at various flow
　　　　　　　　rates for a 2-m long cotton-type sound
　　　　　　　　suppressor

a. Inlet connecting tube

b. perforated plate

c. outer shell

d. outlet short tube
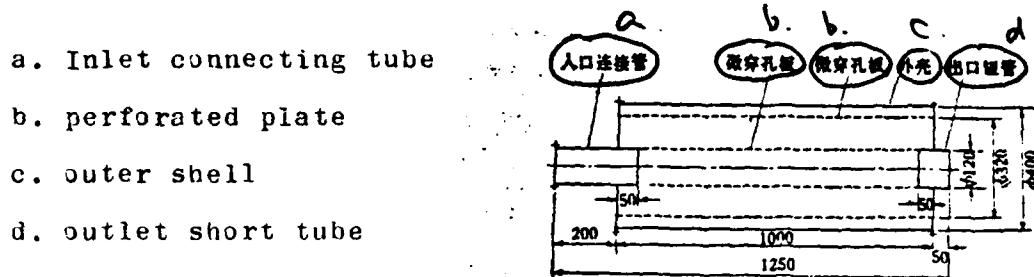
Figure 3.48　Schematic diagram showing the structures
　　　　　　　　of perforated-type sound suppressors

a. inlet connecting tube

b. ultra-fine glass cotton

c. shell

d. perforated plate

e. outlet short tube
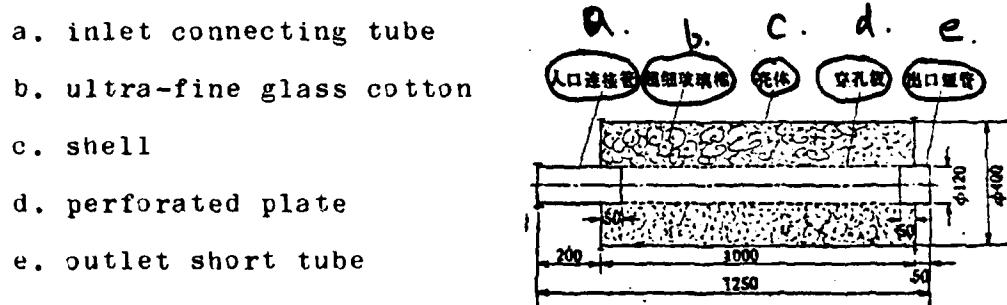
Figure 3.49　Schematic diagram of cotton-type sound
　　　　　　　　suppressors

212

Perforated-type sound suppressors use perforated plates
having the dimensions: plate thickness 0.5 mm, hole diameter
ϕ 0.5 mm, degree of opening 2.7%, front cavity 10 cm, back
cavity 4 cm. Cotton-type sound suppressors have sound absorb-
ing materials with the following specifications: density 30 kg/m^3,
thickness 14 cm, perforated plate hole diameter ϕ 8 mm, plate
thickness 1 mm, degree of opening 20%. Their sound absorption
coefficients as determined by a tube-testing method are listed in
Table 3.16.

Table 3.16   Sound absorption coefficients

a. frequency (Hz)

b. sound absorption
   coefficient

c. material

d. perforated plates

e. glass cotton

c.材料 \ b.吸声系数 \ a.频率(赫)	125	250	500	1K	2K
d. 微穿孔板	55	81	86	82	75
e. 玻璃棉	81	59	77	88	95

Measurements are made in wind tunnels. Figure 3.50 shows
the wind tunnel and testing setup. Two wind generators are used.
Their technical parameters are: wind volume 5000 m^3/hr, wind
pressure 1500 mm water column.

The testing point is selected near the wind tunnel outlet,
at a horizontal distance of 5 cm from the outer diameter. Noise
values are first determined without the sound suppressor, and
re-measured after sound suppressors are installed. The difference
in the two noise values is the sound reduction quantity due to
the sound suppressors.

213

The testing point is located outside the sound suppressor
to avoid interference of high speed stream to microphones.
This also agrees with the actual situations. Other methods
including those based on semi-sound-mixing room and insert-
loss have been used. They are not accurate because of the
noise radiation effect of the tunnel shell.

Sound   also comes from the centrifugal blower. At
5 cm from the wind tunnel outlet, the total sound pressure
level and the A-sound level of the wind tunnel are both at
about 110 db.

Based on these measurements: [32]

1. The sound reduction decreases with increasing wind
velocity. Particularly for the cotton-type sound suppressors,
at high velocities, the sound reduction becomes negative.

a. wind tunnel
b. first sound suppressor
c. second sound suppressor
d. microphone
e. automatic recorder
f. spectrometer
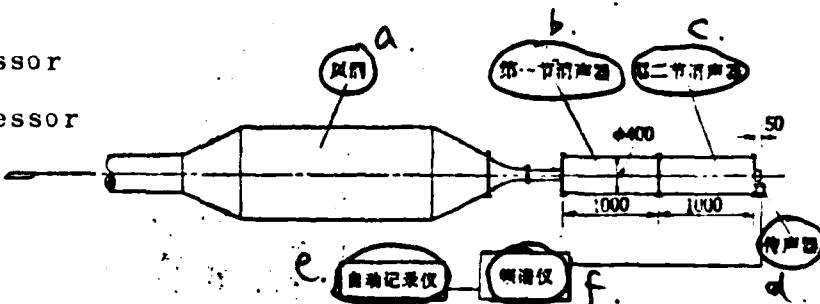
Figure 3.50   Schematic diagram showing
the testing setup for sound
suppressors

214

Figure 3.51 shows the relationship between log v and the average sound reduction ΔL, of the two types of sound suppressors. It can be seen that they are very much linearly related. An empirical equation can thus be derived:

For perforated-type sound suppressors,

$$\Delta L_p = 75 - 34\log v \quad \text{(db)}$$
$$120 \geqslant v \geqslant 20 \quad \text{m/sec}$$

$$(3.75)$$

For cotton-type sound suppressors,

$$\Delta L_p = 102 - 54\log v \quad \text{(db)}$$
$$120 \geqslant v \geqslant 20 \quad \text{m/sec}$$

$$(3.76)$$
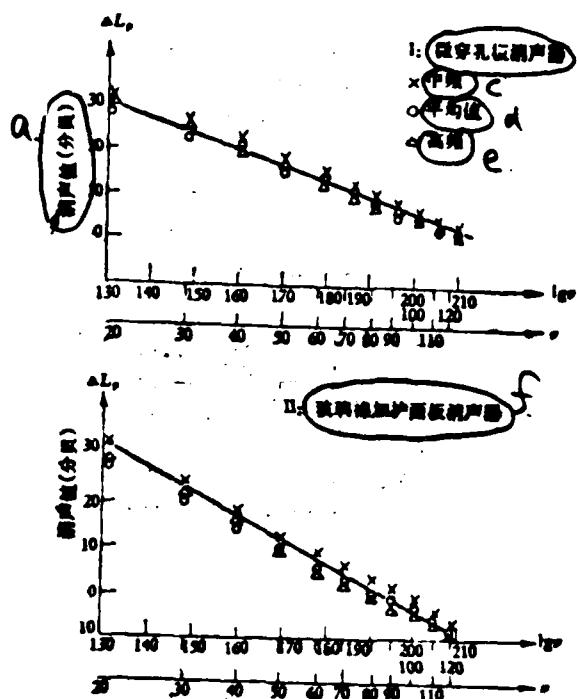
a. sound reduction (db)

b. perforated-plate sound suppressors

c. medium frequencies

d. average values

e. high frequencies

f. glass cotton-type sound suppressors

Figure 3.51   Curves showing the relationships between ΔL, and log v

From Figure 3.46 and Figure 3.47, **3.50** it can be seen that the
average sound reduction has the tendency of decreasing with in-
creasing flow rate v. It can also be seen that, as flow rate
increases, the flow rate effect is much smaller for perforated-
type **than** for cotton-type sound suppressors.

From Equations (3.75)-(3.76), it is obvious that the $\Delta L - \log v$
curve has a slope $K = 34$ for perforated-type sound suppressors
and $K = 54$ for cotton-type sound suppressors. Consequently,
with increasing flow rate v, the drop in sound reduction is
much faster for the latter than for the former.

Judging from the numbers, when the flow rate is 20 m/s, both
sound suppressors have average sound reduction close to 30 db.
When the flow rate is 50 m/s, perforated-type sound suppressors'
average sound reduction decreases only by 10 db, while cotton-
type sound suppressors' average sound reduction decreases by
20 db. When the flow rate is 80 m/s, the former decreases by
20 db, while the latter decreases by 30 db with a null sound
reduction. When the flow rate is 100 m/s, the former still has
an average sound reduction of 5 db, but the latter produces a
negative 3-4 db average sound reduction. At higher than 100 m/s,
the former has 2-3 db in average sound reduction, and the latter
produces a negative 5-9 db average sound reduction.

In the range of 30-80 m/s, when the flow rate doubles,
perforated-type sound suppressors have their sound reduction
decreased by about 15 db. For cotton-type sound suppressors,
the sound reduction decrease is about 10 db.

216

Based on the actual sound reduction effect of sound suppressors (Table 3.17), it is more obvious that sound reduction decreases with increasing flow rate. The table also illustrates the different flow rate effect for the two types of sound suppressors.

Table 3.17   Sound reduction (ΔL_A) at various flow rates

流速 (米/秒) 消声器 类别 ΔL_A (分贝)	集 式 消 声 器	棉 式 消 声 器
10—20	27	27
60	20	12
80—90	14	7
100	12	2
120	5	8

a. flow rate (m/s)

b. sound reduction ΔL_A (db)

c. types

d. perforated-type sound suppressors

e. cotton-type sound suppressors

From these analyses it can be concluded that, under high speed streams, perforated-type sound suppressors have much better sound reduction properties than cotton-type sound suppressors.

2. With increasing flow rate, the effect on sound reduction disappears with increasing length of sound suppressors: For perforated-type sound suppressors at flow rate of 70 m/s and for cotton-type sound suppressors at flow rate of 50 m/s, the

217

average sound reduction is the same (about 10 db) for both 2-m and 1-m long sound suppressors. In other words, at these two flow rates, stream noises have become the major factors; the sound reduction results will not be enhanced anymore by lengthening the sound suppressors. Therefore, the designed length of sound suppressors and flow rates should be appropriate.

a. sound reduction (db/m)

b. m/s

c. frequency (1000 Hz)

d. mineral cotton
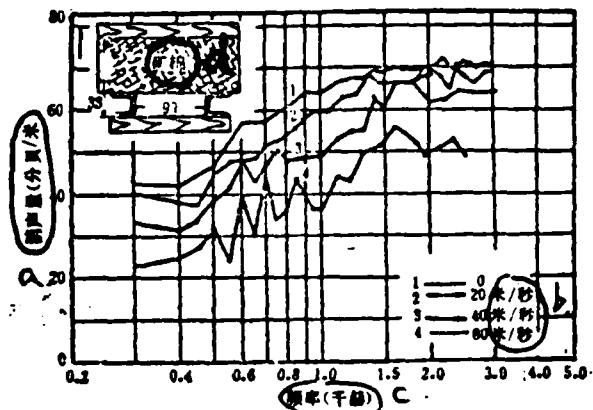

Figure 3.52   Functional relationship between sound
             reduction at various flow rates and frequency.
             10 cm thick mineral cotton is attached to one
             inner side of the tube.

Several foreign authors [33-36] have made high flow rate sound reduction property tests on reactive-type sound suppressors, Helmholtz resonator sound suppressors (with and without the addition of resistive components), and expansion-room type sound suppressors. The results indicate: as shown in Figure 3.52 and Figure 3.53, for sound suppressors with perforated materials with or without the addition of multi-hole layers, the sound reduction decreases with increasing flow rate.

213

As shown in Figure 3.54, similar results occur for expansion-
room type sound suppressors. For Helmholtz resonators with im-
pedance, the results are basically the same. The maximum value
of sound reduction decreases with increasing flow rate, and
moves towards higher frequencies, as shown in Figure 3.55. For
Helmholtz resonators without impedance, the maximum value of
sound reduction also decreases and moves towards higher fre-
quencies as flow rate increases, as shown in Figure 3.56. However,
at high speed, sound signals are enhanced at certain frequencies.

a. sound reduction (db/m)

b. wind velocity

c. m./s

d. mineral cotton

e. frequency (1000 Hz)
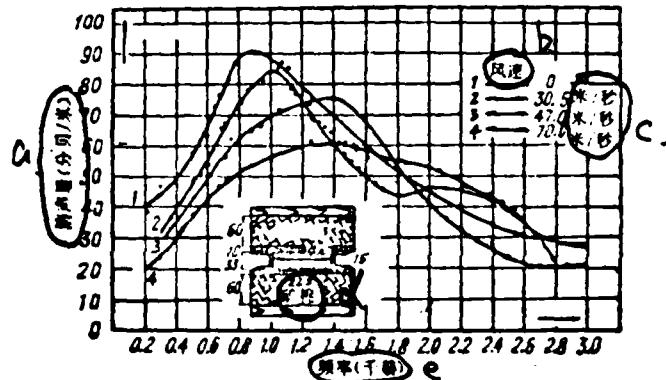
Figure 3.55 Functional relationship between sound
reduction at various flow rates and frequencies.
Six cm of mineral cotton covered with perforated
gypsum plates are attached to the two wider sides
of the passage.

219
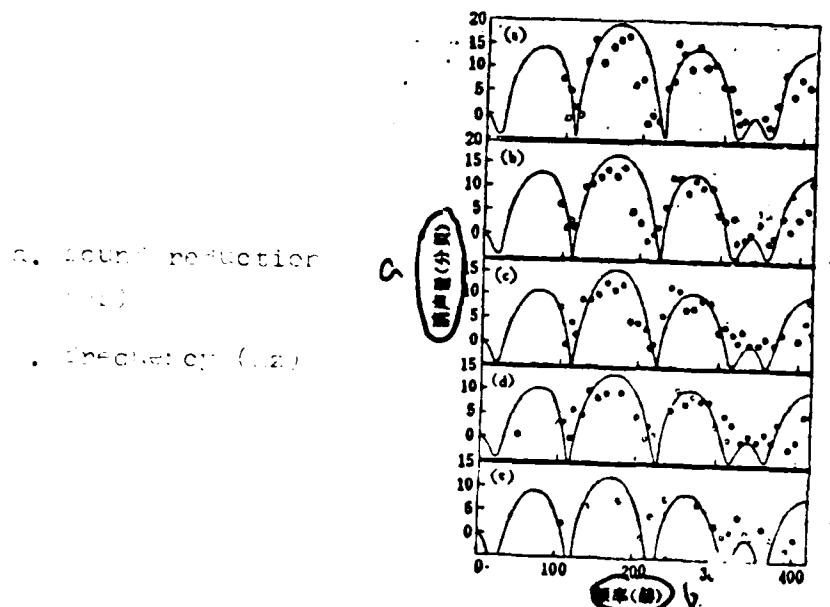
Figure 3.34   Relationship between sound reduction at
various flow rates and frequencies for expansion-room
type sound suppressors

(a)---without stream   (b)---v=10 m/s   (c)---v=20 m s

(d)---v=30 m/s   (e)---v=40 m/s

a. sound reduction (db/m)
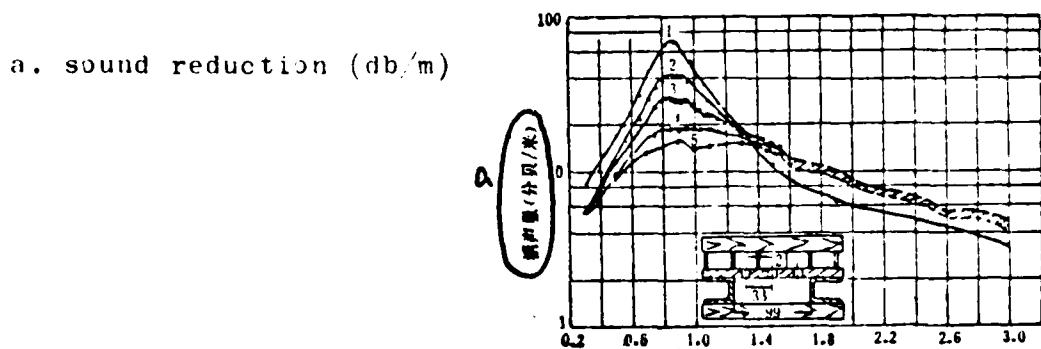
Figure 3.35   Relationship between sound reduction at
various flow rates and frequencies

one side of the tube has a Helmholtz resonator with
impedance.   The resonator is constructed of per-
forated plates and divided back cavities.   Silk
fabric is tightly wrapped in front of the small
holes to produce impedance.

220
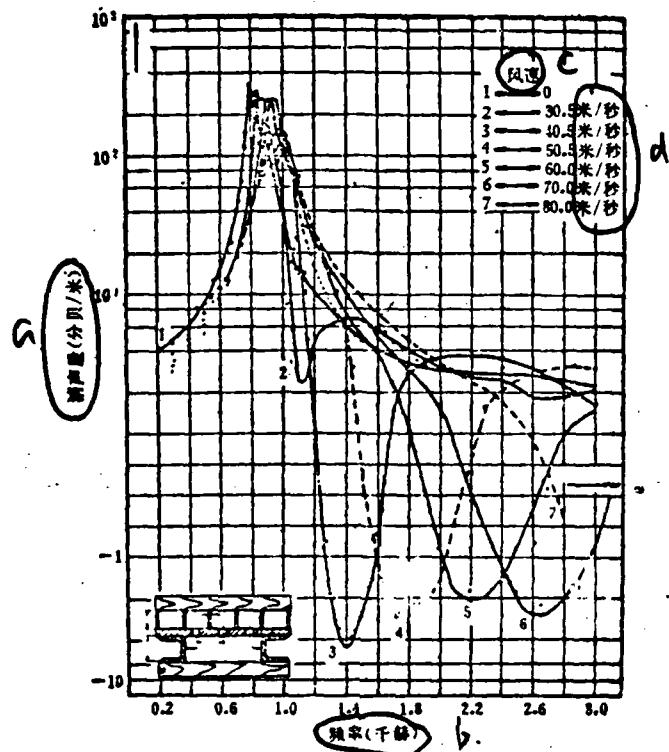
Figure 7.5. Relationship between sound reduction and frequency at various flow rates

The rate is equivalent to ... airbeltz we chosen without impedance, which are at the same rate as that shown in Figure 7.5.

a. sound reduction (db/m)

b. frequency (kHz)

c. ...

...

The main reason for the stream effect on sound reduction properties is the re-generated noise induced when air flows through the sound suppressors.

As stated in chapter 2, when a stream encounters obstacles in its propagation, it will form eddy currents. This is the main cause for the regeneration of noise in sound suppressors. The sound reducing components in sound suppressors can not be very smooth. Sometimes for the purpose of adjusting the sound resistance in the passages, the cross-sections of sound suppressors are intentionally made with changing diameters, bending, and perforated screens. Therefore at low velocities, regenerated noise is not yet obvious. But at high velocities, since the sound power $W \propto \xi^2 v^6$, one can not ignore the regenerated noise thus produced. At high velocities, perforated-type sound suppressors have much lower regenerated noise than cotton-type sound suppressors of the same model. The main reason is that perforated plates with low degree of opening and small and dense holes have a much smaller resistance coefficient ξ than that for glass cotton covered surface with high degree of opening and large and rough holes.

On the other hand, under the impact of high velocity streams, the components and tube walls of the sound suppressors will vibrate. System resonance can sometimes occur. With the formation of solid-regenerated noise, sound suppressors will amplify noise of certain frequencies.

222

Furthermore, when the flow rate reaches very large values, jet noise will form at the outlet and inside sound suppressors. The sound power $W \propto v^8$. At this time, the high noise levels produced by the high-velocity streams themselves greatly overcome the sound reduction achieved by the sound suppressor. The latter becomes not effective.

In addition, the sound reduction pattern change inside a sound suppressor as produced by the stream flow can also affect the sound suppression properties to a certain degree. For instance, for resistive-type sound suppressors, a simple quantitative expression is

$$\Delta L = \frac{\Delta L_0}{1 + M} \quad (\mathrm{db}), \tag{3.77}$$

where ΔL--sound reduction at flow rate v; ΔL_0 --sound reduction without flow; $M = \frac{v}{c}$ -- Mach number. When $M \ll 1$,

$$\frac{1}{1 + M} \approx 1 - M.$$

Therefore, Equation (3.77) can be simplified to

$$\Delta L = \Delta L_0 - M \Delta L_0 \quad (\mathrm{db}), \tag{3.78}$$

i.e., when $M \ll 1$, the decrease in sound reduction is purely determined by the Mach number M.

Figure 3.57 and Figure 3.58 show the variations of sound reduction with stream flow. It can be seen that, when the sound propagation direction is the same as the stream flow direction, sound reductions at low and medium frequency ranges decrease according to Equation (3.78) with increasing flow rate. When the sound propagation direction is opposite to the stream flow direction, sound reductions at low and medium frequency ranges

223

increase with increasing flow rate. At the high frequency
range, sound reductions decrease to below those at no stream
flow. Since when the sound propagation direction is opposite
to the stream flow direction, M value is negative, the ΔL value
in Equation (3.78) increases. Therefore, it can be said that
wind velocity is not advantageous to reduce exhaust sound. It
is advantageous to sound suppressors at the inlet.

a. sound reduction (db/m)

b. frequency (1000 Hz)
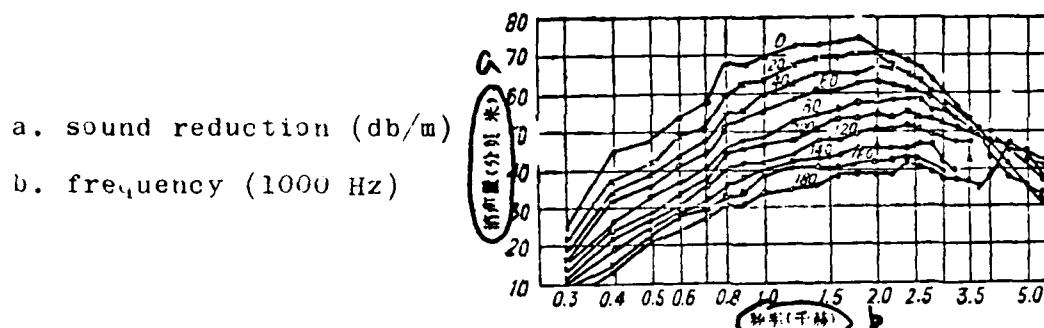
Figure 3.57 Resistive-type sound suppressors: variations
of sound reduction when the sound propagation direction
is the same as the stream flow direction

a. sound reduction (db/m)

b. frequency (1000 Hz)
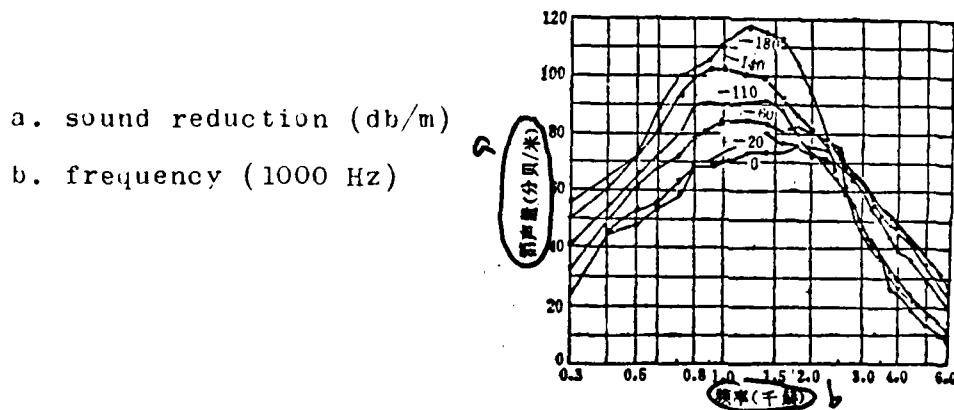
Figure 3.58 Resistive-type sound suppressors: variations
of sound reduction when the sound propagation direction is
opposite to the stream flow direction

224

It can also be seen from Equation (3.78) that the sound reduction decrease, which arises from the variation of sound reduction pattern inside sound suppressors caused by the stream flow, is of the same quantity level as the Mach number M. For example, within a wind velocity of 50-60 m/s, the sound reduction change is 1.5-2%. For a resistive-type sound suppressor with sound reduction of 30-40 db, this only yields an effect of 5-8 db.

For resonance sound suppressors, with stream flow, (two Japanese workers) [35] gave the sound reduction equation:

$$\Delta L = 10\log\left[1 + \frac{(1 - M^2)^2 + \frac{16(1 - M^2)}{3\pi}\frac{F_1\bar{M}}{n\pi a}}{\left(\frac{8}{3\pi}\frac{F_1\bar{M}}{n\pi a^2}\right)^2 + \left(\frac{2F_1}{\sqrt{GV}}\right)^2\left(\frac{\omega}{\omega_r} - \frac{\omega_r}{\omega}\right)^2}\right] \quad \text{(db)}$$

$$(3.79)$$

where M—Mach number; F_1—cross-sectional area of sound suppressor; n—hole number of resonator; a—small hole radius of resonator; V—volume of resonator; G—transmission rate.

Figure 3.59 shows the theoretical and experimental values of sound reduction for resonance sound suppressors under 10-50 m/s flow rate.

(One Japanese worker) also gave the effect on sound reduction due to stream flow for expansion-room type sound suppressors. [36] The mathematical formula:

$$\Delta L = 10\log\left[1 + \left(\frac{m_M}{2}\right)^2 \sin^2(kl)\right] \quad \text{(db)}, \qquad (3.80)$$

where $m_M = m/(1+mM)$ is the equi-effective expansion ratio; m—expansion ratio; M—Mach number. The experimental results

225

(theoretical values and experimental data) are shown in Figure 3.54.

From such analyses one can realize that sound reduction for sound suppressors is not constant. In noise control, the actual sound reductions for sound suppressors depend mainly on the intensity of the noise source, the sound reduction characteristics of the sound suppressors, the intensity of regenerated noise, as well as the level of ambient noise at the outlet.

Assume that the inlet noise level for a sound suppressor is L_i, the noise level at the outlet is L_0, regenerated noise level is L_r, and ambient noise level at the outlet is L_a; then

1. When $L_0 \gg L_r$ (for more than 10 db), the regenerated noise has no effect on the sound reduction properties of the sound suppressors. Under this condition the measured sound reduction $\Delta L = L_i - L_0$ is the actual sound reduction of the sound suppressor.

2. When $L_0 \approx L_r$, the regenerated noise has a certain effect on the sound reduction of the sound suppressors. An approximate value of the actual sound reduction can be obtained after corrections are made:

When $L_0 > L_r$, $\Delta L = L_i - L_0 - \Delta L_{gain}$,

when $L_0 < L_r$, $\Delta L = L_i - L_r - \Delta L_{gain}$;

ΔL_{gain} is determined from Table 1.1 and Figure 1.4 of this book.

3. When $L_r \gg L_0$ (for more than 10 db), the regenerated noise has significant effects on the sound reduction properties. The sound reduction of a sound suppressor is only $\Delta L = L_i - L_r$.

226

Under this condition, due to the regenerated noise, the sound level at the outlet of a sound suppressor will not decrease and a sound reduction effect can not be achieved; even the length of sound suppressor is increased.

4. In any case, the noise level as measured at the outlet of sound suppressors must be $\gg L_a$ (for more than 10 db). Otherwise, due to the interference of ambient noise, the sound reduction can be accurately measured. The effectiveness of sound suppressors, even it is very good, can not be demonstrated.
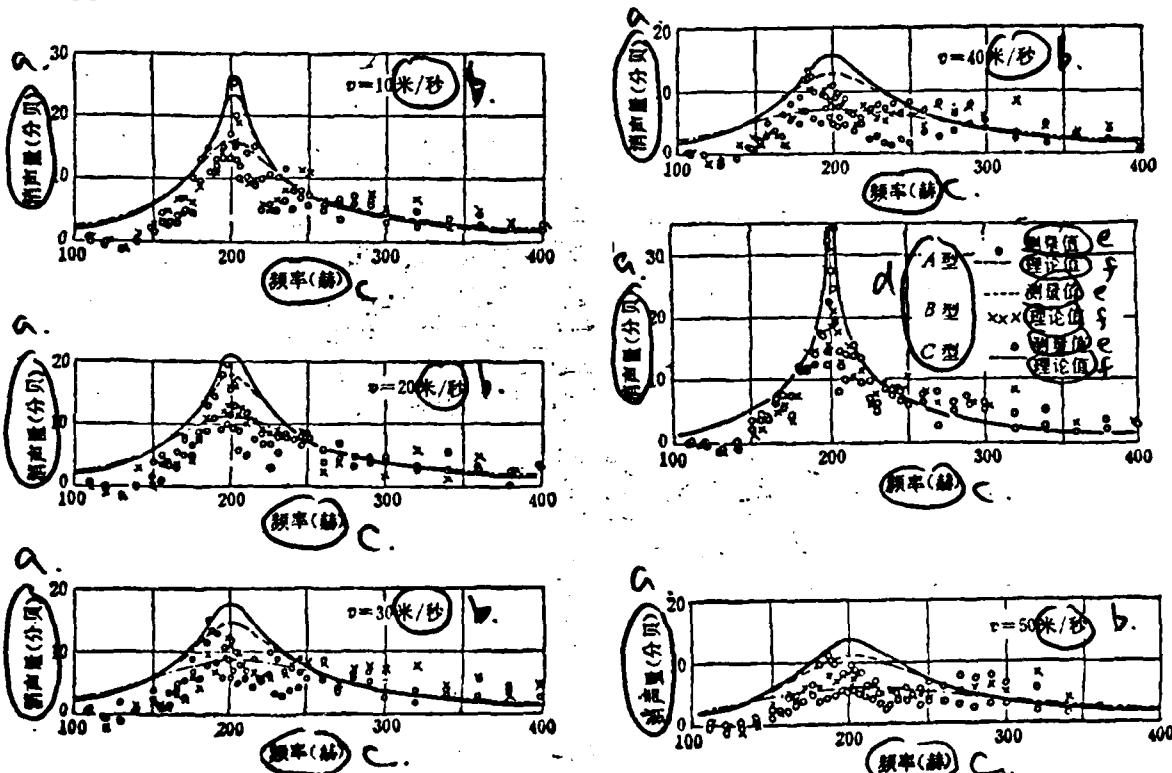

Figure 3.59 Sound reduction curves for resonance sound suppressors with stream flow rate at 10-50 m/s

a. sound reduction (db)   b. m/s   c. frequency (Hz)

d. A-Type, B-Type, C-Type   e. experimental data

f. theoretical values

227

In summary, in designing sound suppressors, one has to consider the intensity of noise sources, the effect of stream flow rate, as well as factors such as the ambient noise at the locations of application. These problems are very complicated. and need detailed analyses based on actual conditions.

In general, for sound suppressors used in air-conditioning units, the intensity of noise sources is not high. The required noise level in applied locations is very low, and the resistance loss requirement is also stringent. The flow rate inside the sound suppressors should be kept under 10 m/s. For sound suppressors with good aerodynamic characteristics (such as perforated plate sound suppressors), the flow rate can be controlled below 15 m/s.

For the inlet and exhaust sound suppressors for blowers, air compressors, and combustion gas rotating machinery, since the noise source intensity levels are relatively high (more than 10 db) and the requirement on noise intensities in the areas of application is not very strict (e.g., required to be less than 90 db(A)), the flow rate inside sound suppressors can be controlled to below 30 m/s.

For internal combustion machinery and jack-hammers, since the noise source intensity is high and the requirement in noise control is strict, compounded with the fact that the ambient noise levels are also high, the flow rate can be allowed to below 50-60 m/s.

228

For sound suppressors with high pressure and large-volume exhaust, since their own noise levels are high, the air volume is large and no people work in the vicinity the flow rate can be controlled based on actual conditions (the distance from residential areas and working locations, etc) to below 30-60 m/s.

Chapter 4. Applications of Sound Suppressors
§4.1 Sound Suppressors for Gas Exhaust

The gas exhaust system has noises with high sound level, broad frequency spectrum, and wide area of influence. Therefore, the required sound suppressors need to be those with large sound suppression volume and broad frequency spectrum for sound suppression. Meanwhile, because of the large flow volume and high pressure, the suppressors should also have the effect of pressure reduction and volume expansion, thus to reduce the pressure drop for gas exhaust.

Due to the different flow volume, pressure and medium, the designs of sound suppressors have to be different in different cases. For instance, for model K-250-61-1 air compressors (intake gas flow volume q = 250 m^3/second, exhaust pressure P = 6 atmosphere), strong noises are produced at total exhaust. Near the exhaust opening (at 0.2 m), both the total sound pressure level and A-sound level reach 137 db. The frequency spectrum is more pronounced at medium and high frequencies, and the spectrum is very broad, seriously containinating the surroundings. However, after installing sound suppressors on the exhaust tube as shown in Figure 4.1, at 0.2 m from the exhaust opening, the total sound pressure level and the A-sound level of the noise reduce to 85 db and 78 db, respectively, with good sound suppression effect. There is no more effect at the neighboring areas. One can make normal conversations near the exhaust opening.

Resistive-reactive combined pressure-reducing sound suppressors have two sections. The first section is for reactively filtering

230

waves and reducing pressure and expanding volume. Sound waves
lose part of the energy through reflections, when encountering the
sudden change in cross-sectional areas, perforated plates, obstacles,
elbows, etc. (Figure 4.2 shows the effect of this section). Mean-
while, the high pressure and high speed gas from the air compressors
becomes one with lower pressure and lower speed (outlet speed is
about 10 m/second) due to continuous pressure reduction and volume
expansion. This process reduces the noise to a certain degree.
The second section is a resistive type sound suppressor. The plates
have thickness of 60 mm, and a separation distance of 120 mm. It
has better effect towards high and medium frequency range noises.

a. direction
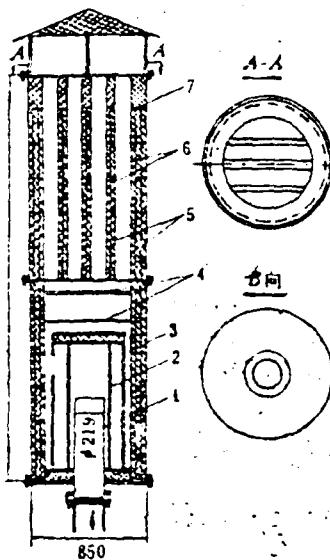
Figure 4.1   Reactive-resistive combined sound suppressor
for air compressor exhaustion

1. Steel tube φ 219x6;   2. steel tube φ 325x7 --- 1000,

6 holes φ 80, 117 holes φ 25 (uniformly arranged in six

rows);   3. steel tube φ 529x6 --- 1100, 14 holes φ 50, 133

holes φ 30 (uniformly arranged in 5 rows);   4. steel plate

133 holes φ 30 uniformly arranged;   5. perforated steel

plate 6, degree of opening 20%, thickness 1.5 mm;   6. glass

fiber: 7. dividing plates
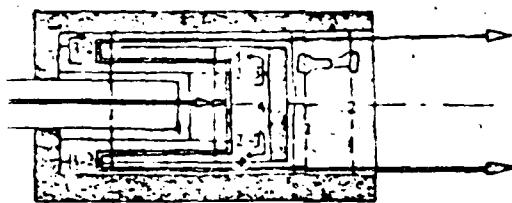
Figure 4.2   Reactive wave filtering and pressure reduction
     and volume expansion section.

1. effective section with sudden change in cross section

2. effective parts of perforated plates

3. effective parts of elbows

4. effective parts of screens

Table 4.1   Evaluation table of reactive-resistive combined
     sound suppressors for air compressor exhaust (testing
     location: 0.2 m from the exhaust opening)

(Table next page)

232

压力(大气压)表压	流量(米³/分)	加消声器前的噪声值(分贝)				加消声器后的噪声值(分贝)				消声量(分贝)		
		L_C	L_s	L_A	频率	L_C	L_s	L_A	频率	ΔL_C	ΔL_s	ΔL_A
0.2	237	127	127	128	高、中	85	80	75	低	42	47	53
1	235	131	131	131.5	高、中	85	80	75	低	46	51	56.5
2	233.5	133.5	133.5	134	高、中	85	90	76	低	48.5	53.5	58
3	227	136	136	137	高、中	85	80	78	低			
4	215	136	136	137	高、中	85	81	78	低			
5	205	137	137.5		高、中	85	80	78	低			
		137	137.5	137.5	高、中	85	80	78	低			

a. pressure (atmosphere, gauge pressure)

b. flow volume (m^3/minute)   c. frequency   d. high,medium

e. low   f. noise level (db) before installing sound
suppressors   g. noise level (db) after installing sound
suppressors   h. sound reduction (db)

Table 4.1 shows the sound reduction effect of this type of
sound suppressors under different pressures and flow rates. It
can be seen that, without the sound suppressors, the noise level
increases with increasing exhaust pressure. With sound suppressors,
because of their effect of gradually reducing pressures, the noise
level becomes independent of the pressure variation. This eliminates
the noises caused by the sudden change in pressures.

For air compressors with flow rates larger than that of the
model K-250, similar type of sound suppressors can be used for the

233

exhaust system. However, the dimensions need to be increased, controlling the flow rate at the exhaust opening to be 10-20 m second. For small-scale air compressors, the required sound suppressors are much simpler (for example, Figure 4.3).
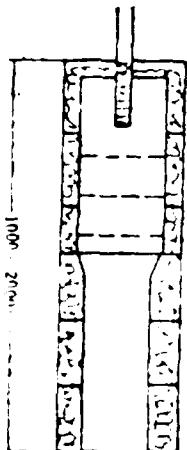

Figure 4.3 Sound suppressor for small-scale air
compressor exhaust

As compared to air compressors, blowers have lower pressure head, but larger flow volume, particularly for large-scale blowers (e.g., the blowers used in tall furnaces for steel mills) with flow rates as high as $1000-5000 \text{ m}^3$ minute, i.e., $60,000-300,000 \text{ m}^3$ hour. Their exhaust noises can reach 120-140 db(A) with broad frequency spectrum and wide area under influence. The influence can sometimes reach several kilometers. Therefore, the dimensions of the exhaust sound suppressors need to be correspondingly larger.

Figure 4.4 is the schematic diagram of the structures of exhaust valve sound suppressor for Model K4250-61 turbine blower (flow volume $= 4250 \text{ m}^3$ min, P_{in} = 1.0 atmosphere, P_{out} = 4.0 atmosphere). This sound suppressor was designed by the Peijing Municipal Workers'

234

Protection and Scientific Research Institute and the Paotou Black Metallurgical Institute. Its structure has also two sections. The first section is a resonant reactive-resistive combined sound suppressor. Its basic component is a diamond-shape sound suppressing structure (see Figure 4.5), with one side being a resonance cavity and another being sound absorbing materials. The resonance cavity is divided into sixteen small compartments, with the design based on the frequencies needed to be removed. Such a diamond-shape sound suppression structure has good effect for a relatively broad frequency band. The second section is a bend-plate type resistive sound suppressor. It suppresses sound through the sound absorbing materials. The bend-plate arrangement is for the purpose of inducing repeated reflections, while sound wave propagates through the passage, thus increasing the loss of sound energy. The sound suppression effect is then raised.

a. fiber glass

b. resonance cavity
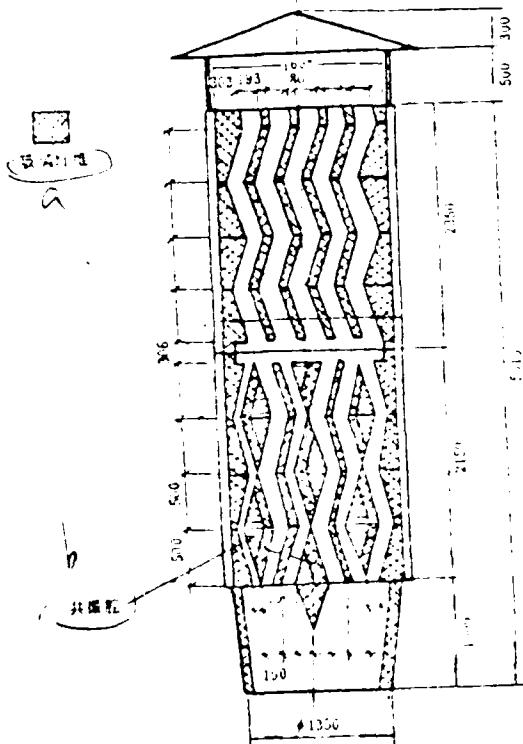
Figure 4.5 Sound suppressor for a tall furnace's exhaust valve

235

Having such a sound suppressor installed on the exhaust valve
of the Model K4250-01-1 blower with φ1400, the noise drops appreciably.
At total exhaust, near the exhaust opening, the noise drops from
131 db(A) to 57 db(A); at small-volume exhaust, the noise there drops
from 121.5 db(A) to 69 db(A). Furthermore, at two meters away from
the exhaust opening, one can make normal conversations. The effect
on environments is already very small.

a. fiber glass 5 cm

b. perforated steel plate
   degree of opening P = 20%
   plate thickness t = 4 mm
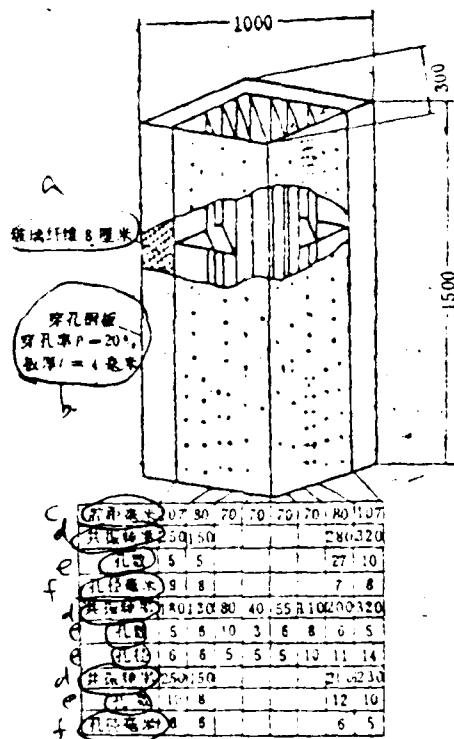
Figure 4.5   Schematic diagram of a resonance sound suppressor

c. cavity distance, mm   d. resonance frequency

e. number of holes   f. hole diameter, mm

Figure 4.6 shows the sound suppression effect curves for each frequency band (octave band) for the above-mentioned sound suppressor at different flow rates.

a. sound reduction (db)

b. frequency (Hz)
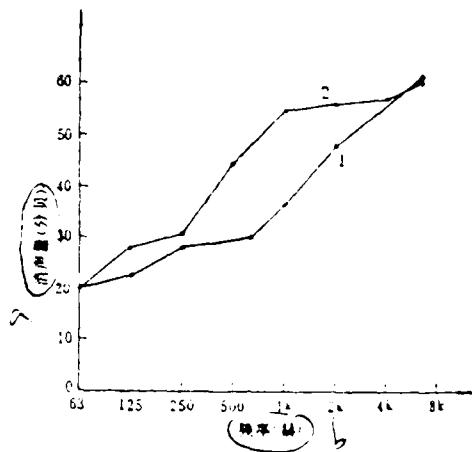

Figure 4.6   Sound suppression effect curves for the exhaust
valve sound suppressors on Model K4250-01-1 blowers
1. sound suppression curve for total exhaust
2. sound suppression curve for small-volume exhaust

Figure 4.7 shows another example of large-scale blower exhaust's sound suppressors. This kind of sound suppressors have the passage in the form of helix. The helix and the wall surface are padded with 9 cm thick glass fiber, covered with perforated steel plates. Sound waves are absorbed over several times through normal and side faces inside the helix. They are greatly reduced. The gas flows along the helix upward to exhaust. This kind of sound suppressors can reduce the noise of blower exhaust valve to 30-40 db.

237
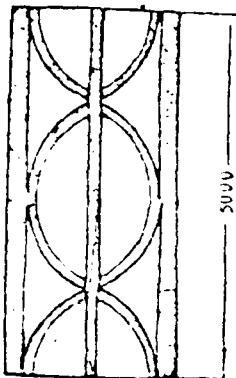
Figure 4.7 another example of large-scale blower exhaust's
sound suppressors

In recent years, large-scale blowers' exhaust systems utilize
sound suppressors in the form of ground hole filled with gravel
(see Figure 4.5). The sound suppression effect is also good. When
the stream passes through the sound suppressing hole, with volume
expansion and reducing speed, it passes through the gaps between
gravel with slow speed of several meters per second. The gravel
reflect the noise sound many times, dissipating greatly the sound
energy. They also change the pressure drop from a sudden drop to
gradual drop. By utilizing such kind of sound suppression on Model
K-4250 and K-3250 large-scale blower's exhaust system, sound reduc-
tion reaches 50 db(A). The original exhaust noise of 130-140 db(A)
is reduced to below 90 db(A). Small volume exhaust noise is as
low as 60-70 db(A). Sometimes they can be even lower than the
factory's ambient noise.

Figure 4.5 is the gravel-ground hole type sound suppressor
for large-scale blower's exhaust system.

238

a. sound-absorbing wedge

b.

c. gravel (ϕ 100), 1000 thick

d. gravel (ϕ 150), 500 thick

e. light rail

f. steel structure

g. blower exhaust pipe
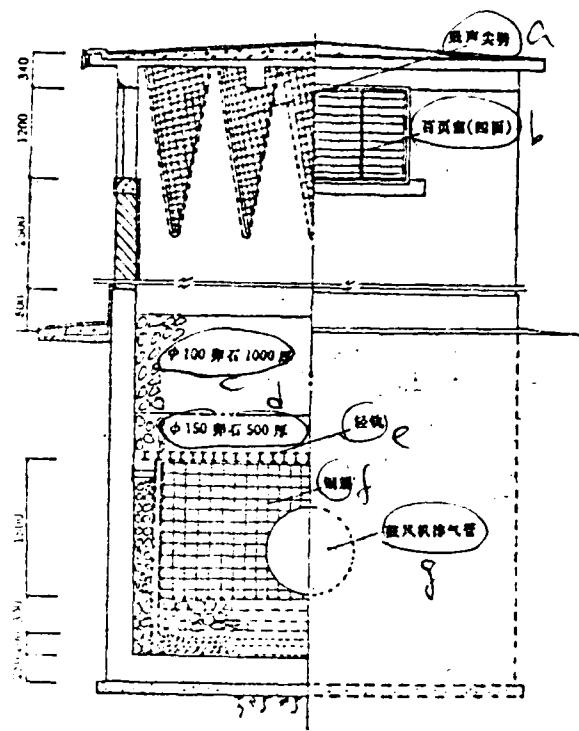
Figure 4.8 Gravel-ground hole type sound suppressor for large-scale blower's exhaust

For medium and small scale blowers' exhaust systems, the sound suppressors can have smaller dimensions and simpler structures. For instance, the exhaust system for the blower with a medium flow rate (q = 1000 m^3/minute approximately) can use one passage of the sound suppressor in Figure 4.4, formed in the configuration as shown in Figure 3.42(f), Figure 4.9 or Figure 4.10. Such sound suppressors have length of nearly 3 m. When the flow rate is below 30 m/s, the sound suppressors have sound reduction of 30-40 db(A).

239

For small-scale blowers (flow rate at several hundred m^3/minute) one can use tube-type sound suppressors, tube type-expansion room combined sound suppressors, or tube type-resonance combined sound suppressors (see Figure 3.11 (a), Figure 3.42 (a), (b), (c), (e), etc.).
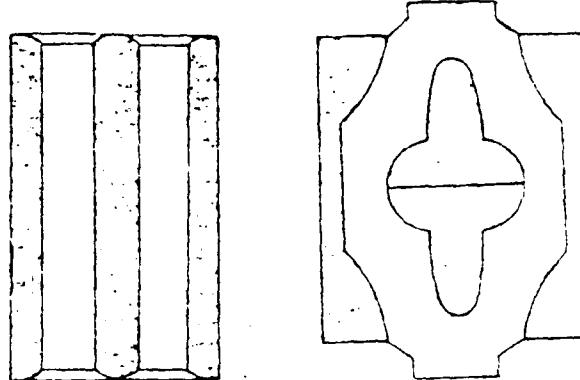
Figure 4.9   An example of exhaust sound suppressor for medium-scale blowers

Figure 4.10   Another example of exhaust sound suppressor for medium-scale blowers

What should be the magnitude of controlled flow speed in the exhaust sound suppressor for blowers? If it is too low, the dimensions of the sound suppressor will be too large for large flow volumes. If it is too high, the re-generated noise will affect the efficiency of the sound suppressor. In general, the flow speed for blowers' exhaust system should be controlled to below 30 m/s. If the requirements on dimensions are more stringent, and the exhaust pipe is high above ground (e.g., above 5 m), then the flow speed can be higher. however, the highest speed should not be more than 50-60 m/s.

240

a. tiny-hole perforated plate

b. perforated plate

c. fiber glass
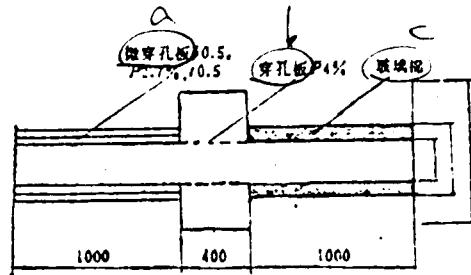
Figure 4.11 Schematic diagram of exhaust valve sound suppressor

for the Model L84 Rotz blower (Q = 5000 m^3/minute)

a. sound reduction (db)

b. before sound reduction,
   near exhaust opening

c. after sound reduction,
   near exhaust opening

d. db

e. frequency (Hz)
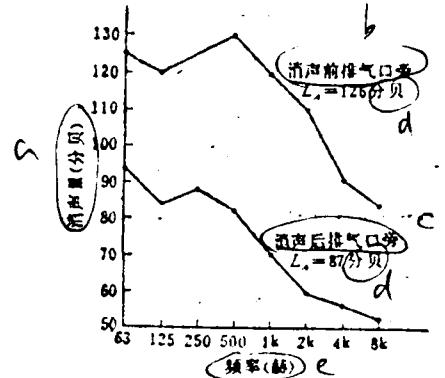
Figure 4.12 Effect of sound reduction of the exhaust valve

sound suppressor for the Rotz blower

The controlled flow speed for sound suppressors is also related
to the buildings (offices, residential) near the exhaust outlet and
with strict noise requirements. If the requirements are not strict,
flow rate can be higher. Otherwise, even the dimensions of sound
suppressors are large, the flow speed should still be reduced as
much as possible.

The exhaust system for boilers in generation facilities has
the characteristics of large flow volume (as high as several tens

241

of tons per hour), high pressure (as high as 100 atmosphere), large noise pollution area (sometimes reaching several tens of kilometers), and high water content in the exhaust steam. Therefore, the sound suppressors are required to be strong and durable, not susceptible to impact, water corrosion. Not only do they reduce sound, they also allow pressure drop and volume expansion.

Figure 4.13 is the schematic diagram for the exhaust sound suppressor for a certain generation facility's medium pressure boiler (pressure at 31 kg/cm^2). This kind of sound suppressor can reduce the boiler's exhaust noise by about 20 db. (The initial
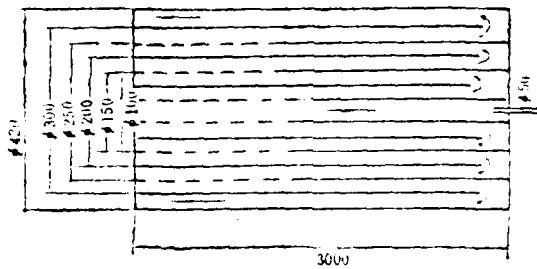

Figure 4.13 Schematic diagram for the exhaust sound suppressor for a certain generation facility's medium pressure boiler (through hole diameter of 10 mm)

a. sound pressure level (db)
b. frequency (Hz)
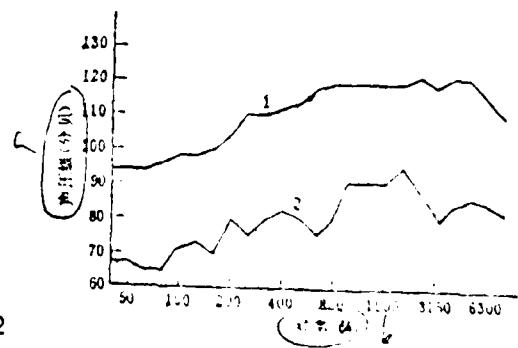
Figure 4.14   Sound reduction effect curves for the exhaust

sound suppressor for a certain generation facility's

medium pressure boiler

1. noise frequency spectrum for a certain medium

pressure boiler's exhaust

2. noise frequency spectrum of the exhaust after

installing sound suppressor

testing point: 1 m from the exhaust opening, at 45^0

noise sound level at 45^0 and 1 m from the exhaust opening is 137.5

db).   Figure 4.14 shows the sound reduction effect curves.

Figure 4.15 is the schematic diagram for the exhaust sound

suppressor for a certain generation facility's high pressure boiler

(95 kg/cm^2).   It has the same principle as that for Figure 1.15.

They both utilize the sound suppressor's continuous change in

reactive-resistive properties, and the continuous pressure reduction

and volume expansion.   Because of the large flow volume, high pres-

sure, therefore the sound suppressor has large dimensions and many

stages.

Such a sound suppressor can reduce exhaust noise by 20-30 db.

The structure has three sections, with the gas passage cross sec-

tions increasing in steps, i.e.,

$$F_5 = 1.25(F_4' + F_4'') = F_5 = 1.25(F_1' + F_2'') = 1.25 F_1,$$

where F_1 is the cross-sectional area of tube 1: $F_1' + F_2''$ is the

total holes' area of tube 1; F_5 is the ring-shape area between tube

1 and tube 2; $F_4' + F_4''$ is the total holes's area of tube 2: F_5 is

the ring-shape area between tube 2 and tube 3.

In general, the boiler's exhaust tubes for generation facilities are installed on top of buildings, more than 10 m from the ground. After sound reduction, and also attenuated over a distance more than 10 m, the boiler's exhaust noise is already not very strong on the ground. If the sound suppressor as shown in Figure 4.16 is used, the sound reduction can be even higher (more than 40 db(λ)).

For boiler's exhaust, one can also use the spraying sound suppressors. For instance, the spraying sound suppressor as shown in Figure 4.17 can reduce the noise from a medium pressure boiler by approximately 20 db.
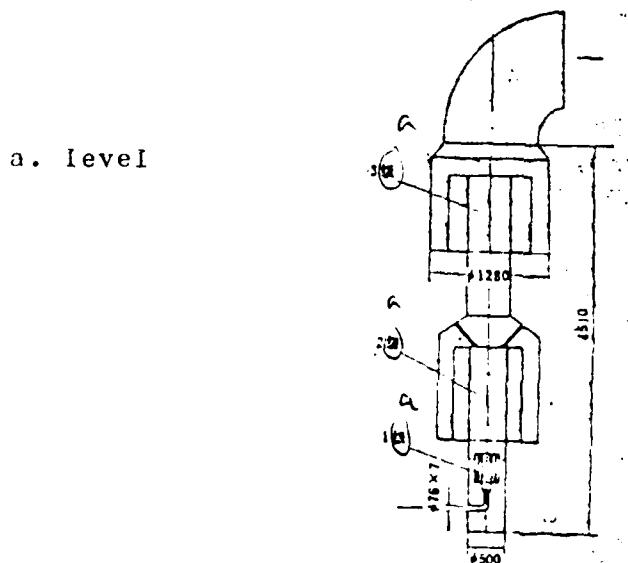
a. level

Figure 4.13 Schematic diagram for the exhaust sound
suppressor for a certain generation facility's
high pressure boiler
(through holes with diameter of $\phi 50$ mm)

a. small hole perforated
   plate
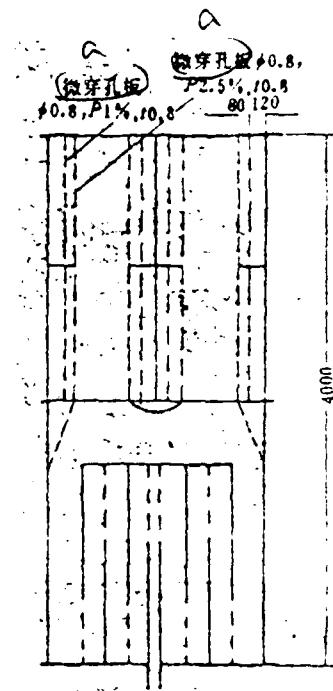
Figure 4.16   Schematic diagram of exhaust sound suppressors
             for boilers

a. exhaust tube

b. spraying tube

c. steel belt

d. water-steam separator

e. dirty water

f. gas inlet

g. water

h. steam
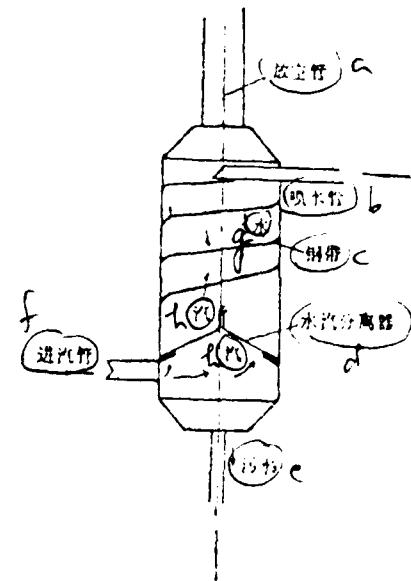
Figure 4.17   Spraying sound suppressor

4.2 Ventilation and Climate Control Noise Silencers

Ventilation and climate control are greatly used in residences and work areas where there is a requirement for peace and comfort. It is also used in many underground structures and in the design and construction of mines. The standards regulating background noise levels in such structures set requirements that are much higher than those for usual industrial structures. Moreover, due to the fact that the pressure heads of blowers are low, the requirements posed by these types of structures in terms of blockage losses are also relatively stringent. It follows from this that, in general, if one takes the flow speed in the noise silencers and controls it so that is below 10 m/sec, it follows that, even if there is high speed circulation, the flow speed will still not exceed 15 - 30 m/sec. In places where there are especially stringent requirements, for example, in the ventilation and climate control equipment of high-class buildings, the flow speeds within the main ventilation ducts do not exceed 5 m/sec.

Concerning the question of the noise silencers in the ventilation and climate control systems of such buildings, it is possible, on the basis of their noise levels, frequency spectra, amounts of flow as well as their conditions of employment, to select for use different lengths and cross sections of tube-type, plate-type, sound-flow-type noise silencers, as well as complex resistance and minute-aperture-plate noise silencers.

Figure 4.18 is an illustration of the national standard tube-type noise silencer. Its noise suppression capabilities as well as its dimensions can be seen in Table 4.2 [10].

When one is employing a tube-type noise silencer, the dimensions of the horizontal cross section cannot be excessively large; if it is excessively large, then, it is possible to take this tube and use it as a part in the construction of a "bee-hive" noise supressor.

246

Figure 4.19 is an illustration of the structure of the national standard plate-type noise silencer. Its noise suppression characteristics and its dimensions can be seen in Table 4.3 [10].

Figure 4.20 is an illustration of the structure of the national standard arc-shaped sound flow-type noise silencer. Its noise suppression characteristics and its dimensions can be seen in Table 4.4.

In recent years, the Shanghai Industrial Architecture Design Academy has made test constructions of a type of wide frequency band complex noise silencer [10]. The noise silencing results of this device were good and its air blockage was also small. An illustration of its structure can be seen in Figure 4.21.

When the wind speed at the intake of the noise silencer is 8m/sec, then the noise silenced on the central frequencies of various frequency bands can be seen in Table 4.5; when the wind speed is 4-12 m/sec, the coefficient of localized air blockage is 0.44.

As far as ventilation and climate control system noise silencers are concerned, recently new requirements have been raised for this type of equipment:

1. When operating in humid air, the acoustic characteristics of sound-absorbing materials, following use, will increase up to a fixed number of years and then deviate from what it should be. This influences the noise silencing results; it follows from this that there exists a requirement to find a type of sound-absorbing material which is new and with which it is not necessary to worry about moisture or humidity.

2. When one is dealing with high-quality precision machine shops, meeting rooms and work areas, it is hoped that one will not use fibrous materials as the type of material used for sound absorptions. The reason for this is that this type of material has a powdery layer blown off from it, and this contamination has an influence on the health of the people in these types of areas as well as on the accuracy of the work which they produce. In this type of situation, it is possible to select for use a minute aperture plate sound flow-type noise silencer (Figure 4.22).

密度为170公斤/米³的矿渣棉底
密度为38公斤/米³的卡普隆纤维

I-I

1000

B

1000
聚酯泡沫塑料密度为34公斤/米³
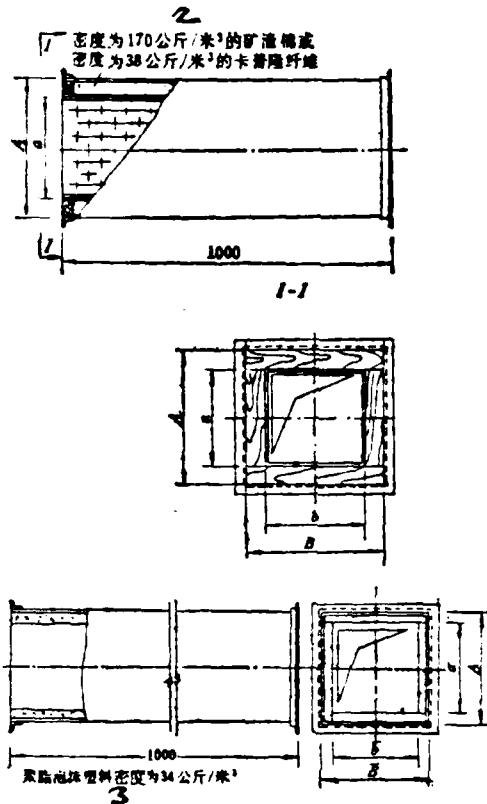
图4.18 国家标准管式消声器示意图

Figure 4.18. 1. An Illustration of the National
Standard Tube-type Noise Silencer. 2. Slag Cotten
with a Density of 170 kg/m^3 or Kaptron Fibers with
a Density of 38 kg/m^3. 3. Sponge Plastic with a
Density of 34 kg/m^3.

Table 4.2 shows the amount of noise eliminated, and the blockage
losses for this type of noise silencer with different flow
speeds.

It is also possible to take a minute aperture plate noise
silencer and make it into a plate-type, a tube-type or a rectangu-
lar-type, as well as other different types of noise silencers
in order to satisfy the requirements of ventilation and climate
control systems for use in different situations. Table 4.7
and Table 4.8 give the amounts of noise eliminated and the blockage

248

表4.2 管式消声器的性能及尺寸

名称	型号	频带中心频率的消声量(分贝)							重量(公斤)	尺寸(毫米)			
		100	200	400	800	1600	3150	6300		A	B	a	b
矿渣棉管式消声器	1	7.7	15.0	20.8	23.4	26.2	27.2	18.0	33	320	320	200	200
	2	6.4	12.5	17.3	19.4	21.8	14.6	7.2	39	320	420	200	300
	3	5.8	11.3	15.6	17.5	19.7	13.2	6.6	45	320	520	200	400
	4	6.2	12.0	16.6	18.8	21.0	14.0	7.0	39	370	370	250	250
	5	5.1	10.0	13.9	15.6	17.5	12.0	6.0	47	370	495	250	375
	6	4.6	9.0	12.5	14.0	15.8	10.5	5.3	54	370	620	250	500
	7	5.1	10.0	13.9	15.6	17.5	11.7	5.8	45	420	420	300	300
	8	4.2	8.3	11.6	12.9	14.6	9.7	4.9	54	420	520	300	450
	9	3.8	7.5	10.4	11.7	13.2	8.8	4.4	63	420	720	300	600
泡沫塑料管式消声器	1	2.6	10.9	25.9	18.5	24.3	25.9	17.8	17	300	300	200	200
	2	2.1	9.7	21.6	15.5	20.3	13.5	6.8	20	300	400	200	300
	3	1.9	8.2	19.4	13.9	18.2	12.0	6.0	23	300	500	200	400
	4	2.1	8.7	20.7	14.8	19.4	12.8	6.4	20	350	350	250	250
	5	1.7	7.3	17.3	12.4	16.2	10.8	5.4	23	350	475	250	375
	6	1.5	6.5	15.5	11.1	14.6	9.8	4.9	27	350	600	250	500
	7	1.7	7.2	17.2	12.3	16.2	10.8	5.4	23	400	400	300	300
	8	1.4	6.1	14.3	10.3	13.4	8.9	4.4	27	400	550	300	450
	9	1.3	5.4	13.0	9.2	12.1	8.0	4.0	31	400	700	300	600
卡普隆管式消声器	1	7.7	17.6	30.0	29.5	26.5	18.5	12.3	28	360	360	200	200
	2	6.4	14.7	25.1	24.6	22.3	14.8	7.4	33	360	460	200	300
	3	5.8	13.2	22.6	22.1	19.9	13.2	6.6	38	360	560	200	400
	4	6.2	14.1	24.1	23.6	21.2	14.1	7.1	33	410	410	250	250
	5	5.1	11.7	20.1	19.6	17.7	11.8	5.9	39	410	535	250	375
	6	4.6	10.5	18.0	17.6	15.9	10.6	5.3	45	410	660	250	500
	7	5.1	11.7	20.0	19.6	17.7	11.8	5.9	38	460	460	300	300
	8	4.2	9.8	16.7	16.4	14.8	9.8	4.9	45	460	610	300	450
	9	3.8	8.8	15.0	14.7	13.8	8.8	4.4	52	460	760	300	600

Table 4.2.   1.   Characteristics and Dimensions of Tube-type Noise Silencers.   2.   Nomenclature.   3. Model Number.   4.   Amount of Noise Reduction on the Center Frequency of a Frequency Band (decibels). 5.   Weight.   6.   Dimensions (mm).   7.   Slag Cotten Tube-type Noise Silencer.   8.   Sponge Plastic Tube-type Noise Silencer.   9.   Kapron Tube-type Noise Silencer.
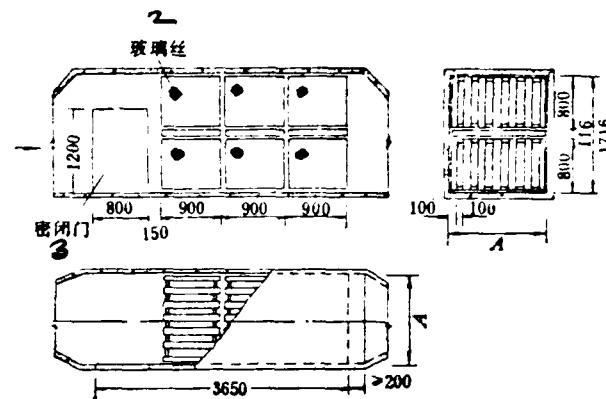
图 4.19 国家标准片式消声器结构示意图

Figure 4.19. 1. An illustration of the Structure of the National Standard Type of Plate-type Noise Silencer. 2. Glass Fibers. 3. Sealed Door.

表 4.3 片式消声器的性能及尺寸

型号	(毫米)	重量[1] (公斤)	风速(米/秒)下的风量(米³/时)		风速(米/秒)下的阻抗(毫米水柱)		频带中心频率下的消声量(分贝)							
			4.0	5.0	4.0	5.0	50	100	200	400	800	1600	3150	6300
1	900	972	9200	11500	6	9								
2	1300	1365	13800	17300	6	9	5	11	22	32	38	32	22	13
3	1700	1758	18400	23000	6	9								
4	2500	2544	27600	34600	6	9								

1) 不包括外壳和密闭门的重量.

Table 4.3 1. Characteristics and Dimensions of Plate-type Noise Silencers. 2. Model Number. 3. (mm). 4. Weight (kg). 5. Wind Speed (m/sec). Amount of Air Coming Down (m³/hour). 6. Wind Speed (m/sec). Amount of Blockage Loss (mm on water column). 7. Amount of Noise Silenced on the Center Frequency of a Frequency Band (Decibels). 8. All this does not include the weights of the exterior shell or the sealed door.

250
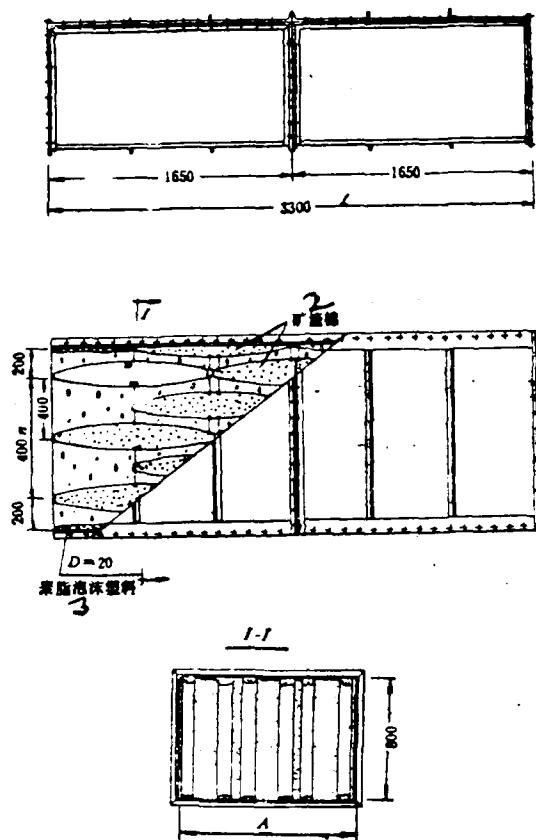
图 4.20 国家纤维弧形声流式消声器结构示意图

Figure 4.20. 1. An Illustration of the Structure
of the National Standard Arc-shaped Acoustic Flow-
type Noise Silencer. 2. Slag Cotton. 3. Sponge
Plastic.

losses for two types of rectangular, minute aperture plate-type
noise silencers (Figure 3.45) given different flow speeds. The
structure of this type of noise silencer is shown in Figure 3.45.

From Tables 4.6 - 4.8 it can be seen that the blockage
losses of minute aperture plate noise silencers are much smaller
than those of drag-type noise silencers or complex resistance-
type noise silencers. Concerning the matter of rectangular

251

minute aperture plate noise silencers, it is almost possible to ignore the blockage or resistance losses, and not consider them in at all. This is of particular significance for ventilation and climate control systems which require unusually stringent controls on blockage or resistance losses.

What follows is an actual example of the use of a minute aperture plate noise silencer in a ventilation and climate control system.

表4.4 国家标准弧形声流式消声器（长: 3300 毫米)的
性能及尺寸

型号	A毫米	n	重量公斤	风速（米/秒）下的风量（米³/时）			风速（米/秒）下的阻损（毫米水柱）			频带中心频率下的消声量(分贝)							
				4.5	5.0	5.5	4.5	5.0	5.5	50	100	200	400	800	1600	3150	6300
1	800	1	629	2460	2730	3000	19	22	26	16	16	38	46	47	49	46	43
2	1200	2	874	3690	4100	4570	19	22	26								

Table 4.4. 1. The Capabilities and Dimensions of the National Standard Arc-shaped Acoustic or Noise Flow-type Noise Silencer (Length 3300 mm). 2. Model Number. 3. mm. 4. Weight (kg). 5. The Amount of Ventilation (m^3/hr) Put Out at a Certain Flow Speed (m/sec). 6. Blockage Losses (mm on a water column) Resulting at a Certain Flow Speed (m/sec). 7. The Amount of Noise Reduced (decibels) On the Center Frequency of a Frequency Band.

A certain fertilizer plant had a newly installed W-1 model climate control unit. After passing through more than ten meters of ducts, the air from the unit entered a sterile chamber. The rooms within this chamber all had small volumes; moreover, due to the fact that there were certain technical requirements, the

whole area was painted with a kind of shiny and slippery oily
lacquer; the area was like a reverberation chamber. In some of
the rooms, the background noise from the climate control unit
reached 81 decibels (A), and exceeded N75; even in the best of
the rooms, the background noise level reached 69 decibels (A),
N65. This monotonous background noise was difficult to listen
to, made people unusually irritable, and affected work efficiency.

After it was arranged to install a rectangular minute aper-
ture plate noise silencer such as the one shown in Figure 4.23,
the average background noise level in all the rooms fell to
below N50 and reached 52 decibels (A); its noise reduction
efficiency is as shown in Figure 4.24.

After the installation of this type of noise silencer, as
far as the particular technical requirements of the sterile chamber
were concerned, it was possible to fundamentally meet them, that
is: (1) The background noise level in the rooms must be
basically similar to that in the factory itself, and (2) with
the use of a pure metal minute aperture plate noise silencer which
is sprayed with a rust preventive paint, it is possible to use
moist gases to clean it; moreover, there is no fibrous powdery
layer.

Figure 4.25 is a diagram of a ventilation and climate con-
trol system which uses a minute aperture plate noise silencer.

4.3. Gas Disposal Noise Silencers for Internal Combustion Engines

The noise which is produced by the exhaust systems of inter-
nal combustion engines is composed primarily of low and medium
frequency sounds with high frequency sounds reaching a certain
level. It follows from this that there is a requirement for
sound silencers which are to be used for this purpose to have
good capabilities in the low and medium frequency ranges and,
at the same time, to have a certain level of capability for high
frequency sound elimination. Besides this, internal combustion
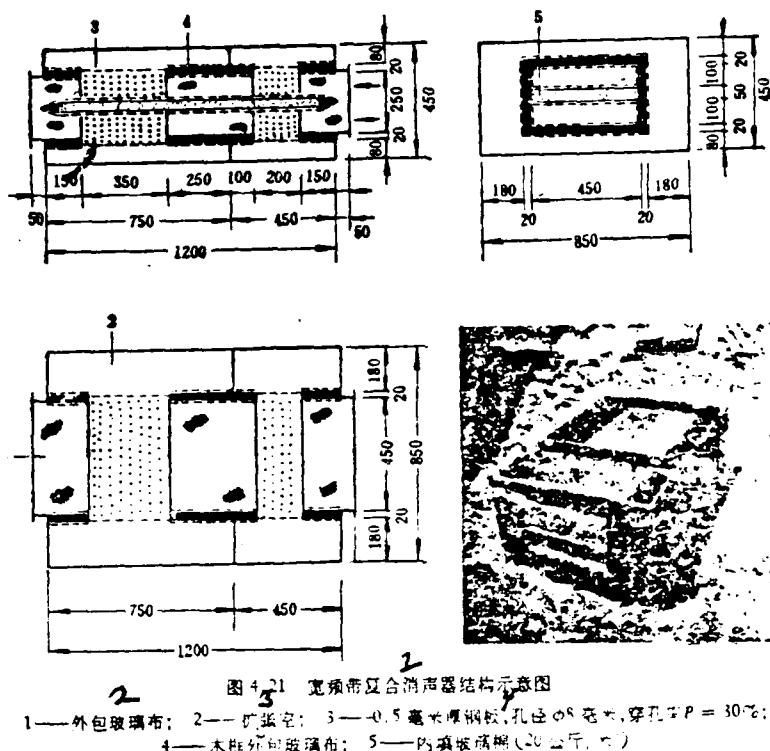
图 4.21 宽频带复合消声器结构示意图

1——外包玻璃布； 2——扩张室； 3——0.5毫米厚钢板，孔径φ8毫米，穿孔率P＝30%；
4——木框外包玻璃布； 5——内填玻璃棉（20公斤/米³）

Figure 4.21. 1. An Illustration of the Structure
of a Wide Frequency Band Complex Noise Silencer. 2.
Outer Wrapper of Poly Vinyl Chloride. 3. Expansion
Chamber. 4. Steel Plate with a Thickness of 0.5 mm,
Aperture Diameter of 8mm, Penetration Rate of P = 30%.
 5. Wooden Framework of the Outer Wrapper of Poly Vinyl
Chloride. 6. Interior Stuffing of Glass Cotton
(20 kg/m^3).

engines put out gases which have a high temperature, a high flow
speed, carry with them pollutants from the fuel and, sometimes
still contain some flames. Because of this situation, noise
silencers for internal combustion engines should be primarily
of a resistance or resistance complex nature, and the sound
absorbant materials which are employed in them need to be resis-
tant to high heat, to shock, and there should be no fear of
pollutants or fire as far as they are concerned.

表 4.5 宽频带复合消声器的消声性能

频带中心频率	50	100	200	400	800	1600	3150	6300
消声量(分贝)	13	14	16	20	28	37	41	36

Table 4.5. 1. The Noise Suppression Capabilities of
a Wide Frequency Band Complex Noise Silencer. 2. Fre-
quency Band Center Frequency. 3. Amount of Noise
Eliminated (decibels).
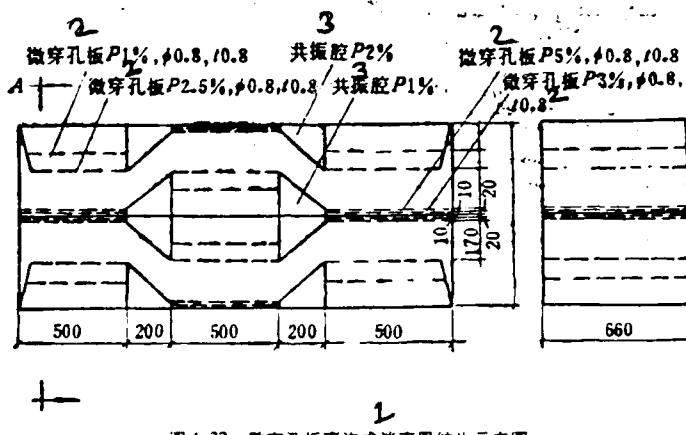
图4.22 微穿孔板声流式消声器结构示意图

Figure 4.22. 1. An Illustration of the Structure of
a Minute Aperture Plate Acoustic or Noise Flow-
Type Noise Silencer. 2. Minute Aperture Plate.
3. Resonance Cavity.

After diesel engines similar to the 4115 type (65 horse-
power and 55 horsepower) were fitted with a minute aperture plate-
drag type noise silencer similar to the one shown in Figure 4.26
as well as a curved head mesh screen noise silencer similar to
the one in Figure 4.27, the noise went down 20 decibels (A);
the noise suppression frequency charts for the various cases
are shown respectively in Figure 4.28 and 4.29.

After a type of noise silencer similar to the one shown in
Figure 4.30 was chosen for employment in a medium size diesel

255

1

表4.6 不同流速下微穿孔板消声器的消声量和阻损

流速(米/秒) 消声量(分贝) 中心频率(赫)	63	125	250	500	1k	2k	4k	8k	阻损毫米水柱
0	18	28	29	33	30	42	51	41	0
7	16	25	29	33	23	32	41	35	0.5
10	15	23	26	29	22	30	35	33	4.9
15	13	19	20	24	20	26	34	30	8

Table 4.6. 1. The Amount of Noise Eliminated and the Blockage Losses for a Minute Aperture Plate Noise Silencer Given Different Flow Speeds. 2. Flow Speed (m/sec). 3. Amount of Noise Eliminated (decibels). 4. Center Frequency (Hertz). 5. Blockage of Resistance Losses in mm on a Water Column.

engine (350 horsepower), its exhaust port was 45°, and, at a distance of one meter, the noise level went down 30 decibels (A); the noise reduction frequency spectrum curves are as shown in Figure 4.31. From 63 - 8000 Hertz, within a wide band of frequencies, the noise level dropped by 30 - 40 decibels.

Figure 4.32 is a simplified drawing of various noise silencers which are used with internal combustion engine exhausts both inside and outside China.

4.4 Air Compressor and Air Blower Noise Silencers

On the basis of the different frequency characteristics of air compressors, it is possible to respectively choose for use expansion chamber noise silencers, expansion chamber-drag type complex noise silencers or resonance resistance complex noise silencers (ss Figure 3.42(a) - (d) and Figure 3.43(e)).

Figure 4.33 is an illustrative diagram of a model 160B-20/8 air compressor noise silencer. When the type of noise silencers we have mentioned are installed in the intake and exhaust ports of this type of air compressor, the noise will be greatly reduced.

表 4.7　微穿孔板矩形消声器（通道为 150 毫米）
在不同流速下的消声量与阻损

流速（米/秒）＼消声量（分贝）＼中心频率（赫）	63	125	250	500	1k	2k	4k	8k	阻损 毫米水柱
0	12	16	25	25	26	26	23	26	0
7	12	16	25	24	22	25	23	25	0.01
10	12	16	25	23	22	25	23	25	0.24
16	11	14	22	20	23	26	23	24	0.65
20	9	12	21	22	20	24	23	24	1.32
25	5	9	19	21	20	26	23	24	1.52

Figure 4.7. 1. The Amount of Noise Eliminated and the Blockage of Resistance Losses for a Minute Aperture Plate Rectangular Noise Silencer (the passageway is 150 mm) Under Different Conditions of Flow Speed. 2. Flow Speed (m/sec). 3. Amount of Noise Eliminated (decibels). 4. Center Frequency (Hertz). 5. Blockage Loss in mm on a Water Column.

表 4.8　微穿孔板矩形消声器（通道 250 毫米）
在不同流速下的消声量和阻损

流速（米/秒）＼消声量（分贝）＼中心频率（赫）	63	125	250	500	1k	2k	4k	8k	阻损 毫米水柱
7	12	18	26	25	20	22	25	25	0
11	12	17	23	23	20	20	26	24	0
17	11	15	23	22	20	22	23	23	0
20	6	12	22	21	20	21	21	20	0.7

Table 4.8. 1. The Amount of Noise Eliminated and the Blockage Losses for a Rectangular Minute Aperture Plate Noise Silencer (with passageway 250 mm) Under Different Conditions of Flow Speed. 2. Flow Speed (m/sec). 3. Amount of Noise Eliminated (decibels). 4. Center Frequency (Hertz). 5. Blockage Losses in mm on a Water Column.
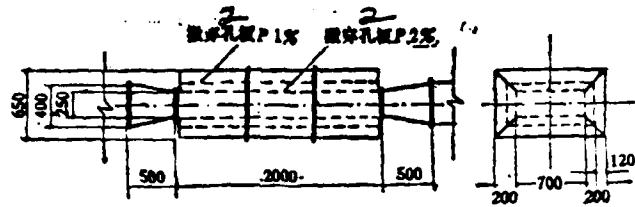
图 4.23 某制药厂 W-1 型空调机矩形微穿孔板消声器
微穿孔板板厚 t = 0.75 毫米, 孔径 φ0.8 毫米

Figure 4.23. 1. The Rectangular Minute Aperture Plate
Noise Silencer on the Model W-1 Climate Control
Unit in a Certain Fertilizer Plant, the Plate Thickness
of the Minute Aperture Plate is t = 0.75 mm, the
Diameter of the Apertures is 0.8 mm.
2. Minute Aperture Perforated Plate
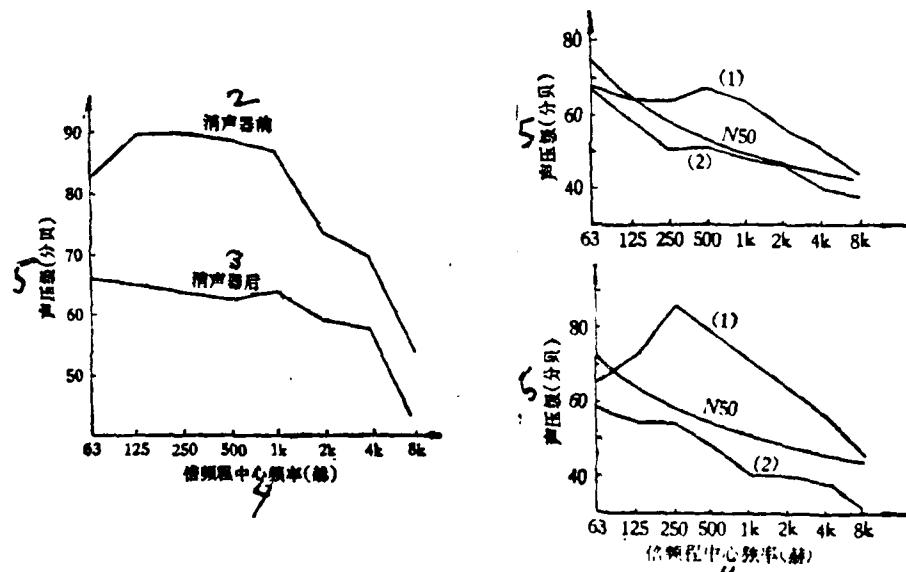
图 4.24 W-1 型空调机微穿孔板消声器消声效果

Figure 4.24. 1. The Noise Silencing Results of the
Minute Aperture Plate Noise Silencer Used With the
Model W-1 Climate Control Unit. 2. Before Use of the
Noise Silencer. 3. After Use of the Noise Silencer.
4. The Center Frequency Among Frequency Multiples
(Hertz). 5. Degree of Acoustic Pressure (decibels).

258

微穿孔板 P 1%

微穿孔板 P 2%

微穿孔板 P 2%

微穿孔板 P 1%

(c)

图 4.25 通风空调系统用消声器
(a) 矩形,适用于流量为 5000—10000 米³/时;
(c) 片式,适用于流量 20000—30000 米³/时;
微穿孔板板厚 t = 0.8毫米

穿孔板消声器系列化图
(b) 声流式,适用于流量为 10000—20000 米³/时;
(d) 声流式,适用于流量为 40000—50000 米³/时
孔径中 = 0.8 毫米
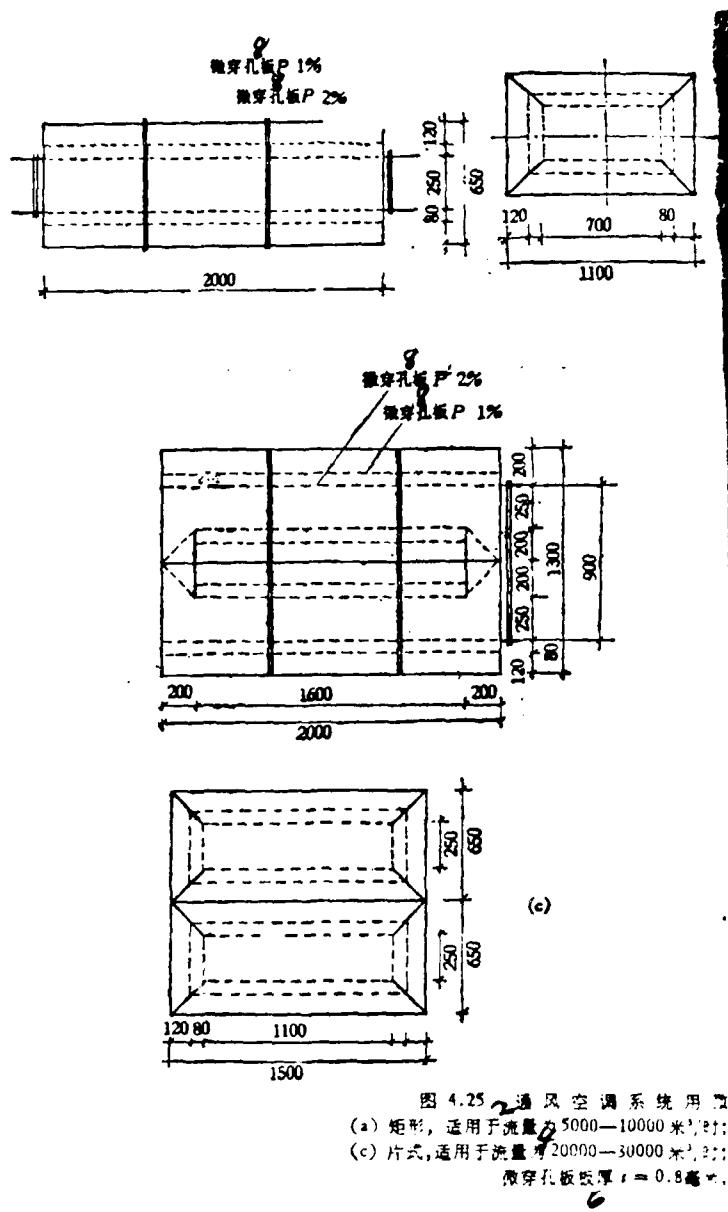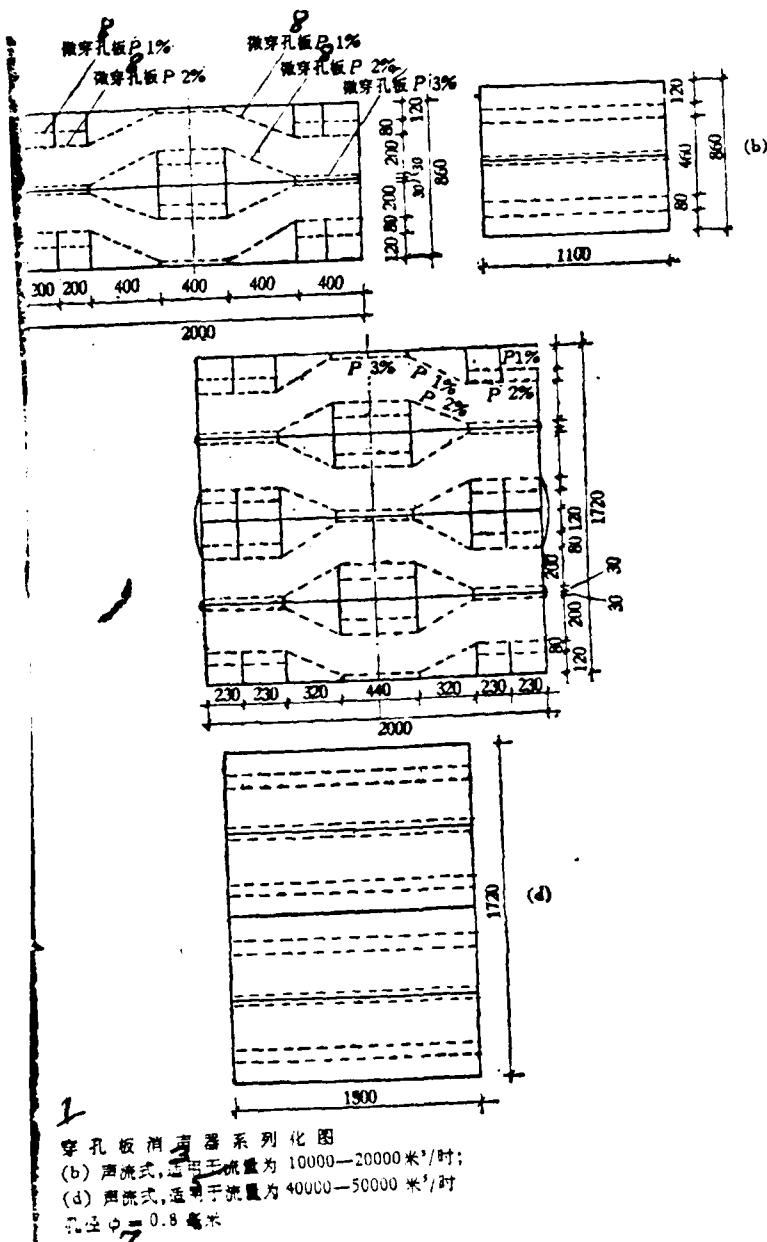
Figure 4.25 (see caption, key next page)

Figure 4.25. 1. An Illustration of a Ventilation
and Climate Control System in Which is Used a Minute
Aperture Plate Noise Silencer. 2. A Rectangular type
is Appropriate for Use When the Amount of Flow is
5000-10000 m³/hr. 3. The Acoustic Flow Type is
Appropriate for Use When the Amount of Flow is 10000-
20000 m³/hr. 4. The Plate Type is Appropriate For
Use when the Amount of Flow is 20000-30000 m³/hr.
5. The Acoustic Flow Type is Appropriate for Use When
The Amount of Flow is 40000-50000 m³/hr. 6. The
Plate Thickness of the Minute Aperture Plate is t =
0.8 mm. 7. The Diameter of the Apertures is ɸ = 0.8 mm.
8. Minute Aperture Perforated Plate.

Figure 4.34 is a graph of the noise values measured in the
air intake port of an air compressor. It can be seen that the
noise, within a relatively wide frequency range, was reduced,
particularly in the vicinity of 250 Hertz, where the drop was
approximately 40 decibels.
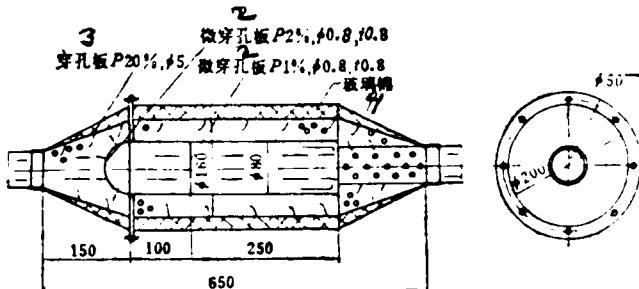
图 4.26 4115 型柴油发动机的微穿孔板-阻性消声器

Figure 4.26. 1. A minute Aperture Plate-Drag-type
Noise Silencer for a model 4115 Diesel Engine. 2.
Minute Aperture Plate. 3. Perforated Plate. 4.
Glass Cotten.

Figure 4.35 is an illustration of the noise silencer used on
a model V-3/8-1 air compressor. When a noise silencer of this
type is installed in the intake port of the air compressor,
there is an obvious reduction in the noise level (see Figure
4.36).

In the case of air blower machinery, their noise level is
high, their frequency spectrum is wide, and their amounts of

260
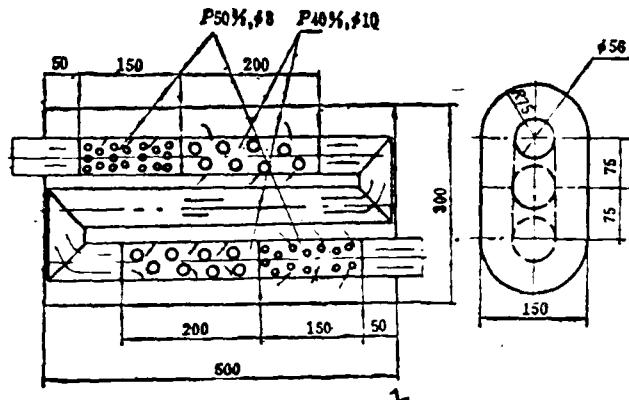
图 4.27 4115型柴油反动机的弯头-穿孔屏消声器

Figure 4.27. 1. A Curved Head Mesh Screen Noise Silencer for a Model 4115 Diesel Engine.

flow are large; it follows from this that one ought to employ with such equipment resonance resistance complex noise surpressors and drag-type noise silencers.

This noise silencer is in the form of an elongated square (outer shell dimensions are 3000 x 600 x 700 mm) with a body proper length of 2.4 m and an extension length or overhang of 0.6 m. The central or core section is the wide frequency band noise silencing body as is shown in Figure 4.38. It is formed from resonance devices and a complex of sound absorbing materials. As was discussed in Section 3.2, the types of resonator devices which have cavity depths of 15 cm, wall thicknesses of t = 2.5 mm and penetration rates of P = 0.6%, 1%, 1.2%, and 2%, within the range of 125 - 400 Hertz, all have sound absorption coefficients which are 70% or above. When these are put together with glass cotton (density 20-30 kg/m^3 with the surface using polyvinyl chloride and an additional system of steel plates or a penetration plate protective surface with a penetration rate of 20% or higher), this causes the noise silencing body, within the wide frequency range of 125-8000 Hertz, to have sound absorption coefficients which reach 70% or higher.

261
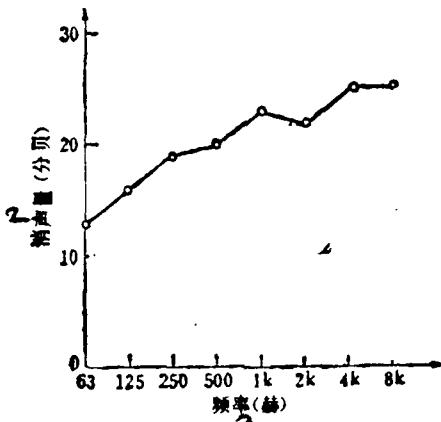
图4.28 4115型柴油发动机的微穿孔板-阻性消声器消声曲线

Figure 4.28. 1. Noise Reduction Curve for a Minute
Aperture Plate - Drag Type Noise Silencer for a
Model 4115 Diesel Engine. 2. Amount of Noise
Reduced (decibels). 3. Frequency (Hertz)
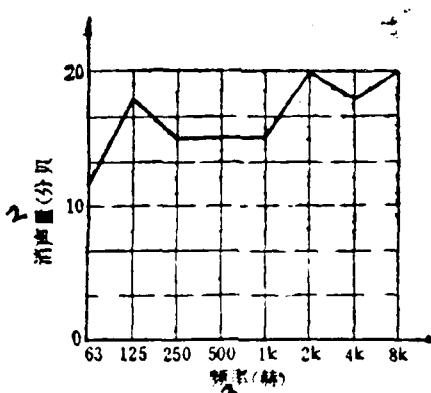
图4.29 4115型柴油发动机的弯火-穿孔罩消声器消声曲线

Figure 4.29. 1. Noise Reduction Curve for the Curved
Head - Perforated Screen of Mesh Screen Noise Silencer
for a Model 4115 Diesel Engine. 2. Amount of Noise
Reduced (decibels). 3. Frequency (hertz)
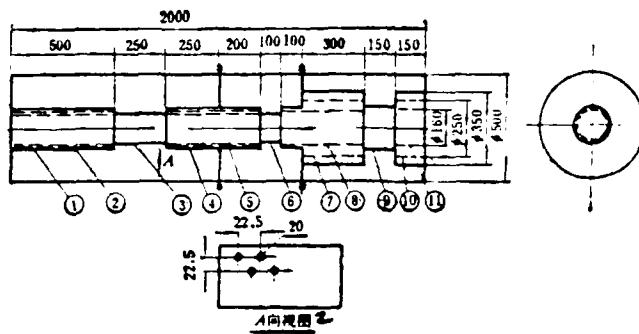
図 4.30 350 马力柴油发动机排气消声器

Figure 4.30. Exhaust Noise Silencer for a 350
Horsepower Diesel Engine. 2. Direction View
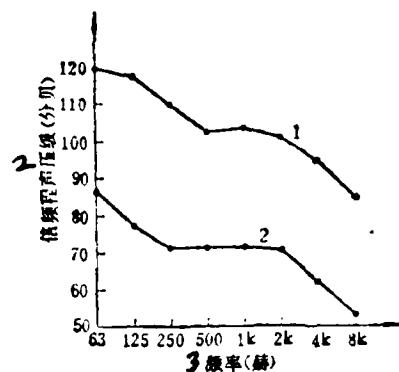
图 4.31 350 马力柴油机消声效果
1——柴油机排气口 45°，1 米处的噪声频谱：2 ——加消声器（包括导管）
后，排气口 45°，1 米处的噪声频谱

Figure 4.31. 1. Noise Reduction Results with a 350
Horsepower Diesel Engine. 2. Frequency Multiple
Acoustic Pressure Level (decibels). 3. Frequency
(Hertz). ---. Noise Frequency Spectrum for the Diesel
Engine Exhaust Port 45° at a Distance of one Meter

1. Noise Frequency Spectrum Taken at one Meter away from the
Exhaust Port at 45° after the Addition of the Silencer (including
Guide Tubes)

263
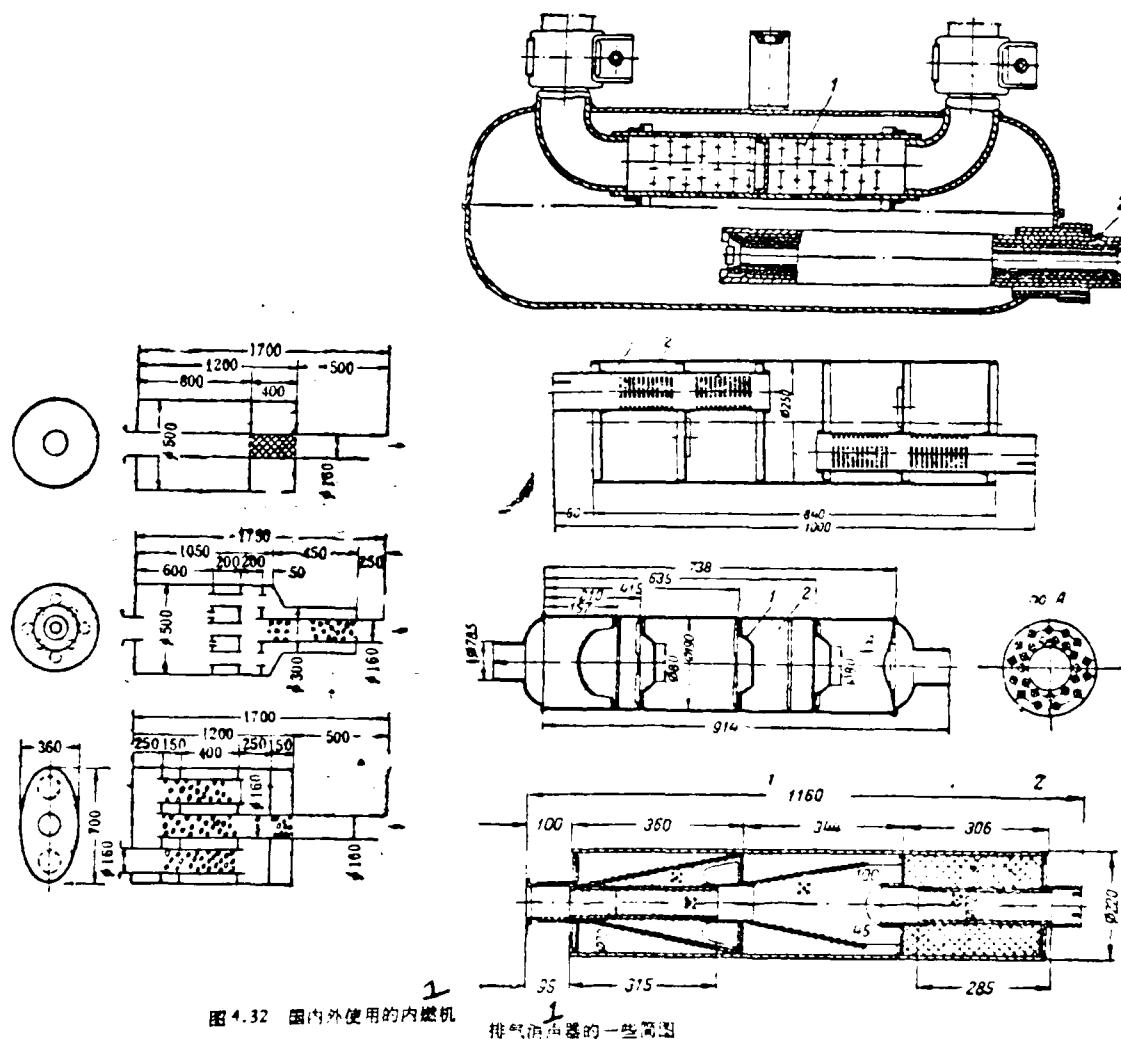
図 4.32 国内外使用的内燃机

排气消声器的一些简图

Figure 4.32. 1. Some Simplfied Diagrams of
Internal Combustion Engine Exhaust Noise Silencers
Which Are Used Both Inside and Outside of China.
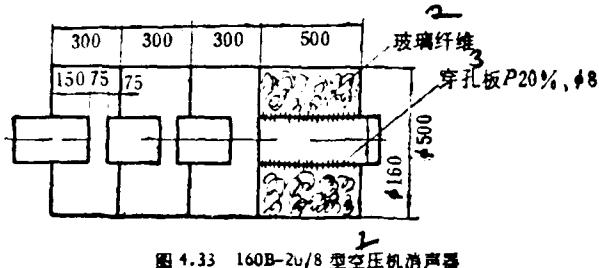
图 4.33 160B-2u/8 型空压机消声器

Figure 4.33. 1. The Noise Silencer for a Model
160B-20/8 Air Compressor. 2. Glass Fibers. 3.
Perforated Plate.
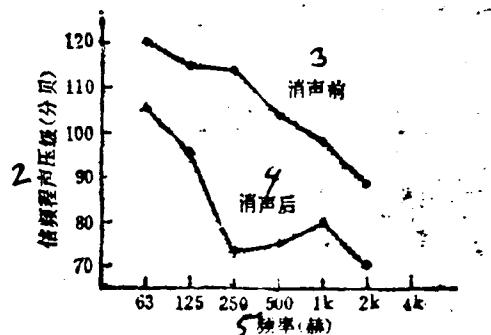
图 4.34 空压机进风口安装消声器后的消声效果

Figure 4.34. 1. Noise Reduction Results After the
Installation of Noise Silencers in the Intake Port of
an Air Compressor.
2. Multiple Frequency Acoustic Pressure Level (Decibels)
3. Before Noise Silencing 4. After Noise Silencing
5. Frequency (Hertz)
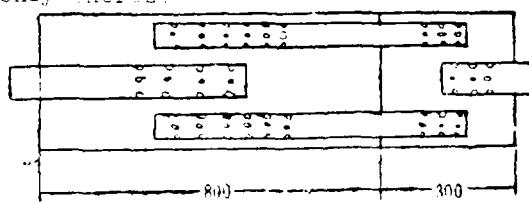
图 4.35 V-3/8-1 型空压机消声器示意图

Figure 4.35. 1. An Illustration of the Noise Silencer
for a Model v-3/8-1 Air Compressor.

265
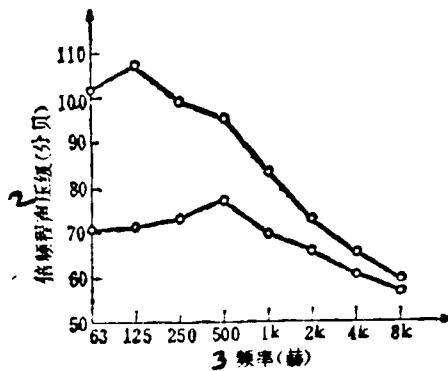
図 4.36 V-3/8-1 型空压机安装消声器后的消声效果

Figure 4.36. 1. The Noise Reuction Results After
Installation of Noise Suppressors in the Model
V-3/8-1 Air Compressor. 2. Frequency Multiple
Acoustic Pressure level (decibels). 3. Frequency
(Hertz).
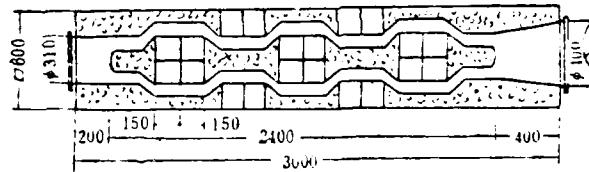
图 4.37 L84 型罗茨鼓风机用共振阻抗复合消声器结构示意图

Figure 4.37. 1. A Structural Diagram for a Model
L84 Blower Using a Resonance Resistance Complex
Noise Silencer.

If noise silencers are installed in ductwork according to
the method put forward in Figure 4.39, then, the noise level is
lowered in the following way:

1. When the flow speed in the noise silencer is 35 m/sec,
then, the overall acoustic pressure from the noise is lowered
from 131 decibels to 79 decibels; the A sound level is lowered
from 126 decibels to 72 decibels; these reductions in noise
occur when the exhaust port of the ducting is at 45°, and
measurements are taken at a one meter point. The frequency
spectrum is lowered to N70 (see Figure 4.40) and is eventually

266
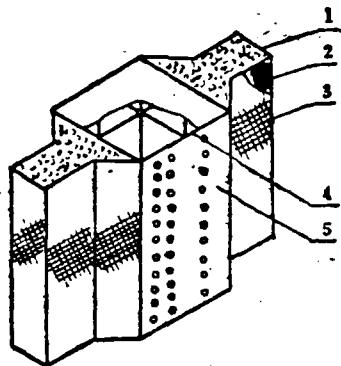
图4.38 宽频带消声体结构示意图
1——玻璃棉: 2——玻璃布: 3——钢板网: 4——钢板,厚度 $t=2.5$ 毫米:
5——穿孔板,孔径 φ10 毫米.

Figure 4.38. 1. An Illustration of the Structure of a Wide Frequency Band Noise Silencer. 2. Glass Cotton. 3. Polyvinyl Chloride. 4. Steel Plate Net. 5. Steel Plate Thickness t = 2.5 mm. 6. Perforated Plate with Hole Diameter φ 10 mm.
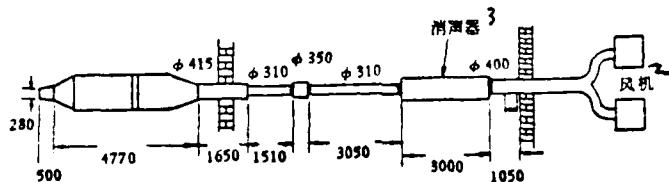
Figure 4.39. An Illustration of the Installation of a Noise Silencer. 2. Blower 3. Noise Silencer

lowered to N85.

At medium flow speeds, with a ductwork exhaust port at 45° and at a distance of one meter, the A sound level is lowered to 56 decibels. When one is dealing with small flow speeds (for example, 10 m/sec), then, the A sound level is lowered to 52 decibels.

2. The level of overall acoustic power is lowered from 133 decibels to 86 decibels; the overall acoustic power is lowered from 20 Watts to 0.0004 Watts.

3. The level of interference with speech is lowered from

267
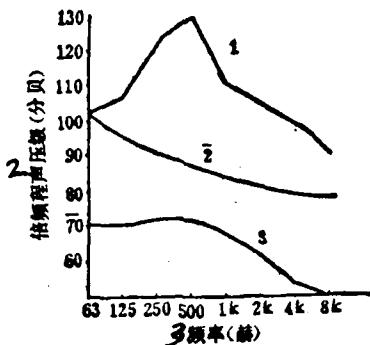
图4.40 风洞消声器消声效果评定
1——风洞噪声；2——N85 曲线；3——消声后的风洞噪声
测点：距风洞出风口 45°、1 米处

Figure 4.40. 1. An Evaluation of the Noise Reduction
Results From a Noise Silencer in the Ductwork. 2.
Frequency Miltiple Acoustic Level (Decibels). 3.
Frequency (Hertz). 4. Duct Noise. 5. Curve. 6.
Noise Measurement Points in the Ductwork After Noise
Reduction: Ductwork Exhaust Port 45° at one meter.

114 decibels to 67 decibels which means that there is no influ-
ence on oral communication.

4. The surrounding offices and laboratores cannot hear the
noise from the operation of the ventilation system.

The Shanghai Industrial Architectural Design Academy [37]
has recently made successful test production of a serial noise
suppressor which is fitted to be used with a Luo Ci-gu blower
(it is called a Model D Noise Silencer, see Figure 4.41), and
this noise suppressor is of a folded plate resistance type which
comes in seven types all together and in varying sizes; these
types are respectively suitable for use with Luo Ci-gu blowers
having rates of flow from 1.25 - 200 m^3/minute. Table 4.9 is a
display of their sizes and specifications. These seven types of
noise silencers are already in definitive production form in the
Xiang Yang Noise Silencer Plant in Changsha City, Hunan.
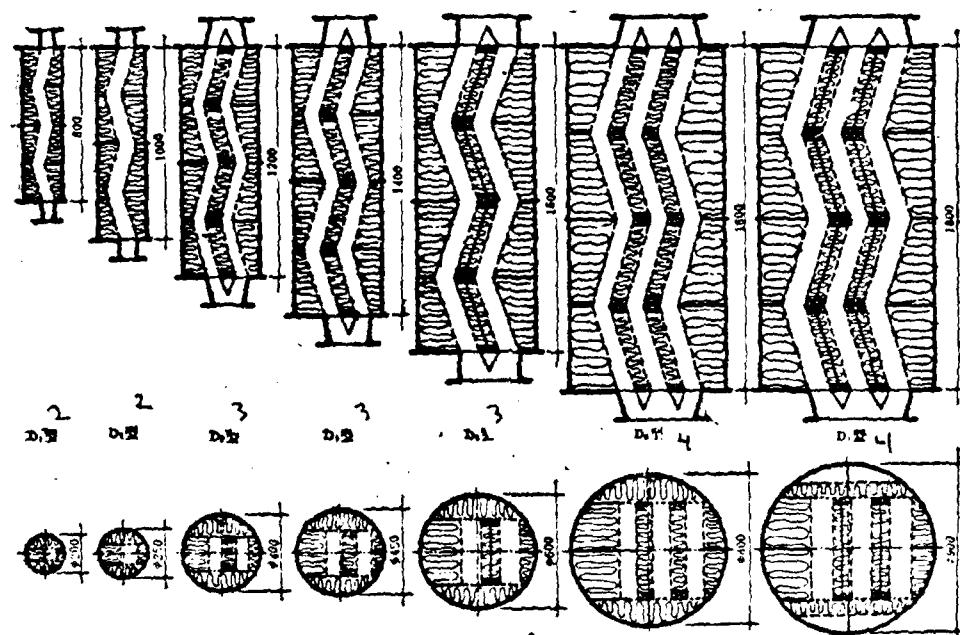
图 4.41 罗茨鼓风机用 D 型阻性折板式消声器系列示意图

Figure 4.41. 1. An Illustration of the Series of
Model D Folded Plate Resistance-Type Noise Silencers
For Use With Luo Ci-gu Blowers.
2. single passages 3. double passages 4. triple passages

269

表4.9　D型消声器系列规格

消声器型号	有效长度(毫米)	外形直径(毫米)	法兰孔径(毫米)	收声片厚(毫米)	吸声片距(毫米)	通道面积(米²)	通过流速(米/秒)	配用流量(米³/分)	重(公斤/只)
D₁	800	φ200	φ50	—	60	0.0036	5.8 / 11.6	12.5 / 2.5	18
D₂	1000	φ250	φ80 (φ100)	—	30	0.008	10.4 / 14.6	5 / 7	25
D₃	1200	φ400	φ150 (φ200)	80	60	0.0216	7.8 / 11.6 / 15.5	10 / 15 / 20	69
D₄	1400	φ450	φ200	80	30	0.0384	13.0 / 17.4	30 / 40	84
D₅	1600	φ600	φ300	100	100	0.068	14.7 / 19.6	60 / 80	162
D₆	1800	φ800	φ350 (φ400)	80	90	0.135	14.8 / 19.8	120 / 160	248
D₇	1800	φ900	φ450	100	100 / 110	0.173	19.3	200	358

Table 4.9. 1. Series Specifications for Model D
Noise Silencers. 2. Model Designation of Noise
Suppressor. 3. Effective Length in mm. 4. External
Diameter (mm). 5. Flange Hole Diameter (mm). 6.
Noise Absorbing Section Thickness (mm). 7. Noise
Absorbing Section Distance (mm). 8. Area of the
Passage (m^2). 9. Transit Flow Speed (m/sec). 10.
Amount of Flow Used (m^3/minute). 11. Weight
(kg/ unit).

In Figure 4.41, D_1 and D_2 are single passageways; D_3, D_4 and
D_5 are double passageways, and D_6 and D_7 have three passageways;
all of these variants are composed of two parts or sections and
have an angle of fold which is approximately 20°. The sound
absorbing plates are all made with exceedingly fine glass cotton
stuffed to a density of 20 kg/m^3; on the surface is used a
fiber glass covering with perforated steel plates as a protec-
tive covering (thickness 0.75-1.2 mm, hole diameter is φ 6 mm,
rate of penetration or perforation is P27%). For the sound

absorbing layers in the lateral direction on the D_7 model noise silencer, there was employed a double layer of perforated steel; the utilization of the empty cavity which has sound absorbing

表4.10 D₄, D₅, D₇型消声器的实测值		
实测条件	消声效果	⊿声级(分贝A)
风机流量 30—40 米³/分	未装消声器(距1米)	115
	装D₄型消声器(距1米)	90
风机流量 60—80 米³/分	未装消声器(距1米)	122
	装D₅型消声器(距1米)	93
风机流量 200 米³/分	未装消声器(距1.5米)	115
	装D₇型消声器(距1.5米)	92

Figure 4.10. 1. Experimental Values for D_4, D_5 and D_7 Models of Noise Silencer. 2. Conditions for Experimental Measurement. 3. Results of Noise Suppression. 4. Acoustic Level (Decibels A). 5. Amount of Flow Through the Blower in M^3/Min. 6. Without the Installation of a Noise Silencer (Distance of One Meter). 7. With the Installation of Noise Silencer (Various Models) (Distance of One Meter).

material improves the noise silencing characteristics in low frequency ranges, and, since this economizes on glass cotton, it is also possible to increase the strength of the outer shell of the noise silencer. Concerning the layer of thin steel plates that are installed between the folded sound silencing plates or sections in the middle section of the D_6 and D_7 model noise silencers, these are installed in order to prevent the sound waves in the interior of the noise silencer from passing through directly; the installation of a round horizontal wall plate on the sides of the sound absorbing cavities not only make it possible to raise the level of integral rigidity of the body but also makes it possible to avoid the lateral propagation of sound waves within the sound absorbing cavity.

The D model series of drag or resistance type folded plate noise silencers which have been discussed above are primarily suitable for use with Luo Ci-gu blowers and are used to silence noise in the intakes of these blowers. If one is using noise

271

silencers on the exhaust of a blower, then, one should arrange for a suitable strengthening of the structure of the noise silencer to be used. This type of noise suppressor is also suitable for general use in the elimination of noise from the intakes of medium and low pressure blower ductwork as well as from those of other types of high pressure blowers (such as 9-27 types and 8-18 types) which have similar specifications for their amounts of flow.

Table 4.10 is a table of the experimental values which were determined for model D_4, D_5 and D_7 noise silencers.

If one is considering the case of large scale drum blowers, then, it is possible, on the basis of the flow conducting equipment in the ducts, to design an appropriate noise silencer to suppress the noise; it is also possible, at the same time, to improve the air-moving characteristics of the blower involved. Figure 4.42 - Figure 4.45 are illustrations of the structures of large scale drum blower noise silencers.

In recent years, in the intakes and exhausts of drum blowers, there have been used mesh plate noise silencers similar to those found in Figure 3.44, 4.22 and 4.30; with the use of this type of noise silencer, it has been possible to obtain excellent noise silencing results.

In the case of drum blowers and air compressors, besides the addition of sound silencers, there are occasions when it is also appropriate to carry out the operations of noise isolation and the reduction of resonance [38] and, by the use of these methods, to effect an overall reduction in the noise level.

4.5 Noise Silencers for Jet Aircraft and Rockets

If we are dealing with the case of jet aircraft and rockets, there is no question that, in flight, whether it is during take-off and landing or during operation on the ground, the noise levels are extremely high, and there is a need for control. Below we will introduce the problem of noise silencers for this application by considering it from three points of view.
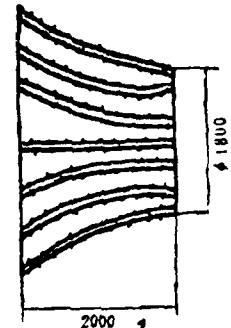
图 4.42 进风导流消声器
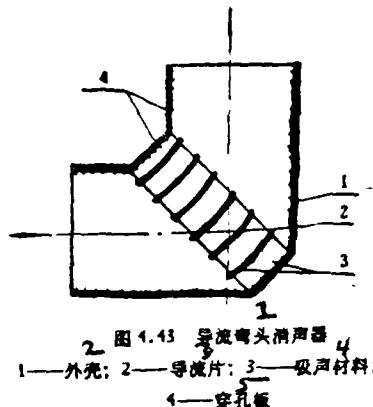
图 4.43 导流弯头消声器
1——外壳；2——导流片；3——吸声材料；
4——穿孔板

Figure 4.42. 1. An Intake Directed Flow Noise Silencer.

Figure 4.43. 1. Directed Flow Elbow Noise Silencer. 2. Outer Shell. 3. Guide Vane. 4. Sound Absorbing Material. 5. Perforated Plate.
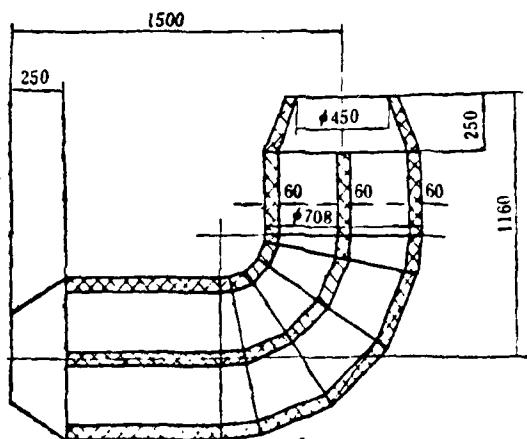

图 4.44 D700/3-2 型鼓风机出风口消声器结构示意图

Figure 4.44. 1. An Illustration of the Structure of a Model D700/3-2 Exhaust Port Noise Supressor for a Drum Blower.

273

4.5.1 The Noise Which is Put Out By Jet Engines During Flight

Ordinary drag or resistance type noise silencers have large volumes, are clumsy and cumbersome and are only able to meet the requirements of aircraft during operations on the ground or when used during take off. Many years of research demonstrates that [3, 5, 24, 39, 40, 41] the reduction of the noise which is put out by engines during flight is a problem which can be come to grips with through a study of the construction of the engines which are producing the noise in terms of the jet flow which occurs within them.
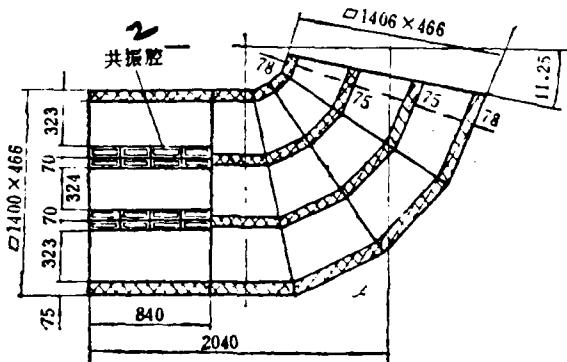
图 4.45 D700/3-2 型鼓风机进风口消声器结构示意图

Figure 4.45. 1. An Illustration of the Structure of a Model D700/3-2 Intake Port Noise Silencer for a Drum Blower. 2. Resonance Cavity

The type of noise silencer required for this application are ones which go through and destroy jet flow patterns and organize new jet flow patterns in order to arrive at the required reduction in noise. We know it is true that the acoustic power of the noise produced by a jet and the jet speed of the engine in question form an eighth power direct proportion, and we also know that there is a direct square relationship between the thrust of a jet engine and the jet flow speed of that engine. On the basis of this, it follows that the most effective method one could use to reduce jet noise is to lower the jet flow speed. Because of this, the widespread application or utilization

of many engines to take the place of one engine guarantees that the thrust will not vary, and this approach, when it is used in conjunction with a lowering of the jet flow speed of the engines, makes it possible to achieve the objective of noise reduction. However, it is not possible to increase the number of engines without limit. Because of this fact, there has been intensive and large scale research and test production of jet nozzle sound silencers with a view on the one hand to a lowering of the jet flow speed and, on the other, to the problem of not excessively influencing the thrust of the engine.

The simplest type of jet nozzle noise silencer is illustrated in Figure 4.46; this type is a jet flow guide of a tubular type which is installed in the jet nozzle of the engine in question. Air is induced to enter the jet apparatus and mix with the original jet flow; this causes the amount of flow of the jet flow to be increased, the speed to be lowered, and, as a consequence, the jet noise to also be lowered. This method is simple and convenient; however, in order to achieve a certain amount of noise reduction, the tube must be quite long.

引入二次气流

原始喷射气流

喷射器套管
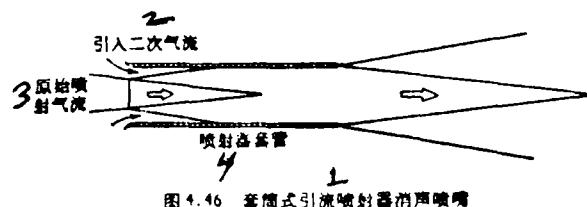
图4.46 套筒式引流喷射器消声喷嘴

Figure 4.46. 1. A Tubular-type Induced Flow Jet Apparatus for Noise Silencing in Jet Nozzles. 2. Entry of Induced Secondary Air Flow. 3. Original Jet Flow. 4. The Outer Tube of the Jet Apparatus.

A relatively better method is to change the configuration of the shape of the jet nozzle of the engine. In recent years, the largest part of the research and experimentation that has been done into this aspect of the problem has been concentrated in the area of the improvement of the configuration or shape of the jet intake nozzle. In the earliest days, use was made

275
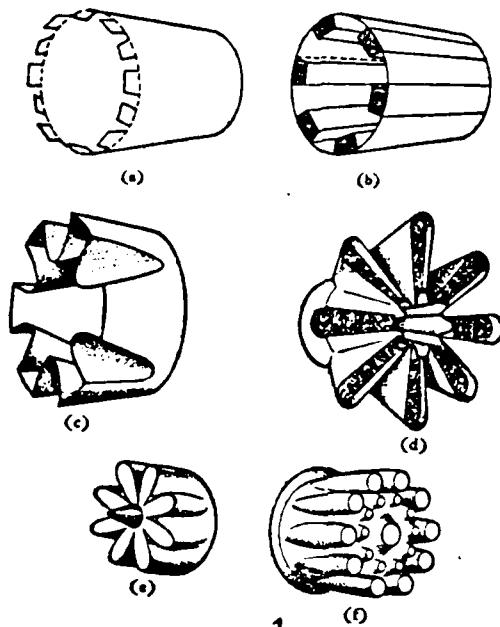
图4.47 各种不同形状的消声喷嘴

Figure 4.47. 1. Various Types of Noise
Silencing Jet Nozzles With Different Shapes.

of tooth-shaped jet nozzles to take the place of straight tubular
jet nozzles (Figure 4.47a); after further progress was made,
this concept was developed into a wave-shaped jet nozzle (Figure
4.47b), and, at present, the method which is generally utilized
is one in which multiple tubular jet nozzles are used or a
similar one in which multiple wave-shaped jet nozzles are used
Figure 4.47 e-f).

If one is considering these noise suppressing jet nozzles,
they can induce more secondary flow than is the case with the
original simple tube-type, round jet nozzles; this causes the
area of the new jet flow which is formed to be enlarged, the
jet flow speed to be lowered, and, consequently, this allows the
objective of noise reduction to be achieved. These noise
suppressing jet nozzles also are capable of causing the frequency

spectrum of the noise to shift from low frequencies to high frequencies. Because of the fact that there is a relationship between the frequency composition of the noise and the diameter of the jet nozzle; this means that, if the diameter of the jet nozzle is small, then, the frequency of the jet noise will be high; if we reverse this, then, the frequency of the jet noise will be low. Noise suppressive jet nozzles take one large diameter jet nozzle and change it into several small jet nozzles with a fixed distance between them; this approach causes the frequency spectrum of the jet noise to shift toward the high end. Air absorbs high frequency sounds much faster than it absorbs low frequency sounds; this, to a certain extent, also lowers the jet noise from the engine.

Figure 4.48 is a display of the noise reduction results from noise silencing jet nozzles. In the figure, the two curves in the top of the graph represent data which was taken when an aircraft was flying over at an altitude of 150 m; the bottom two curves represent data taken on frequency spectra when the engine was on the ground; the curves with the high acoustic levels are the ones which were obtained from data taken on engines which had not been fitted with noise silencing devices and had the ordinary tube-shaped jet nozzles; the curves with the lower values represent data taken from engines after they had been fitted with the noise silencing jet nozzles. It can be seen from the figure that the noise suppressive jet nozzles caused a relatively large reduction in the low frequency noise; moreover, there was caused a reduction of 7 decibels in the overall level of acoustic pressure, and there was a perceptible reduction in the noise level of 5 decibels. The lower two curves represent the sound spectra for two for the noise for two types of jet nozzles when an aircraft was flying at an altitude of 450 m. It is possible to see that the noise silencing jet nozzles, at one time, cause the low frequency noise to be reduced in a relatively large way; moreover, it causes the overall level of acoustic pressure to be reduced by 10 decibels as well as causing a reduction of the perceptible noise level of 7 decibels. It is also possible to see from the chart that when

277

the altitude of the aircraft changed from 450 m to 150 m, and
the distance increased 1.5 times, the corresponding differen-
tial in acoustic pressure is 9 decibels; this corresponds appro-
priately with the inverse square law requirements. However,
in the high frequency range, due to the fact that there is
atmospheric absorption, the corresponding differential is more
than 9 decibels.

Because of these facts, after sound silencing jet nozzles
are installed in the jet tubes of jet aircraft, as far as take
off and landing periods are concerned, it is generally possible
to lower the noise 4-15 EPN; from Table 2.9 it is possible to
see that, after the employment of sound silencing jet nozzles,
the take off noise of a DC 10 is reduced 4 EPN decibels, and
its landing noise is reduced 5 EPN decibels; it can also be
seen that the take off noise and the landing noise of a DC 8 are
both reduced 12 EPN decibels; and, it can be seen as well that
the take off noise of a Boeing 707 is lowered 11 EPN decibels,
and its landing noise is lowered 15 EPN decibels, and so on.
In general, these sound silencing jet nozzles are capable of
causing the production of a 1-5% loss in the thrust produced
by the engines; moreover, the installation of them causes the
weight of the engines to be increased by several hundred kg.
If one is dealing with the case of a Ru Tu 104 passenger plane,
then, after the installation of noise suppressing jet nozzles,
the power level of the noise was lowered 7-8 decibels; however,
the thrust of the aircraft was reduced 1.4 - 2.2%.

In recent years, as far as the problem of the reduction of
the noise of jet aircraft engines is concerned, there has also
been done a good deal of work on the problem of the absorbtion
of noise by the arrangement of engine compartments in aircraft.
Figure 4.49 is an illustrative diagram of the use of a JT-9D
engine compartment arrangement as it appears in a Boeing 747
passenger plane. As far as the question of sound absorbing
arrangements in the engine compartments of aircraft is concerned,
there is a very great requirement for noise absorbing materials
which are capable of resisting high temperatures and the shock
of high speed air flow: Figure 4.50 is an illustrative diagram

279

of the structure of some materials which can be considered for
use in such conditions.

4.5.2 Silencing of Noise from the Take Off
or Ground Operation of Jet Aircraft

The use of exhaust noise silencers is a relatively effective
way of lowering the jet noise which is produced during the take off
or ground operation of jet aircraft.

On the basis of the occasions on which their use is called for
and the environment in which that use takes place, it is possible
to divide noise silencers into three types: fixed noise silencers;
moveable noise silencers; and, noise silencing aircraft beds which
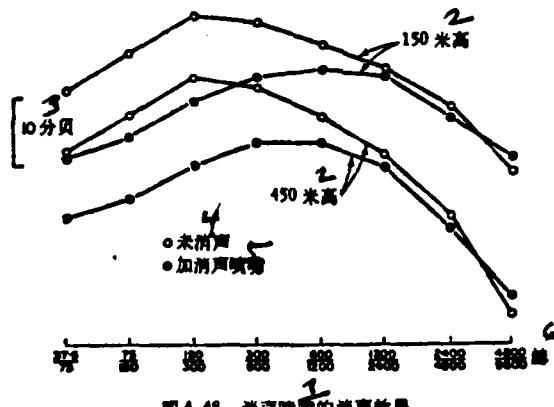
图4.48 消声喷管的消声效果

Figure 4.48. 1. Noise Silencing Results From
Noise Suppressive Jet Nozzles. 2. Meters Alti-
tude. 3. Decibels. 4. Without Sound Silencing.
5. With the Addition of Sound Suppressive Jet
Nozzles. 6. Hertz.

are capable of containing the entire aircraft involved. All of
these noise silencers are relatively clumsy, have very large volumes
and have lengths that reach to ten or twenty meters. In principle,
they are composed of three main sections or parts (see Figure
4.51).

279
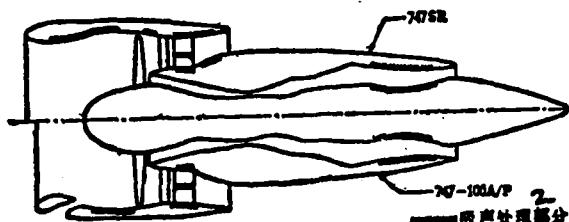
图 4.49　波音747客机 JT-9D 发动机舱的吸声处理示意图

Figure 4.49.　1.　An Illustrative Diagram of
the Sound Absorbing Arrangement in the JT-9D
Engine Compartment of a Boeing 747 Passenger
Plane.　2.　Sound Absorbing Sections of the
Arrangement.
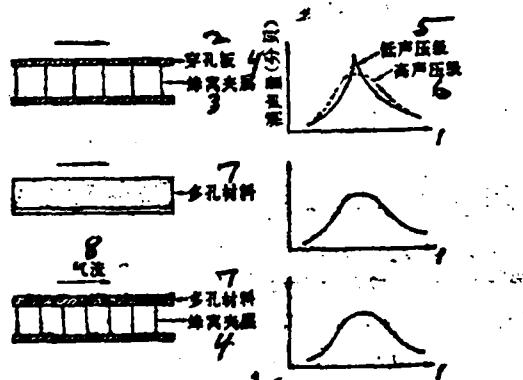
图 4.50　发动机舱的吸声结构基本形式示意图

Figure 4.50.　1.　An illustrative Diagram of the
Basic Structure of the Sound Absorbing Components
of Engine Beds.　2.　Perforated Plate.　3.　A
Honeycomb Sandwiched Between the Perforated
Plates.　4.　The Amount of Noise Reduction (Decibels).
5.　Low Acoustic Pressure Level.　6.　High Acoustic
Pressure Level.　7.　Pourous Material.　8.　Air Flow.

1.　Induced Flow Section:　Concerning the high temperature,
high speed gases which are put out by the jet nozzle, the jet noise
silencers take large amounts of air which is at normal temperature

280

(the secondary flow) and induce them to enter the noise silencers; in this way, not only is the temperature of the air flow of the jet lowered, causing the noise silencers to be unlikely to lose their effectiveness due to the effects of high temperatures, but also, this procedure causes the lowering of the speed of the jet air flow, which causes the level of noise to be reduced somewhat.

2. Diffusion Apparatus: These apparatuses are, structurally speaking, formed in the shape of a plate or an arc or a sharp cone, and they are formed out of perforated steel plate; they are positioned on a horizontal cross section of a jet gas flow. The function of these apparatuses is to break up the formation of jet noise, to lower the speed of the jet gas flow, to take the low frequency portion of the jet noise and turn it into a high frequency component and, thereby, to achieve a relatively large decrease in the amount of jet noise, particularly low frequency noise.
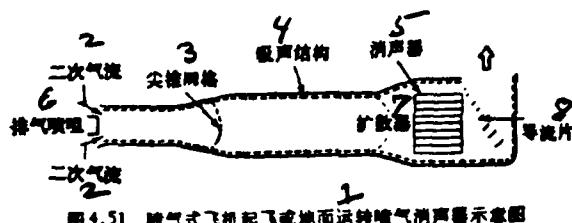
图4.51 喷气式飞机起飞或地面运转喷气消声器示意图

Figure 4.51. An Illustrative Diagram of a Noise Silencer for Use During the Take Off of Jet Aircraft or During Their Ground Operation. 2. Secondary Flow. 3. Cone-shaped Grid. 4. Noise Absorbing Structure. 5. Noise Silencer. 6. Jet Exhaust. 7. Diffusion Apparatus. 8. Induced Flow Blades.

3. Noise Silencers Which Carry With Them Noise Absorbing Structures: The flow induction section and the diffusion apparatus section are capable of lowering the jet speed and the temperature of the jet flow; moreover, they are capable of causing a reduction of a certain size in the noise produced. However, large scale reductions in noise from jets is still dependent upon noise silencing sections which have noise absorbing structures which accompany them. These noise silencing sections are similar to the exhaust air release noise silencer in Section 4.1; most such devices are of a blade type, a folded plate type or an acoustic flow type.
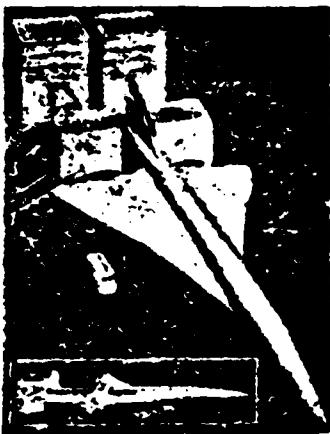
图4.52 飞机起飞或地面运转消声器的例子

Figure 4.52. 1. An Example of a Noise Silencer
for Use During the Take Off of Aircraft or
During Their Ground Operation.

However, one ought to pay attention to the fact that noise absorb-
ing materials and noise absorbing structures should be resistant
to high heat and fuel vapor as well as to shock erosion (it is
possible to employ glass cotton with a high silicon oxide component,
fire resistant brick or sound absorbing structures made out of
perforated metallic plates); in the jet exhausts, the placement of
elbow-shaped devices which have noise absorbing materials in them
as well as the placement of induction flow plates causes the
exhaust put out through the noise silencers to be turned skyward.

Figure 4.52 is an example of a noise silencer for use during
the take off of aircraft or during their ground operation.

4.5.3   The Lowering of Noise From Rockets

Ordinarily, rockets experience ignition on the launching pad
and take off vertically from there; the noise they put out is
extremely strong. Due to the fact that the noise from these
rockets has a maximum frequency value which is in the extremely
low range, it is relatively difficult to eliminate; moreover, the

282

rockets put out jet gases which are at 2000°C and over, and it is
not easy to find materials which have good properties in the areas
of resistance to high temperatures and resistance to high speed
air flow shock; because of these factors, the problem of the
control of the ground noise put out by rockets has still not reached
a thoroughgoing solution.

At present, concerning the methods for the lowering of the
noise put out by rockets, the principal ones are the use of various
models of jet blast deflection plates. These deflection plates
cause the jet blast from the rockets to be diffused, and, as a result
of this, lowers the noise produced by the jet from the rocket,
particularly the low frequency noise.

Besides this, concerning the building of underground launching
silos, the installation on the walls within the silos of heat resis-
tant and blast resistant sound absorbing materials or of sound
absorbing structures is also a method for reducing the noise put
out by rockets; the sound absorbing structures in the engine bed
which is illustrated in Figure 4.50 as well as the double layer
perforated plate noise absorbing structure are both methods which
can be selected for use.

Appendix 1   Resistance Losses (Pressure Reductions) in Commonly Seen Piping[1]

1. Friction Resistance Losses.

If we use a formula to represent them, then, it is

$$\Delta p = \Sigma \xi_{\text{F}} \frac{l}{d_e} \cdot \frac{v^2}{2g} \cdot \gamma \cdot 10^{-4} \quad (kg/cm^2)$$

In this formula, ξ_F is the coefficient of friction resistance;
l is the length of the piping in meters; d_e is the effective diameter
of the piping in meters; v is the average flow speed in meters
per second; g is the acceleration of gravity which is 9.81 m/sec²;
and, γ is the gas density in kg/m³.

Concerning the generality of noise silencers, most of them are
rough pipes; their coefficients of friction resistance are dependent
on the corresponding degree of roughness of the walls of the pipes,
and the numerical values for these two quantities are as shown in

Appendix Table 1.

附表1 摩擦阻力系数 ξ_m （雷诺数 $R_e > 10^4$）

2 相对粗糙度 s/d_o (%)	0.2	0.4	0.6	0.8	1.0	1.5	2	3	4	5
摩擦阻力系数 ξ_m	0.024	0.028	0.032	0.036	0.039	0.044	0.049	0.057	0.065	0.072

Appendix Table 1. 1. Appendix Table 1 The
Coefficients of Friction Resistance ξ_F (Reynolds
No Re > 10^5). 2. Corresponding Degree of Rough-
ness. 3. Coefficient of Friction Resistance.

In the Table, ε is the absolute degree of roughness of the
wall surface. As far as cast iron pipe is concerned, ε = 0.25 mm;
as far as cold drawn and cold rolled steel pipe is concerned,
ε = 0.04 mm; and, as far as perforated plate is concerned, it has
an order of magnitude which is the same as the diameter of the
perforations.

In ordinary diameter piping, ε/d_e can be chosen as 2%. ξ_F
can be chosen as 0.05. In general, friction resistance losses
are not the main source of resistance losses in noise silencers.

2. Local Resistance Losses
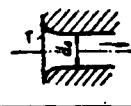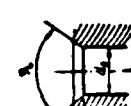
The local friction losses which are caused when changes are
produced in the direction and cross section area of the gas flow
are

$$\Delta p = \Sigma \zeta \cdot \frac{v^2}{2g} \cdot \gamma \times 10^{-4} \qquad (\text{kg/cm}^2)$$

In this formula, ζ is the coefficient of local resistance, see
Appendix Table 2; v is the gas flow flow speed at d_o.

---
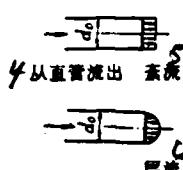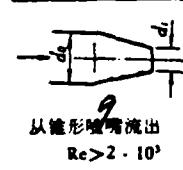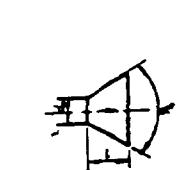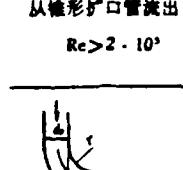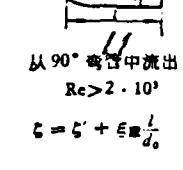
[1]Taken from "Mechanical Design Handbook", Fuel Chemical
Industry Publishing House, 1972.

附表2 管道入口处的局部阻力系数

入口型式	局部阻力系数 ζ
入口处为尖角 凸边 Re>10⁴	when $\delta:d_0<0.05$ and $b:d_0>0.5$ 时, $\zeta=1$ when $\delta:d_0>0.05$ and $b:d_0<0.5$ 时, $\zeta=0.5$

入口处为尖角 Re>10⁴

$\alpha°$	20	30	45	60	70	80	90
ζ'	0.96	0.91	0.81	0.70	0.63	0.56	0.5

一般垂直入口, $\alpha=90°$

入口处为圆角

r/d_0	0.12	0.16
ζ	0.1	0.06

入口处为倒角 Re>10⁴ ($\alpha=60°$时最佳)

$\alpha°$	ζ — l/d_0					
	0.025	0.050	0.075	0.10	0.15	0.60
30	0.43	0.36	0.30	0.25	0.20	0.13
60	0.40	0.30	0.23	0.18	0.15	0.12
90	0.41	0.33	0.28	0.25	0.23	0.21
120	0.43	0.38	0.35	0.33	0.31	0.29
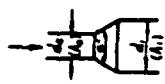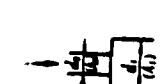
Appendix Table 2. 1. The Coefficient of Local Drag in the Intake of Piping. 2. Form of the Intake of Entrance . 3. Coefficient of Local Drag or Resistance ζ. 4. The Entrance Is at an Acute Angle with a Convex Side Re > 10⁴. 5. The Entrance Is at an Acute Angle With Re > 10⁴. 6. An Entrance With a Rounded Edge. 7. In the General Case of Vertical Entrances, a = 90°. 8. A Chamfered Entrance With Re > 10⁴ (It is optimum when a = 60°.

285

附表3 管道出口处的局部阻力系数

出 口 型 式	局 部 阻 力 系 数 ζ

从直管流出　紊流 / 层流

紊流时, ζ=1

层流时, ζ=2

从锥形喷嘴流出 Re>2·10³

$$\zeta = 1.05 \, (d_0/d_1)^4$$

d_0/d_1	1.05	1.1	1.2	1.4	1.6	1.8	2.0	2.2	2.4	2.6	2.8	3.0
ζ	1.28	1.54	2.18	4.03	6.88	11.0	16.6	24.8	34.8	48.0	64.6	85.0

从锥形扩口管流出 Re>2·10³

	ζ									
l/d_0	$\alpha°$									
	2	4	6	8	10	12	16	20	24	30
1	1.30	1.15	1.03	0.90	0.80	0.73	0.59	0.55	0.55	0.58
2	1.14	0.91	0.73	0.60	0.52	0.46	0.39	0.42	0.49	0.62
4	0.86	0.57	0.42	0.34	0.29	0.27	0.24	0.47	0.54	0.66
6	0.49	0.34	0.25	0.22	0.20	0.22	0.29	0.39	0.50	0.62
10	0.40	0.20	0.15	0.14	0.16	0.18	0.26	0.35	0.45	0.60

从90°弯管中流出 Re>2·10³

$$\zeta = \zeta' + \xi \cdot \frac{l}{d_0}$$

	ζ							
r/d_0	l/d_0							
	0	0.5	1.0	1.5	2.0	3.0	5.0	10.0
0	2.95	3.13	3.23	3.00	2.72	2.40	2.10	2.00
0.2	2.15	2.15	2.08	1.84	1.70	1.60	1.52	1.38
0.5	1.80	1.54	1.43	1.36	1.32	1.26	1.19	1.14
1.0	1.46	1.19	1.11	1.0?	1.0?	1.0?	1.0?	1.0?
2.0	1.1?	1.10	1.0?	1.0?	1.04	1.0?	1.01	1.0?

Appendix Table 3. 1. Coefficients of Local Resistance or Drag For the Exits or Exhausts of Piping. 2. The Form of the Exit or Exhaust. 3. Coefficient of Local Drag or Resistance ζ. 4. Flowing Out From a Straight Pipe. 5. Turbulence Flow. 6. Laminar Flow. 7. During Turbulence Flow. 8. During Laminar Flow. 9. Flowing Out From a Cone-shaped Jet Nozzle. 10. Flowing Out from the Conical Diffuser Exhaust or Exit of a Pipe. 11. Flowing Out From a Pipe Bent 90°.

286

管道扩大型式	局 部 阻 力 系 数 ζ					
	α°	ζ				
		d_0/d_1				
		1.2	1.5	2.0	3.0	4.0	5.0

α°	1.2	1.5	2.0	3.0	4.0	5.0
5	0.02	0.04	0.08	0.11	0.11	0.11
10	0.02	0.05	0.09	0.15	0.16	0.16
20	0.04	0.12	0.25	0.34	0.37	0.38
30	0.06	0.22	0.45	0.55	0.57	0.58
45	0.07	0.30	0.62	0.72	0.75	0.76
60		0.36	0.68	0.81	0.83	0.84
90		0.34	0.63	0.82	0.88	0.89
120		0.32	0.60	0.82	0.88	0.89
180		0.30	0.56	0.82	0.88	0.89

当 α = 180°，为突然扩大：

注：A_0、A_1 为管道相应于内径 d_0、d_1 的通过面积

表中未计摩擦损失，其值按下式决定：

$$\frac{\zeta}{8\sin\frac{\alpha}{2}}\left[1-\left(\frac{A_0}{A_1}\right)^2\right]$$

Appendix Table 4. 1. Coefficients of Local Resistance or Drag Where There is an Expansion in a Pipe. 2. The Form of the Expansion in the Pipe. 3. Coefficients of Local Resistance or Drag ζ. 4. When a = 180°, this is a sudden expansion. 5. Note: A and A are the passage areas of the pipe which correspond to the interior diameters d and d . 6. Within this table the effects of friction losses have not yet been figured in; their values are figured according to the formula below.

管道缩小型式	局 部 阻 力 系 数 ζ									
$Re > 10^4$	$\zeta = 0.5\left(1 - \frac{A_0}{A_1}\right)^n$									
	A_0/A_1	0.1	0.2	0.3	0.4	0.5	0.6	0.7	0.8	0.9	1.0
	ζ	0.45	0.40	0.40	0.35	0.30	0.25	0.20	0.15	0.05	0

管道缩小型式	
$Re > 10^4$	$\zeta = \zeta'\left(1 - \frac{A_0}{A_1}\right)$

ζ'——按附表2第4项"管道入口处为倒角"的ζ值

1) A_0、A_1 为管道相应于内径 d_0、d_1 的通过面积

Appendix Table 5. 1. Coefficients of Local Drag or Resistance in Places where Pipes are Contracted. 2. The Form of the Contraction of the Pipe. 3. Coefficients of local Friction or Drag ζ. 4. ζ is the value of ζ according to the "Quantity 4"

Appendix Table 5 (continued). "The Entrance or Intake of the Pipe is Chamfered" as it is found in Appendix Table 2. 5. A_o and A_1 are the passage areas of the pipe which correspond to the interior diameters d_o and d_1.

附表6　弯管局部阻力系数

弯　管　型　式	局　部　阻　力　系　数　ζ								
折　管	$\alpha°$	10	20	30	40	50	60	70	80	90
	ζ	0.04	0.1	0.17	0.27	0.4	0.55	0.7	0.9	1.12

$$\zeta = \zeta' \cdot \frac{\alpha°}{90°}$$

均匀弯管

$d_o/2R$	0.1	0.2	0.3	0.4	0.5
ζ	0.13	0.14	0.16	0.21	0.29

注: ①对于粗管壁的铸造弯头,当紊流时,ζ'数
值当较上表大 3~4.5 倍.
②两个弯管相连的情况:

$\zeta = 2\zeta_{90°}$　$\zeta = 3\zeta_{90°}$　$\zeta = 4\zeta_{90°}$

Appendix Table 6. 1. Coefficients of Local Drag or Resistance for a Bent Pipe. 2. The Form of the Bent Pipe. 3. Coefficients of Local Drag or Resistance ζ. 4. A Folded Tube. 5. A Tube With an Even Bend. 6. Note: (1) Concerning the cast elbow of the coarse pipe wall, when there is turbulence flow, the numerical value of ζ' should be 3-4.5 times larger than the values found in the table above. (2) The situation when two bent pipes are hooked together.

附表7 分支管的局部阻力系数

型式及流向						
ζ	0.13	0.1	0.5	3	0.05	0.15

注: ①根据上表可以组合成各种分流或合流情况;
②局部阻力计算公式中的 v 应为主管道内油流平均速度.

Appendix Table 7. 1. Coefficients of Local Resistance or Drag in Branch Tubes. 2. Form and Direction of Flow. 3. Note: (1) On the basis of the Table above, it is possible to organize the situation into various types of branching flows or converging flows; (2) v in the formula for figuring the local resistance or drag ought to be the average flow speed of the fuel flow in the main tube path.

$$Re = \frac{v \cdot \delta}{\nu} \geqslant 400, \quad \zeta = 1.3\left[1 - \frac{A_0}{A}\right] + \left[\frac{A}{A_0} - 1\right]^2$$

A_0/A	0.1	0.15	0.2	0.25	0.3	0.35	0.4	0.45	0.5	0.55	0.6	0.65	0.7	0.75	0.8	0.85	0.9
ζ	82	33.3	17	10	6.4	4.3	3	2.2	1.65	1.26	0.97	0.75	0.58	0.44	0.32	0.23	0.14

$$Re = \frac{v \cdot \delta}{\nu} < 400, \quad \zeta' = \eta \cdot \zeta$$

Re	50	100	150	200	300	400
η	1.44	1.24	1.13	1.08	1.03	1.01

A_0——滤网的有效通过面积(米²)；　A——滤网的全部面积(米²)；　v——滤网前面油的流速(米/秒)(经过网的全部面积)；　δ——网丝平均直径；　ν——油的运动粘度(δ 及 ν 在原资料中，没有给出具体单位，但由于 Re 为无量纲的准数，因此建议在选择单位时应满足此条件)。

当有 n 层滤网时，每层间隔不小于 15δ 时，总的局部阻力系数

Appendix Table 8. Coefficients of Local
Resistance or Drag for Filter Nets. 2. A$_0$
is the effective passage area of the filter
net (m^2); A is the total area of the filter
net (m^2); v is the flow speed of the fuel
flowing in the front of the filter (m/sec)
(the total area going through the net);
δ is the average diameter of the filter
filaments; v is the kinetic viscosity of
the fuel (δ and v), in the original material,

(Appendix Table 8 continued) are not given in actual units; however, due to the fact that Re is a non-dimensional standard, when there is an n layer filter net, and the intervening space between each of the layers is not smaller than 15δ, then, the total coefficients of local resistance or drag are

$$\zeta = \sum_{i=1}^{n} \zeta_i$$

Appendix 2. Thermal Capability Coefficients of Several Sound Absorbing Materials.

| 吸 声 材 料	密 度 (公斤/米³)	导热系数 (千卡/米·时·度)	最高使用温度 (℃)	最低使用温度 (℃)
泡沫塑料	20—50	0.03—0.04	80	− 35
玻璃纤维制品	<150	0.03—0.04	250—350	− 35
普通超细玻璃棉	10—20	0.03	450—550	−100
无碱超细玻璃棉	10—20	0.03	600—700	−100
高硅氧玻璃棉	40—80	0.03	1000—1200	−100
矿渣棉制品	<150	0.04—0.05	250—350	− 35
矿渣棉	120—150	0.04—0.05	500—600	−100
微孔吸声砖	300—800	0.08—0.12	900—1000	—
金属微穿孔板	—	—	1000 以上	—

1. Sound Absorbing Material. 2. Density (kg/m³). 3. Coefficient of Thermal Conductivity (kilo-calories/m·sec·degree). 4. Highest Temperature of Employment. 5. Lowest Temperature of Employment (C°). 6. Sponge Plastic. 7. Fiber Glass Products. 8. Ordinary Very Fine Glass Cotton. 9. Non-alkaline Very Fine Glass Cotton. 10. High Silicon Oxide Content Glass Cotton. 11. Slag Cotton Products. 12. Slag Cotton. 13. Pourous Sound-absorbing Brick. 14. Perforated Metallic Plate. 15. and up.

Appendix 3. Relationships between the Rate of
Perforation and the Hole Diameter and Distance
From the Center of One Hole to the Center of
Another.

In the case of a triangular arrangement $P = \frac{\pi}{2\sqrt{3}}\left(\frac{d}{l}\right)^2,$

In the case of a square arrangement $P = \frac{\pi}{4}\left(\frac{d}{l}\right)^2,$

In these equations: P is the perforation rate; d is the diameter
of the circular holes; and, l is the distance between the center of
one hole and the center of another.
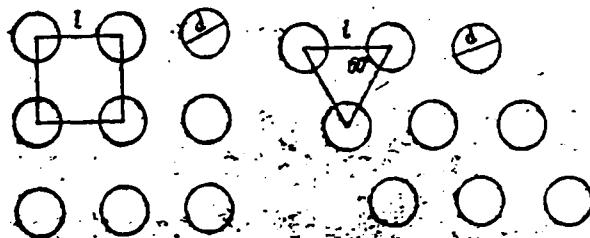
The relationships between P, d and l can be used as they are dis-
played in the table below.

P(%)	l/d 三角排列	l/d 正方排列	P(%)	l/d 三角排列	l/d 正方排列	P(%)	l/d 三角排列	l/d 正方排列
0.5	13.5	12.5	2.5	6.0	5.6	12	2.7	2.6
0.6	12.3	11.4	3.0	5.5	5.1	14	2.5	2.4
0.7	11.4	10.6	3.5	5.1	4.7	16	2.3	2.2
0.8	10.6	9.9	4.0	4.6	4.3	18	2.2	2.1
0.9	10.0	9.3	4.5	4.5	4.2	20	2.1	2.0
1.0	9.6	8.9	5.0	4.3	3.9	25	1.9	1.8
1.2	8.7	8.1	6.0	3.9	3.6	30	1.7	1.6
1.4	8.0	7.5	7.0	3.6	3.4	35	1.6	1.5
1.6	7.5	7.0	8.0	3.4	3.1	40	1.5	1.4
1.8	7.1	6.6	9.0	3.2	2.9	45	1.4	1.3
2.0	6.6	6.2	10.0	3.0	2.8	50	1.3	1.2

1. Triangular Arrangement. 2. Square
Arrangement.

Appendix 4.   A Calculation Diagram for the
Resonant Frequencies of Perforated Plate Sound
Absorbing Materials.
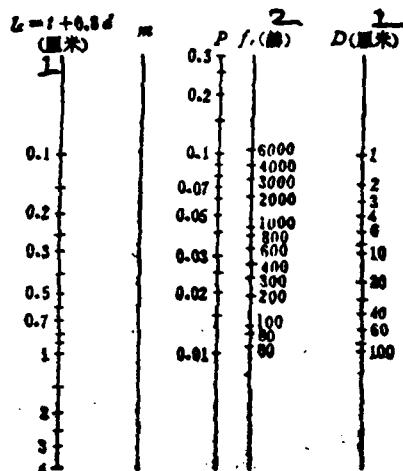
穿孔板构造体的共振频率计算图表

t——板厚； d——孔径； P——穿孔率； D——背后空气层厚度

已知 t，d，P，D，f₀ 中的 4 项时，可以求出另外一项。例如已知
穿孔板厚和背后空气层时，要求出 f₀。先把和穿孔板相对应的（t +
0.8d）和 P 用直线连接起来，交 m 轴上的一点，再把这一点与 D 上的点
连接，截之点就是所求的共振频率。

1.   cm.   2.   Hertz.   3.   A Calculation Diagram for
the Resonant Frequencies of Structural Bodies Made
From Perforated Plate.   4.   Plate Thickness.   5.
Hole Diameter.   6.   Perforation Rate.   7.   Rear Air
Layer Thickness.   8.   When we already know four of
the quantities in t, d, P, D and f_o, then, it is
possible to solve for the other quantity.   For exam-
ple, if we already know the thickness of the perforated
plate and the rear air layer thickness, then, if we
are going to solve for f_o, we must first take the
(t+0.8d) which corresponds to the perforated plate and,
using a straight line, connect it to P; then, take the
point at which this first straight line crossed m and
join this point to the appropriate point on D; the
point at which this line crosses the f_o line is the
resonant frequency we are looking for.

293

References

[1] 守田栄, PPM公害対策と技術調査, 4 (1973), 107.
[2] L. L. Beranek, Noise and Vibration Control, McGraw-Hill, 1971.
[3] A. T. Мунин, В. Е. Квитка, Авиационная акустика, Машиностроение, 1973.
[4] 福田基一, 奥田襄介, 騒音対策と消音設計, 共立出版株式会社, 1973.
[5] E. J. Richards, D. J. Mead, Noise and Acoustic Fatigue in Aeronautics, John Wiley & Sons, 1968.
[6] Glenne, Warnaka, H. T. Miller, J. M. Zalas, American Industrial Hygiene Association Journal, 33(1972), 1.
[7] E. Я. Юдин, Борьба с шумом, Стройиздат, 1964.
[8] M. J. Lighthill, Proc. Roy. Soc. Ser., A211(1952), No. 1107.
[9] L. L. 白瑞纳克, 声学, 高等教育出版社 (章启铎等译), 1959.
[10] 四帆郎十度等编, 空气调节与制冷设计手册, 中国工业出版社, 1970.
[11] P. A. Franken, Review of Information on Jet Noise, Noise Control, 4, 1958, No. 3.
[12] H. E. Glarke, Aircraft Noise Sources, C. Harris, Handbook of Noise Control, McGraw-Hill, 1957.
[13] F. B. Greatex, Jet noise, I, II and III, Engineer, 200 (1955), No. 5188, 5189, 5190.
[14] W. L. Howes, Similarity of Far Noise Fields of Jets, NASA, TRR52, 1960.
[15] A. T. Мунин, Связь аэродинамических и акустических параметров дозвуковой газовой струи, Труды ЦАГИ «Промышленная аэродинамика», № 23, Оборонгиз, 1962.
[16] 福田基一, 内燃機関の排気騒音と消音効果の現状, 内燃機関, 10 (1971), 123—125.
[17] D. Anderton, E. C. Grover, N. Lalor, T. Priede, ASME Publication 70-WA/DGP-3, Aug. 11, 1970.
[18] RRL Report Ln 357, A review of road traffic noise, 1970.
[19] W. Walter, Soroka, Chi-Shing, P. Chien, Automotive Pistonengine Noise and Its Reduction—A literature survey, SAE Paper 690452, May 19—23, 1969.
[20] CIMAC-Arbeitsgruppe "Geräusch", Statistische Erhebung über Dieselmotorengeräusche, MTZ, 31(1970), Nr. 4, 153—156.
[21] 上海工业建筑设计院章蕴生, 环境保护, 1975, No. 1, 21.
[22] 公害と防災編集委員会編, 騒音・振动, 白亞書房, 1966.
[23] N. A. C., Noise in the Next Ten Years, 1972.
[24] H. E. von Gierke, Proceedings of the ICA Congress 1959. Stuttgart, 2(1961), 1055—1070. (中译本, 声学译丛, 总第11号, 建筑声学, 114页).
[25] Handbook of Noise and Vibration Control, 1st. edition, 1970.
[26] B & K, Tech. Rev., 1960, No. 2.
[27] Д. И. Блохинцев, Акустика неоднородной движущейся среды, Гостехиздат, 1946.
[28] 马大猷, 中国科学, 1 (1975), 38.
[29] 伊藤毅, 騒音制御工学, コロナ社, 1969.
[30] C. Eckel, JEP, 86 (1964), No. 1.
[31] W. L. Martin, British Power Engineering, 3(1961), 44—49.
[32] 方丹群, 孙家其, 冯翔正, 物理, 4 (1975), 300.
[33] E. Meyer, F. Mecnel, G. Kurtze, J. Acoust. Soc. Am., 30(1958), 165.
[34] F. Mechel, P. Mertens, Acustica, 13(1963), 154—165.
[35] 平田能睦, 伊藤毅, 日本音响学会誌, 26 (1970), 16.
[36] 平田能睦, 日本音响学会誌, 27 (1971), 501.
[37] 上海工业建筑设计院, 环境保护, 1976, No. 1, 24.
[38] 方丹群, 噪声的危害及防治, 中国建筑工业出版社, 1975 第1版, 1977 年修订第二版.
[39] N. D. Sanders, W. J. North, Combustion and Propulsion Third AGARD Colloquium, 3(1958), 185—196.
[40] E. J. Richards, Combustion and Propulsion Third AGARD Colloquium, 3 (1958), 197—223.
[41] F. B. Greatrex, D. M. Brown, Proceedings of the First Congress in the Aeronautical Sciences, Madrid, 8—13, September, 1958, Vol. 1, 1959, 364—392.

DATE
FILMED

-8